IL
NUOVO CIMENTO
ORGANO DELLA SOCIETÀ ITALIANA DI FISICA
SOTTO GLI AUSPICI DEL CONSIGLIO NAZIONALE DELLE RICERCHE

VOL. VIII, N. 1 *Serie decima* 1° Aprile 1958

Sulla « Bremsstrahlung interna » associata al decadimento beta del $^{204}_{81}Tl$.

R. A. RICCI

Istituto di Fisica Sperimentale del Politecnico - Torino

(ricevuto il 17 Ottobre 1957)

Riassunto. — Lo spettro continuo di bremsstrahlung interna associato al decadimento β del ^{204}Tl è stato determinato sperimentalmente per mezzo di uno spettrometro γ a scintillazione, nell'intervallo di energie 80÷400 keV, e confrontato con le distribuzioni teoriche calcolate sia con il metodo di Knipp e Uhlenbeck, sia con quello di Nilsson, che tiene conto dell'influenza del campo coulombiano del nucleo sul decadimento β. Tale influenza è dimostrata, nel nostro caso, dal fatto che i risultati sperimentali, mentre sono in disaccordo con lo spettro teorico di Knipp e Uhlenbeck, si accordano invece in modo soddisfacente con lo spettro teorico corretto per tale effetto, almeno fino ad energie superiori a 150 keV circa. Tuttavia, per energie più basse si ha un evidente eccesso di fotoni anche rispetto allo spettro teorico di Nilsson. Ciò sembra in accordo con i risultati sperimentali di Starfelt e collaboratori e con quelli di Langevin-Joliot relativi ad altri nuclidi. Nell'intervallo di energie considerato si è trovata una intensità di $(1.0 \pm 0.1) \cdot 10^{-3}$ fotoni di bremsstrahlung emessi per disintegrazione; la teoria di Knipp e Uhlenbeck prevede una intensità pari a $0.637 \cdot 10^{-3}$ fotoni per disintegrazione, negli stessi limiti di energia; quella di Nilsson $0.789 \cdot 10^{-3}$ fotoni per disintegrazione.

1. – Introduzione.

Uno degli effetti secondari che accompagnano sempre la disintegrazione β è costituito dall'emissione di radiazioni elettromagnetiche (bremsstrahlung interna) che si distribuiscono secondo uno spettro continuo nell'intervallo di energie che va da zero all'energia massima W_0 (in unità mc^2) della disintegrazione.

Teoricamente interessa calcolare la distribuzione spettrale di tali radiazioni, partendo dall'ipotesi che la probabilità di emissione di un fotone di bremsstrahlung di energia K (in unità mc^2), da parte di un nucleo radioattivo β, sia, in generale, funzione della probabilità di emissione di un elettrone di data energia W_e (energia dell'elettrone in unità mc^2, compresa l'energia di riposo) e della probabilità che tale emissione sia accompagnata dall'espulsione di una parte dell'energia stessa sotto forma di radiazione elettromagnetica.

In generale si dovrà anche tener conto dell'eventuale influenza del campo coulombiano del nucleo sul decadimento β e sull'interazione elettrone-campo di radiazione, nonchè del tipo di transizione β, ossia della forma dello spettro β.

Si può, in prima approssimazione, trascurare l'influenza del campo coulombiano del nucleo e considerare la probabilità di emissione di un fotone di energia K come prodotto delle probabilità di due eventi indipendenti: emissione di un elettrone di energia W_e e irradiazione da parte di quest'ultimo di un fotone di energia K. Si ha quindi per tutto lo spettro di energie, indicando con $S(K)$ la probabilità di distribuzione spettrale dei fotoni di bremsstrahlung:

$$S(K) = \int_{1+K}^{W_0} P(W_e)\,\Phi(W_e, K)\,\mathrm{d}\,W_e\,, \tag{1}$$

dove $P(W_e)$ è la distribuzione in funzione dell'energia W_e degli elettroni dello spettro β; (W_e, K) è la probabilità che un elettrone di energia W_e irradi un fotone di energia K, ed è data, nei limiti delle approssimazioni suddette, dalla relazione:

$$\Phi(W_e, K) = \frac{\alpha p'}{\pi p K}\left[\frac{W_e^2 + W_e'^2}{W_e p'} \ln (W_e + p') - 2\right], \tag{2}$$

con $\alpha = e^2/\hbar c = 1/137$, costante di struttura fine p e p' sono. rispettivamente gli impulsi dell'elettrone (in unità mc) prima e dopo l'espulsione del quanto; $W_e' = W_e - K$, è l'energia dell'elettrone dopo l'emissione elettromagnetica.

Le relazioni (1) e (2) sono alla base della teoria sviluppata da Knipp e Uhlenbeck [1] per transizioni β permesse.

Chang e Falkoff [2] hanno dimostrato che, nei limiti di tale teoria, le transizioni β proibite danno luogo a distribuzioni di bremsstrahlung interna, ad esse associata, leggermente diverse; le differenze non essendo tuttavia rivelabili sperimentalmente, nei limiti degli errori che si hanno nelle misure di questo tipo.

Ove si tenga conto dell'influenza del campo coulombiano del nucleo sulla disintegrazione β, secondo i calcoli eseguiti da Nilsson [3], si ottiene una distri-

(1) J. Knipp e G. Uhlenbeck: *Physica*, **3**, 425 (1936).
(2) C. S. Chang e D. L. Falkoff: *Phys. Rev.*, **76**, 365 (1949).
(3) S. B. Nilsson: *Ark. f. Fys.*, **10**, 467 (1956).

buzione formalmente analoga alla (1):

$$S(K) = \int_{1+K}^{W_0} P(W_e, Z)\, \Phi_Z(W_e, K)\, \mathrm{d}\, W_e\,, \tag{3}$$

dove $P(W_e, Z)$ è la distribuzione sperimentale ($Z \neq 0$) degli elettroni dello spettro β e $\Phi_Z(W_e, K)$ è data da:

$$\Phi_Z(W_e, K) = \Phi(W_e, K)\, \frac{F(W_e', Z)}{F(W_e, Z)}\,, \tag{4}$$

essendo $\Phi(W_e, K)$ la funzione di Knipp e Uhlenbeck e $F(W_e, Z)$ la funzione di Coulomb nel decadimento β. La teoria di Nilsson è stata sviluppata solo per transizioni β permesse.

Sperimentalmente la distribuzione spettrale della bremsstrahlung interna associata ad un processo di decadimento β, si può determinare con una delle tecniche ormai usuali nella spettroscopia γ; di particolare utilità si è dimostrato l'uso dello spettrometro γ a scintillazione, utilizzato per la prima volta a questo scopo, indipendentemente da Bolgiano, Madanski e Rasetti e da Novey [4]; tali misure richiedono particolare cura nel discriminare la bremsstrahlung interna da rivelare, da altri tipi di radiazioni eventualmente presenti (particelle β, bremsstrahlung esterna, effetti secondari), e nella taratura del dispositivo sperimentale.

Le ricerche compiute da diversi Autori con nuclei a decadimento β semplice e ben definito danno luogo a risultati non sempre in accordo fra loro e con i calcoli teorici.

Mentre da una parte i risultati di Bolgiano, Madanski e Rasetti (^{32}P e ^{91}Y), di Novey (^{32}P e RaE), di Boehm e Wu (^{147}Pm), di Renard (^{32}P) e di Michalowicz (^{32}P, ^{90}Y, RaE) [4] sono in soddisfacente accordo con la teoria di Knipp e Uhlenbeck, dall'altra Lidèn e Starfelt (^{32}P), Starfelt e Svantesson (^{35}S), Langevin-Joliot (^{32}P, ^{143}Pr, ^{147}Pm, ^{35}S), Hakeem e Goodrick (^{90}Y), e, infine, Starfelt e Cederlund (^{143}Pr, ^{147}Pm) [5] giungono a conclusioni diverse pur usando in generale dispositivi sperimentali analoghi.

Il confronto con le distribuzioni teoriche ottenute con il metodo di Nilsson è riportato da Starfelt e Cederlund per il ^{147}Pm e il ^{143}Pr, e da Langevin-

[4] F. Boehm e C. S. Wu: *Phys. Rev.*, **90**, 369 (1953); **93**, 518 (1954); P. Bolgiano, L. Madansky e F. Rasetti: *Phys. Rev.*, **89**, 679 (1953); T. B. Novey: *Phys. Rev.*, **89**, 672 (1953); G. Renard: *Journ. de Phys. et Rad.*, **14**, 361 (1953); A. Michalowicz: *Ann. de Phys.*, **2**, 116 (1957).

[5] K. Lidèn e N. Starfelt: *Phys. Rev.*, **97**, 419 (1955); N. Starfelt e N. L. Svantesson: *Phys. Rev.*, **97**, 708 (1955); M. A. Hakeem e M. Goodrick: *Bull. Am. Phys. Soc.*, II, **1**, 264 (1956); H. Langevin-Joliot: *Ann. de Phys.*, **2**, 16 (1957); N. Starfelt e J. Cederlund: *Phys. Rev.*, **105**, 241 (1957).

Joliot per il ^{32}P, il ^{35}S, il ^{143}Pr e il ^{145}Pm. In entrambi i casi si ha un netto miglioramento nel confronto con i risultati sperimentali; tuttavia esso non è ancora sufficiente, soprattutto alle basse energie. In generale il disaccordo cresce al crescere di Z e al diminuire di W_0. L'influenza del grado di proibizione è pure considerata da Starfelt e Cederlund, nell'approssimazione di Chang e Falkoff, ma senza risultati confortanti. D'altra parte Ford e Lewis [6] segnalano che il calcolo delle correzioni coulombiane del 1° ordine non conduce a risultati tali da spiegare le deviazioni sperimentali osservate per il ^{32}P e per il ^{35}S.

Il caso da noi preso in esame è quello del ^{204}Tl. A causa dell'elevato numero atomico e del valore non troppo grande dell'energia massima della disintegrazione β (0.760 MeV), l'influenza del campo coulombiano del nucleo non può ritenersi trascurabile, a priori. D'altra parte la transizione β è del tipo « unique first forbidden » ($\Delta I = 2$, cambio di parità) [7].

Ci è sembrato quindi di un certo interesse tentare di determinare sperimentalmente lo spettro di bremsstrahlung associato al decadimento β di questo nuclide e confrontare i risultati ottenuti sia con le previsioni teoriche di Knipp e Uhlenbeck sia con quelle di Nilsson, al fine di stabilire l'importanza nel confronto esperienza-teoria dell'influenza del campo coulombiano del nucleo e del tipo di transizione β.

2. – Distribuzione teorica della bremsstrahlung interna del ^{204}Tl.

Il $^{204}_{81}Tl$ decade per il 98% circa per emissione β^- nel $^{204}_{82}Pb$ ($E_{max} = 0.760$ MeV) e, per l'1.5% per cattura elettronica trasformandosi in $^{204}_{80}Hg$ [7]. Lo spettro β è semplice, e nessuna radiazione γ dovuta a diseccitazione nucleare è presente.

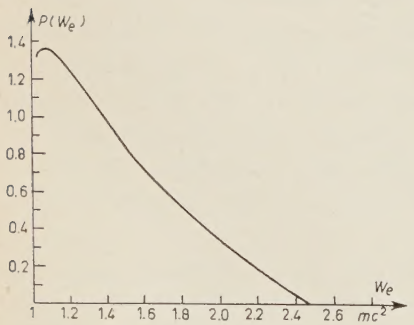

Fig. 1.

In Fig. 1 è riportato lo spettro β sperimentale ottenuto da Der Mateosian [7] e normalizzato ponendo

$$\int_1^{W_0} P(W_e)\,\mathrm{d}W_e = 1\,.$$

Si ha così la distribuzione della probabilità $P(W_e)$ in funzione dell'energia W_e (in unità mc^2). Le funzioni $P(W_e)\cdot K\cdot\Phi(W_e, K)$ (Knipp e Uhlenbeck) e

[6] G. Ford e R. R. Lewis: *Bull. Am. Phys. Soc.*, II, **1**, 195 (1956).
[7] E. Der Mateosian e A. Smith: *Phys. Rev.*, **88**, 1186 (1952).

$P(W_e)\cdot K\cdot \Phi_z(W_e, K)$ (NILSSON), calcolate a partire dalle formule (2) e (4) e dallo spettro sperimentale di Fig. 1, sono riportate rispettivamente in Fig. 2

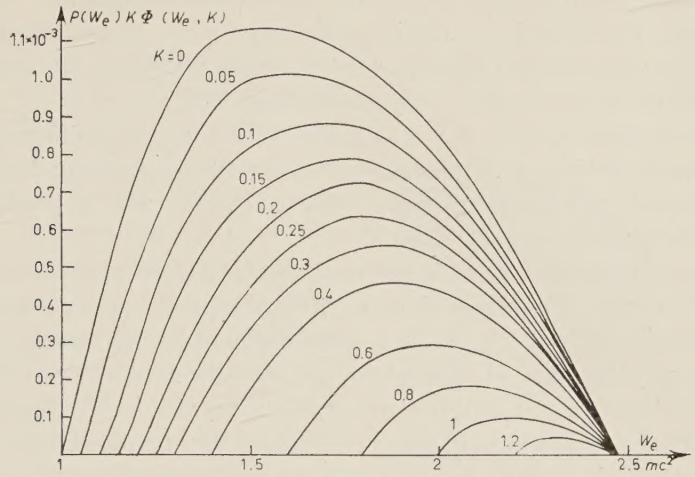

Fig. 2.

e 3, in funzione di W_e e per vari valori di K. Per integrazione grafica di tali curve si hanno i vari punti dello spettro

$$KS(K) = \int_{1+K}^{W_0} P(W_e)\cdot K\cdot \Phi(W_e, K)\,\mathrm{d}W_e\ ,$$

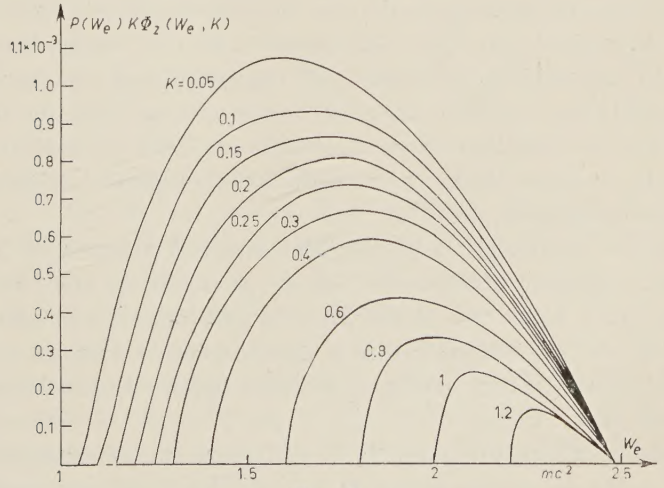

Fig. 3.

in funzione di K: energia (in unità mc^2) emessa nell'intervallo K, $K+\mathrm{d}K$, sotto forma di bremsstrahlung, per intervallo di energia mc^2.

Lo spettro di bremsstrahlung interna $S(K)$ (numero di fotoni emessi per disintegrazione e per intervallo di energia mc^2) si ottiene a partire dallo spettro $KS(K)$ dividendo ogni punto per la corrispondente energia K.

Gli spettri teorici $S(K)$ e $KS(K)$, calcolati sia con il metodo di Knipp e Uhlenbeck sia con quello di Nilsson, sono riportati rispettivamente nelle Fig. 11 e 12 in confronto con i nostri risultati sperimentali.

L'integrale dello spettro $KS(K)$ da 0 a $W_0 - 1$ dà, in unità mc^2, l'energia totale emessa sotto forma elettromagnetica, per disintegrazione: $0.309 \cdot 10^{-3}\ mc^2$ e $0.392 \cdot 10^{-3}\ mc^2$ per disintegrazione, rispettivamente per la teoria di Knipp e Uhlenbeck e per quella di Nilsson.

Nel calcolo dello spettro di bremsstrahlung associato al decadimento β non si è tenuto conto dell'influenza della bremsstrahlung interna associata alla cattura elettronica (1.5%), dovuta essenzialmente a catture K. In effetti, assumendo, per l'energia di transizione per cattura K il valore 0.335 MeV ([7]) (corrispondente a 0.250 MeV come limite superiore dell'energia W_c della bremsstrahlung di cattura), il numero di fotoni di bremsstrahlung di cattura per ogni cattura K è dato da ([8]): $(\alpha/12\pi)(W_c/mc^2)^2 = 4.65 \cdot 10^{-5}$.

Si hanno quindi, per ogni disintegrazione β circa $7 \cdot 10^{-7}$ fotoni di bremsstrahlung di cattura, mentre la bremsstrahlung associata al decadimento β è dell'ordine di 10^{-3} fotoni per disintegrazione.

3. – Determinazione sperimentale dello spettro di bremsstrahlung interna del ^{204}Tl.

Il dispositivo sperimentale è di tipo convenzionale ([4,5]) ed è mostrato in Fig. 4. S è la sorgente di $^{204}_{81}$Tl (16.5 μcurie $= 6.1 \cdot 10^5$ disintegrazioni al secondo) la cui intensità fu misurata per confronto con una sorgente tarata ($3.486 \cdot 10^3$ dis/s); una seconda sorgente meno intensa ($2.3 \cdot 10^5$ dis/s) è stata utilizzata al fine di controllare l'eventuale influenza della bremsstrahlung esterna prodotta nella sorgente stessa. L'intensità delle sorgenti è stata determinata con una approssimazione del 5%.

Il ricevitore è costituito da un cristallo di NaI(Tl) Harshaw (2 cm diam $\times$ $\times$ 2 cm spess.) connesso otticamente con il catodo di un tubo fotomoltiplicatore DuMont 6292 scelto per la stabilità del guadagno ed il basso fondo termico. L'anodo del fotomoltiplicatore è direttamente collegato, attraverso un amplificatore lineare a larga banda, ad un analizzatore di impulsi ad un canale, della « Atomic Instr. Co. ».

Un canalizzatore di Pb converge le radiazioni provenienti dalla sorgente sul cristallo sotto un angolo solido $\Omega/2\pi = 7.7 \cdot 10^{-4}$ (distanza sorgente-ricevi-

([8]) K. Siegbahn: *Beta and Gamma-ray Spectroscopy* (Amsterdam, 1955), p. 659; P. Morrison e L. Schiff: *Phys. Rev.*, **58**, 24 (1940).

tore 18.00 cm). A metà strada tra sorgente e ricevitore ed all'inizio del canalizzatore è posta una pasticca di Be (0.36 g/(cm)²) sufficiente ad assorbire completamente i raggi β del ^{204}Tl ($E_{max} = 0.760$ MeV).

La forma del canalizzatore è tale da rendere trascurabile il contributo di fotoni secondari per effetto Compton sulle pareti.

La massa di Pb che circonda completamente il ricevitore al fine di ridurre al minimo l'influenza del fondo esterno, è ricoperta, sulla superficie vista dalla sorgente, da uno spessore di plexiglass sufficiente ad assorbire i raggi β, evitando in tal modo la produzione di raggi X caratteristici e di bremsstrahlung esterna nel Pb.

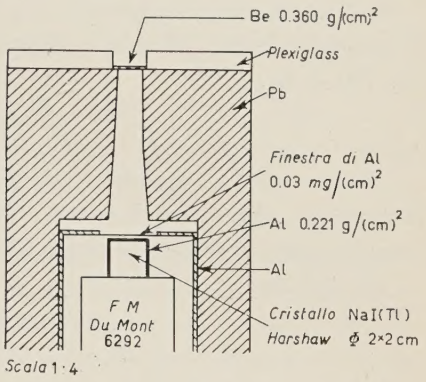

Fig. 4.

La bremsstrahlung esterna prodotta nell'assorbitore di berillio viene rivelata sotto un angolo solido $\Omega/4\pi = 3.1 \cdot 10^{-3}$. Il contributo della frazione di bremsstrahlung esterna rivelata alla bremsstrahlung interna si può valutare con un semplice calcolo approssimato.

La perdita di energia per emissione di bremsstrahlung subita da un elettrone nell'attraversare 1 cm di materiale di numero atomico Z, peso atomico A e densità ϱ è data da [9]:

$$\frac{dE}{dx} = 3.44 \cdot 10^{-4} (E + mc^2) \frac{Z^2}{A} \varrho \left[4 \ln \frac{2(E + mc^2)}{mc^2} - \frac{4}{3} \right] \frac{\text{MeV}}{\text{cm}},$$

dove E è l'energia cinetica dell'elettrone (in MeV).

Assumendo come energia media degli elettroni provenienti dal decadimento β del ^{204}Tl 0.260 MeV circa, e nell'ipotesi di una distribuzione isotropica della bremsstrahlung esterna, la frazione di energia emessa sotto forma di bremsstrahlung esterna ad elettrone assorbito in 0.2 cm di Be e rivelata sotto un angolo solido $\Omega/4\pi = 3.1 \cdot 10^{-3}$, è pari a circa $5 \cdot 10^{-7}$ MeV/elettrone.

L'energia emessa sotto forma di bremsstrahlung interna ad elettrone è al minimo (validità della teoria di Knipp e Uhlenbeck), uguale a $1.6 \cdot 10^{-4}$ MeV/elettrone; la bremsstrahlung esterna rivelata sta alla bremsstrahlung interna rivelata nel rapporto $5/1600 \simeq 3 \cdot 10^{-3}$.

[9] W. Heitler: *Quantum Theory of Radiation* (Oxford, 1948); H. Bethe e W. Heitler: *Proc. Roy. Soc.*, A **146**, 83 (1954).

Sperimentalmente la frazione di bremsstrahlung esterna rivelata è stata determinata nel modo seguente. La sorgente in istudio è stata ricoperta successivamente con assorbitori di Be e di Pb sufficienti ad arrestare completamente gli elettroni del ^{204}Tl. Il numero totale di impulsi al secondo contati nel caso dell'assorbitore di Be era pari all'88.6 % di quelli rivelati bel caso del Pb (fondo detratto).

Indicando rispettivamente con R_i, R_{Be}, R_{Pb} le intensità delle radiazioni di bremsstrahlung interna e della bremsstrahlung esterna prodotta nel Be e nel Pb, si ha:

$$(R_i + R_{Be}) = 0.886\,(R_i + R_{Pb}) .$$

D'altra parte, secondo i calcoli di BETHE e HEITLER ([9]), confermati dall'esperienza, il numero di fotoni di bremsstrahlung esterna creati da un elettrone completamente assorbito è proporzionale a $\varrho Z^2/A$; si ha quindi: $R_{Be}/R_{Pb}=1.3\cdot 10^{-2}$.

Ne risulta:

$$R_{Be}/R_i = 1.5\cdot 10^{-3}$$

a parità di angolo solido. Tenendo conto che, nelle condizioni sperimentali effettive la bremsstrahlung esterna è rivelata sotto un angolo solido 4 volte più grande, la frazione di bremsstrahlung esterna rivelata è dunque pari allo 0.6 % della bremsstrahlung interna rivelata.

In conclusione è lecito assumere che il contributo alle radiazioni rivelate dovuto a fotoni di bremsstrahlung interna è certamente inferiore all'1 % e di esso non è stato tenuto conto nei risultati sperimentali.

Lo spettrometro a scintillazione è stato tarato per le energie e per la risoluzione, e l'efficienza del cristallo è stata determinata con un metodo che si è dimostrato semplice e conveniente, e che verrà segnalato a parte. Esso consiste essenzialmente nel sostituire alla sorgente in studio una sfera di Al (scatteratore) e nel rivelare i fotoni di scattering Compton prodotti sulla sfera e nella direzione del cristallo da un fascio di raggi γ monocromatici (nel nostro caso i raggi γ di energia 662 keV provenienti da una sorgente di ^{137}Cs) fatti incidere a diversi angoli rispetto alla direzione scatteratore-cristallo. Poichè si può conoscere, in funzione dell'angolo d'incidenza, l'energia del fascio di fotoni di scattering, ciò permette di tarare lo spettrometro per sufficienti valori dell'energia (da 190 a 450 keV nel nostro caso). Altri punti di taratura sono stati ottenuti con raggi X e γ di isotopi radioattivi a schema di decadimento noto (raggi γ di 93 keV e raggi X_K di 51 keV del $^{183}_{73}$Ta; raggi γ di 279 keV del $^{203}_{81}$Hg e i raggi X_K di 69 keV provenienti dalle catture K dello stesso ^{204}Tl). In tal modo si è anche potuto controllare la validità del metodo suddetto.

La tarature ed il controllo sono stati eseguiti anche per il potere risolutivo dello spettrometro misurando la larghezza dei vari picchi fotoelettrici a metà del massimo corrispondente.

La determinazione dell'efficienza del cristallo si effettua per confronto tra l'area compresa nel picco fotoelettrico prodotto dai fotoni di scattering di una data energia e l'intensità corrispondente, calcolata secondo la formula di Klein-Nishina, purchè siano note l'intensità della sorgente di γ primari e la geometria usata.

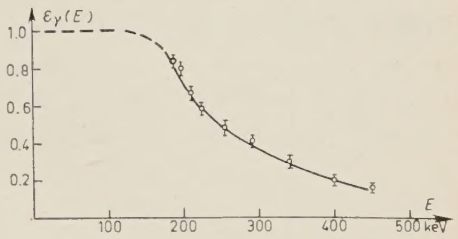

Fig. 5.

In Fig. 5 sono riportate le efficienze del cristallo usato alle varie energie e per la particolare geometria usata; ε_γ ha qui il significato di rapporto tra il numero di fotoni che dànno luogo ad impulsi fotoelettrici « contati » ed il numero corrispondente di fotoni di data energia E effettivamente incidenti sul cristallo.

I punti sperimentali sono stati ottenuti nell'intervallo di energie (190 ÷ 450) keV; la curva è stata estrapolata per energie inferiori tenendo conto che per fotoni di bassa energia (fino a circa 100 keV) e per grandi distanze sorgente-cristallo è certamente $\varepsilon_\gamma = 1$, per un cristallo di spessore 2 cm.

Lo spettro X del ^{204}Tl ottenuto sperimentalmente e corretto per il rumore di fondo (determinato rimuovendo la sorgente) è mostrato in Fig. 6; è riportato anche il picco a 69 keV, corrispondente ai raggi X_K provenienti dalle transizioni di cattura K.

Esso è stato sottratto, assumendo una distribuzione gaussiana della riga e tenendo conto della risoluzione dello spettrometro. Nella stessa Fig. 6 è riportata la distribuzione sperimentale, così ottenuta, corrispondente alla sola bremsstrahlung. Tale distribuzione è stata opportunamente corretta al fine di valutare lo spettro continuo di bremsstrahlung da confrontarsi con gli spettri teorici. Le correzioni apportate ed il procedimento usato sono riportati qui di seguito.

a) *Risoluzione dello spettrometro.* Un modo semplice per correggere lo spettro di bremsstrahlung interna tenendo conto del potere risolutivo dello spettrometro è quello segnalato da Novey [4]. Si usa la formula seguente, dovuta a Palmer e Laslett [10]:

$$N_2(E) = N_1(E) - A \cdot N_1'(E) - \tfrac{1}{2} A N_1''(E) \cdot E \,,$$

dove $N_2(E)$ è lo spettro corretto per la risoluzione; $N_1(E)$, $N_1'(E)$, $N_1''(E)$ sono rispettivamente lo spettro sperimentale e le sue derivate prima e seconda. A è dato dalla relazione:

$$A = 0.181\,(\Delta E)^2/E \,,$$

[10] J. P. Palmer e L. J. Laslett: *AEC Report AECU*-1220, 14 (1951).

essendo ΔE la larghezza, a metà del massimo, della riga fotoelettrica prodotta dai fotoni di energia E. Le correzioni così ottenute variano dallo 0.1% all'8% circa nell'intervallo di energia compreso tra 80 e 400 keV, in cui lo spettro sperimentale è stato determinato. L'approssimazione con cui tali correzioni si possono ottenere è del 3% circa.

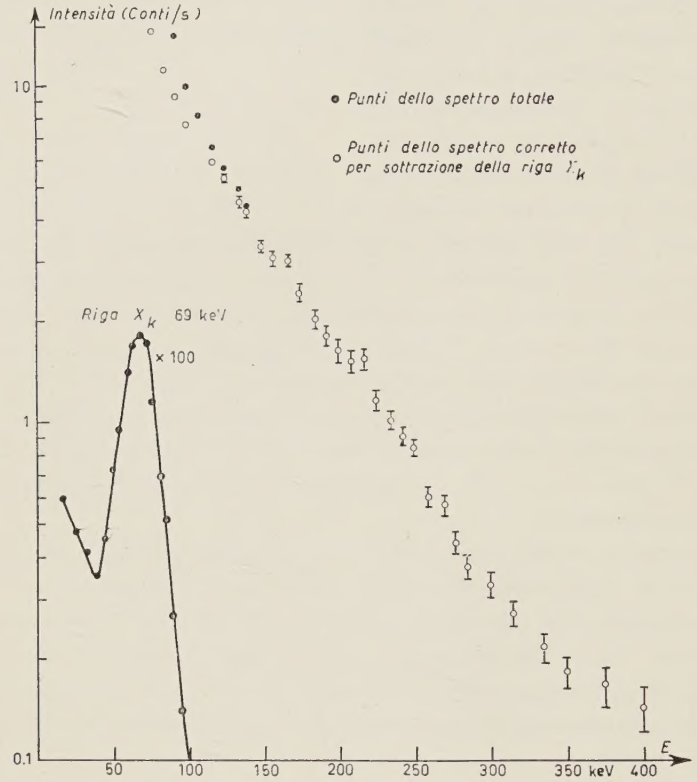

Fig. 6.

b) *Assorbimento.* Il fattore di assorbimento C per fotoni in 0.360 g/(cm)^2 di Be (assorbitore dei β) e in 0.221 g/(cm)^2 di Al (finestra del contatore e rivestimento del cristallo) è stato calcolato a partire dai coefficienti di assorbimento totali tabulati da C. M. Davisson ([11]). Esso è riportato in Fig. 7; nell'intervallo di energia da noi considerato l'accuratezza con cui il fattore C può essere calcolato è dell'1% ([11]).

([11]) P. M. Davisson: K. Siegbahn, *Beta and Gamma-ray Spectroscopy* (Amsterdam, 1955), p. 85.

Lo spettro corretto per l'assorbimento è dato quindi da:

$$N_3(E) = C N_2(E) .$$

c) Impulsi dovuti alle distribuzioni Compton. Se $N_f(E)\,\mathrm{d}E$ è il numero di impulsi (al secondo) prodotti nell'intervallo di energia $(E,\ E+\mathrm{d}E)$ da fotoni di energia compresa tra E e $E+\mathrm{d}E$, per assorbimento fotoelettrico, ad essi si sovrappongono un certo numero $N_c(E)\,\mathrm{d}E$ di impulsi di uguale energia dovuti alle distribuzioni Compton prodotte da fotoni incidenti di energia più elevata. La frazione Compton per ogni picco fotoelettrico di energia E_γ è stata determinata usando lo stesso metodo descritto per la determinazione delle efficienze ε_γ, nell'intervallo $190 < E < 450$ keV; il rapporto tra l'area $S_c(E_\gamma)$ della banda Compton e l'area $S_f(E_\gamma)$ del picco fotoelettrico corrispondente, misurati sperimentalmente, dà la frazione Compton $N_c(E_\gamma)/N_f(E_\gamma)$. Per energie superiori a 450 keV la curva è stata estrapolata tenuto conto del punto sperimentale a 662 keV, determinato misurando lo spettro γ di una sorgente di ^{137}Cs.

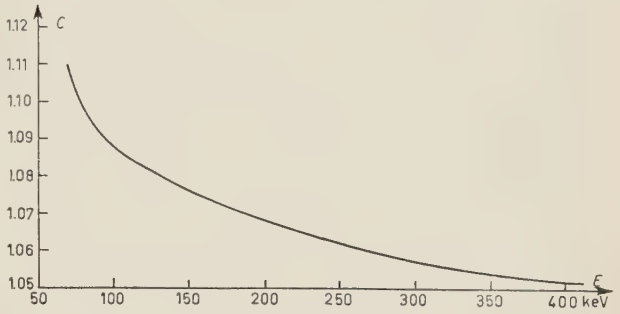

Fig. 7.

L'energia massima $E_c(E_\gamma)$ della distribuzione Compton dovuta a fotoni di energia primaria E_γ viene ad essere compresa tra 80 keV e 450 keV per E_γ compreso nell'intervallo (190 ÷ 662) keV; poichè lo spettro sperimentale è stato ottenuto fino a 400 keV circa, data la rapidità con cui decresce l'intensità dei fotoni di bremsstrahlung, il contributo Compton dovuto ai fotoni di energia compresa tra 400 e 662 keV è stato calcolato in prima approssimazione, estrapolando lo spettro sperimentale fino a 662 keV; per energie superiori il contributo Compton è stato trascurato. Tali approssimazioni non possono comunque contribuire in maniera importante, essendo l'intensità dei fotoni, a tale energia, molto piccola. Già il contributo Compton dei fotoni di 400 keV agli impulsi contati nell'intervallo di energia tra 80 e 120 keV è inferiore allo 0.1 %.

Lo spettro $N_3(E)$ è stato suddiviso in intervalli ΔE uguali alla larghezza del canale usata, considerando ciascuno dei rettangoli di base ΔE e di altezza $N_f(E)$ come un picco fotoelettrico di area $N_f(E)\Delta E$. Il continuo Compton corrispondente a fotoni di energia primaria compresa tra E_γ e $E_\gamma+\Delta E$ e che indicheremo con $N_c(E_\gamma)\Delta E$, si può approssimare, con sufficiente accuratezza ([12]),

([12]) K. Lidèn e N. Starfelt: *Ark. f. Fys.*, **7**, 36, 450 (1953).

con un rettangolo di base $E_C(E_\gamma)$ e di altezza $N_C(E_\gamma)\Delta E/E_C(E_\gamma)$, estendentesi da zero a $E_C(E_\gamma)$.

Tale distribuzione contribuisce al numero di impulsi compresi nell'intervallo $(E, E+\Delta E)$ con la frazione:

$$N_C(E)\Delta E = \frac{N_C(E_\gamma)}{E_C(E_\gamma)}(\Delta E)^2 ,$$

per $E \leqslant E_C(E_\gamma)$.

Il contributo totale agli impulsi compresi nell'intervallo $(E, E+\Delta E)$, dovuto a tutte le distribuzioni Compton provenienti da fotoni di energia primaria E_γ, tale che $E_C(E_\gamma) \geqslant E$, si ottiene sommando tutte le frazioni $N_C(E)\Delta E$ corrispondenti. Il contributo Compton $N_{C_{tot}}(E)/N_f(E)$ agli impulsi fotoelettrici di energia E è quindi dato da:

$$\frac{N_{C_{tot}}(E)}{N_f(E)} = \sum \frac{N_C(E_\gamma)\Delta E}{E_C(E_\gamma)} \cdot \frac{1}{N_f(E)} .$$

In Fig. 8 è mostrato il grafico di $N_{C_{tot}}(E)/N_f(E)$ così ottenuto.

Lo spettro corretto per le distribuzioni Compton è dato da:

$$N_4(E) = N_3(E)\cdot\{1 - [N_{C_{tot}}(E)/N_f(E)]\} .$$

È possibile determinare il rapporto $N_{C_{tot}}(E)/N_f(E)$ con una approssimazione dell'ordine del 10%; l'errore corrispondente nella determinazione di $N_4(E)$ è, in generale, inferiore allo 0.3%.

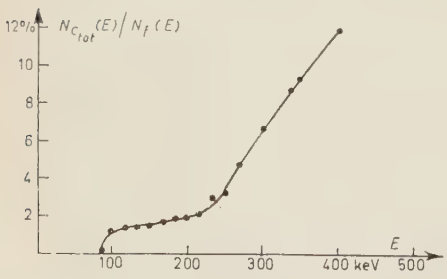

Fig. 8.

d) Backscattering. Si è proceduto in modo analogo al precedente. L'energia $E_B(E_\gamma)$ del picco di backscattering dovuto a fotoni di energia primaria E_γ varia da 80 keV a 185 keV per E_γ compreso tra 120 e 760 keV (limite massimo dello spettro di bremsstrahlung). Per energie superiori a 185 keV, quindi, il contributo di backscattering è nullo e per energie inferiori a 80 keV non ha interesse nel nostro caso.

Il rapporto $N_B(E_\gamma)/N_f(E_\gamma)$ tra il numero di impulsi di backscattering ed il numero di impulsi fotoelettrici prodotti da fotoni di energia primaria E_γ è stato ottenuto sperimentalmente come in *c*).

Ad ognuno dei picchi $N_f(E)\Delta E$, per $E \leqslant 185$ keV, contribuisce un picco di backscattering $N_B(E_\gamma)\Delta E$, per E_γ tale che $E_B(E_\gamma)$ cada nell'intervallo

$(E, E+\Delta E)$. In Fig. 9 è mostrato il rapporto $N_B(E)/N_f(E)$ che così si ottiene e che dà la frazione di impulsi di backscattering che si sovrappongono agli impulsi fotoelettrici di energia E.

Si ha allora per lo spettro corretto del contributo di backscattering:

$$N_5(E) = N_4(E) \cdot \{1 - [N_B(E)/N_f(E)]\} .$$

L'errore apportato dal computo dell'effetto di backscattering è dello 0.1 %.

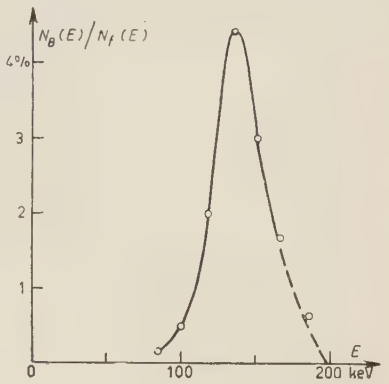

Fig. 9.

e) «*Escape*» *dei raggi* X_K *dello Iodio.* La correzione è stata fatta seguendo il metodo suggerito da LIDÈN e STARFELT [12]. Se $N_6(E)$ è lo spettro corretto per l'effetto di «escape», si ha:

$$N_6(E) = \frac{N_5(E) - N_6(E + E_K)F(E + E_K)}{1 - F(E)} ,$$

dove E_K è il valor medio delle energie dei raggi X_K dello iodio (~ 30 keV); $F(E)$ è il numero totale di fotoni di « escape » per impulso nel picco fotoelettrico di energia E.

Il calcolo di $F(E)$ è stato eseguito tenendo conto degli effetti di « escape » attraverso le superficie superiore, inferiore e laterale del cristallo e dell'assorbimento fotoelettrico di fotoni secondari generati nel cristallo [12]. $F(E)$ è mostrato in Fig. 10 in funzione di E.

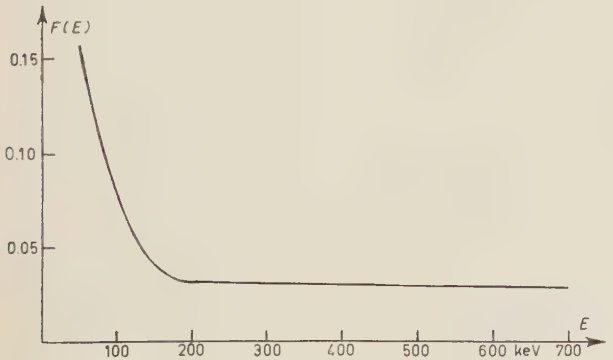

Fig. 10.

f) *Efficienza di rivelazione* γ. Se $\varepsilon_\gamma(E)$ è l'efficienza effettiva del cristallo per fotoni di energia E, definita e misurata come precedentemente descritto, si ha:

$$N_7(E) = N_6(E)/\varepsilon_\gamma(E) .$$

L'approssimazione con cui $\varepsilon_\gamma(E)$ è stato determinato e con cui, quindi, contribuisce al computo di $N_7(E)$ è del 5 % circa.

g) *Fattore geometrico e intensità della sorgente.* Lo spettro $N_7(E)$ è stato finalmente corretto per l'angolo solido di rivelazione, moltiplicando per $G = 1.3 \cdot 10^3$, e normalizzato a radiazioni per disintegrazione β dividendo per

l'intensità della sorgente I, ottenendo:

$$N_8(E) = (G/I)\, N_7(E)\,.$$

L'errore percentuale dovuto a G e I è del 6%.

Infine dallo spettro $N_8(E)$ si risale allo spettro $S(K)$ sperimentale normalizzando a intervalli di energia in unità mc^2.

In Fig. 11 e 12 rispettivamente sono riportati i punti sperimentali relativi agli spettri $S(K)$ e $KS(K)$ in confronto con le distribuzioni teoriche.

4. – Conclusioni.

Come si vede dalle Fig. 11 e 12, nell'intervallo di energie considerato ($(0.15 \div 0.78)$ mc^2) l'eccesso di fotoni rispetto alla curva di Knipp e Uhlenbeck è

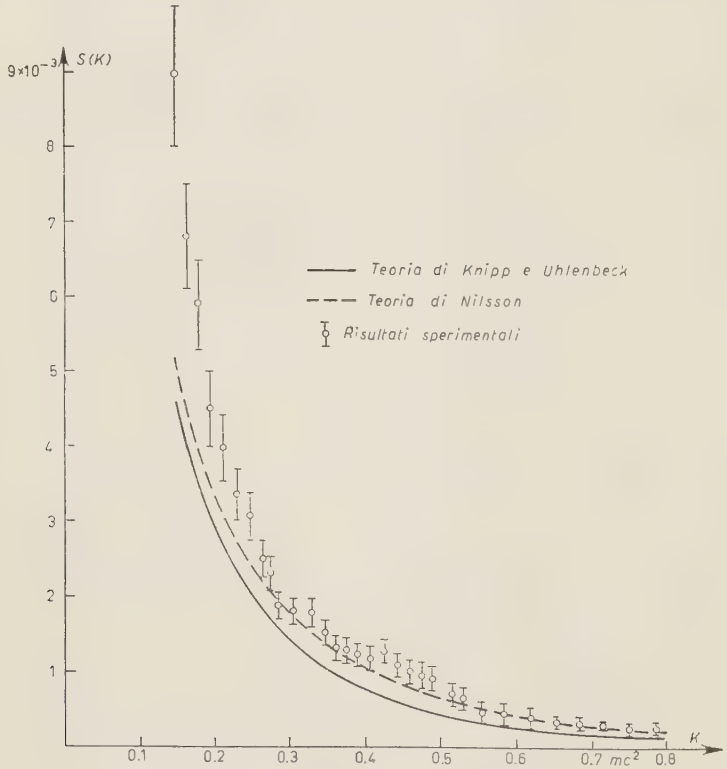

Fig. 11.

evidente, mentre, nei limiti degli errori sperimentali, vi è soddisfacente accordo con la curva corretta per l'effetto coulombiano del nucleo, fino ad energie non

inferiori a 0.28 mc^2 (145 keV). Tale accordo viene a mancare nettamente per le energie più basse, dimostrando anche, nel caso del ^{204}Tl, l'insufficienza della correzione coulombiana almeno nell'approssimazione di Nilsson. Tale risultato sembra quindi in accordo con quelli di STARFELT e coll. e di LANGEVIN-JOLIOT

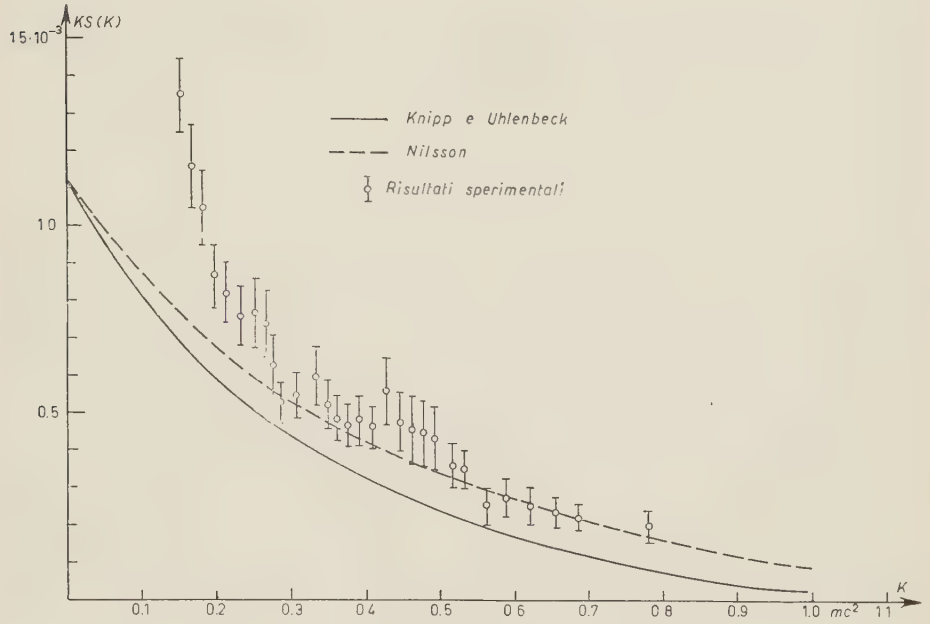

Fig. 12.

relativi a nuclei come il ^{143}Pr e il ^{147}Pm. Anche in questi casi si tratta di spettri proibiti, sebbene a forma permessa; per il ^{204}Tl da noi preso in esame lo spettro β ha energia massima compresa tra le energie massime degli spettri suddetti (225 keV per il ^{147}Pm e 922 keV per il ^{147}Pr), ed è del tipo proibito con forma proibita. Se si tiene conto che anche le correzioni coulombiane nell'approssimazione di Nilsson sono calcolate per spettri permessi, non si può escludere, sulla base dei nostri risultati una influenza del tipo della disintegrazione β sulla distribuzione della bremsstrahlung interna, oltre che del campo coulombiano del nucleo.

Nell'intervallo di energie, da noi considerato ((80 ÷ 400) keV) il numero di fotoni di bremsstrahlung emessi a disintegrazione è pari a $(1.0 \pm 0.1) \cdot 10^{-3}$, mentre la teoria di Knipp e Uhlenbeck prevede una intensità di $0.637 \cdot 10^{-3}$ fotoni a disintegrazione e quella di Nilsson $0.789 \cdot 10^{-3}$ fotoni a disintegrazione.

* * *

L'autore intende esprimere il proprio ringraziamento al prof. E. PERUCCA per il gradito interessamento.

SUMMARY

The experimental distribution of the internal bremsstrahlung in the case of ^{204}Tl β-decay has been measured, with the help of a γ scintillation spectrometer. The method used in calibrating the experimental apparatus and in evaluating the « true » experimental spectrum is reported. In the energy interval considered $((80 \div 400)$ keV) the experimental distribution has been compared with the theoretical spectra calculated on the basis of the method developed by Knipp and Uhlenbeck and of the Nilsson method, which take into account, in first approximation, the influence of the Coulomb field of the nucleus. The experimental results are in disagreement with the Knipp and Uhlenbeck distribution and agree well with the Nilsson corrected distribution up to a lower limit of about 150 keV, showing, in our case, the importance of the nuclear Coulomb field. Nevertheless, for energies lower than 150 keV, also the corrected theoretical spectrum is unsatisfactory; the excess of photons in the lower part of the experimental spectrum is the outstanding feature of the ^{204}Tl internal bremsstrahlung. This seems to be in agreement with the results of STARFELT and co-workers, and LANGEVIN-JOLIOT, for other nuclides. Owing to the fact that the Nilsson theoretical distribution is calculated for allowed transition only, the influence of the β spectrum shape (« unique first forbidden » in the case of ^{204}Tl) cannot be excluded. Between 80 and 400 keV an intensity of $(1.0 \pm 0.1) \cdot 10^{-3}$ photons per disintegration has been found; the predicted intensities are $0.637 \cdot 10^{-3}$ and $0.789 \cdot 10^{-3}$ photons per disintegration, for the Knipp and Uhlenbeck theory and for the Nilsson corrected theory, respectively.

Überprüfung der allgemeinen Relativitätstheorie durch Erdsatelliten (*).

F. Winterberg

Gesellschaft für Kern-Energie - Hamburg (+)

(ricevuto il 1° Novembre 1957)

Zusammenfassung. — Die Schaffung künstlicher Satelliten bringt eine Reihe von Möglichkeiten zur Überprüfung der allgemeinen Relativitätstheorie. Mit den bisherigen Nachweismöglichkeiten als gleichwertig anzusehen sind bei küntlichen Satelliten die Periheldrehung und die Rotverschiebung. Die relativistische Periheldrehung wird durch eine von der Erdabplattung herrührende viel größere Periheldrehung überlagert und daher schwer erfaßbar. Bei der Rotverschiebung muß der Einfluß der Eigenbewegung des Satelliten mitberücksichtigt werden. Wegen der geringen Größe der Rotverschiebung ist ein Nachweis durch Messung der Spektrallinien-Verschiebung ausgeschlossen. Es ist aber möglich, durch Vergleich des Ganges von Atomuhren auf Erde und Satellit diese Rotverschiebung zeitlich direkt zu messen. Für die Zweistundenbahn beträgt diese Zeitverschiebung jährlich $4.1 \cdot 10^{-3}$ s. Eine weitere Folgerung der allgemeinen Relativitätstheorie besteht in der Änderung der Lichtgeschwindigkeit in Abhängigkeit vom Gravitationspotential. Der Effekt ist aber so klein, daß er nicht meßbar ist. Schließlich hat die Erdrotation relativistische Folgerungen, die nicht mehr zu vernachlässigen sind. Die Erdrotation erzeugt nach der allgemeinen Relativitätstheorie ein zusätzliches Gravitationsfeld. Dieses zusätzliche Gravitationsfeld führt zu einer zusätzlichen relativistischen Periheldrehung sowie zu einem Vorrücken der Knoten der Satellitenbahn. Das jährliche Vorrücken der Knotenlinie beträgt für eine Zweistundensatellitenbahn $0.13''$. Die genannten relativistischen Bahnstörungen sind mit astronomischen Methoden und mit Radar nachweisbar.

(*) Vortrag gehalten auf der Physikertagung zu Heidelberg am 30. September 1957.

(+) Gesellschaft für Kern-Energie, Forschungsreaktor Geesthacht bei Hamburg, Geesthacht.

1. – Einleitung.

Es gibt drei klassische Überprüfungsmöglichkeiten der allgemeinen Relativitätstheorie. Diese drei Überprüfungsmöglichkeiten beruhen auf der Nachweisbarkeit von drei beobachtbaren Effekten. Alle drei Effekte werden aus den bei Kugelsymmetrie vorliegenden Lösungen der Einstein'schen Feldgleichungen abgeleitet. Diese kugelsymmetrische Lösung ist bekanntlich durch das Schwarzschild'sche Linienelement

$$(1) \qquad ds^2 = \frac{dr^2}{1-(2\alpha/r)} + r^2(d\vartheta^2 + \sin^2\vartheta\, d\varphi^2) - c^2\left(1-\frac{2\alpha}{r}\right)dt^2 ,$$

gegeben, wo $\alpha = GM/c^2$ der Gravitationsradius ist mit der Gravitationskonstanten G, der Masse M und der Lichtgeschwindigkeit c.

Nimmt man als ein in der Natur vorliegendes Beispiel das kugelsymmetrische Gravitationsfeld der Sonne an, so liegen die drei genannten Effekte innerhalb der Nachweismöglichkeit der Meßinstrumente.

Die Effekte sind der Reihe nach als Rotverschiebung, Lichtablenkung am Sonnenrand und Periheldrehung eines Planeten bekannt.

Von allen drei Effekten ist die Rotverschiebung bei der Sonne in dem theoretisch geforderten Umfang nur am Rand beobachtet worden und muß in der Mitte durch irgend einen anderen entgegengesetzt wirkenden Effekt überlagert werden. Dagegen hat man den in Frage stehenden Effekt bei weissen Zwergtsternen beobachtet, ohne jedoch wegen der Unsicherheit der Kenntnis des Gravitationspotentials an deren Oberfläche zu einer quantitativ genauen Aussage über die Größe der Rotverschiebung zu gelangen. Der Rotverschiebungseffekt darf auch nicht als ein entscheidender Beleg für die Richtigkeit der Theorie betrachtet werden, da er eine unmittelbare Folge des Energiesatzes ist und somit auch aus anderen Vorstellungen wie z.B. aus der Photonentheorie abgeleitet werden kann. Diesen drei Effekten gesellt sich noch zusätzlich ein vierter Effekt hinzu, dessen Messung bisher nicht möglich war, und der sich in einer Abhängigkeit der Lichtgeschwindigkeit vom Gravitationspotential äußert. Dieser Effekt besagt, daß die Lichtgeschwindigkeit mit wachsendem Gravitationspotential abnimmt.

2. – Die Überprüfung der Theorie durch Erdsatelliten.

Es soll jetzt auf die Verhältnisse eingegangen werden, die bei künstlichen Erdsatelliten vorliegen.

Wie im Fall der Sonne bildet die Erde ein nahezu kugelsymmetrisches Feld, für das die Schwarzschild'sche Lösung zuständig ist.

Darüberhinaus treten aber im Rahmen der allgemeinen Relativitätstheorie Abweichungen von der Schwarzschild'schen Lösung auf, die in der nicht mehr zu vernachlässigenden Rotation des Zentralkörpers liegen. Wegen der Bedeutung der Gravitation für den Rahmen einer zukünftigen Theorie der Elementarteilchen wird es besonders wichtig sein, die Theorie im größeren Umfang als bisher einer Prüfung zu unterziehen. Als besonders bedeutungsvoll scheint es zu sein, daß die Schaffung von Erdsatelliten die Möglichkeit gibt, die Theorie über den Rahmen der Schwarzschild'schen Lösung hinaus zu überprüfen.

3. – Satellitentests.

Beschränken wir uns zunächst auf die beobachtbaren Folgerungen aus der Schwarzschild'schen Lösung. Im Vergleich zu den an der Sonne untersuchten drei Effekten stehen bei Erdsatelliten vorläufig nur die Periheldrehung und die Rotverschiebung als nachweisbar in Aussicht. Die Lichtablenkung ist zu gering, als daß sie erfaßbar ist. Dasselbe gilt für die Messung der Änderung der Lichtgeschwindigkeit in Abhängigkeit vom Gravitationspotential.

Dagegen bringt der Einfluß der Erdrotation weitere Bahnstörungen, deren Nachweis zur Überprüfung der Theorie herangezogen werden kann. Diese zusätzlichen Bahnstörungen haben den Charakter einer Periheldrehung und einer Knotenbewegung.

4. – Relativistische Drehung des Satellitenperigäums ohne Berücksichtigung der Erdrotation.

Eine Prüfung der allgemeinen Relativitätstheorie durch Bestimmung des Vorausschreitens eines Satellitänperigäums ist zuerst von L. La Paz [1] vorgeschlagen worden. Unter Vernachlässigung der Erdrotation beträgt die Größe dieser Drehung für eine nahezu kreisförmige Bahn nach Einstein:

$$\delta\omega = \frac{3\alpha}{a} v \,. \tag{2}$$

In Gleichung (2) bedeutet a die große Achse der Satellitenbahn und v die wahre Anomalie. Dabei gilt für eine kreisförmige Bahn:

$$v = nt = c\sqrt{\frac{\alpha}{a^3}}\, t \,. \tag{3}$$

[1] L. La Paz: *Publs. Astron. Soc. Pacific*, **66**, 13 (1954).

Wählt man eine Satellitenbahn, die nach zwei Stunden durchlaufen ist, so erhält man als Wert der großen Achse

$$a = 8060 \text{ (km)} .$$

Mit dem Wert des Erdradius $R = 6370$ km beträgt die Höhe dieser sog. «Zweistundenbahn» 1690 km. Für diese Zweistundenbahn berechnet man eine jährliche Perigäumsdrehung von

$$\delta\omega = 8.54'' \qquad \text{pro Jahr.}$$

Dieser Effekt ist so groß, daß er sich ohne Schwierigkeiten messen läßt. Leider ist aber die Erde keineswegs mehr kugelförmig, sondern leicht abgeplattet. Diese Abplattung führt zu einer viel größeren Perigäumsdrehung als die relativistische. Wir kommen darauf weiter unten noch zurück.

5. – Die Rotverschiebung.

Als zweiter nachweisbarer Effekt soll jetzt die Rotverschiebung untersucht werden.

Im Gegensatz zur Sonne ist dieser Effekt bei der Erde so klein, daß nicht an eine Messung mit spektroskopischen Methoden zu denken ist.

Dagegen wurde jedoch in zwei früheren Veröffentlichungen ([2,3]) gezeigt, daß der in Frage stehende Effekt sich durch Vergleich von zwei Atomuhren, die auf Satellit und Erde synchron laufen, direkt als Zeitverschiebung nachweisen läßt. Die dabei auftretende Zeitverschiebung ist im Vergleich zu der bekannten Rotverschiebung jedoch einer Modifikation zu unterziehen. Diese Modifikation ergibt sich aus der Notwendigkeit, die nicht mehr vernachlässigbare Eigenbewegung des Satelliten mitzuberücksichtigen.

Diese Mitberücksichtigung führt nach der Theorie zu einem Ergebnis, das sich anschaulich als eine Überlagerung der Einstein'schen Schwererotverschiebung und dem der Einstein'schen Zeitdilatation äquivalenten transversalen Dopplereffekt eines bewegten Körpers deuten läßt. Für eine bestimmte Höhe der Satellitenbahn über der Erdoberfläche kompensieren sich beide Effekte zu null. Die Schwerkraft bringt für den Erdbeobachter eine Blauverschiebung, die Eigenbewegung des Satelliten eine Rotverschiebung der Satellitenhur gegenüber der Erduhr. Die Blauverschiebung bedeutet ein Vorgehen, die Rotverschiebung ein Nachgehen der Satellitenuhr gegenüber der Uhr des

---

([2]) F. WINTERBERG: *Astronautica Acta*, **2**, 25 (1956).

([3]) S. F. SINGER: *Phys. Rev.*, **104**, 11 (1956).

Erdbeobachters. In den zitierten Arbeiten wird für die Größe der Zeitverschiebung einer kreisförmigen Satellitenbahn der Ausdruck abgeleitet (R ist der Erdradius):

$$\frac{\delta t}{t} = \alpha\left[\frac{1}{R} - \frac{3}{2}\frac{1}{a}\right]. \tag{4}$$

Aus Gleichung (4) entnimmt man, daß δt für $a = (3/2)R$ verschwindet. Zerlegt man (4) in die Form

$$\frac{\delta t}{t} = \alpha\left[\frac{1}{R} - \frac{1}{a}\right] \quad \frac{\alpha}{2}\frac{1}{a}, \tag{4a}$$

so entspricht das erste Glied auf der rechten Seite von (4a) der Schwererotverschiebung, das zweite Glied der Zeitdilatation.

Für die Zweistundenbahn folgt als Zeitverschiebung

$$\frac{\delta t}{t} = -1.3 \cdot 10^{-10}.$$

Im Laufe eines Jahres geht die Satellitenuhr gegenüber den Erduhren um den Betrag

$$\delta t = -4{,}1 \cdot 10^{-3}\,\mathrm{s}$$

nach.

Atomuhren laufen mit einer sehr großen Genauigkeit. Caesiumuhren haben eine Genauigkeit von $\Delta t/t = 10^{-12}$. Solche Uhren sind daher geeignet, den Effekt mit großer Präzision zu messen, im Laufe eines Jahres mit einer Genauigkeit von vielen Zehnerpotenzen.

Das größte Hindernis, das einer Überprüfung der Theorie mit Atomuhren im Wege steht, ist in der technischen Schwierigkeit, eine Atomuhr in einen künstlichen Satelliten einzubauen zu sehen. Im Hinblick auf die ungenügende Überprüfung der Rotverschiebung würde sich aber ein solcher Aufwand rechtfertigen lassen.

Darüberhinaus hat der hier vorgeschlagenen Weg zur Überprüfung der Rotverschiebung eine gewisse grundsätzliche Bedeutung. Der Atomuhrtest ist nämlich ein integraler Effekt im Gegensatz zum differentiellen Effekt der Spektrallinienverschiebung. Er läßt sich daher nicht wie die Spektrallinienverschiebung auch aus einer Photonentheorie unter Zugrundelegung der speziellen Relativitätstheorie ableiten. Er kann im übrigen auch durch die relativistische Massenveränderung der schwingenden Atome im Schwerefeld gedeutet werden.

6. – Die Lichtablenkung.

Die Lichtablenkung im Gravitationsfeld der Erde ist so klein, daß an einen Nachweis nicht zu denken ist.

Nach Einstein beträgt die gesamte Lichtablenkung eines den Himmelskörper vom Radius R tangierenden Strahls:

$$\delta\psi = \frac{4\alpha}{R} . \tag{5}$$

Für die Erde ist die Größe dieser Ablenkung:

$$\delta\psi = 5.8 \cdot 10^{-4''}$$

also weit unterhalb der Nachweismöglichkeit.

7. Änderung der Lichtgeschwindigkeit in Abhängigkeit vom Gravitationspotential.

Nach der allgemeinen Relativitätstheorie geschieht die Ausbreitung des Lichts nach der Gleichung $ds = 0$.

Die Lichtgeschwindigkeit beträgt danach z.B. in radialer Richtung nach Gleichung (1):

$$\frac{dr}{dt} = \left(1 - \frac{2\alpha}{r}\right) \cdot c . \tag{6}$$

Da die Frequenz für jeden Beobachter als feststehendes Zeitmaß konstant anzusehen ist, folgt aus der Änderung der Lichtgeschwindigkeit eine Änderung der Wellenlänge wegen $c = \lambda\nu$ zu

$$\frac{\delta\lambda}{\lambda} = \frac{2\alpha}{r} . \tag{7}$$

Als Änderung der Wellenlänge zwischen Satellit und Erde erhält man:

$$\frac{\delta\lambda}{\lambda} = 2\alpha\left[\frac{1}{R} - \frac{1}{a}\right] . \tag{8}$$

Dieser Wert beträgt für die Zweistundenbahn:

$$\frac{\delta\lambda}{\lambda} = 2.9 \cdot 10^{-10} .$$

Nachweisbar müßte der Effekt sein durch Mitnahme eines Interferometers auf den Satelliten und Beobachtung der Änderung des Interferenzbildes. Heute übliche Interferometer haben aber höchstens eine Genauigkeit von

$$\frac{\Delta\lambda}{\lambda} \simeq 10^{-6}.$$

Es besteht daher kaum eine Aussicht, den Effekt nachzuweisen.

8. – Der Einfluß der Erdrotation.

Die Schwarzschild'sche Lösung vernachlässigt die Tatsache, daß sich der in Frage kommende Zentralkörper in Rotation befindet. Die Rotation führt zu Beiträgen im Energieimpulstensor, die ihrerseits zu Zusatzgliedern im metrischen Fundamentaltensor nach Lösung der Feldgleichungen Anlaß geben müssen. Die hier sich anschließenden Folgerungen gehen daher ihrem Gehalt nach über den Rahmen der Schwarzschild'schen Lösung hinaus.

Bekanntlich kann nach der allgemeinen Relativitätstheorie die Wirkung der Zentrifugal- und Corioliskraft als durch Umwälzen des gesamten Universums um einen festen Punkt hervorgebracht gedacht werden. Dasselbe gilt für die Trägheitskraft, die durch relative Beschleunigung des gesamten Universums auftritt. Andererseits sagt die Theorie voraus und wurde bereits durch Einstein gezeigt, daß durch relative Beschleunigung jeder Materie, die nicht notwendig das ganze Universum umfassen muß, eine Kraft auftritt, die der Trägheitskraft analog ist. Quantitativ wird die Kraft im Allgemeinen aber viel kleiner sein als die von der Beschleunigung der Gesamtheit aller Sterne herrührende Trägheitskraft. Das für die Trägheitskraft Gesagte überträgt sich sinngemäß auf die Zentrifugal- und Corioliskraft.

Wie THIRRING ([4]) gezeigt hat, tritt nach der allgemeinen Relativitätstheorie ein dem Zentrifugal- und Corioliskraftfeld analoges Feld im Innern einer mit Masse belegten rotierenden Hohlkugel auf.

Andererseits muß auch bei einer rotierenden Vollkugel zusätzlich zum üblichen Schwerefeld ein dem Coriolis- und Zentrifugalkraftfeld ähnliches Feld auftreten. Der Fall einer rotierenden Vollkugel ist bei der Erde gegeben. In einer Arbeit von LENSE und THIRRING ([5]) werden die von der Rotation des Zentralkörpers herrührenden relativistischen Bahnstörungen für den Fall der Jupitermonde angegeben. Die Autoren kommen zu dem Ergebnis, daß die Störungen bei Jupiter so klein sind, daß es praktisch ausgeschlossen ist, sie von der Erde aus zu beobachten. Anders verhält es sich bei dem Problem

([4]) H. THIRRING: *Phys. Zeits.*, **19**, 33 (1918).
([5]) I. LENSE und H. THIRRING: *Phys. Zeits.*, **19**, 156 (1918).

der Bahnstörungen eines Erdsatelliten. Die Störungen sind im Fall der Erde so groß, daß sie einer Beobachtbarkeit gerade noch zugänglich werden. Das sich aus der Arbeit von LENSE und THIRRING ergebende Linienelement hat in sphärischen Polarkoordinaten die Gestalt:

$$(9) \qquad ds^2 = \frac{dr^2}{1-(2\alpha/r)} + r^2(d\vartheta^2 + \sin^2\vartheta\, d\varphi^2) - \frac{8\alpha R^2\omega \sin^2\vartheta}{5r}\, dt\, d\varphi - c^2\left(1-\frac{2\alpha}{r}\right)dt^2 .$$

Im Linienelement (9) ist ω die Winkelgeschwindigkeit der Erdrotation. Die sich aus der Erdrotation ergebenden neu hinzukommenden Bahnstörungen sind dann den Störungen der Einstein'schen Merkurarbeit, der das Schwarzschild'sche Linienelement zugrundeliegt zu überlagern.

9. Die relativistische Drehung des Satellitenperigäums unter Berücksichtigung der Erdrotation.

Die Erdrotation führt zu einer zusätzlichen Drehung des Satellitenperigäums vom Betrag:

$$(10) \qquad \delta\omega = -\frac{8\alpha\omega R^2}{5na^3}\left|1 \quad 3\sin^2\left(\frac{i}{2}\right)\right|\cdot r .$$

In Gleichung (10) ist i die Neigung der Bahn gegen die Aequatorebene. Für eine über den Pol gelegte Zweistundenbahn z.B. erhält man eine jährliche Perigäumsdrehung von

$$\delta\omega = 0.13'' \qquad \text{pro Jahr.}$$

Die gesamte relativistische Perigäumsdrehung ergibt sich dann durch Addition dieses Betrags zum Einstein'schen zu

$$\delta\omega = 9.07'' \qquad \text{pro Jahr.}$$

10. Das durch die Erdrotation verursachte relativistische Vorrücken der Knoten.

Die Erdrotation führt zu einer Störung der Bahn, die in einem Vorrücken der Knoten besteht, welche die Satellitenbahn mit der Äequatorebene bildet.

Diese relativistische Störung beträgt:

$$(11) \qquad \delta\Omega = \frac{4\alpha\omega R^2}{5na^3}\, v .$$

Für die Zweistundenbahn ergibt sich daraus ein jährliches Vorrücken der Knoten wom Betrag

$$\delta\Omega = 0.13'' \qquad \text{pro Jahr.}$$

Diese Art einer relativistischen Störung ist für den Einfluß der Erdrotation auf das Gravitationsfeld charakteristisch und fehlt bei der Schwarzschild'schen Lösung (*).

11. – Ortung der Bahn durch Radarinterferometer.

Um die genannten Bahnstörungen zu bestimmen, sind genaueste Ortsbestimmungen der Satellitenbahn erforderlich. Der Wert von 0.1″ bedeutet bereits auf der Erdoberfläche eine Entfernung von etwa nur 3 m. Der Satellit sollte danach bis möglichst auf 1 m genau in seiner Bahn bestimmt werden. Zu diesem Zweck werden sich Vorrichtungen eignen, die man als Radarinterferometer bezeichnen kann. Zwei Radarstationen legen als Fläche konstanter Wellenlängendifferenz eine räumliches Hyperboloid fest. Drei Radarstationen legen paarweise je eine solche Fläche fest. Alle drei Flächen schneiden sich in einen Punkt. Drei Stationen genügen daher bereits zur örtlichen Fixierung eines Satelliten zu einen bestimmten Zeitpunkt mit der örtlichen Genauigkeit von einer Wellenlänge. Technisch dürfte allerdings eine solches Verfahren wegen des benötigen Aufwandes nicht ohne Schwierigkeiten sein. Immerhin ist eine große Präzision in der Bahnbestimmung mit solchen Mitteln zu erwarten.

12. – Einfluß der Erdrotation auf den Uhrengang.

In der unter (2) zitierten Arbeit wurde bereits der Einfluß der Erdrotation auf den Gang der Atomuhren in erster Näherung untersucht. Dabei ergab sich ein Einfluß der Erdrotation in der Zeitverschiebung von der Größe

$$\frac{\delta t}{t} = \frac{R^2\omega^2 \cos^2\varphi}{2c^2} = 1.19 \cdot 10^{-12} \cos^2\varphi \,, \tag{12}$$

(*) *Anmerkung bei der Korrektur.* - Wie mir Herr Prof. Hönl freundlicherweise mitteilte hat dieser « Thirringeffekt » deshalb eine so grundlegende Bedeutung, weil er entscheiden wird, ob die Newtonsche Gravitationstheorie sich an Stelle der allgemeinen Relativitätstheorie nicht im Sinne der Maxwellschen Theorie vektoriell erweitern läßt. Die Einsteinsche tensorielle Theorie ergibt ein um den Faktor 4 größeren Effekt als die elektrodynamische Analogie erwarten läßt. Vergl. dazu H. Hönl und A. W. Maue: *Zeits. f. Phys.*, **144**, 152 (1956).

wobei φ die geographische Breite ist. Dieser Effekt ist so groß, daß er sich mit Atomuhren nachweisen lassen wird. Der hier abgeleitete Einfluß der Erdrotation auf die Rotverschiebung läßt sich als Zeitdilatation der durch die Kinematik der rotierenden Erde verursachten Bewegung deuten und steht daher den beiden anderen relativistischen Rotationseffekten an Bedeutung nach. Er läßt sich bereits ohne die Verwendung der Thirring'schen Lösung aus dem Schwarzschild'schen Linienelement begründen. Der Einfluß der Thirring'schen Lösung auf den Uhrengang ist von höherer Ordnung und daher ebenso zu vernachlässigen wie die anderen Glieder höherer Ordnung, die sich aus der Schwarzschild'schen Lösung für die Größe der Zeitverschiebung ergeben.

13. – Einfluß der Erdabplattung.

Leider liegen die Verhältnisse bei der Erde insofern nicht so glücklich und erschweren es, die relativistischen Bahnstörungen einwandfrei zu ermitteln. Die starke Abplattung der Erde ist die Ursache von Störungen, die sich den gleichartigen relativistischen Störungen überlagern. Glücklicherweise wird es aber trotzdem möglich sein, durch Beobachtung verschiedener Satellitenbahnen eine Trennung der Abplattungseinflüsse von den relativistischen Störungen zu erreichen.

Der Einfluß der Erdabplattung führt, wie im Anhang gezeigt wird, zu einer Drehung des Perigäums für eine in der Äquatorebene umlaufende Bahn vom Betrag:

$$\Delta\omega = \chi\left(\frac{R}{a}\right)^2 v \quad \text{mit} \quad \chi = \frac{3[C-A]}{2MR^2} = 1.3\cdot 10^{-3}\,, \tag{13}$$

C ist das Trägheitsmoment der Erde in Bezug auf die Äquatorachse und A dasjenige in Bezug auf die Polachse. Der numerische Wert von χ ist in einer Arbeit von SPITZER (6) angegeben.

Für die Zweistundenbahn folgt aus (13)

$$\Delta\omega = 0.294^\circ \qquad \text{pro Umlauf.}$$

Die Erdabplattung führt weitherin zu einem Zurückweichen der Bahnknoten vom Betrag (vgl. Anhang)

$$\Delta\Omega = -\chi\left(\frac{R}{a}\right)^2 \cos i\cdot v\,, \tag{14}$$

(6) L. SPITZER Jr.: *Journ. Brit. Interplan. Soc.*, **9**, 131 (1950).

was für eine den Äquator umlaufende Zweistundenbahn den Wert annimmt:

$$\Delta\Omega = -0.294^\circ \qquad \text{pro Umlauf.}$$

Die Knotenstörung verschwindet bei einer über den Pol gelegten Bahn. Jedoch wird sich eine Satellitenbahn nicht so genau über den Pol legen lassen, um die Abplattungsstörung kleiner als die relativistische Störung zu machen. Für eine über den Pol gelegte Bahn verschwindet die störende Kraft der Erdabplattung im Raummittel und daher für sehr viele Umläufe auch im Zeitmittel. Das Perigäum wird bei einer solchen Lage der Bahn im Allgemeinen nur periodischen Störungen unterliegen, wenn die relativistischen Einflüsse nicht berücksichtigt werden. Letztere führen zu einem säkularen Voranschreiten des Perigäums.

Es ist schließlich denkbar, den Einfluß der Erdabplattung durch genaue Beobachtung der Perigäum- und Knotenstörung zu eliminieren. Die gesamten Perigäums- und Knotenstörungen stellen sich durch Ausdrücke der Form dar:

$$(15)\qquad \begin{cases} \Delta\omega = \chi\left(\dfrac{R}{a}\right)^2 \cdot v + \delta\omega\,, \\ \Delta\Omega = -\chi\left(\dfrac{R}{a}\right)^2 \cos i \cdot v + \delta\Omega\,. \end{cases}$$

Für die Perigäumsdrehung haben wir der Einfachheit halber eine in der Äquatorebene liegende Satellitenbahn gewählt. Aus beiden Gleichungen (15) läßt sich die Unbekannte $\chi r(R/a)^2$ eliminieren und damit die Größe der relativistischen Glieder ermitteln. Dieses Verfahren setzt aber wegen der benötigten Genauigkeit eine große Anzahl von Beobachtungsdaten voraus, die erst in vielen Jahren zu gewinnen sind.

Schließlich können andere Unregelmäßigkeiten der Erde als deren Abplattung zu Bahnstörungen führen. Wie in der astronomischen Störungstheorie kann eine solche Unregelmäßigkeit in der Massenverteilung als störende Kraft eingeführt werden. Es werden, wenn die Umlaufszeit des Satelliten mit dem Einfluß der störenden Kraft keine zeitliche Kommensurabilität besitzt, nur kurzperiodische Störungen auftreten. Bei Vorhandensein von Kommensurabilitäten treten säkulare une langperiodische Störungen auf. Diese zeitlichen Kommensurabilitäten können zwischen der Umlaufszeit der Satelliten und der Rotationsdauer der Erde auftreten.

Das Eintreten von solchen durch Kommensurabilitäten verursachten Bahnstörungen kann unter Umständen zur Feststellung von Unregelmäßigkeiten im Erdaufbau erwünscht sein. Für unsere Zwecke dagegen wird man darauf zu achten haben, daß die Umlaufszeit der Satellitenbahn mit der Rotationszeit der Erde in hohen Maße inkommensurabel ist, d.h. in keinem einfachen Zahlenverhältnis oder in der Nähe davon steht.

Anhang

Bahnstörungen durch die Erdabplattung.

Nach Brouwer (7) wird das Gravitationspotential einer abgeplatteten Kugel näherungsweise durch den Ausdruck dargestellt:

$$U = -\frac{GM}{r} - \frac{kGM}{r^3}(1 - 3\cos^2\theta)\,. \tag{16}$$

In (16) ist θ der Winkel zwischen dem Radiusvektor der Satellitenbahn und der Polachse. Die Größe k hat den Wert

$$k = \frac{C - A}{2M}$$

und hängt daher mit der Größe χ der Gleichung (13) durch die Beziehung zusammen:

$$\chi = \frac{3k}{R^2}\,.$$

In Gleichung (16) ist der zweite Summand auf der rechten Seite das Störpotential S,

$$S = \frac{kGM}{r^3}(1 - 3\cos^2\theta)\,.$$

Die Berechnung der Bahnstörungen geschieht in üblicher Weise wie in der astronomischen Störungstheorie. Die Störungsgleichungen für die Bahnelemente sind in dem Werk von Moulton (8) zusammengestellt.

Für die Störung des Perihels gilt die Gleichung:

$$\frac{\mathrm{d}\omega}{\mathrm{d}t} = -\frac{\sqrt{1-e^2}\cos v}{nae}R + \frac{\sqrt{1-e^2}}{nae}\left[1 + \frac{r}{p}\right]\sin v \cdot T - \frac{r\sin u \cdot \operatorname{ctg} i}{na^2\sqrt{1-e^2}}W\,. \tag{17}$$

In (16) sind R, T und W die Komponenten der störenden Kraft in radialer Richtung, T in der Bahnebene senkrecht zum Radiusvektor und W senkrecht zur Bahnebene. u ist das Argument der Breite, das ist der Winkel zwischen Radiusvektor und Knotenlinie. Läuft der Satellit in der Äquatorebene, so verschwinden die Komponenten W und T der störenden Kraft. Es verbleibt

(7) Brouwer: *Astronom. Journ.*, **51**, 223 (1946).

(8) F. R. Moulton: *Einführung in die Himmelsmechanik* (Leipzig-Berlin, 1927).

die Komponente R, die sich aus

$$R = -\frac{\partial S}{\partial r}$$

berechnet zu

$$R = -\frac{3kGM}{r^4} \,. \tag{18}$$

Damit erhält man als Gleichung für die Störung von ω:

$$\frac{\mathrm{d}\omega}{\mathrm{d}t} = 3kGM \frac{\sqrt{1-e^2}}{nae} \frac{\cos v}{r^4} \,. \tag{19}$$

Zur Berechnung der Störungen erster Ordnung setzt man, wie es in der Himmelsmechanik üblich ist, die Bahnelemente auf der rechten Seite von (19) konstant und erhält in Verbindung mit dem Flächensatz

$$r^2 \dot{v} = na^2\sqrt{1-e^2} \,,$$

$$\frac{\mathrm{d}\omega}{\mathrm{d}t} = \frac{3kGM}{n^2a^3e} \frac{\dot{v}\cos v}{r^2} \,. \tag{20}$$

Wegen Bestehens der Ellipsengleichung:

$$r = \frac{a(1-e^2)}{1+e\cos v}$$

folgt aus (20):

$$\frac{\mathrm{d}\omega}{\mathrm{d}t} = \frac{3kGM}{n^2a^5e(1-e^2)^2} (1+e\cos v)^2 \cdot \cos v \cdot \dot{v} \,. \tag{21}$$

Durch Integration von (21) folgt unter Fortlassung der in v periodischen Glieder als säkulare Störung:

$$\Delta\omega = \frac{3kGM}{n^2a^5(1-e^2)^2} v \,, \tag{22}$$

was für eine Kreisbahn mit $e = 0$ und wegen

$$n^2 = \frac{GM}{a^3}$$

sich vereinfacht zu

$$\Delta\omega = \frac{3k}{a^2} v \tag{23}$$

oder nach Einführung von χ

$$\Delta\omega = \chi \left(\frac{R}{a}\right)^2 \cdot v \,. \tag{24}$$

Die Störung von Ω berechnet sich aus der Gleichung

$$\frac{\mathrm{d}\Omega}{\mathrm{d}t} = \frac{r \sin u}{na^2\sqrt{1-e^2}\sin i} \cdot W \,. \tag{25}$$

was sich für eine Kreisbahn vereinfacht zu

$$\frac{\mathrm{d}\Omega}{\mathrm{d}t} = \frac{\sin u}{na\sin i} W \,. \tag{26}$$

Die Komponente W der störenden Kraft, die senkrecht auf der Bahnebene steht, berechnet sich aus der Gleichung

$$W = -K_\theta \sin\varepsilon \,. \tag{27}$$

In (27) ist K_θ die Komponente der störenden Kraft in der θ-Richtung und ε der Winkel, den die Bahnebene mit der Meridianebene einschließt.
Es gilt

$$K_\theta = -\frac{1}{r}\frac{\partial s}{\partial\theta} = \frac{6kGM}{r^4}\sin\theta\cos\theta \,. \tag{28}$$

Weiterhin folgt aus den Formeln der sphärischen Trigonometrie

$$\begin{cases} (a) & \sin\varepsilon = \dfrac{\cos i}{\sin\theta} \,, \\ (b) & \cos\theta = \sin i \cdot \sin u \,. \end{cases} \tag{29}$$

Damit ergibt sich für W:

$$W = -\frac{6kGM}{r^4}\sin i\cos i\sin u \tag{30}$$

und für eine Kreisbahn:

$$W = -\frac{6kGM}{a^4}\sin i\cos i\sin u \,. \tag{30a}$$

Wird (30a) in (26) eingesetzt, erhält man:

$$\frac{\mathrm{d}\Omega}{\mathrm{d}t} = -\frac{6kGM}{na^3}\cos i\sin^2 u \,, \tag{31}$$

wegen $u = nt$ folgt durch Integration von (31) unter Beschränkung auf den säkularen Anteil:

$$\Delta\Omega = -\frac{3kGNM}{n^2 a^3} \cos i \cdot nt \,, \tag{32}$$

wegen $u = v = nt$, wegen $n^2 = GM/a^3$ und nach Einführung der Größe χ läßt sich (32) auf die Form bringen

$$\Delta\Omega = -\chi \left(\frac{R}{a}\right)^2 \cos i \cdot v \,. \tag{33}$$

RIASSUNTO (*)

La creazione di satelliti artificiali offre una serie di possibilità per la verifica della teoria della relatività generale. La precessione del perielio e lo spostamento delle linee spettrali dei satelliti artificiali sono da considerare equivalenti alle possibilità di verifica finora esistenti. Alla precessione relativistica del perielio si sovrappone una precessione assai maggiore dovuta all'appiattimento della terra e la prima è pertanto difficilmente osservabile. Nelle osservazioni dello spostamento delle linee spettrali verso il rosso si deve tener conto del moto proprio del satellite. Data la debole entità dello spostamento spettrale è da escludere una prova per mezzo della misura diretta dello spostamento stesso. È però possibile la misura diretta nel tempo dello spostamento verso il rosso confrontando le indicazioni di orologi atomici sulla terra e sul satellite. Per la traiettoria di due ore questo spostamento temporale è annualmente di $4.1 \cdot 10^{-3}$ s. Un'ulteriore predizione della teorie della Relatività generale è quella della variazione della velocità della luce in dipendenza del potenziale gravitazionale. L'effetto è però tanto piccolo da non essere misurabile. Finalmente, anche la rotazione della terra ha conseguenze relativistiche che non sono più trascurabili. Secondo la teoria della Relatività generale la rotazione della terra genera un campo gravitazionale aggiunto. Tale campo conduce ad una ulteriore rotazione relativistica del perielio, nonchè ad una precessione dei nodi della traiettoria del satellite. La precessione annua dei nodi del satellite è, per una traiettoria di due ore, di 0.13″. Le suddette perturbazioni relativistiche della traiettoria sono osservabili con metodi astronomici e col radar.

(*) *Traduzione a cura della Redazione.*

Relativistic Equation for the Distinguished Component of the State Vector.

K. L. Nagy

Institute for Theoretical Physics of the Roland Eötvös University Budapest, Hungary

(ricevuto il 2 Novembre 1957)

Summary. — An integro-differential equation for the distinguished component of the state vector has been deduced from the Schwinger-Tomonaga equation of the interacting fields. We have proved that this equation is completely equivalent to a differential equation. These equations are the relativistic generalizations of those of W. Królikowski and J. Rzewuski: the interaction picture and arbitrary space-like surfaces have been used. As an example the dressing and the oscillation of a bare V particle in the Lee's model have been studied.

1. – Introduction.

Recently W. Królikowski and J. Rzewuski in a series of papers [1] treated the problem of the motion of a distinguished component of a system. They have derived equations describing the change in time of the distinguished state. Their calculations are however not relativistically invariant using Schrödinger picture and $t = \text{const}$ planes. We frequently meet calculations in the course of which we are not interested in states other than a distinguished one, so we have generalized in a preliminary paper [2] their results to relativistically invariant form. Here we summarize our calculations, prove the equivalence of the integro-differential and differential equations obtained and apply

[1] W. Królikowski and J. Rzewuski: *Bull. Acad. Pol. Sci., Cl. III*, **1**, 1 (1956); *Nuovo Cimento*, **3**, 260 (1956); **4**, 1212 (1956).

[2] K. L. Nagy: *Acta Phys. Hung.*, **7**, 167 (1957).

our method to the Lee's model ([3]). In this case the kernel of the integral equation opposed to other more realistic problems is exact. At the end however we work in g^2 approximation.

2. – The equation for the distinguished component.

We start with the Schwinger-Tomonaga equation

$$i\hbar c \frac{\delta |\sigma\rangle}{\delta\sigma(x)} = H(x)|\sigma\rangle , \tag{1}$$

where H is the interaction Hamiltonian. Denote by $P_{\parallel}$ the projection operator projecting the state vector into its distinguished component: $|\sigma\rangle_{\parallel} = P_{\parallel}|\sigma\rangle$. We suppose $\delta P_{\parallel}/\delta\sigma(x) = 0$. Defining $P_{\perp} = 1 - P_{\parallel}$ it is shown: $P_{\parallel}^2 = P_{\parallel}$, $P_{\perp}^2 = P_{\perp}$, $P_{\perp}P_{\parallel} = P_{\parallel}P_{\perp} = 0$. Now we perform a unitary transformation on (1) with the operator

$$U[\sigma, \sigma_0] = P \exp\left\{-\frac{i}{\hbar c}\int_{\sigma_0}^{\sigma}(P_{\parallel}HP_{\parallel} + P_{\perp}HP_{\perp})\,\mathrm{d}x\right\} , \tag{2}$$

where P is Dyson's chronological operator. Thus we obtain

$$i\hbar c \frac{\delta |\sigma\rangle'}{\delta\sigma(x)} = (P_{\parallel}H'P_{\perp} + P_{\perp}H'P_{\parallel})|\sigma\rangle' . \tag{3}$$

Multiplying this equation with $P_{\parallel}$ or $P_{\perp}$, respectively, we obtain two equations. After eliminating the state vector $|\sigma\rangle_{\perp}$ from the first equation by means of the second equation and returning again to the interaction picture we obtain the following integro-differential equation for $|\sigma\rangle_{\parallel}$:

$$i\hbar c \frac{\delta |\sigma\rangle_{\parallel}}{\delta\sigma(x)} - P_{\parallel}H(x)P_{\perp}|\sigma\rangle + P_{\parallel}H(x)P_{\perp}P \exp\left\{-\frac{i}{\hbar c}\int_{\sigma_0}^{\sigma}P_{\perp}HP_{\perp}\,\mathrm{d}x'\right\}|\sigma_0\rangle - \\ - \frac{i}{\hbar c}\int_{\sigma_0}^{\sigma}K(x, x';\, \sigma, \sigma')|\sigma'\rangle_{\parallel}\,\mathrm{d}x' \tag{4}$$

where

$$K(x, x';\, \sigma, \sigma') = P_{\parallel}H(x)P_{\perp}P \exp\left\{-\frac{i}{\hbar c}\int_{\sigma}^{\sigma}P_{\perp}H(x'')P_{\perp}\,\mathrm{d}x''\right\}P_{\perp}H(x')P_{\parallel} . \tag{5}$$

([3]) T. D. Lee: *Phys. Rev.*, **95**, 1329 (1954).

If $(x_\mu - x'_\mu)^2 > 0$ then $[H(x), H(x')] = 0$ and thus it is shown that the integrability condition

$$\frac{\delta^2 |\sigma\rangle_\parallel}{\delta\sigma(x)\,\delta\sigma(y)} - \frac{\delta^2 |\sigma\rangle_\parallel}{\delta\sigma(y)\,\delta\sigma(x)} = 0$$

is fulfilled. In the following we suppose that $|\sigma_0\rangle_\perp = 0$.

Now we prove that the integro-differential equation (4) is completely equivalent to the following differential equation

$$(6) \qquad i\hbar c \frac{\delta_\parallel |\sigma\rangle_\parallel}{\delta\sigma(x)} = [P_\parallel H(x) P_\parallel + V(x; \sigma, \sigma_0)]\,|\sigma\rangle_\parallel ,$$

where V (which is in general not Hermitian) satisfies

$$(7) \qquad V(x; \sigma, \sigma_0) = -\frac{i}{\hbar c}\int_{\sigma_0}^{\sigma} K(x, x'; \sigma, \sigma') P^{-1} \exp\left\{\frac{i}{\hbar c}\int_{\sigma'}^{\sigma} [P_\parallel H(x'') P_\parallel + V(x'', ; \sigma, \sigma_0)]\,\mathrm{d}x''\right\}\mathrm{d}x' ,$$

from which V can be determined. The equivalence is unterstood in the following sense: if there is a unique solution of (7) for V than each solution of (6) satisfies (4) and reversely each solution of (4) satisfies (6) V given by (7).

From the equation (6) we obtain for every σ'

$$(8) \qquad |\sigma\rangle_\parallel = P \exp\left\{-\frac{i}{\hbar c}\int_{\sigma'}^{\sigma} [P_\parallel H(x'') P_\parallel + V(x''; \sigma'', \sigma_0)]\,\mathrm{d}x''\right\}|\sigma'\rangle_\parallel ,$$

from which

$$V(x; \sigma, \sigma_0)\,|\sigma\rangle_\parallel = -\frac{i}{\hbar c}\int_{\sigma_0}^{\sigma} K(x, x'; \sigma, \sigma') P^{-1} \exp\left\{\frac{i}{\hbar c}\int_{\sigma'}^{\sigma} [P_\parallel H(x'') P_\parallel +$$

$$+ V(x''; \sigma, \sigma_0)]\,\mathrm{d}x''\right\}\mathrm{d}x' P \exp\left\{-\frac{i}{\hbar c}\int_{\sigma'}^{\sigma} [P_\parallel H(x'') P_\parallel + V(x''; \sigma'', \sigma_0)]\,\mathrm{d}x''\right\}|\sigma'\rangle_\parallel =$$

$$= -\frac{i}{\hbar c}\int_{\sigma_0}^{\sigma} K(x, x'; \sigma, \sigma')\,|\sigma'\rangle_\parallel \mathrm{d}x' ,$$

that is each solution of (6) V given by (7) satisfies (4). Inversely the transition is the following. From (4) in the lowest order of approximation we get

$$|\sigma\rangle_\perp - |\sigma'\rangle_\perp .$$

Substituting this into (4) we obtain

$$i\hbar c\,\frac{\delta|\sigma\rangle_{\parallel}}{\delta\sigma(x)} = \left[P_{\parallel}H(x)P_{\parallel} - \frac{i}{\hbar c}\int_{\sigma_0}^{\sigma} K(x, x';\, \sigma, \sigma')\,\mathrm{d}x'\right]|\sigma\rangle_{\parallel}\,, \tag{9}$$

which is noting but (7) with

$$\overset{(1)}{V} = -\frac{i}{\hbar c}\int_{\sigma_0}^{\sigma} K(x, x';\, \sigma, \sigma')\,\mathrm{d}x'\,.$$

The solution of the approximate form (9) of (4) is

$$|\sigma\rangle_{\parallel} = P\exp\left\{-\frac{i}{\hbar c}\int_{\sigma'}^{\sigma}[P_{\parallel}H(x'')P_{\parallel} + \overset{(1)}{V}(x'';\, \sigma'', \sigma_0)]\,\mathrm{d}x''\right\}|\sigma'\rangle_{\parallel}.$$

Substituting $|\sigma'\rangle_{\parallel}$ into (4) this equation gives

$$i\hbar c\,\frac{\delta|\sigma\rangle_{\parallel}}{\delta\sigma(x)} = \left[P_{\parallel}H(x)P_{\parallel} - \frac{i}{\hbar c}\int_{\sigma_0}^{\sigma} K(x, x';\, \sigma, \sigma')P^{-1}\exp\left\{\frac{i}{\hbar c}\int_{\sigma'}^{\sigma}[P_{\parallel}H(x'')P_{\parallel} + \overset{(1)}{V}(x'';\, \sigma'', \sigma_0)]\,\mathrm{d}x''\right\}\mathrm{d}x'\right]|\sigma\rangle_{\parallel}\,,$$

which is also (7) with

$$\overset{(2)}{V} = -\frac{i}{\hbar c}\int_{\sigma_0}^{\sigma} K(x, x';\, \sigma, \sigma')P^{-1}\exp\left\{\frac{i}{\hbar c}\int_{\sigma'}^{\sigma}[P_{\parallel}H(x'')P_{\parallel} + \overset{(1)}{V}(x'';\, \sigma'', \sigma_0)]\,\mathrm{d}x''\right\}\mathrm{d}x'\,.$$

Repeating the procedure and assuming that there exists the limit $\overset{(n)}{V} \to V$ where

$$\overset{(n)}{V} = -\frac{i}{\hbar c}\int_{\sigma_0}^{\sigma} K(x, x';\, \sigma, \sigma')P^{-1}\exp\left\{\frac{i}{\hbar c}\int_{\sigma'}^{\sigma}[P_{\parallel}H(x'')P_{\parallel} + \overset{(n-1)}{V}(x'';\, \sigma'', \sigma_0)]\mathrm{d}x''\right\}\mathrm{d}x'\,,$$

we obtain (6) V given by (7). Thus we proved the equivalence.

In analogy with the usual eigenvalue equation the equation

$$\left\{P_{\mu}^{0} - \frac{1}{c}\int_{\sigma}[P_{\parallel}H(x)P_{\parallel} + V(x;\, \sigma, \sigma_0)]\,\mathrm{d}\sigma_{\mu}\right\}|\sigma\rangle_{\parallel} = \pi_{\mu}(\sigma, \sigma_0)\,|\sigma\rangle_{\parallel} \tag{10}$$

—if it is fulfilled—can be regarded as the four-momentum eigenvalue equation in the distinguished state. So $\mathrm{Re}\,(c/i)\pi_4 = E$ might be the energy in the distinguished state, $\mathrm{Im}\,(c/i)\pi_4 = \Gamma$, Γ/h is the probability of the transition to

other states per unit time. E is in general time-dependent because of the energy exchange between the components of the whole system.

In the following we shall apply the above formalism to the Lee's model.

3. – The solution of the equations.

Lee's model in the interaction picture has the interaction Hamiltonian

$$H(x) = g(\psi_V^* \psi_N \varphi^{(+)} + \psi_N^* \psi_V \varphi^{(-)}) - \delta M_V c^2 \psi_V^* \psi_V \,. \tag{11}$$

The operators ψ_V, ψ_N and φ satisfy the equations of motion

$$\begin{cases} (\partial_4 + \varkappa_V)\psi_V = 0 \,, \\ (\partial_4 + \varkappa_N)\psi_N = 0 \,, \\ (\Box - \mu^2)\varphi = 0 \,, \end{cases} \tag{12}$$

and the commutation relations

$$\begin{cases} \{\psi_V(x), \psi_V^*(x')\} = \delta(\boldsymbol{x} - \boldsymbol{x}') \exp[-ic\varkappa_V(t - t')] \,, \\ \{\psi_N(x), \psi_N^*(x')\} = \delta(\boldsymbol{x} - \boldsymbol{x}') \exp[-ic\varkappa_N(t - t')] \,, \\ [\varphi(x), \varphi(x')] = i\hbar c\, \Delta(x - x') \,, \\ \text{others commute or anticommute} \,, \end{cases} \tag{13}$$

because

$$\psi(\boldsymbol{x}, t) = \psi(\boldsymbol{x}, 0) \exp[-ic\varkappa t] \,. \tag{14}$$

Here everything is unrenormalized, but $\varkappa$ and μ are the observed masses. We solve (6) and (7) in this case. Choosing $|\sigma\rangle_\parallel$ as the bare N or θ particle state we easily obtain $P_\parallel H P_\parallel = V = 0$, thus $\delta|\sigma\rangle_\parallel/\delta\sigma(x) = 0$ showing that these particles are the stable dressed ones. We now study the bare V particle state. Then

$$\begin{cases} P_\parallel = i\int_t \psi_V^*(x)\,|0\rangle\langle 0|\,\psi_V(x)\,\mathrm{d}\sigma_4 \,, \\ 1 - \sum_{N,V,\theta} \frac{1}{N!V!\theta!}(i)^{N+V}\left(\frac{i}{hc}\right)^\theta \int_t \dots \int_t \psi_V^*(x^1)\dots\psi_V^*(x^V)\psi_N^*(y^1)\dots\psi_N^*(y^N)\cdot\varphi^{(-)}(z^1)\dots \\ \qquad \dots\varphi^{(-)}(z^\theta)\,|0\rangle \prod_{N,V}\mathrm{d}\sigma_4 \prod_\theta \left(\frac{\overleftarrow{\partial}}{\partial z_4^i} - \frac{\overrightarrow{\partial}}{\partial z_4^i}\right)\mathrm{d}\sigma_4(z^i)\langle 0|\,\varphi^{(+)}(z^\theta) \\ \qquad\qquad \dots\psi_N(y^N)\dots\psi_V(x^V)\dots\psi_V(x^1) \,. \end{cases} \tag{15}$$

First we wish to determine V from (7). In g^2 approximation V is

$$V^{(2)}(x;\,\sigma,\,\sigma_0) = -\frac{i}{\hbar c}\int_{\sigma_0}^{\sigma} P_{\parallel} H(x) P_{\perp} H(x') P_{\parallel}\,\mathrm{d}x' \,. \tag{16}$$

Using (15), (13) and the definition of the vacuum state $\psi\,|\,0\rangle = \varphi^{(+)}\,|\,0\rangle = 0$, substituting $\Delta^{(+)}$ and $\psi_V(\boldsymbol{x}', t') = \psi_V(\boldsymbol{x}', t)\exp\left[-i\varkappa_V c(t'-t)\right]$ (16) gives (with $\sigma \to t = \text{const} \leqslant 0$, and $\sigma_0 \to t_0 = \text{const}$ planes)

$$\left\{\begin{aligned} &V^{(2)}(x;\,t,\,t_0) = -\frac{g^2}{4\pi^2}\exp\,[2c\varepsilon t]\cdot \\ &\quad\cdot\int_0^{\infty} k^2\{1-\exp\left[-ic(t-t_0)\right]\left[\varkappa_N-\varkappa_V+\omega-i\varepsilon\right]\}\\ &\qquad\qquad \omega[\varkappa_N-\varkappa_V+\omega-i\varepsilon]\end{aligned}\,\mathrm{d}k\;\psi_V^{*}(x)\,|\,0\rangle\langle 0\,|\,\psi_V(x)\,, \right. \tag{17}$$
$$\omega = \sqrt{k^2+\mu^2}\,,$$

where we have taken care of the adiabatic switching on of the interaction, because we wish to allow t_0 to tend to $-\infty$ too. From (17) it is shown that $V^{(2)}(x;\,t_1,\,-\infty)$ would be—disregarding ε—the exact solution of (7) with

$$\delta M_V = -\frac{g^2}{4\pi^2 c^2}\int_0^{\infty}\frac{k^2}{\omega[\varkappa_N-\varkappa_V+\omega]}\,\mathrm{d}k\,, \tag{18}$$

(that is with the value given by Lee) because

$$P_{\parallel} H(x) P_{\parallel} = -\,\delta M_V c^2 \psi_V^{*}(x)\,|\,0\rangle\langle 0\,|\,\psi_V(x)$$

and

$$\varkappa(x,\,x';\,\sigma,\,\sigma') = P_{\parallel} H(x) P_{\perp} H(x') P_{\parallel}\,, \tag{19}$$

exactly for $P_{\perp} H P_{\perp} H P_{\parallel} = 0$. Using (17) and taking the limit $\varepsilon \to 0$ at the end of calculations we obtain from (6) and (10) for $t_0 \to -\infty$ in g^2 approximation

$$\left\{\begin{aligned} &\frac{\mathrm{d}\,|\,t\rangle_{\parallel}}{\mathrm{d}t} = 0\,,\\ &\mathrm{d}\,{}_{\parallel}\langle t\,|\,t\rangle_{\parallel} - \frac{2\Gamma}{\hbar}\,{}_{\parallel}\langle t\,|\,t\rangle_{\parallel} = 0\,,\\ &|\,t\rangle_{\parallel} = \left\{1-\frac{g^2}{8\pi^2\hbar c}\int_0^{\infty}\frac{k^2\,\mathrm{d}k}{\omega\,[\varkappa_N-\varkappa_V+\omega]^2}\right\}|-\infty\rangle_{\parallel}\,,\\ &{}_{\parallel}\langle t\,|\,t\rangle_{\parallel} = 1-\frac{g^2}{4\pi^2\hbar c}\int_0^{\infty}\frac{k^2\,\mathrm{d}k}{\omega\,[\varkappa_N-\varkappa_V+\omega]^2}\,,\\ &E = M_V c^2\,, \end{aligned}\right. \tag{20}$$

that is the bare particle V dresses infinitely slowly for infinite time interval, its energy is always the observed one. The analogous terms are for finite t_0

$$
(21)\qquad
\begin{cases}
\dfrac{\mathrm{d}\,|t\rangle_{\parallel}}{\mathrm{d}t} = \dfrac{g^2}{4\pi^2\hbar i}\displaystyle\int_0^\infty \frac{k^2 \exp\left[-ic(t-t_0)\{\varkappa_N-\varkappa_V+\omega\}\right]}{\omega\left[\varkappa_N-\varkappa_V+\omega\right]}\,\mathrm{d}k\,|t\quad, \\[2ex]
\dfrac{\mathrm{d}\,{}_{\parallel}\langle t|t\rangle_{\parallel}}{\mathrm{d}t} = \dfrac{2\Gamma}{\hbar}\,{}_{\parallel}\langle t|t\rangle_{\parallel} = -\dfrac{g^2}{2\pi^2\hbar}\displaystyle\int_0^\infty \frac{k^2 \sin\left\{c(t-t_0)[\varkappa_N-\varkappa_V+\omega]\right\}}{\omega[\varkappa_N-\varkappa_V+\omega]}\,\mathrm{d}k\;{}_{\parallel}\langle t|t\rangle_{\parallel}\,, \\[2ex]
{}_{\parallel}|t\rangle_{\parallel} = \left\{1-\dfrac{g^2}{4\pi^2\hbar c}\displaystyle\int_0^\infty \frac{k^2\left(1-\exp\left[-ic(t-t_0)\{\varkappa_N-\varkappa_V+\omega\}\right]\right)}{\omega\left[\varkappa_N-\varkappa_V+\omega\right]^2}\,\mathrm{d}k\right\}|t_0\rangle_{\parallel}\,, \\[2ex]
t|t\rangle_{\parallel} = 1-\dfrac{g^2}{2\pi^2\hbar c}\displaystyle\int_0^\infty \frac{k^2\left[1-\cos\left\{c(t-t_0)[\varkappa_N-\varkappa_V+\omega]\right\}\right]}{\omega[\varkappa_N-\varkappa_V+\omega]^2}\,\mathrm{d}k\,, \\[2ex]
E = M_V c^2 + \dfrac{g^2}{4\pi^2}\displaystyle\int_0^\infty \frac{k^2\cos\left\{c(t-t_0)\left[\varkappa_N-\varkappa_V+\omega\right]\right\}}{\omega[\varkappa_N-\varkappa_V+\omega]}\,\mathrm{d}k\,,
\end{cases}
$$

showing that V and its energy rapidly oscillate.

Our calculations were only approximate but their approximate character did note originate from neglecting several graphs; for according to (19) all the allowed ones were taken into consideration. From (20) and (21) it is shown that when we wish to obtain reasonable results we must cut-off the integrals at a value at which the integral

$$
\frac{1}{\pi}\int_0^\infty \frac{k^2\, f(k^2)\,\mathrm{d}k}{\omega[\varkappa_N-\varkappa_V+\omega]^2} \qquad \text{should be less than} \qquad \frac{4\pi\hbar c}{g^2}\,.
$$

* * *

The author is indebted to Dr. G. Marx and F. Károlyházi for stimulating discussions.

RIASSUNTO (*)

Dall'equazione dei campi interagenti di Schwinger-Tomonaga abbiamo dedotto un'equazione integro-differenziale per la « componente distinta » del vettore di stato. Abbiamo provato che questa equazione equivale completamente a un'equazione differenziale. Tali equazioni sono le generalizzazioni relativistiche di quelle di W. Królikowski e J. Rzewuski: ci siamo valsi della rappresentazione d'interazione e di superfici tipo spazio arbitrarie. A titolo d'esempio abbiamo studiato la particella V fisica e l'oscillazione di una particella V matematica nel modello di Lee.

(*) *Traduzione a cura della Redazione.*

On the Quantization of Fermion Fields with Zero Mass.

C. G. Bollini

Comisión Nacional de la Energía Atómica - Argentina

(ricevuto l'8 Novembre 1957)

Summary. — The formulation of quantum field theory for massless tensor fields given in a previous paper, is here extended to fermion fields with zero mass. The fermion field, which in the Rarita-Schwinger formalism is represented by a tensor spinor, is here expressed in terms of simple Dirac spinors. These Dirac spinors are free components of the field and the usual anticommutation relations are imposed on them. The corresponding anticommutation relations of the field components are given. They are compatible with the supplementary conditions.

1. – Introduction.

In the Rarita-Schwinger formalism [1] the general fermion field is represented by means of a symmetric tensor-spinor $\Psi_{\nu_1 \dots \nu_s}$. When this field corresponds to massless particles with zero mass, it satisfies the equations

$$\gamma_\mu \partial_\mu \Psi_{\nu_1 \dots \nu_s} = 0 \,, \tag{1.1}$$

$$\gamma_{\nu_1} \Psi_{\nu_1 \dots \nu_s} = 0 \,. \tag{1.2}$$

The matrices γ_μ satisfying the relations

$$\gamma_\mu \gamma_\nu + \gamma_\nu \gamma_\mu = 2\delta_{\mu\nu} \,. \tag{1.3}$$

[1] W. Rarita and J. Schwinger: *Phys. Rev.*, **60**, 61 (1941).

It is easily seen that these equations imply.

$$\partial_{\nu_1} \Psi_{\nu_1 \ldots \nu_s} = 0 , \tag{1.4}$$

$$\delta_{\nu_1 \nu_2} \Psi_{\nu_1 \ldots \nu_s} = 0 . \tag{1.5}$$

(1.1) is the field equation and (1.2) is the supplementary condition which reduces to $2s+2$ the number of independent components of the tensor-spinor $\Psi_{\nu_1 \ldots \nu_s}$. This is the right number of possible orientations of a particle with spin $s-\frac{1}{2}$. The gauge invariance condition reduces further this number to two ([2]).

We intend to take (1.2) as constraint equations and so our first aim is the extraction of the independent components from the field entity (in a covariant manner). To get this result we are going to use a method for the tensorial field, already developed in a previous paper ([3]) (hereafter referred to as I).

2. – Decomposition of the field entity.

We first arbitrarily choose a time-like unit vector: $n_\mu n_\mu = -1$. Then, let us define by recurrence the following tensor spinors: (see also I (2.1) (2.2) (2.3) (2.4))

$$\Psi^{(0)} = n_{\nu_1} \ldots n_{\nu_s} \Psi_{\nu_1 \ldots \nu_s}$$

$$\Psi^{(1)}_{\nu_1 \ldots \nu_s} = \partial^{\ s} \partial_{\nu_1} \ldots \partial_{\nu_s} \Psi^{(0)}$$

$$\left.\begin{aligned} \Psi^{(r)}_{\nu_1 \ldots \nu_r} &= n_{\nu_{r+1}} \ldots n_{\nu_s} \Big(\Psi_{\nu_1 \ldots \nu_s} - \sum_{t=0}^{r-1} \Psi^{(t)}_{\nu_1 \ldots \nu_s} \Big) \qquad (2.1) \\ \Psi^{(r)}_{\nu_1 \ldots \nu_s} &= \partial^{\ (s-r)} \partial_{\nu_{r+1}} \ldots \partial_{\nu_s} \Psi^{(r)}_{\nu_1 \ldots \nu_r} + (\text{symm.}) \qquad (2.2) \end{aligned}\right\} \quad r = 0, 1, \ldots, s.$$

Here $\partial = n_\nu \partial_\nu$ and ∂^{-1} is the inverse operator. « Symm. » means terms necessary to make symmetric the right hand side of (2.2).

The quantities defined by (2.1) and (2.2), all satisfy (1.1), (1.2).

It can be proved by recurrence that

$$n_{\nu_{r+1}} \ldots n_{\nu_s} \Psi^{(r)}_{\nu_1 \ldots \nu_s} = \Psi^{(r)}_{\nu_1 \ldots \nu_r} \tag{2.3}$$

$$n_{\nu_1} \Psi^{(r)}_{\nu_1 \ldots \nu_r} = 0 . \tag{2.4}$$

([2]) J. S. De Wet: *Phys. Rev.*, **58**, 236 (1940).
([3]) C. G. Bollini: *Nuovo Cimento*, **6**, 1034 (1957).

The last equation of the recurrence chain is

$$\Psi^{(s)}_{\nu_1 \dots \nu_s} = \Psi_{\nu_1 \dots \nu_s} - \sum_0^{s-1} \Psi^{(t)}_{\nu_1 \dots \nu_s}$$

which brings the decomposition

$$\Psi_{\nu_1 \dots \nu_s} = \sum_{t=0}^{s} \Psi^{(t)}_{\nu_1 \dots \nu_s} \tag{2.5}$$

of the field quantities in $s+1$ new tensor-spinors satisfying (1.1), (1.2), (2.3) and (2.4). We are going to prove that each one of this new tensor-spinors has only one independent component which is a simple spinor (without tensorial index).

3. – Polarization matrices.

In I (Eq. (3.1)) we introduced two derivation operators α_ν, β_ν such that

$$\left\{ \begin{array}{ll} n_\nu \alpha_\nu = 0 , & n_\nu \beta_\nu = 0 , \\ \alpha_\nu \partial_\nu = 0 , & \beta_\nu \partial_\nu = 0 , \\ \alpha_\nu \alpha_\nu = 1 , & \beta_\nu \beta_\nu = 1 , \\ \multicolumn{2}{c}{\alpha_\nu \beta_\nu = 0 .} \end{array} \right. \tag{3.1}$$

By means of these operators and the γ_μ matrices, we define now

$$\Gamma_\nu = \alpha_\nu + \beta_\nu \gamma \cdot \alpha \, \gamma \cdot \beta , \tag{3.2}$$

$$\Gamma_{\nu_1 \dots \nu_r} = \Gamma_{\nu_1} \dots \Gamma_{\nu_r} . \tag{3.3}$$

(From now on, we put $\gamma_\mu \alpha_\mu = \gamma \cdot \alpha$, etc.).

The Γ_μ are commuting matrices:

$$\Gamma_\mu \Gamma_\nu - \Gamma_\nu \Gamma_\mu = 0 . \tag{3.4}$$

It follows from (3.1) and (3.2) that

$$n_\nu \Gamma_\nu = 0 , \qquad \partial_\nu \Gamma_\nu = 0 . \tag{3.5}$$

We also have

$$\gamma_\nu \Gamma_\nu = 0 , \qquad \Gamma_\nu \Gamma_\nu = 0 , \tag{3.6}$$

because

$$\begin{cases} \gamma\cdot\alpha\,\gamma\cdot\beta = -\gamma\cdot\beta\,\gamma\cdot\alpha\,, \\ \gamma\cdot\alpha\,\gamma\cdot\alpha - \gamma\cdot\beta\,\gamma\cdot\beta = 1\,. \end{cases} \tag{3.7}$$

According to these equations (3.3) defines a symmetric set of matrices satisfying

$$\begin{cases} \delta_{\nu_1\nu_2}\Gamma_{\nu_1\ldots\nu_r} = 0\,, \\ \gamma_{\nu_1}\Gamma_{\nu_1\ldots\nu_r} = 0\,, \\ \partial_{\nu_1}\Gamma_{\nu_1\ldots\nu_r} = 0\,, \\ n_{\nu_1}\Gamma_{\nu_1\ldots\nu_r} = 0\,, \end{cases} \tag{3.8}$$

also

$$\gamma\cdot\partial\,\Gamma_{\nu_1\ldots\nu_r} = \Gamma_{\nu_1\ldots\nu_r}\gamma\cdot\partial\,. \tag{3.9}$$

Analogously, putting

$$\tilde{\Gamma}_\nu = \alpha_\nu + \beta_\nu\,\gamma\cdot\beta\,\gamma\cdot\alpha \tag{3.10}$$

and

$$\tilde{\Gamma}_{\nu_1\ldots\nu_r} = \tilde{\Gamma}_{\nu_1}\ldots\tilde{\Gamma}_{\nu_r}\,, \tag{3.11}$$

we have

$$\begin{cases} \delta_{\nu_1\nu_2}\tilde{\Gamma}_{\nu_1\ldots\nu_r} = 0\,, \\ \tilde{\Gamma}_{\nu_1\ldots\nu_r}\gamma_{\nu_1} = 0\,, \\ \partial_{\nu_1}\tilde{\Gamma}_{\nu_1\ldots\nu_r} = 0\,, \\ n_{\nu_1}\tilde{\Gamma}_{\nu_1\ldots\nu_r} = 0\,, \\ \gamma\cdot\partial\,\tilde{\Gamma}_{\nu_1\ldots\nu_r} = \tilde{\Gamma}_{\nu_1\ldots\nu_r}\gamma\cdot\partial\,. \end{cases} \tag{3.12}$$

4. – Field co-ordinates.

The tensor-spinors defined by (2.1) are orthogonal to n_ν, ∂_ν and γ_ν. Because of this we can put

$$\begin{aligned} 0 = \gamma_{\nu_1}\Psi^{(r)}_{\nu_1\ldots\nu_r} &= \gamma_\mu(\alpha_\mu\alpha_{\nu_1} + \beta_\mu\beta_{\nu_1})\Psi^{(r)}_{\nu_1\ldots\nu_r} \\ &= \gamma\cdot\alpha\,\alpha_{\nu_1}\Psi^{(r)}_{\nu_1\ldots\nu_r} + \gamma\cdot\beta\,\beta_{\nu_1}\Psi^{(r)}_{\nu_1\ldots\nu_r} \end{aligned}$$

$$\gamma\cdot\alpha\,\alpha_{\nu_1}\Psi^{(r)}_{\nu_1\ldots\nu_r} = -\gamma\cdot\beta\,\beta_{\nu_1}\Psi^{(r)}_{\nu_1\ldots\nu_r}\,. \tag{4.1}$$

Then

$$\begin{aligned} \Gamma_\mu \alpha_{\nu_1} \Psi^{(r)}_{\nu_1 \dots \nu_r} &= \alpha_\mu \alpha_{\nu_1} \Psi^{(r)}_{\nu_1 \dots \nu_r} + \beta_\mu \gamma \cdot \alpha \, \gamma \cdot \beta \, \beta_{\nu_1} \Psi^{(r)}_{\nu_1 \dots \nu_r} \\ &= \alpha_\mu \alpha_{\nu_1} \Psi^{(r)}_{\nu_1 \dots \nu_r} + \beta_\mu \beta_{\nu_1} \Psi^{(r)}_{\nu_1 \dots \nu_r} \\ &= \Psi^{(r)}_{\mu \nu_2 \dots \nu_r} . \end{aligned}$$

In the same way we can deduce that

$$\Gamma_{\mu_1 \dots \mu_r} \alpha_{\nu_1} \dots \alpha_{\nu_r} \Psi^{(r)}_{\nu_1 \dots \nu_r} = \Psi^{(r)}_{\mu_1 \dots \mu_r} . \tag{4.2}$$

Equivalently, but more symmetrically

$$2^{-r} \Gamma_{\mu_1 \dots \mu_r} \tilde{\Gamma}_{\nu_1 \dots \nu_r} \Psi^{(r)}_{\nu_1 \dots \nu_r} = \Psi^{(r)}_{\mu_1 \dots \mu_r} \tag{4.3}$$

on account of

$$\begin{aligned} \tilde{\Gamma}_{\nu_1} \Psi^{(r)}_{\nu_1 \dots \nu_r} &= \alpha_{\nu_1} \Psi^{(r)}_{\nu_1 \dots \nu_r} + \gamma \cdot \beta \, \gamma \cdot \alpha \, \beta_{\nu_1} \Psi^{(r)}_{\nu_1 \dots \nu_r} \\ &= \alpha_{\nu_1} \Psi^{(r)}_{\nu_1 \dots \nu_r} + \alpha_{\nu_1} \Psi^{(r)}_{\nu_1 \dots \nu_r} \\ &= 2 \alpha_{\nu_1} \Psi^{(r)}_{\nu_1 \dots \nu_r} . \end{aligned}$$

The equation (4.2) allows then to express the tensor spinor $\Psi^{(r)}_{\mu_1 \dots \mu_r}$ as a function of one spinor, namely:

$$\Psi^{(r)} = \alpha_{\nu_1} \dots \alpha_{\nu_r} \Psi^{(r)}_{\nu_1 \dots \nu_r} , \tag{4.4}$$

$$\Psi^{(r)}_{\mu_1 \dots \mu_r} = \Gamma_{\mu_1 \dots \mu_r} \Psi^{(r)} . \tag{4.5}$$

(4.5) shows an explicit separation of the tensorial part from $\Psi^{(r)}_{\mu_1 \dots \mu_r}$.

The tensor-matrix operator $\Gamma^{(r)}_{\mu_1 \dots \mu_r}$ carries all the subsidiary properties of $\Psi^{(r)}_{\mu_1 \dots \mu_r}$, whereas the purely spinorial part $\Psi^{(r)}$ satisfies only the field equation:

$$\gamma \cdot \partial \, \Psi^{(r)} = 0 \tag{4.6}$$

without any other condition.

The $s+1$ Dirac spinors $\Psi^{(r)}$ are then free components of the field. (4.5), (2.2) and (2.5), allow one to express the field entity as a function of these co-ordinates.

When a gauge transformation is made, all but one of these spinors are changed. The only really free component is $\Psi^{(s)}$, i.e. the completely « transversal » component of $\Psi_{\nu_1 \ldots \nu_s}$ (see I).

5. – Adjoint components.

The adjoint spinor of $\Psi^{(r)}$ is defined by [4]

$$\Psi^{(r)} = \Psi^{(r)*} A \,,$$

$\Psi^{(r)*}$ being the transposed conjugate, and A the matrix such that

$$\gamma_\mu^* = -A\gamma_\mu A^{-1} \,. \qquad A^* = A \tag{5.1}$$

From (4.6) we deduce

$$\Psi^{(r)*}\gamma^* \cdot \partial = 0 \,. \tag{5.2}$$

(In the expressions like (5.2) it is understood that the derivation operator operates on the left).

With (5.1) equation (5.2) is transformed into

$$-\Psi^{(r)*} A\, \gamma \cdot \partial\, A^{-1} = -\bar{\Psi}^{(r)} \gamma \cdot \partial\, A^{-1} = 0 \,,$$

i.e.

$$\bar{\Psi}^{(r)} \gamma \cdot \partial = 0 \,. \tag{5.3}$$

(5.3) is the equation adjoint to (4.6).

Applying the star operation to the matrix Γ_ν, we have

$$\begin{aligned} \Gamma_\nu^* &= \alpha_\nu + \beta_\nu \gamma^* \cdot \beta\ \gamma^* \cdot \alpha \,, \\ &= \alpha_\nu + \beta_\nu A\, \gamma \cdot \beta A^{-1} A\, \gamma \cdot \alpha\, A^{-1} \,, \\ &= \alpha_\nu + \beta_\nu A\, \gamma \cdot \beta\, \gamma \cdot \alpha\, A^{-1} \,, \\ &= A(\alpha_\nu + \beta_\nu \gamma \cdot \beta\ \gamma \cdot \alpha) A^{-1} \,, \\ \Gamma_\nu^* &= A\, \tilde{\Gamma}_\nu A^{-1} \,. \end{aligned}$$

[4] J. M. Jauch and F. Rohrlich: *The Theory of Photons and Electrons* (Cambridge, Mass., 1955), p. 53.

In general

$$\Gamma^*_{\nu_1\dots\nu_r} = A\,\tilde{\Gamma}_{\nu_1\dots\nu_r}A^{-1}\,. \tag{5.4}$$

Transposing (4.5) and taking the complex conjugate

$$\Psi^{(r)*}_{\mu_1\dots\mu_r} = \Psi^{(r)*}\Gamma^*_{\mu_1\dots\mu_r} = \Psi^{(r)*}A\,\tilde{\Gamma}_{\mu_1\dots\mu_r}A^{-1}\,,$$

$$= \Psi^{(r)}\tilde{\Gamma}_{\mu_1\dots\mu_r}A^{-1}\,.$$

Putting

$$\overline{\Psi^{(r)}}_{\mu_1\dots\mu_r} = \Psi^{(r)*}_{\mu_1\dots\mu_r}A$$

one has

$$\overline{\Psi^{(r)}}_{\mu_1\dots\mu_r} = \Psi^{(r)}\tilde{\Gamma}_{\mu_1\dots\mu_r}\,. \tag{5.5}$$

The decomposition (2.5) is now transformed into the adjoint decomposition

$$\overline{\Psi}_{\nu_1\dots\nu_s} = \sum_{t=0}^{s}\Psi^{(t)}_{\nu_1\dots\nu_s}\,, \tag{5.6}$$

where

$$\Psi^{(r)}_{\nu_1\dots\nu_s} = \Psi^{(r)*}_{\nu_1\dots\nu_s}A = \partial^{-(s-r)}\partial_{\nu_{r+1}}\dots\partial_{\nu_s}\Psi^{(r)}_{\nu_1\dots\nu_r} + (\text{symm.})\,. \tag{5.7}$$

6. – Quantization.

The $s+1$ spinors $\Psi^{(r)}$ are free co-ordinates satisfying the Dirac equation (with zero mass). It seems logical then to impose the anticommutation relations:

$$\{\Psi^{(r)}(x),\,\overline{\Psi^{(r')}}(x')\} = i\,\delta^{rr'}\,\gamma\cdot\partial\,D(x-x')\,, \tag{6.1}$$

where we take

$$\delta^{rr'} = 0 \qquad \text{when } r \neq r'$$

and

$$\delta^{rr} = \varepsilon^{(r)} \qquad \text{(not necessarily 1).}$$

$\varepsilon^{(r)}$ is the « weight » of the r-th free co-ordinate and depends on the way

in which it appears in the field Lagrangian. (4.5), (5.5) and (6.1) give:

$$\{\Psi^{(r)}_{\mu_1\dots\mu_r}(x),\ \Psi^{(r')}_{\nu_1\dots\nu_{r'}}(x')\} = \{\Gamma_{\mu_1\dots\mu_r}\Psi^{(r)}(x),\ \overline{\Psi}^{(r')}(x')\widetilde{\Gamma}_{\nu_1\dots\nu_{r'}}\} =$$
$$= \Gamma_{\mu_1\dots\mu_r}\{\Psi^{(r)}(x),\ \Psi^{(r')}(x')\}\widetilde{\Gamma}_{\nu_1\dots\nu_{r'}} = i\,\delta^{rr'}\,\Gamma_{\mu_1\dots\mu_r}\gamma\cdot\partial\,\widetilde{\Gamma}_{\nu_1\dots\nu_{r'}}\,D(x-x')\,,$$

$$\{\Psi^{(r)}_{\mu_1\dots\mu_r}(x),\ \overline{\Psi}^{(r')}_{\nu_1\dots\nu_{r'}}(x')\} = i\,\delta^{rr'}\,\Gamma_{\mu_1\dots\mu_r}\widetilde{\Gamma}_{\nu_1\dots\nu_r}\gamma\cdot\partial\,D(x-x')\,. \tag{6.2}$$

Now, with (2.2), we have

$$\{\Psi^{(r)}_{\mu_1\dots\mu_s}(x),\ \Psi^{(r')}_{\nu_1\dots\nu_s}(x')\} = i\,\delta^{rr'}\,\Gamma^{(r)}_{\mu_1\dots\mu_s}\widetilde{\Gamma}^{(r)}_{\nu_1\dots\nu_s}\gamma\cdot\partial\,D(x-x')\,, \tag{6.3}$$

where

$$\Gamma^{(r)}_{\mu_1\dots\mu_s} = \partial^{-(s-r)}\partial_{\mu_{r+1}}\dots\partial_{\mu_s}\Gamma_{\mu_1\dots\mu_s} + (\text{symm.})\,. \tag{6.4}$$

From (6.3) and the decompositions (2.5) and (5.6) we obtain

$$\{\Psi_{\mu_1\dots\mu_s}(x),\ \overline{\Psi}_{\nu_1\dots\nu_s}(x')\} = i\,\Gamma_{\mu_1\dots\mu_s;\nu_1\dots\nu_s}\gamma\cdot\partial\,D(x-x') \tag{6.5}$$

with

$$\Gamma_{\mu_1\dots\mu_s;\nu_1\dots\nu_s} = \sum_{t=0}^{s}\varepsilon^{(t)}\,\Gamma^{(t)}_{\mu_1\dots\mu_s}\widetilde{\Gamma}^{(t)}_{\nu_1\dots\nu_s}\,. \tag{6.6}$$

The anticommutation relations (6.5) are compatible with the supplementary condition.

7. – Example spin $\frac{3}{2}$.

The decomposition (2,5) is now

$$\Psi_\nu = \partial^{-1}\partial_\nu\Psi^{(0)} + \Gamma_\nu\Psi^{(1)}\,,$$
$$\Psi^{(0)} = n_\nu\Psi_\nu\,; \qquad \Psi^{(1)} = \alpha_\nu\Psi_\nu\,.$$

And the anticommutation relations are

$$\{\Psi^{(0)}(x),\ \overline{\Psi}^{(0)}(x')\} = i\varepsilon^{(0)}\gamma\cdot\partial\,D(x-x')\,,$$
$$\{\Psi^{(1)}(x),\ \overline{\Psi}^{(1)}(x')\} = i\varepsilon^{(1)}\gamma\cdot\partial\,D(x-x')\,,$$
$$\{\Psi_\mu(x),\ \overline{\Psi}_\nu(x')\} = i\,\Gamma_{\mu;\nu}\gamma\cdot\partial\,D(x-x')\,,$$
$$\Gamma_{\mu;\nu} = \varepsilon^{(0)}\partial^{-2}\partial_\mu\partial_\nu + \varepsilon^{(1)}\Gamma_\mu\widetilde{\Gamma}_\nu$$
$$\Gamma_\mu\widetilde{\Gamma}_\nu = \alpha_\mu\alpha_\nu + \beta_\mu\beta_\nu - (\alpha_\mu\beta_\nu - \beta_\mu\alpha_\nu)\,\gamma\cdot\beta\,\gamma\cdot\alpha\,.$$

It is easily seen that the last expression is actually independent of a particular choice for α_ν and β_ν. In fact

$$\Gamma_\mu \tilde{\Gamma}_\nu = \gamma_\nu \gamma_\mu - \partial^{-2} \partial_\mu \partial_\nu - \partial^{-1} (\partial_\mu \gamma_\nu \gamma \cdot n + \gamma \cdot n \, \partial_\nu \gamma_\mu) \, .$$

When both sides act on $\gamma \cdot \partial D(x - x')$.

RIASSUNTO (*)

Nel presente lavoro si estende ai campi di fermioni di massa nulla la formulazione della teoria quantistica dei campi di tensori privi di massa. Il campo fermionico che nel formalismo di Rarita-Schwinger è rappresentato da uno spinore tensoriale è espresso qui in termini di semplici spinori di Dirac. Tali spinori di Dirac sono componenti libere del campo e si impongono loro le solite relazioni di anticommutazione. Si danno le corrispondenti relazioni di anticommutazione delle componenti del campo, che sono compatibili con le condizioni supplementari.

(*) *Traduzione a cura della Redazione.*

On the Decay of ^{133}Ba.

R. K. Gupta, S. Jha, M. C. Joshi and B. K. Madan

Tata Institute of Fundamental Research - Bombay

(ricevuto il 28 Novembre 1957)

Summary. — The results of β-ray spectrometer studies and scintillation spectrometer studies of ^{133}Ba are being presented. A new level in ^{133}Cs at 160 keV has been found. The γ-rays of energies 56 keV, 79 keV, 160 keV, 224 keV, 277 keV, 302 keV, 358 keV, 383 keV and 437 keV have been detected. The conversion coefficients of some of the γ-rays have been estimated. It has been found by a combination of the summing technique and the conventional coincidence technique that ^{133}Ba decays with an energy of (53 ± 2) keV to the 437 keV state of ^{133}Cs by K-electron captures (46%) and L-electron captures (54%). A decay scheme is suggested.

1. – Introduction.

The isotope $^{133}_{56}$Ba, which decays by electron captures with a half-life of ten years, has been studied, in recent years, by Langevin [1] and Hayward *et al.* [2]. Langevin found that ^{133}Ba decays predominantly by L-electron captures only to the 440 keV state of ^{133}Cs. He found γ-rays of energies 70 keV, 80 keV, 290 keV and 360 keV. He estimated the decay energy of this isotope to the 440 keV state of ^{133}Cs to be less than 40 keV. The decay scheme proposed by him is given in the inset of Fig. 2. Hayward *et al.* [2] found that there are electron capture transitions to both the 439 keV and 382 keV states of ^{133}Cs. He found γ-rays of energies 57 keV, 82 keV, 300 keV and 357 keV. The difference in the results of Langevin and Hayward *et al.* is that the 440 keV state decays, according to Langevin by the emission of 70 keV, 290 keV and 80 keV γ-rays in cascade but according to Hayward *et al.* it decays by emission of 57 keV, 300 keV and 82 keV γ-rays in cascade. Re-

[1] M. Langevin: *Ann. de Phys.*, **1**, 57 (1956).

[2] R. W. Hayward, D. D. Hoppes and H. Ernst: *Phys. Rev.*, **93**, 916A (1954).

cently Coulomb excitation of ^{133}Cs has been studied and the γ-rays of energies 82 keV ([3,4]), 160 keV ([3,4]), 302 keV ([4]) and 379 keV ([4]) have been observed.

The results being reported here were obtained from the studies of a carrier-free source of ^{133}Ba in a scintillation coincidence spectrometer and β-ray spectrometer. A new level in ^{133}Cs has been found and some new γ-rays have been detected. The energy values of some of the γ-rays have been revised. The conversion coefficients of some of the γ-rays have been estimated. Finally, it has been found that ^{133}Ba decays to the 437 keV level by K-electron captures in 46% cases and by L-electron captures in 54% cases, the decay energy to the 437 keV level being (53 ± 2) keV.

2. – Beta-ray spectrometer studies.

The source of ^{133}Ba was obtained by chemical separation from CsCl target bombarded with about 25 MeV protons in the cyclotron of the Oak Ridge National Laboratory. The spectrum of the electrons from this source was

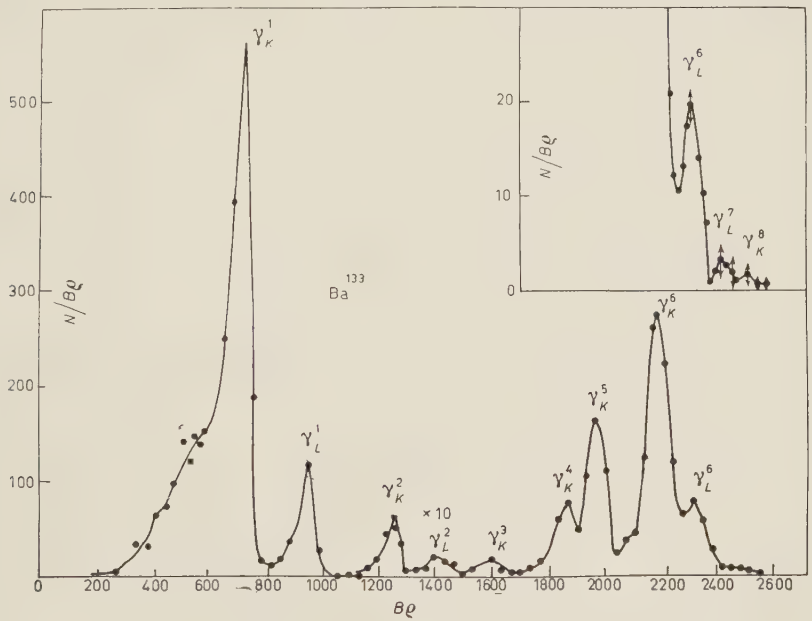

Fig. 1. – The spectrum of electrons from ^{133}Ba taken in a β-ray spectrometer. The main spectrum is a reproduction from our studies with Siegbahn-Slätis β-ray spectrometer. The inset in the figure gives the spectrum of the higher energy electrons taken in a lens spectrometer.

([3]) G. M. Temmer and N. P. Heydenburg: *Phys. Rev.*, **93**, 351 (1954); **104**, 967 (1956).

([4]) L. W. Fagg: *Bull. Am. Phys. Soc.*, **2**, No. 4, 207 P_2 (1957).

studied in the Siegbahn-Slätis type intermediate focussing β-ray spectrometer and in a lens spectrometer ([5]). The spectrum is reproduced in Fig. 1. The high energy portion of the spectrum studied in the lens spectrometer is reproduced in the inset of the Fig. 1.

The results of β-ray spectrometer measurements are summarized in Table I.

TABLE I.

Electron line energy in keV	Possible assignment	γ-ray energy in keV	Relative intensity	Notation in Fig. 1
42.6	K conversion	78.6	100	γ_K^1
72.9	L »	78.6	14.7	γ_L^1
124.3	K »	160.3	0.25	γ_K^2
153	L »	158.7	0.06	γ_L^2
188.3	K »	224.3	0.06	γ_K^3
241	K »	277	0.5	γ_K^4
266	K »	302	1.08	γ_K^5
320.5	K »	356.5	2.3	γ_K^6
352.3	L »	358	0.53	γ_L^6
377.2	L »	383	0.08	γ_L^7
401	K »	437	0.04	γ_L^8

In Table I, the first column gives the energy in keV of the electron lines appearing in the spectrum reproduced in Fig. 1, the possible origin of the electron lines is given in column 2. On the basis of the origin of the electron lines given in column 2, the energies of the γ-rays are calculated and are given in column 3. Taking the intensity of the 42.6 keV line to be 100, the relative intensities of the other electron lines are given in column 4. The fifth column gives the notation by which the electron lines are marked in Fig. 1. Due to the thickness of the source, the possible electron lines below 42 keV are not resolved. It may be pointed out that on the basis of our interpretation, the L conversion line of the 277 keV γ-ray is superposed on the K conversion line of the 302 keV γ-ray, the L conversion line of which is not well resolved. The K conversion line of the 383 keV γ-ray falls on the L conversion lines of the 358 keV γ-ray. It may be emphasized that although the counts for the peak γ_k^8 in the inset of Fig. 1 were not large enough to give good statistics, the hump kept appearing in all the runs. This hump has been interpreted as the K conversion line of a γ-ray of energy 437 keV. It is concluded that γ-rays of energy 78.6 keV, 160.3 keV, 224 keV, 277 keV, 302 keV, 357.5 keV, 383 keV and 437 keV are emitted in the decay of ^{133}Ba.

([5]) T. D. NAINAN, H. G. DEVARE and AMBUJ MUKERJI: *Proc. Ind. Acad.*, **44** A, 111 (1956).

3. – Scintillation spectrometer studies.

The γ-ray spectrum of ^{133}Ba source deposited on a mylar film fixed to an aluminium ring, was studied in a NaI(Tl) scintillation spectrometer. In order to prevent the summing of the γ-rays, the source was placed at a distance of 39 mm from the crystal. The spectrum is reproduced in Fig. 2.

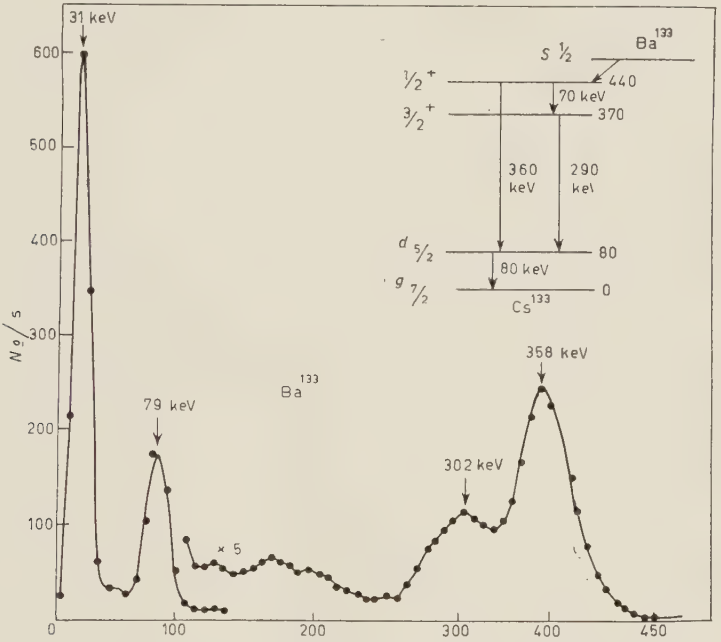

Fig. 2. – The spectrum of γ-rays from ^{133}Ba taken in a scintillation spectrometer. The inset gives the decay scheme proposed by LANGEVIN.

One can see from the spectrum that γ-rays of energy 358 keV, 302 keV, 277 keV, 79 keV and 56 keV are emitted along with 31 keV K X-rays. The 56 keV γ-ray appears better in the spectrum of Fig. 6 and in coincidence experiments which will be discussed later.

In order to get the intensities of the 302 keV and the 277 keV γ-rays, the peak at the 358 keV in Fig. 2 was resolved by making the Gaussian shape fits first for the 358 keV γ-ray and then for the 302 keV γ-ray. In this way one could accommodate a peak for the 277 keV γ-ray also. The intensities of the γ-rays relative to the intensity of the 358 keV γ-ray are given in the Table II. In Table II the intensity of a γ-ray of energy 160 keV also is given. This γ-ray was not observed in the spectrum in Fig. 2. It was observed in the β-ray spectrometer and in the coincidence studies with the scintillation

spectrometer. The intensity of this γ-ray was estimated from coincidence studies. The intensity of 56 keV γ-ray was obtained from the spectrum given in Fig. 6, where 160 mg/cm^2 of Cu were inserted between source and crystal to cut down the high intensity K X-ray for better resolution of the 56 keV γ-ray.

TABLE II.

γ-ray	56 keV	78.6 keV	160.3 keV	277 keV	302 keV	358 keV
Intensity	7.3±2%	45.5±2%	0.4%	3.3±2%	22±2%	100%

4. – Coincidence studies.

The radiation fron ^{133}Ba were studied with two NaI(Tl) scintillation spectrometers in coincidence, with a resolving time of 0.5 μs. The source was mounted on a holder with an anti-Compton shield. The photo-peak of a particular γ-ray was accepted in one channel and the spectrum in coincidence was scanned in the other channel. The spectrum of the γ-rays in coincidence with the 302 keV γ-ray photo-peak in the gate and that with the 358 keV γ-ray photo-peak in the gate are given in Fig. 3*a* and 3*b* respectively.

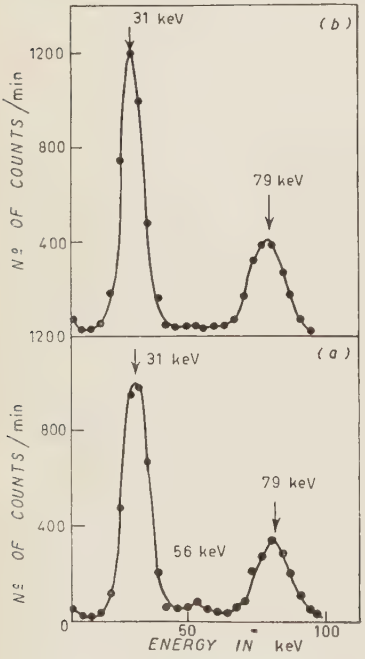

Fig. 3. – *a*) The spectrum of low energy γ-rays in coincidence with the 302 keV γ-ray : *b*) The spectrum of the low energy γ-rays in coincidence with the 358 keV γ-ray.

In coincidence with the 358 keV γ-ray, one gets the 79 keV γ-ray and one can see that the intensity of the scape peak is negligible. In coincidence with the 302 keV γ-ray, one gets a peak at 79 keV and another at 56 keV. This latter peak cannot be explained as anything but a γ-ray peak. In view of this result and the results obtained with the β-ray spectrometer, it is concluded that there is a level in ^{133}Cs at 437 keV which de-excites itself by the emission of 358 keV γ-ray and 79 keV γ-ray in cascade, and that it also de-excites itself by the emission of 56 keV, 302 keV and 79 keV γ-rays in cascade. For accommodating the 277 keV γ-ray observed in the β-ray spectrometer (Fig. 1,

Table I) and suspected in the scintillation spectrometer studies (Fig. 2, Table II), the obvious thing to do is to assume a level in between the ground state and the 437 keV state of ^{133}Cs either at 277 keV or at 160 keV. One would expect to get a 160 keV γ-ray in coincidence with the 277 keV γ-ray. One can see from Fig. 4 and 5 that one does get the 160 keV γ-ray peak in

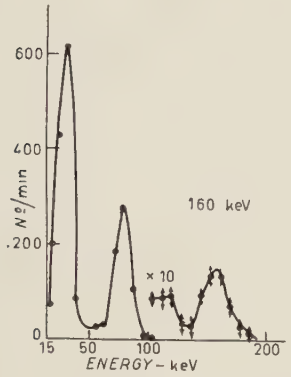

Fig. 4. – The observed peak of the 160 keV γ-ray in coincidence with the 277 keV γ-ray.

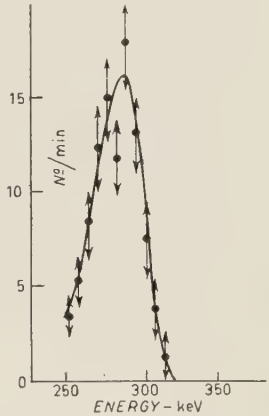

Fig. 5. – The observed peak of the 277 keV γ-ray in coincidence with the 160 keV γ-ray.

coincidence with the 277 keV pulses in the gate, and also the 277 keV γ-ray peak in the coincidence spectrum with the 160 keV pulses in the gate. It is therefore concluded that the 437 keV state in ^{133}Cs has another branching; it de-excites itself also by the emission in cascade of 160 keV and 277 keV γ-rays.

5. – The determination of the decay energy.

The decay energy of ^{133}Ba has been estimated to be less than 40 keV ([2]). This estimate was rather indirect, and involved the accurate knowledge of the intensities of the K X-rays and the γ-rays and their conversion coefficients, and lastly the K fluorescence yield in $_{55}$Cs. The decay energy has been measured here by a combination of the conventional coincidence technique and the summing technique, developed in connection with the determination of the decay energy of $^{196}_{79}$Au ([6]). The decay energy of ^{133}Ba can be calculated ([7]) from the ratio of the probability of the L electron captures and the proba-

([6]) R. K. Gupta: To be published.
([7]) H. Brysk and M. E. Rose: *ORNL* 1830 (January, 1955).

bility of the K electron captures, P_L/P_K. In order to find the ratio P_L/P_K in ^{133}Ba, one needs to know the number of K X-rays in coincidence with the 358 keV γ-ray as well as the 79 keV γ-ray (cf. the decay scheme in Fig. 7). One needs thus to perform a triple coincidence study. Instead, one puts the source on the top of one of the crystals (in a conventional coincidence set up) so that one gets the sum peak of the 79 keV γ-ray and the 358 keV γ-ray at 437 keV. This is shown in Fig. 6.

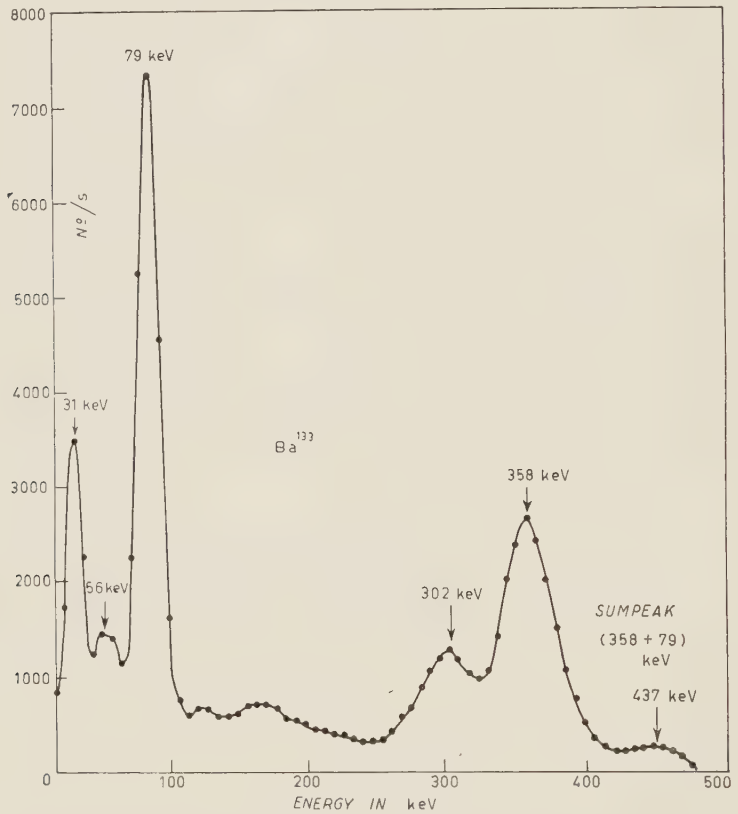

Fig. 6. – The spectrum of γ-rays from ^{133}Ba in a scintillation spectrometer with a copper absorber to cut down the K X-rays. It shows the sum peak of 358 keV and 79 keV γ-rays at 437 keV.

With this sum peak in the gate, the number of coincidence counts were found when the scanning analyser gate was widened to accept the full K X-ray peak. This gave the number of K X-rays in simultaneous coincidence with the 79 keV and the 358 keV γ-rays. The sum peak area is proportional to $I_{\gamma_1\gamma_2}$

$$I_{\gamma_1\gamma_2} = N\varepsilon_{\gamma_1}\varepsilon_{\gamma_2}\delta_1^2(1 - X_1)(1 - X_2) \tag{1}$$

and the number of K X-ray counts found in the coincidence experiment is is proportional to $I_{\gamma_1\gamma_2 X}$

$$I_{\gamma_1\gamma_2 X} = N_K \varepsilon_X \varepsilon_{\gamma_2} \varepsilon \, S_1^2 S_2 \omega_K (1 - X_1)(1 - X_2) \,, \tag{2}$$

where N is the number of disintegrations reaching the 437 keV level per unit time, N_K, the number of K electron captures per unit time leading to the same level. The number of L electron captures per unit time is, therefore, $N_L = (N - N_K)$. ε_{γ_1} and ε_{γ_2} are the efficiencies of the detection of the 79 keV and the 358 keV γ-rays in the crystal where the summing takes place, and ε_X is efficiency of detection of the K X-rays in the scanning crystal; this efficiency is taken to be 1. S_1 is the solid angle subtended by the source at the gate crystal, and S_2 the solid angle subtended at the scanning crystal. X_1 and X_2 are the total conversion probabilities of the 79 keV and the 358 keV γ-rays. The total conversion probability is related to the total conversion coefficient α by the relation

$$X = \alpha/(1 + \alpha)$$

and ω_K is the K fluorescence yield in Cs atoms.

From the relation (1) and (2), one gets

$$(N_K/N) = (I_{\gamma_1\gamma_2 X}/I_{\gamma_1\gamma_2}) \times (1/\omega_K \varepsilon_X S_1) \tag{3}$$

and

$$(P_L/P_K) = \{1 - (N_K/N)\}/(N_K/N) \,, \tag{4}$$

from the relations (3) and (4), the value of P_L/P_K for the transition to the 437 keV state can be calculated, and so one can get the decay energy from the ground state of ^{133}Ba to the 437 keV state of ^{133}Cs (7). In the table below are given the results of a representative measurement.

TABLE III.

Solid angle	Gate counts	Coincidence counts		
S_2	$I_{\gamma_1\gamma_2}$	$I_{\gamma_1\gamma_2 X}$	$I_{\gamma_1\gamma_2 X}/I_{\gamma_1\gamma_2}$	P_L/P_K
0.113	1740	65	0.037	$1.7^{+0.26}_{-0.20}$

From the P_L/P_K value of $1.17^{+0.26}_{-0.20}$ in $^{135}_{56}$Ba, the decay energy comes out to be (53 ± 2) keV. The total decay energy of this isotope is thus (491 ± 4) keV.

6. – The conversion of γ-rays.

The K conversion coefficient and the K/L ratio of the 79 keV γ-ray has been measured both from the decay of ^{133}Ba and the decay of ^{133}Xe; the values found are $\alpha_K = 1.51 \pm 0.15$ ([8]), 1.75 ([1]) and $K/L + M = 4.9 \pm 0.15$ ([8]). In the spectrum reproduced in Fig. 1 the K and L conversion lines of the 79 keV γ-ray are well resolved. The K/L conversion ratio was found from the ratio of the areas of the two peaks. The K conversion coefficient of the 79 keV γ-ray was found by taking the spectrum of the low energy γ-rays and X-rays in coincidence with the 358 keV γ-ray (Fig. 3*b*). The ratio of the K X-ray peak area including the escape peak and the area of the 79 keV γ-ray peak, corrected for the K fluorescence yield in $_{55}$Cs and for K X-rays due to K electron capture, gave α_K for the 79 keV γ-ray. The value of $\alpha_K = 1.5$ found here agreed with the value found by Bergström, but our value of the K/L ratio is some 30% higher. For finding out the conversion coefficient of the 56 keV γ-ray, the low energy γ-ray and the K X-ray spectrum was taken in coincidence with the 302 keV γ-ray (Fig. 3*a*). In this experiment one found the number of 79 keV γ-ray, the number of 56 keV γ-ray and a number of K X-rays due to the internal conversion of these γ-rays. Making corrections for the contribution to the K X-ray intensity from the K conversion of the 79 keV γ-ray and the K capture one got the K conversion coefficient of the 56 keV γ-ray from the ratio of the corrected K X-ray peak area and the 56 keV γ-ray peak area.

From the β-ray spectrometer studies (Fig. 1), one can get the ratio of the intensities of the internal conversion lines. From the scintillation spectrometer studies (Table II) the ratio of the intensities of the unconverted part of the γ-rays were found. From these two sets of values and the known conversion coefficient of the 79 keV γ-ray, the K conversion coefficients of the other γ-rays were found.

In Table IV are given the energy of some of the γ-rays emitted from ^{133}Ba, the theoretical K conversion coefficients of these γ-rays, if they have E_1, M_1 and E_2 character, found by extrapolation from the values of Rose ([9]) and the theoretical K/L conversion ratio ([10]). Comparing these values with the experimentally found values, the multipole character of some of the γ-rays have been suggested.

([8]) I. Bergström: *Arkiv för Fysik*, **5**, 191 (1952).

([9]) M. E. Rose: *Beta and Gamma Spectroscopy*, edited by Kai Siegbahn, Appendix IV.

([10]) M. E. Rose: *Beta and Gamma-Ray Spectroscopy*, edited by Kai Siegbahn, page 410.

TABLE IV.

γ-ray	Theoretical α_K			Theoretical K/L			Experimental		Assigned Multipolarity
Energy	$E1$	$M1$	$E2$	$E1$	$M1$	$E2$	α_K	K/L	assignment
56 keV	0.93	4.2	6.4		—		3.35	—	$M1$
79 keV	0.33	1.55	2.1	7.2	7.5	2	1.5	6.9	$M1$
160 keV	$5.0\cdot10^{-2}$	0.22	0.25	7.5	7.5	3.8	0.4	4	$E2$?
277 keV	$1.0\cdot10^{-2}$	$4.6\cdot10^{-2}$	$4.7\cdot10^{-2}$	—	—		0.106	—	—
302 keV	$8.5\cdot10^{-3}$	$3.8\cdot10^{-2}$	$3.8\cdot10^{-2}$	—	—	—	$2.35\cdot10^{-2}$	—	—
358 keV	$5.2\cdot10^{-3}$	$2.2\cdot10^{-2}$	$2.0\cdot10^{-2}$	7.7	7.5	6.2	$1.65\cdot10^{-2}$	4.35	$E2$?

7. – Decay scheme.

The γ-rays emitted from the electron capture decay of ^{133}Ba can be fitted into a decay scheme given in Fig. 7.

The excited levels of ^{133}Cs as a result of the decay of ^{133}Ba, at 79 keV and 437 keV have been suggested both by LANGEVIN [1] and HAYWARD *et al.* [2]. Our assignment of a level at 381 keV in place of the one at 370 keV agrees with the assignment of HAYWARD *et al.* [2]. In the decay scheme proposed here, a new level at 160 keV has been suggested. If one depended entirely on the results of the coincidence work described above, one could not have been able to decide if this new level was at 160 keV or at 277 keV. In view of the results of Coulomb excitation on ^{133}Cs [3,4]; which gives a γ-ray of 160 keV but not one of 277 keV, it appeared more likely that the 437 keV level de-excites itself by transition to a level at 160 keV. It was then possible to fit the weak intensity 224 keV γ-ray, observed in the β-ray spectrometer, as due to the transition between the 381 keV and 160 keV levels. The β-ray spectrometer evidence for the direct transition from the 381 keV level to the ground level is consistent with the Coulomb excitation result. In the decay

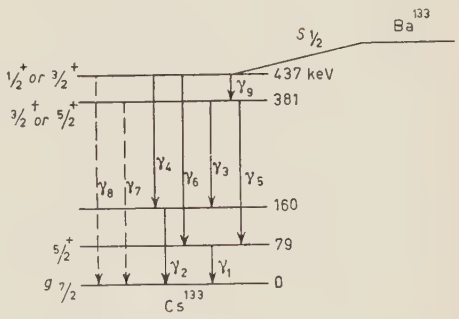

Fig. 7. A tentative decay scheme of ^{133}Ba.

scheme above, a direct transition from the 437 keV level to the ground state has been shown with a dotted arrow because, although a hump was observed (Fig. 1 inset) in the electron spectrum in the β-ray spectrometer, an evidence for the occurrence of the unconverted part of this γ-ray could not be obtained from the scintillation spectrometer studies. It was difficult because of the occurrence at this energy of the sum peak of the high intensity 79 keV γ-ray and the 358 keV γ-ray. By cutting down the intensity of the 79 keV γ-ray with critical absorbers, all one could gather was that the intensity of the 437 keV γ-ray could not be more than about 5 per thousand disintegrations. It may be pointed out here that the intensity of the unconverted 277 keV γ-ray has been observed to be very much larger than that of the 160 keV γ-ray. Although the intensity figures are not very accurate, it seems that perhaps the 160 keV level decays not only to the ground state but also to the 79 keV state.

The decay energy of the electron capture transition from the ground state of ^{133}Ba to the 437 keV state of ^{133}Cs has been measured to be (53 ± 2) keV. From this value of the decay energy and the half-life of 10 years, the log *ft* value has been calculated to be 5.6. The ground state of ^{133}Ba has been shown to be $\frac{1}{2}^+$ ([11]). Since the log *ft* value is consistent with the allowed character of the electron capture transition, the spin and parity of the 437 keV level of ^{133}Cs are perhaps $\frac{1}{2}^+$ or $\frac{3}{2}^+$. The ground state of ^{133}Cs has a spin and parity $\frac{7}{2}^+$. From the allowed nature of the β-decay of ^{133}Xe the ground state of which is $\frac{3}{2}^+$ to the 79 keV level of ^{133}Cs, one can perhaps conclude that the first excited state of ^{133}Cs is $\frac{1}{2}^+$ or $\frac{3}{2}^+$ or $\frac{5}{2}^+$. From the conversion coefficient of the 79 keV γ-ray, one can conclude that this γ-ray is M_1 in character; and from this one can conclude that the 79 keV state is $\frac{5}{2}^+$. From the conversion coefficient values, it seems likely that the 358 keV γ-ray is E_2 in character. This would then indicate that the 437 keV state is $\frac{1}{2}^+$. The conversion coefficients of the 160 keV γ-ray are not very reliable, but it seems that this γ-ray also is E_2. It seems likely that the 160 keV state is $\frac{3}{2}^+$.

Lastly, it may be pointed out that the findings of LANGEVIN ([1]) and HAYWARD *et al.* ([2]) are different regarding the percentage of electron capture transitions to different levels in ^{133}Cs. It has been estimated that the percentage of electron capture transition to the 381 keV level is not more than about 5%.

([11]) R. D. HILL, G. SCHARFF-GOLDHABER and M. MCKEOWN: *Phys. Rev.*, **84**, 382 (1951).

* * *

Our thanks are due to Mr. K. S. Bhatki who performed the chemical separation for us. We are grateful to Mr. H. G. Devare and Mr. B. N. Subba Rao for their help in β-ray spectrometer work. Our grateful thanks are due to Dr. B. V. Thosar for his help in preparing this paper.

RIASSUNTO (*)

Si presentano i risultati degli studi sul ^{133}Ba eseguiti con lo spettrometro per raggi β e con lo spettrometro a scintillazione. È stato trovato un nuovo livello del ^{133}Cs a 160 keV. Si sono scoperti i raggi γ di energie 56 keV, 79 keV, 160 keV, 224 keV, 277 keV, 302 keV, 358 keV, 383 keV e 437 keV. Si sono stimati i coefficienti di conversione di alcuni dei raggi γ. Con una combinazione della tecnica d'addizione con la tecnica di coincidenza convenzionale si è trovato che il ^{133}Ba decade con l'energia di (53 ± 2) keV allo stato 437 keV del ^{133}Cs con catture di elettroni K (46%) e di elettroni L (54%). Si propone uno schema di decadimento.

(*) *Traduzione a cura della Redazione.*

Electronic Spectra of Mono-, Di- and Tri-Azines of the Naphtalene Series.

G. Favini, S. Carrà, V. Pierpaoli, S. Polezzo and M. Simonetta

Istituto di Chimica Industriale
Laboratorio di Chimica Fisica dell'Università - Milano

(ricevuto l'11 Dicembre 1957)

Summary. — The electronic absorption spectra of quinoline, isoquinoline, quinoxaline, phtalazine, quinazoline and cinnoline were taken. The bands are assigned to the different electronic transitions and for the $\pi - \pi^*$ transitions the experimental results for position and intensity were compared with values from theoretical calculation, to which they closely agreed.

The ultraviolet spectra of quinoline, isoquinoline and benzodiazines have been described by different authors [1] in different solvents, but a complete comparison of the spectra of all these molecules in the same conditions is still lacking. In the present paper the spectra in cyclohexane and in methanol of quinoline, isoquinoline, phtalazine, quinoxaline, quinazoline and cinnoline are presented, the bands are assigned to electronic transitions and the results are compared with positions and intensities predicted for the same electronic transitions by the Pariser and Parr's theory.

1. – Experimental procedure and results.

Materials: quinoline and isoquinoline were pure Eastman Kodak products purified by repeated distillation under vacuum; quinoxaline was a pure « Fluka »

[1] R. A. Friedel and M. Orchin: *Ultraviolet Spectra of Aromatic Compounds* (New York, 1951); H. M. Hershenson: *Ultraviolet and Visible Absorption Spectra* (New York, 1956); A. R. Osborn and K. Shofield: *Journ. Chem. Soc.*, 4191 (1956); R. C. Hirt, F. T. King and J. C. Cavagnol: *Journ. Chem. Phys.*, **25**, 574 (1956).

product, m.p. 27.5 °C; all the other azines were prepared and purified in our laboratory; quinazoline from o-nitrobenzaldehyde according to J. D. RIEDEL [2] (m.p. 48.5 °C); phtalazine from o-phtalic aldehyde, according to GABRIEL and PINKUS [3] (m.p. 91 °C); cinnoline according to DRAKE and PECK [4] (m.p. 38 °C). Eastman Kodak cyclohexane and methanol were used as solvent.

Spectra were obtained by the standard technique [5]; the data are plotted in Fig. 1 to 6, as the log of the molar extinction versus wave length (in Å).

Wave lengths and molar extinctions of the observed bands are collected in Table I; the band origin is also indicated.

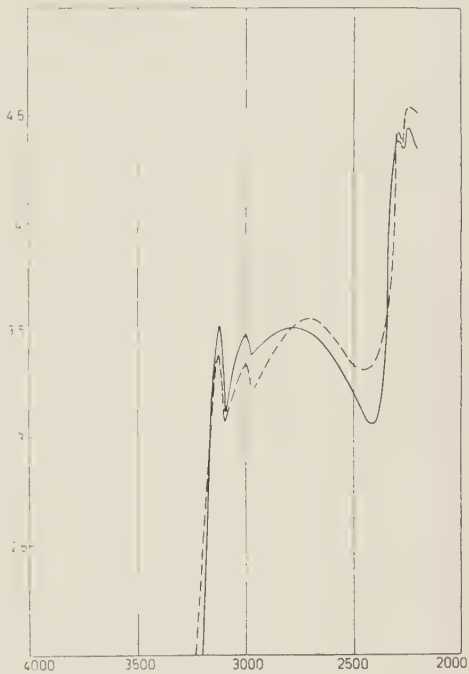

Fig. 1. – Quinoline in: methanol ———; cyclohexane – – – – –.

2. – Theoretical treatment.

The Pariser and Parr approximation of the SCF LCAO MO method has proved to be useful in the interpretation and prediction of electronic absorption spectra of azines [5,6]. To test the soundness of our band assignment to electronic transitions a Pariser and Parr treatment was performed for all the molecules studied. The details of the calculations are not reported here, as the scheme followed was the same as in a previous work [5]. Also the values for all the parameters were already known. The geometry of the molecules was assumed from data for pyridine, pyrimidine and pyrazine by PARISER and PARR [6], on the assumption that in our molecules the benzene ring is a regular hexagon with C-C bond distance equal to 1.39 Å. As starting orbitals naphtalene LCAO molecular orbitals were used [5].

Results are summarized in Table II.

[2] P. FRIEDLÄNDER: *Fortschritte der Teerfarbenfabrikation*, **8**, 1238 (1907).

[3] S. GABRIEL and G. PINKUS: *Ber.*, **26**, 2210 (1893).

[4] N. L. DRAKE and R. M. PECK: *Journ. Am. Chem, Soc.*, **68**, 1313 (1946).

[5] M. SIMONETTA, G. FAVINI, S. CARRÀ and V. PIERPAOLI: *Nuovo Cimento*, **4**, 1364 (1956).

[6] R. PARISER and R. PARR: *Journ. Chem. Phys.*, **21**, 767 (1953).

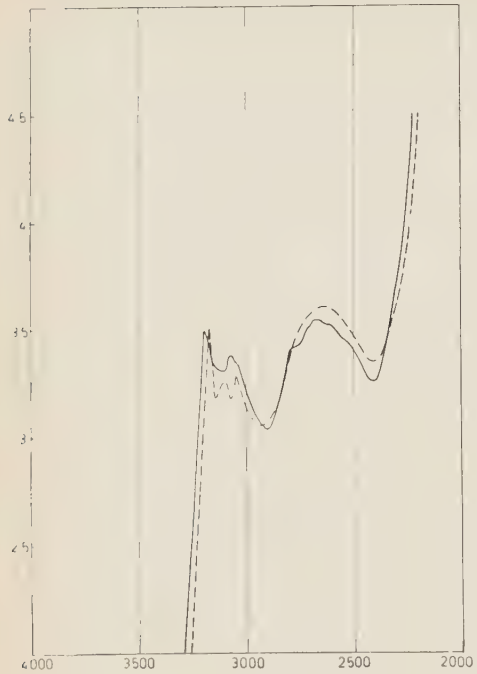

Fig. 2. – Isoquinoline in: methanol ———; cyclohexane – – – –.

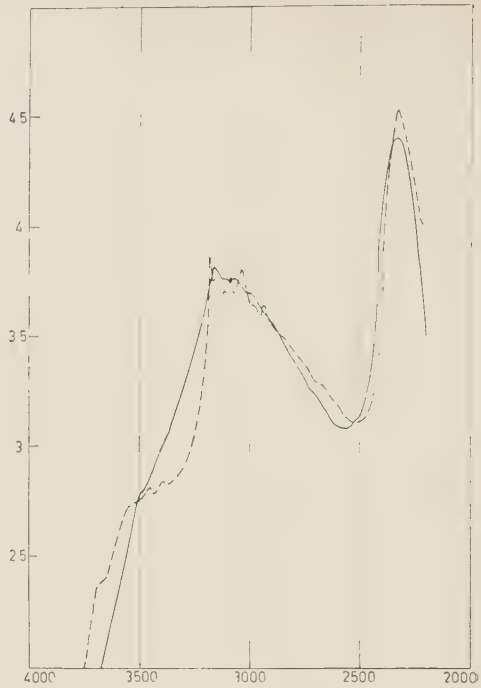

Fig. 3. – Quinoxaline in: methanol ———; cyclohexane – – – – –.

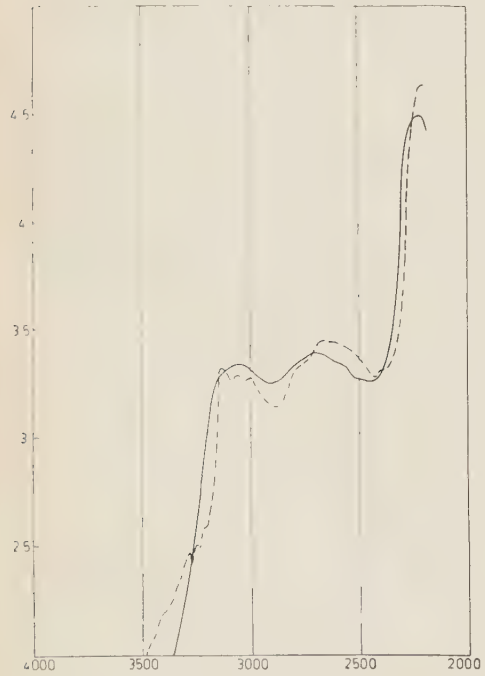

Fig. 4. – Quinazoline in: methanol ———; cyclohexane - - - -.

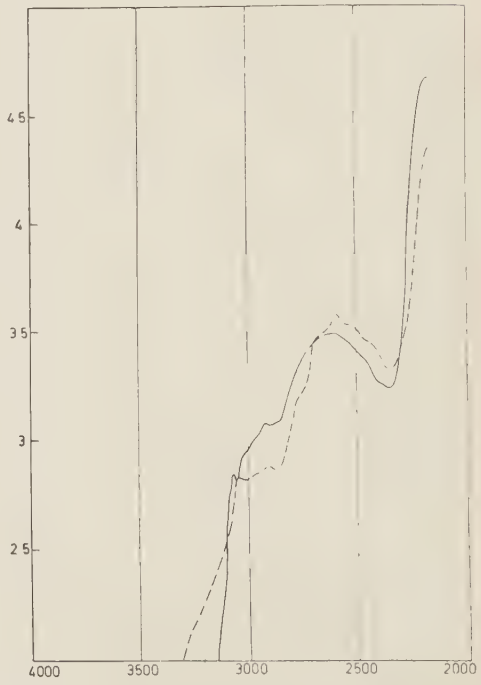

Fig. 5. – Phtalazine in: methanol ———; cyclohexane ———.

TABLE I. – *Observed bands of quinoline, isoquinoline and benzodiazines.*

Compounds	Solvent	Band origin $n - \pi^*$		Band origin $1^\circ\ \pi - \pi^*$		Band origin $2^\circ\ \pi - \pi^*$	
		λ_{max} (Å)	log ε	λ_{max} (Å)	log ε	λ_{max} (Å)	log ε
Quinoline	C	3130	3.344	2700	3.569	2300	4.428
		3000	3.338			2260	4.548
	M	3130	3.428	2775	3.532	2306	4.365
		3000	3.485			2270	4.425
Isoquinoline	C	3180	3.509	2650	3.606	2200	4.550
		3110	3.235				
		3050	3.288				
	M	3200	3.497	2680	3.543	2200	4.550
		3060	3.373				
Quinoxaline	C	(3670)	2.400	3170	3.869	2330	4.541
		(3520)	2.750	3080	3.728		
		3450	2.820	3030	3.734		
		3390	2.850	2940	3.650		
	M	—	—	3150	3.809	2340	4.418
Quinazoline	C	3130	3.313	2650	3.445	2180	4.629
		3050	3.293				
		2990	3.285				
	M	3050	3.342	2700	3.394	2210	4.490
Phtalazine	C	3050	2.836	(2680)	3.500	2180	4.350
		(2960)	2.857	2600	3.585		
		2900	2.893	(2520)	3.540		
	M	2920	3.080	2620	3.502	2180	4.670
Cinnoline	C	3925	2.451	2870	3.483	2220	4.663
		3220	3.398	2760	3.515		
		3180	3.300				
		3100	3.353				
	M	3200	3.410	2800	3.395	2250	4.598

C = cyclohexane; M = methanol; ( ) shoulder.

TABLE II. – *Wave functions and state energies* (*).

	ψ_{V_0}	$\psi_{V_{46}}$	$\psi_{V_{35}}$	$\psi_{V_{45}}$	$\psi_{V_{36}}$	Energy (eV)
			A) Quinoline			
ψ_0	0.994 43	—0.001 34	0.001 65	—0.104 55	0.013 06	—0.068 47
ψ_1	0.002 02	0.538 21	—0.842 82	—0.001 41	—0.000 38	4.353 81
ψ_2	0.082 99	—0.011 38	—0.005 53	0.699 39	0.709 80	5.477 06
ψ_3	0.002 63	0.859 34	0.510 99	0.019 07	0.004 79	6.483 40
ψ_4	0.065 06	0.033 10	0.021 86	0.706 98	—0.703 05	7.101 88
			B) Isoquinoline			
ψ_0	0.990 33	—0.052 48	—0.063 81	0.056 74	0.0957 8	—0.117 61
ψ_1	0.025 82	—0.762 60	0.597 72	—0.110 52	—0.219 66	4.382 42
ψ_2	0.113 07	0.294 51	0.034 99	—0.797 58	—0.512 95	5.553 35
ψ_3	0.032 87	0.465 74	0.746 04	—0.090 74	0.466 08	6.517 70
ψ_4	0.068 43	0.335 79	0.283 80	0.583 35	—0.679 50	7.311 40
			C) Quinoxaline			
ψ_0	0.999 98	—0.003 04	0.004 02	—	—	—0.000 11
ψ_1	0.004 95	0.398 51	—0.918 17	—	—	4.140 46
ψ_2	—	—	—	0.681 53	0.731 80	5.494 51
ψ_3	0.001 20	0.917 22	0.398 54	—	—	6.788 84
ψ_4	—	—	—	0.731 80	—0.681 53	7.197 15
			D) Phtalazine			
ψ_0	0.979 96	—0.194 91	—0.041 13	—	—	—0.232 90
ψ_1	0.136 36	0.807 11	—0.574 64	—	—	4.362 65
ψ_2	—	—	—	0.574 67	0.818 37	5.361 58
ψ_3	0.145 26	0.557 43	0.817 41	—	—	6.758 15
ψ_4	—	—	—	0.818 37	—0.574 67	7.050 88
			E) Quinazoline			
ψ_0	0.985 16	—0.052 11	—0.058 47	—0.111 49	—0.104 39	—0.174 02
ψ_1	0.006 16	—0.629 83	0.751 79	—0.156 25	0.116 77	4.433 83
ψ_2	0.129 99	—0.185 26	—0.108 66	0.704 06	0.664 28	5.625 32
ψ_3	0.104 88	0.727 03	0.640 65	0.215 96	0.057 81	6.679 70
ψ_4	0.009 17	0.204 25	—0.071 12	—0.647 20	0.730 94	7.326 32
			F) Cinnoline			
ψ_0	0.985 57	0.010 74	—0.131 49	—0.056 91	0.089 53	—0.163 92
ψ_1	0.120 11	—0.656 25	0.722 84	0.161 35	—0.079 92	4.259 85
ψ_2	0.030 84	0.106 86	0.209 51	—0.798 47	—0.553 33	5.183 66
ψ_3	0.060 54	0.713 14	0.644 65	0.089 94	0.253 18	6.441 38
ψ_4	0.098 06	0.223 33	—0.027 30	0.570 10	—0.784 06	7.202 42

(*) Energies are with reference to zero energy for V_0: Each row gives the coefficients of the configurational functions on the top of columns in the final wave functions listed in the first column.

From the energy values in Table II the energies of the two lowest $\pi \rightarrow \pi^*$ singlet transitions were calculated and from the wave function coefficients the theoretical oscillator strengths for the same transitions were obtained. Results are reported in Table III and compared with experiment.

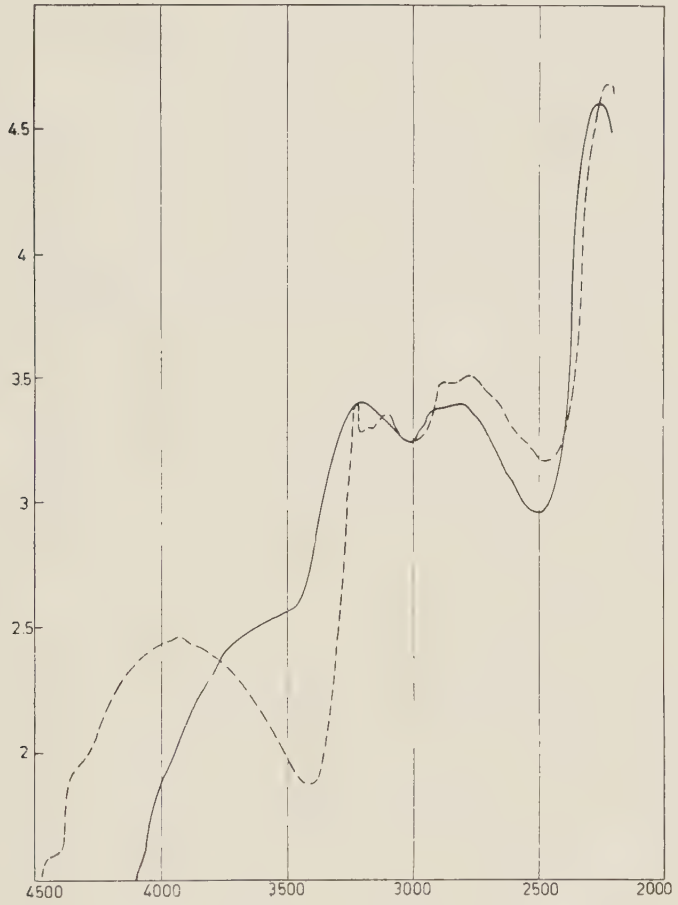

Fig. 6. – Cinnoline in: methanol ———; cyclohexane – – – – –.

For comparison in Table IV energy values, wave functions energy differences and oscillator strengths for benzotriazine, and in Table V ΔE and f for (1,2-e)-as-naphtotriazine and the azines of the benzene series are shown.

Consideration of Tables III, IV and V shows that the differences between calculated and experimental energies is never greater than 12% and that f values are always of the right order of magnitude.

TABLE III. – *Theoretical and experimental energy differences and oscillator strengths for the two lowest singlet transitions.*

Molecule	ΔE_1 (eV)		f_1		ΔE_2 (eV)		f_2	
	calc.	exp.	calc.	exp.	calc.	exp.	calc.	exp.
Quinoline	4.422	4.46	0.076	0.104	5.546	5.45	0.005	0.385
Isoquinoline	4.500	4.63	0.026	0.088	5.671	5.74	0.189	—
Quinoxaline	4.140	3.93	0.208	0.110	5.495	5.31	0.000	0.285
Phtalazine	4.596	4.73	0.033	0.093	5.594	5.69	0.000	(0.410)
Quinazoline	4.608	4.60	0.046	0.068	5.799	5.60	0.112	0.402
Cinnoline	4.424	4.43	0.025	0.064	5.348	5.50	0.161	0.605

TABLE IV. – *Wave functions, energy differences and oscillator strengths for benzotriazine* (*).

	ψ_{V_0}	$\psi_{V_{46}}$	$\psi_{V_{35}}$	$\psi_{V_{45}}$	$\psi_{V_{36}}$	Energy (eV)
ψ_0	0.986 06	0.003 42	—0.123 23	—0.049 57	—0.100 16	—0.147 95
ψ_1	0.105 97	—0.520 28	0.830 33	—0.150 11	0.078 29	4.182 19
ψ_2	0.112 84	0.050 77	0.104 48	0.789 35	0.592 20	5.494 71
ψ_3	0.034 87	0.764 97	0.529 69	0.129 74	—0.340 90	6.835 10
ψ_4	0.050 11	0.377 80	0.058 29	—0.578 14	0.719 10	7.411 90

ΔE_1: calc. 4.330; exp. 4.06 f_1: calc. 0.082; exp. 0.10
ΔE_2: calc. 5.643; exp. 5.37 f_2: calc. 0.073; exp. 0.43

(*) The values reported here are slightly different from values in our previous paper [5] owing to a small numerical mistake discovered in two matrix elements.

TABLE V. – *Energy differences and oscillator strengths for* (1,2-e)-*as-naphtotriazine and azines of the benzene series.*

Molecule	ΔE_1 (eV)		f_1		ΔE_2 (eV)		f_2		Reference
	calc.	exp.	calc.	exp.	calc.	exp.	calc.	exp.	
Pyridine . . .	4.90	4.95	0.046	0.041	—	—	—	—	[6]
Pyrimidine .	5.05	5.15	0.038	—	—	—	—	—	[6]
Pyrazine . . .	4.71	4.77	0.121	0.130	—	—	—	—	[6]
Pyridazine . .	5.15	5.00	0.027	0.019	—	—	—	—	[5]
s-triazine . .	5.29	5.29	0.000	~ 0	—	—	—	—	[6]
(1,2-e-)-as-naphtotriazine	3.73	3.35	0.043	0.058	4.65	4.54	0.130	0.360	[7]

[7] M. SIMONETTA, G. FAVINI and V. PIERPAOLI: *Nuovo Cimento*, **5**, 1814 (1957).

Therefore the Pariser and Parr treatment with the adopted parameter values can be employed with confidence in the prediction and interpretation of the $\pi \rightarrow \pi^*$ singlet transitions in the electronic absorption spectra of all the azines of the benzene and naphtalene series.

RIASSUNTO

Sono riportati gli spettri in metanolo e cicloesano delle seguenti molecole: chinolina, isochinolina, chinossalina, ftalazina, chinazolina e cinnolina. Le varie bande sono assegnate alle opportune transizioni elettroniche; le loro intensità e posizioni sono in accordo con quelle calcolate col metodo degli orbitali molecolari nell'approssimazione di Pariser e Parr.

Parity Violation and the Polarization of Nucleons from Hyperon Decay (*).

J. Leitner

Duke University - Durham, North Carolina

(ricevuto l'11 Dicembre 1957)

Summary. — A general expression for the polarization of nucleons from hyperon decay is obtained. It is shown that this polarization is purely longitudinal in the rest frame of the hyperon. Such longitudinal polarization will have a component transverse to the nucleon momentum in the laboratory system and is thus detectable by means of nuclear scattering.

1. – Introduction.

Dalitz's (1) analysis of K particle decays has shown, subject only to angular momentum and parity conservation, that in spite of the identity of mass and lifetime of the θ and τ mesons, that the latter must be two particles of different spin-parity values. This τ-θ puzzle led Lee and Yang (2) to propose the hypothesis of parity non-conservation in weak interactions. The hypothesis has been partially verified in a series of experiments on β decay (3), π and μ decay (4) and K_{μ} (5) decay. All of these interactions involve neutrino couplings, and the observed parity violation can thus be explained on the basis of the special properties of mass 0 fermion couplings, as developed in the two-component theory (6).

(*) This work is supported by the United States Atomic Energy Commission.

(1) R. Dalitz: *Phil. Mag.*, **44**, 1068 (1953); *Phys. Rev.*, **94**, 1046 (1954).

(2) T. D. Lee and C. N. Yang: *Phys. Rev.*, **104**, 254 (1956).

(3) C. S. Wu *et al.*: *Phys. Rev.*, **105**, 1413 (1957).

(4) R. L. Garwin, L. M. Lederman and M. Weinrich: *Phys. Rev.*, **105**, 1415 (1957).

(5) B. Cork and W. Wentzel: private communication.

(6) T. D. Lee and C. N. Yang: *Phys. Rev.*, **105**, 1671 (1957).

More recently, the domain of verification of the parity non-conservation hypothesis has been extended to include the Λ^0 hyperon decay ([7,8]). Since the Λ^0 decay does not involve a neutrino, the observed parity violation is strong evidence that the parity non-conservation hypothesis holds for all weak interactions. However the Columbia ([7]) and Berkeley ([8]) experiments find no evidence for parity violation in the Σ^- decay. This result is not conclusive, however, since the parity violation is detected by observation of an asymmetry in the decay angular distribution which is present only if the hyperon is polarized at production ([9]).

It is therefore of great interest to find a test of parity non-conservation in hyperon decay which is independent of the hyperon production process. Determination of the nucleon polarization provides such a test.

It is clear that an unpolarized hyperon can have no recollection of its production, and hence that the polarization state of its decay nucleon can depend only on properties of the decay interaction. It is shown below that the decay of an unpolarized beam of spin $\frac{1}{2}$ hyperons, if parity is not conserved, gives rise to purely longitudinally polarized nucleons in the rest system of the hyperon ([10]). It is also shown that the complete sample of hyperons from any production process constitutes such an unpolarized beam; and then the detection of this longitudinal nucleon polarization by means of nucleon scattering, provides an unambiguous method for the detection of parity violation in hyperon decay, independent of the state of hyperon polarization at production.

2. – Nucleon polarization in the decay of polarized spin $\frac{1}{2}$ hyperons.

Consider, for the sake of definiteness, the production and decay processes: $\pi^+ + \mathrm{p} \to \Sigma^+ + \mathrm{K}^+ \to \pi^0 + \mathrm{p} + \mathrm{K}^+$. Let the momentum of the incoming pion in the laboratory system be p_{in}, the momentum of the hyperon be p_{H}, and that of the decay nucleon, in the hyperon rest frame, be p. The production plane is the plane of p_{in} and p_{H}, the decay plane is the plane of p and p_{H}. Then as production frame co-ordinate system, choose x along p_{H}, z along $(p_{\mathrm{H}} \times p_{\mathrm{in}})$ and y perpendicular to p_{H} in the production plane. As decay frame

([7]) F. Eisler *et al.*: *Nevis Laboratory Report* No. 58, to be published (Columbia).

([8]) Crawford *et al.*: to be published (Berkeley).

([9]) T. D. Lee, J. Steinberger, G. Feinberg, P. Kabir and C. N. Yang: *Phys. Rev.*, **106**, 1367 (1957).

([10]) These results have recently been reported by Lee and Yang. They were brought to the author's attention, after the completion of this work, by a private communication (*A Partial Wave Analysis of Hyperon Decay*, to be published) from C. N. Yang.

reference system, choose X along p:, Z along $(p_{\mathrm{H}} \times p)$ and Y in the decay plane, perpendicular to p_{H}.

We will write first the wave function, Ψ, of a hyperon beam with polarization of magnitude P and in the direction of the normal to the production plane, since the production reaction is parity conserving (2). Such a polariezd beam is an incoherent mixture of hyperons of spin up and spin down; then, in the production reference system,

$$\Psi = \begin{pmatrix} \sqrt{\frac{1+P}{2}} & \psi_{\frac{1}{2}}^{\frac{1}{2}} e^{i\gamma} \\ \sqrt{\frac{1-P}{2}} & \psi_{\frac{1}{2}}^{-\frac{1}{2}} \end{pmatrix},$$

where γ is an arbitrary phase factor and $\psi_{\frac{1}{2}}^{\frac{1}{2}}$, $\psi_{\frac{1}{2}}^{-\frac{1}{2}}$ are spin-angle functions for spin up and spin down respectively.

Angular momentum conservation allows only s and p waves to enter into the final state, since the hyperon is assumed to be spin $\frac{1}{2}$. If the s wave amplitude be α, (chosen real) and the p wave amplitude be β, then the expansion into final states takes the following form

$$\psi_{\frac{1}{2}}^{\frac{1}{2}} = \frac{1}{\sqrt{4\pi}} \{(\alpha - \beta \cos \xi)\chi_{\frac{1}{2}} - (\beta \sin \xi) e^{i\eta} \chi_{-\frac{1}{2}}\},$$

$$\psi_{\frac{1}{2}}^{-\frac{1}{2}} = \frac{1}{\sqrt{4\pi}} \{(-\beta \sin \xi) e^{-i\eta} \chi_{\frac{1}{2}} + (\alpha + \beta \cos \xi)\chi_{-\frac{1}{2}}\},$$

where $\chi_{\frac{1}{2}}$ and $\chi_{-\frac{1}{2}}$ are nucleon spinors for spin $\frac{1}{2}$ and spin $-\frac{1}{2}$ respectively and ξ, η are the polar and azimuthal angles of $\boldsymbol{p}$ in the production frame system (PF). The expansion amplitudes for nucleon spin up and down can then be used to write the nucleon wave function, ψ_{N}, in the PF,

$$\psi_{\mathrm{N}}(\xi, \eta) = \frac{1}{\sqrt{4\pi}} \begin{pmatrix} \sqrt{\frac{1+P}{2}} (\alpha - \beta \cos \xi) e^{i\gamma} - \sqrt{\frac{1-P}{2}} (\beta \sin \xi) e^{-i\eta} \\ \sqrt{\frac{1+P}{2}} (-\beta \sin \xi) e^{i(\eta + \gamma)} + \sqrt{\frac{1-P}{2}} (\alpha + \beta \cos \xi) \end{pmatrix}.$$

In order to calculate the nucleon polarization in the decay frame system, (DF), it is convenient to transform the spinor $\psi_{\mathrm{N}}(\xi, \eta)$, via the well known unitary transformation R (11), into $\psi'_{\mathrm{N}}(\Theta, \xi, \eta)$. This transformation corresponds

(11) See, for example, J. Goldstein: *Classical Mechanics* (Cambridge Mass., 1951), p. 97.

to a rotation of co-ordinate system through the Euler angles Θ, $\Phi = \psi = 0$, since the x axis is common to both the PF and DF. Using the right handed convention of Goldstein, one finds

$$R = \begin{pmatrix} \cos \Theta/2 & i \sin \Theta/2 \\ i \sin \Theta/2 & \cos \Theta/2 \end{pmatrix}.$$

Then,

$$\psi'_{\mathrm{N}}(\Theta, \xi, \eta) = R\psi_{\mathrm{N}}(\xi, \eta) ,$$

$\psi'_{\mathrm{N}}(\Theta, \xi, \eta)$ can be written in terms of two independent planar angles, Θ and φ, where Θ is the angle between the production and decay plane normals and φ is the angle between the nucleon momentum and the hyperon momentum. If one does this and calculates the matrix elements of σ_x, σ_y, σ_z, it is easily seen that the nucleon polarization $\boldsymbol{P}$ in the hyperon rest system is

$$\boldsymbol{P} = \left(\frac{A + P \sin \Theta \sin \varphi}{|\psi_{\mathrm{N}}|^2}\right) \hat{p} + \\ + \frac{P\{B \cos \Theta + (1 + |A|^2 + |B|^2) \sin \Theta \cos \varphi\}}{|\psi_{\mathrm{N}}|^2} (\hat{p}_{\mathrm{H}} \times \hat{p}) \times \hat{p} + \\ + \frac{P\{(1 - |A|^2 - |B|^2) \cos \Theta + B \sin \Theta \cos \varphi\}}{|\psi_{\mathrm{N}}|^2} \hat{p}_{\mathrm{H}} \times \hat{p} , \tag{2}$$

where

$$A = -\frac{2 \operatorname{Re}(\alpha\beta^*)}{\alpha^2 + \beta^2} , \qquad B = -\frac{2 \operatorname{Im}(\alpha\beta^*)}{\alpha^2 + \beta^2} ,$$

and $|\psi_{\mathrm{N}}|^2 = 1 + PA \sin \Theta \sin \varphi$, and $\wedge$ indicates a *unit* vector.

Using (2), one sees that the polarization, $\bar{\boldsymbol{P}}$, of the « beam » of nucleons consisting of all nucleons from the hyperon decay averaged over Θ, is

$$\bar{\boldsymbol{P}}(\varphi) = \frac{\int_0^{2\pi} \boldsymbol{P}(\Theta, \varphi) |\psi_{\mathrm{N}}|^2 \, \mathrm{d}\Theta}{\int_0^{2\pi} |\psi_{\mathrm{N}}|^2 \, \mathrm{d}\Theta} = A\hat{p} .$$

3. – Conclusions and discussions.

From (2), the following conclusions follow readily:

a) If the hyperon beam is unpolarized, the nucleon polarization is purely longitudinal in the rest frame of the hyperon and is of magnitude A.

b) Since A is proportional to the product of the opposite parity amplitudes, the nucleon polarization exists only if parity is not conserved in the decay.

The longitudinal polarization (in the DF) has, of course, a component $\boldsymbol{P}_{\perp}$, transverse to the nucleon momentum in the laboratory system and thus can be detected by means of nuclear scattering. In particular, as is well known ([12]), $\boldsymbol{P}_{\perp}$ can be detected by the observation of a term in the angular distribution, of the form $\boldsymbol{N}\cdot\boldsymbol{P}$, where $\boldsymbol{N}$ is the normal to the plane of scattering. Observation of such a term is equivalent to the observation of an asymmetry with respect to the normal to the decay plane, in the distribution of scattered nucleon momenta, $\boldsymbol{p}^1$. From conclusions *a*) and *b*), it follows then that an observation of a correlation of the form $(p_{\mathrm{H}}\times p)\cdot\boldsymbol{p}^1$ is an unambiguous proof of parity non-conservation in hyperon decay. For the case of the Σ hyperons, the results of the Columbia and Berkeley experiments (along with charge independence), indicate that the Σ's are indeed unpolarized at production, and the above experiment can be performed.

From (2) it is clear that the nucleon « beam » consisting of nucleons in events with a given Θ and φ, from polarized hyperon beam decays, has a non-zero polarization whether parity is conserved in the decay or not. However, it should be emphasized that since the detection of the *longitudinal* polarization requires only an observation of the correlation $(p_{\mathrm{H}}\times p)\cdot p'$, it does not involve the angle Θ which indeed specifies the hyperon polarization.

Therefore if one averages over Θ, as is done in (3), one observes, as expected, that the nucleon polarization is $A\hat{p}$ regardless of the state of hyperon polarization at production. It then follows that observation of an asymmetry in the distribution of p^1 with respect to the decay plane normal, is an unambiguous proof of parity violation in hyperon decay, independent of the state of hyperon polarization at production. In fact, the above statement is true, independent of the type of production process, since the hyperon polarization direction is always defined by $p_{\mathrm{H}}\times p_{\mathrm{in}}$ even if the production process involves more than two particles or if the hyperon is scattered in nuclear material before emerging from the production process. A polarization experiment to detect parity non-conservation is then quite feasible for Λ as well as Σ hyperons, from any number of bubble chamber exposures.

Finally, it should be noted that the above results depend only on angular momentum conservation which places no restrictions on the s and p wave amplitudes α and β. It is well known that assumptions as to the invariance of the interaction under symmetry operators, do place restrictions on α and β. In particular, if the hyperon decay interaction is invariant under time re-

([12]) L. Wolfenstein: *Annual Review of Nuclear Science*, **6**, 43 ff. (1956).

versal α and β must both be real ([13]); i.e. A is maximum. Thus, a measurement of the nucleon polarization provides a test of time reversal invariance, as well as parity invariance, in hyperon decay.

* * *

The author would like to express his thanks to Dr. G. FEINBERG for many stimulating discussions on the subjects treated above. He would also like to acknowledge an enlightening discussion with C. N. YANG and to thank him for communication of his results on this problem. The author should like to express his appreciation of helpful discussions with Drs. M. BLOCK, E. GREULING, M. DUNCAN, L. LANDOWITZ and M. SCHWARTZ.

([13]) W. PAULI: *Niels Bohr and the Development of Physics* (1955), p. 30.

RIASSUNTO (*)

Si ottiene un'espressione generale per la polarizzazione dei nucleoni nel decadimento degli iperoni. Si dimostra che tale polarizzazione è puramente longitudinale nel sistema di riposo dell'iperone. Tale polarizzazione longitudinale ha una componente trasversale al momento del nucleone nel sistema del laboratorio ed è pertanto osservabile per mezzo dello scattering nucleare.

(*) *Traduzione a cura della Redazione.*

Higher Order Spinor Lagrangians.

T. W. B. Kibble and J. C. Polkinghorne

Tait Institute of Mathematical Physics - University of Edinburgh, Scotland

(ricevuto il 13 Dicembre 1957)

Summary. — Certain higher order spinor Lagrangians arise naturally in an attempt to write a recent theory of Feynman and Gell-Mann in conventional terms. Their quantization is investigated together with the possible forms for interactions. The theory that seems closest in spirit to that of Feynman and Gell-Mann leads to only a pseudovector interaction with pseudoscalar mesons and a Fermi interaction that is a mixture of A and V.

1. – Introduction.

Feynman and Gell-Mann [1] have recently proposed a universal Fermi interaction that seems to arise most naturally if the fermions are described in terms of the two-component solutions of a second-order equation rather than in terms of the (equivalent) first-order four-component Dirac equation. They introduce quantization by means of Feynman's path integral formalism.

In this paper we wish to discuss the extent to which this scheme may be reproduced in the more conventional terms of the canonical formalism applied to a Lagrangian. If we first consider only free fields the equation to be satisfied is simply

$$(\Box + m^2)\chi = 0 \,. \tag{1}$$

Initially we shall consider a four-component χ and make the reduction to a two-component quantity later. The Lagrangian that corresponds most directly

[1] R. P. Feynman and M. Gell-Mann: *Phys. Rev.*, **109**, 193 (1958).

to equation (1) is

$$-\frac{1}{m}\,\bar{\chi}(\Box + m^2)\chi\,. \tag{2}$$

However it is well known that difficulties with an indefinite metric arise in the quantization of higher order spinor Lagrangians (2). We discuss the quantization of (2) in Sect. **2** and find the form these difficulties take in that case. Another difficulty is that the Lagrangian (2) can not be reduced to a two-component form.

In Sect. **3** and **4** we discuss two other Lagrangians that are connected with linearizations of equation (1) but which are not linearizations of (2). They are in fact limits of linearizations of

$$-\frac{1}{m^2}\,\bar{\chi}\,i\gamma\partial(\Box + m^2)\chi\,. \tag{3}$$

The regular linearizations of (3) have the twin disadvantages of corresponding to an indefinite metric and including the unwanted mass-zero solution of the equation

$$i\gamma\partial(\Box + m^2)\chi = 0\,. \tag{4}$$

It is a remarkable fact that the improper linearizations we discuss have neither disadvantage.

For the first of these linearizations the reduction to two-component form can be made quite simply by replacing (3) by its two-component counterpart

$$-\frac{1}{m^2}\,\chi^{\dagger} i\sigma_\mu\partial_\mu(\Box + m^2)\chi\,, \tag{5}$$

where $\sigma_0 = 1$, and σ_k $(k = 1, 2, 3)$ are the Pauli matrices. However this linearization does not correspond to the way in which Feynman and Gell-Mann construct their solutions and does not lead naturally to their Fermi interaction.

The other linearization is closer to the spirit of their paper. Here the reduction to an effective two-component form must be made using a subsidiary condition.

We also discuss how the interactions may be written in terms of these linearizations. The second linearization seems to exclude a pseudoscalar interaction with pseudoscalar mesons in favour of a pseudo vector interaction. It leads to a Fermi interaction containing A and V only.

(2) Cf. A. Pais and G. E. Uhlenbeck: *Phys. Rev.*, **79**, 145 (1950); R. J. N. Phillips: *Nuovo Cimento*, **1**, 823 (1955).

2. – Second order free Lagrangian.

We consider a four-component $\chi(x)$ satisfying the equation

$$(\Box + m^2)\chi = 0 \,, \tag{6}$$

which may be derived from the Lagrangian

$$-\frac{1}{m}\,\overline{\chi}(\Box + m^2)\chi = 0 \,. \tag{7}$$

A systematic way of using the canonical formalism to obtain the commutation rules is given by the Schwinger principle ([3]). For this purpose it is easier to work with a linearized form of the Lagrangian. The procedure of linearizing the Lagrangian (7) may seem somewhat perverse since (6) was originally obtained by FEYNMAN and GELL-MANN from the Dirac equation, but it is the most systematic way of investigating its properties.

A linearized form of the equations of motion (6) is

$$(i\gamma\partial + m)\chi \;\; = m\psi_1 \,, \tag{8}$$

$$(i\gamma\partial - m)\psi_1 \; = 0 \,. \tag{9}$$

These are in fact the equations originally used by FEYNMAN and GELL-MANN. They may be derived from the Lagrangian

$$-2\overline{\chi}(i\gamma\partial + m)\chi + \overline{\chi}(i\gamma\partial + m)\psi_1 + \overline{\psi}_1(i\gamma\partial + m)\chi - m\overline{\psi}_1\psi_1 \,. \tag{10}$$

This is a true linearization of (7) in the sense that the equation of motion for χ given by (10) is the same as that given by (7), and moreover if a substitution is made for ψ_1 from (8) into (10), the resulting Lagrangian is (7).

The anticommutation relations derived from (10) by the use of the Schwinger principle are

$$\left\{\begin{aligned}
&[\chi(\boldsymbol{x}, t),\ \chi^\dagger(\boldsymbol{x}', t)]_+ = 0 \,, \\
&[\psi_1(\boldsymbol{x}, t),\ \chi^\dagger(\boldsymbol{x}', t)]_+ = \tfrac{1}{2}\delta(\boldsymbol{x} - \boldsymbol{x}') \,, \\
&[\chi(\boldsymbol{x}, t),\ \psi_1^\dagger(\boldsymbol{x}', t)]_+ = \tfrac{1}{2}\delta(\boldsymbol{x} - \boldsymbol{x}') \,, \\
&[\psi_1(\boldsymbol{x}, t),\ \psi_1^\dagger(\boldsymbol{x}', t)]_+ = \;\; \delta(\boldsymbol{x} - \boldsymbol{x}') \,.
\end{aligned}\right. \tag{11}$$

([3]) J. SCHWINGER: *Phys. Rev.*, **82**, 914 (1951); **91**, 713 (1953); T. W. B. KIBBLE and J. C. POLKINGHORNE: *Proc. Roy. Soc.*, A **242**, 252 (1957).

all other equal-time anticommutators vanishing. Equations (6) and (11) yield the four-dimensional anticommutator

$$[\chi(x),\ \chi^{\dagger}(x')]_{+} = \tfrac{1}{2} i m \gamma_0 \Delta(x - x') ,$$

where $\Delta(x - x')$ is the familiar invariant function for mass m.

To find a representation of (11) we write

$$\chi = \tfrac{1}{2}(\psi_1 + \psi_2) , \tag{12}$$

Then relations (11) are satisfied if

$$[\psi_2(\boldsymbol{x}, t),\ \psi_1^{\dagger}(\boldsymbol{x}', t)]_{+} = [\psi_1(\boldsymbol{x}, t),\ \psi_2^{\dagger}(\boldsymbol{x}', t)]_{+} = 0 , \tag{13}$$

and

$$[\psi_2(\boldsymbol{x}, t),\ \psi_2^{\dagger}(\boldsymbol{x}', t)]_{+} = -\delta(\boldsymbol{x} - \boldsymbol{x}') . \tag{14}$$

From (8) and (9), ψ_2 satisfies the equation

$$(i\gamma\partial + m)\psi_2 = 0 . \tag{15}$$

These results are hardly surprising, as the solutions of (6) are clearly connected with the Dirac equations for both positive and negative mass. If we substitute (12) into (10) we obtain

$$\overline{\psi}_1(i\gamma\partial - m)\psi_1 - \overline{\psi}_2(i\gamma\partial + m)\psi_2 , \tag{16}$$

a superposition of the two first order Dirac Lagrangians for masses $+m$ and $-m$. However these two Lagrangians appear in (16) with opposite sign and it is this fact that yields the negative sign on the right side of (14). This implies that the field ψ_2 is quantized with a negative metric, producing an indefinite metric ([2]) for the χ field. The corresponding negative probabilities can be removed by redefining the scalar product in Hilbert space, replacing $\langle\alpha|\beta\rangle$ by $\langle\alpha|(-1)^{n_2}|\beta\rangle$, where n_2 is the number operator for the ψ_2 field.

The Lagrangian (10) has the additional disadvantage that it cannot be written in terms of a purely two-component χ. If we set

$$\chi_{\pm} = \tfrac{1}{2}(1 \pm i\gamma_5)\chi , \tag{17}$$

then the term $\overline{\chi} m \chi$ couples χ_+ to χ_-. If we wish to remove one of these fields

this can therefore only be done by a subsidiary condition of the form

$$\begin{cases} \chi_-^{(+)}|\rangle = 0\,, \\ \overline{\chi_-^{(-)}}|\rangle = 0\,. \end{cases} \tag{18}$$

Clearly it would be an advantage to be able to write a Lagrangian in terms of a purely two-component χ, thus avoiding the necessity of introducing a subsidiary condition. The possibility of doing this will be considered in the next section.

3. – Two-component Lagrangian.

Rather than impose a subsidiary condition (18), we might start from a two-component χ satisfying (6). However it is now impossible to derive this equation from a Lagrangian of the form (7). In order to see what Lagrangian we may use we consider the linearization of (6)

$$i\sigma_\mu \partial_\mu \chi = m\varphi\,, \tag{19}$$

$$i\sigma'_\mu \partial_\mu \varphi = m\chi\,, \tag{20}$$

where $\sigma_0 = \sigma'_0 = 1$ and $\sigma_k = -\sigma'_k$ are the three Pauli spin matrices. These equations may be derived from the Lagrangian

$$\chi^\dagger i\sigma\partial\chi + \varphi^\dagger i\sigma'\partial\varphi - m\chi^\dagger\varphi - m\varphi^\dagger\chi\,. \tag{21}$$

This however is not a linearization of a second order Lagrangian. Indeed, if we substitute for φ from (19) into (21) we obtain the third-order Lagrangian

$$-\frac{1}{m^2}\,\chi^\dagger i\sigma\partial(\Box + m^2)\chi\,. \tag{22}$$

The simplest linearized Lagrangian corresponding to (22) is given by

$$\chi^\dagger i\sigma\partial\chi + \varphi^\dagger i\sigma'\partial\varphi - m\chi^\dagger\varphi - m\varphi^\dagger\chi + \lambda(m\xi^\dagger\varphi + m\varphi^\dagger\xi - \xi^\dagger i\sigma\partial\chi - \chi^\dagger i\sigma\partial\xi) \tag{23}$$

for any non-zero value of λ. The equations of motion are then

$$i\sigma\,\partial\chi = m\varphi\,, \tag{24}$$

$$i\sigma'\partial\varphi = m\chi + \lambda m\xi\,, \tag{25}$$

$$i\sigma\,\partial\xi = 0\,. \tag{26}$$

Substituting from (24) and (25) in (23) yields (22) so that (23) is certainly a true linearization of (22). It yields commutation relations corresponding to an indefinite metric. A change from one finite value of λ to another is evidently a trivial change in the normalization of ξ. However the Lagrangian (21) corresponds in some sense to taking an improper limit $\lambda \to 0$ in (23). The taking of this limit is of course not a strictly permissible procedure, in view of the fact that λ^{-1} appears in the commutation relations; and (21) will therefore be termed an *improper linearization* of (22). It is remarkable that the choice of the Lagrangian (21) avoids both the difficulties of an indefinite metric and of the extra mass-zero field ξ which occurs for (23) with non-zero λ.

However, the Lagrangian (21) is merely the Dirac Lagrangian

$$\psi^\dagger \gamma_0 (i\gamma\partial - m)\psi \tag{27}$$

written in terms of two-component spinors, and correspondingly the equations (19) and (20) do not give a preferred position to either χ and φ. This linearization is not at all close to the spirit of Feynman and Gell-Mann, in that they start by assigning a preferred position to one two-component spinor. We therefore seek a linearized Lagrangian which gives the equations of motion in the form (8) and (9) but avoids the difficulties of an indefinite metric.

4. – Third order free Lagrangian.

A Lagrangian which satisfies the requirements stated is

$$2\bar{\chi}(i\gamma\partial + m)\chi + \bar{\psi}_1 i\gamma\partial\psi_1 - \bar{\chi}(i\gamma\partial + m)\psi_1 - \bar{\psi}_1(i\gamma\partial + m)\chi\,. \tag{28}$$

The equations of motion are (8) and (9) and the commutation relations are

$$\begin{cases} [\chi(\boldsymbol{x}, t),\ \chi^\dagger(\boldsymbol{x}', t)]_+ = \tfrac{1}{2}\delta(\boldsymbol{x} - \boldsymbol{x}')\,, \\ [\psi_1(\boldsymbol{x}, t),\ \chi^\dagger(\boldsymbol{x}', t)]_+ = \tfrac{1}{2}\delta(\boldsymbol{x} - \boldsymbol{x}')\,, \\ [\chi(\boldsymbol{x}, t),\ \psi_1^\dagger(\boldsymbol{x}', t)]_+ = \tfrac{1}{2}\delta(\boldsymbol{x} - \boldsymbol{x}')\,, \\ [\psi_1(\boldsymbol{x}, t),\ \psi_1^\dagger(\boldsymbol{x}', t)]_+ = \delta(\boldsymbol{x} - \boldsymbol{x}')\,, \end{cases} \tag{29}$$

all other equal-time anticommutators vanishing. Equations (8) and (9) then yield the four-dimensional anticommutator

$$[\chi(x),\ \chi^\dagger(x')]_+ = \tfrac{1}{2}\gamma\partial\gamma_0\Delta(x - x')\,. \tag{30}$$

If as in Sect. **2** we write

$$\chi = \tfrac{1}{2}(\psi_1 + \psi_2) ,$$

then (13) is satisfied but (14) becomes

$$[\psi_2(\boldsymbol{x}, t), \psi_2^\dagger(\boldsymbol{x}', t)]_+ = \delta(\boldsymbol{x} - \boldsymbol{x}') . \tag{31}$$

Again, ψ_2 satisfies (15) and the Lagrangian (28) becomes

$$\bar{\psi}_1(i\gamma\partial - m)\psi_1 + \bar{\psi}_2(i\gamma\partial + m)\psi_2 . \tag{32}$$

The Lagrangian (28) is an improper linearization of the four-component Lagrangian corresponding to (22), namely

$$-\frac{1}{m^2}\bar{\chi}i\gamma\partial(\Box + m^2)\chi , \tag{33}$$

since it may be obtained be taking the improper limit $\lambda \to 0$ in

$$\begin{aligned} 2\bar{\chi}(i\gamma\partial + m)\chi + \bar{\psi}_1 i\gamma\partial\psi_1 - \bar{\chi}(i\gamma\partial + m)\psi_1 - \bar{\psi}_1(i\gamma\partial + m)\chi + \\ + \lambda\{m\bar{\psi}\xi + m\bar{\xi}\psi - \bar{\xi}(i\gamma\partial + m)\chi - \bar{\chi}(i\gamma\partial + m)\xi\} , \end{aligned} \tag{34}$$

which for non-zero λ is a true linearization of (33) and yields an indefinite metric.

Unfortunately, although (33) may be written in the two-component form (22), its improper linearization (28) cannot. Thus if we wish to have a Lagrangian which gives directly the equations of motion (8) and (9) we must use the four-component forms (33) and (28). The two-component form (22) allows only the (improper) linearization (21), not (28). Therefore we shall continue to use the four-component form (33) and remove the unwanted components of χ by a subsidiary condition.

The fields $\chi_\pm$ defined by (17) satisfy the commutation relations

$$\begin{cases} [\chi_+(x), \chi_+^\dagger(x')]_+ = \tfrac{1}{4}(1 + i\gamma_5)\gamma\partial\gamma_0\Delta(x - x') , \\ [\chi_-(x), \chi_-^\dagger(x')]_+ = \tfrac{1}{4}(1 - i\gamma_5)\gamma\partial\gamma_0\Delta(x - x') , \\ [\chi_+(x), \chi_-^\dagger(x')]_+ = [\chi_-(x), \chi_+^\dagger(x')] = 0 . \end{cases} \tag{35}$$

Thus the fields $\chi_\pm$ are both dynamically and kinematically independent and it is therefore consistent to impose the subsidiary condition (18) on all physical states.

We now define a field ψ by

$$m\psi = \sqrt{2}\,(i\gamma\partial + m)\chi_+ , \tag{36}$$

which therefore satisfies the Dirac equation (9) and the commutation rules

$$[\psi(x),\ \psi^\dagger(x')]_+ = (\gamma\partial - im)\gamma_0\Delta(x - x') . \tag{37}$$

Comparing (35) and (37) we see that although χ_+ possesses a definite « handedness », ψ constructed from it does not.

One could of course define another field ψ' by

$$m\psi' = \sqrt{2}\,(i\gamma\partial + m)\chi_- ,$$

but if physical states contain no quanta of the χ field then they cannot contain any of the ψ' field either, and so ψ' is not of physical interest.

5. – Interactions.

We may consider how to form interaction terms by first considering bilinear spinor expressions of the form

$$\overline{\chi}B_1\chi + \overline{\chi}B_2\psi_1 + \overline{\psi}_1B_2\chi + \overline{\psi}_1B_3\psi_1 . \tag{38}$$

The B's appearing in (38) may be functions of position and depend upon Bose field operators. The Lagrangian (28)+(38) gives the equations

$$(i\gamma\partial - m)\psi_1 = (B_1 + 2B_2)\chi + (B_1 + 2B_3)\psi_1 , \tag{39}$$

$$(i\gamma\partial + m)\chi \ = m\psi_1 + (B_1 + B_2)\chi + (B_2 + B_3)\psi_1 . \tag{40}$$

If we want equation (39) to be just an equation for ψ_1 and so impose the condition (*) (+)

$$B_1 + 2B_2 = 0 . \tag{41}$$

(*) It is interesting to note that in terms of the indefinite metric quantization of Sect. 2 (41) is just the condition that there are no cross terms between the ψ_1 and ψ_2 fields, i.e. the condition that the redefinition of the scalar product removes all negative probabilities.

(+) This condition is only strictly necessary for parity conserving interactions. The interaction proposed by FEYNMAN and GELL-MANN is obtained by taking $B_2 = B_3 = 0$, and B_1 constructed from the χ's of the other two fields participating in the four-field Fermi interaction. After the subsidiary condition has been imposed χ is effectively $\frac{1}{2}(1 + i\gamma_5)\psi_1$.

Furthermore, so that we may obtain an equation for χ alone by elimination between (39) and (40) we also impose the condition

$$B_2 + B_3 = 0 \,. \tag{42}$$

The form of (38) that we consider is simply

$$2\overline{\chi}B\chi + \overline{\psi}_1 B\psi_1 - \overline{\chi}B\psi_1 - \overline{\psi}_1 B\chi \,. \tag{43}$$

The resulting equation for χ is

$$(\Box + m^2)\chi = (Bi\gamma\partial + i\gamma\partial B)\chi + B^2\chi \,. \tag{44}$$

If this is to be consistent with the subsidiary condition removing the field χ_- from physical states we require that B should contain a linear combination of γ_μ and $\gamma_\mu\gamma_5$ only. In this way we may introduce the interaction with the electromagnetic field, A_μ, and a pseudovector interaction with a pseudoscalar meson field, Φ, by writing

$$B = -e\gamma_\mu A_\mu + ig\gamma_\mu\gamma_5\partial_\mu\Phi \,. \tag{45}$$

It does not seem possible however to introduce a pseudoscalar coupling to Φ and simultaneously to reduce χ to a two-component quantity.

If the Fermi-interactions are thought of as occurring through a coupling with an intermediate very heavy meson the considerations given above, show that they must be a combination, in general parity non-conserving, of A and V and no other invariants. We are led to the unique form (A-V) obtained by FEYNMAN and GELL-MANN by writing an interaction involving χ only.

The (A-V) interaction corresponds to the addition for the term

$$\chi_1^\dagger\sigma_\mu\chi_2\chi_3^\dagger\sigma_\mu\chi_4 \tag{46}$$

to the Lagrangian (21). However we are unable to suggest why, in terms of our formalism, φ should not appear in the weak interaction Lagrangian. One might argue that χ is to be taken as fundamental and φ treated as « derivative » but the choice between χ and φ is arbitrary and the parity conserving strong interactions require the presence of both.

6. – Discussion.

In a conventional form of theory, it is necessary that we should be able to write down a Lagrangian, and if we are to regard χ as the fundamental quantity, it must be expressible in terms of χ. If this Lagrangian is linearized

it must involve some other quantity besides χ, just as $F_{\mu\nu}$ appears in the linearized electromagnetic Lagrangian in addition to A_μ. The most natural choice from the present point of view would appear to be ψ_1. However, it does not seem possible to express the Lagrangian in terms of ψ_1 and a two-component χ, so that the difficulties of a subsidiary condition appear.

The only perfectly consistent Lagrangian which can be written down, involving all interactions, is that in terms of χ and φ, i.e. the usual Dirac Lagrangian in terms of two-component spinors. The problem here is that the free Lagrangian is perfectly symmetric with respect to χ and φ (apart from the trivial sign of the spin matrices), so that there is no apparent reason for giving χ a preferred position.

* * *

We wish to thank Dr. R. SHAW and Dr. J. C. TAYLOR for a most stimulating correspondence. One of us (T.W.B.K.) wishes to thank the Department of Scientific and Industrial Research for a maintenance allowance.

RIASSUNTO (*)

Nel tentativo di mettere in termini convenzionali una recente teoria di Feynman e Gell-Mann sorgono spontaneamente alcuni lagrangiani spinoriali di ordine superiore. Si esamina la loro quantizzazione assieme alle possibili forme per le interazioni. La teoria che, nello spirito, appare essere la più prossima a quella di Feynman e Gell-Mann conduce solamente a un'interazione pseudovettoriale con mesoni pseudoscalari e a un'interazione di Fermi che è un miscuglio di A e V.

(*) *Traduzione a cura della Redazione.*

Antiprotons in Nuclear Emulsions (*).

A. G. Ekspong, S. Johansson and B. E. Ronne

Institute of Physics - Uppsala, Sweden

(ricevuto il 29 Dicembre 1957)

Summary. — In one stack of nuclear emulsions exposed at the Bevatron, Berkeley, we have found 10 events identified as due to antiprotons. The interaction characteristics have been analyzed and are reported. Of special interest is the observation of an elastic collision between an antiproton and a free proton.

1. – The experiment and the scanning.

In the joint exposure of nuclear emulsions to antiprotons set up and carried out by the Berkeley groups in May 1956, we had one stack exposed which has been examined at the Physics Institute in Uppsala. The stack consisted of 120 pellicles, 4 in. × 7 in., 600 μm thickness. The thickness of each individual sheet was measured prior to exposure. The average thickness being 616 μm. The beam momentum was 700 MeV/c in the reference orbit. The stack was positioned with its center line 4 in. from the reference orbit on the higher momentum side. The momentum at the center of our stack being 720 MeV/c. The exposure time was 2.5 hours and the number of 6.2 GeV protons on the target $\simeq 1.5 \cdot 10^{13}$. The beam into the stack contains on the average $0.88 \cdot 10^5$ pions/cm^2. Our observation of 10 antiprotons thus corresponds to a ratio of 1 antiproton in 650 000 pions. Applying a correction for scanning loss (discussed below) the ratio is 1:550 000.

The scanning method has been « along-the-track » scanning starting 3 mm from the leading edge of the plate. All tracks were recorded which had a

(*) Research supported in part by contract AF61(514)-1015 with the Air Research and Development Command, USAF, through its European Office.

grain density relative to minimum grain density in the same plate of 2.0 ± 0.4 and with entrance angles within $\pm 5°$ of the beam direction as measured in the same plate. Occasionally tracks with greater divergence were recorded. The grain density of minimum ionization has been found quite constant throughout the stack; the gap coefficient is 180 mm^{-1}.

The stack has been completely scanned twice. In the first search 7 antiprotons were found, in the second search 3 more. The total number being 10 antiprotons. Judging from the experience of the two scanning runs one may estimate the scanning efficiency to about 60% or 70%. In scanning twice the effective scanning has then been 85-90%. We thus estimate the loss to 1 or 2 antiprotons in the whole stack.

2. – Antiproton identification and interactions.

Ten p^- have been identified by mass measurements and in that they give rise to stars with a visible energy which is greater than their kinetic energies. All of these tracks which correspond to positively identified antiprotons enter the stack with less than $\pm 0.5°$ angle to the beam direction as defined by 10 pions entering the stack at the same point as the track under investigation. The grain density was also close to $2.0 \times g_{\min}$ (within 5%).

We have also three more events which fulfill the above stringent entrance criteria. Two of the particles come to rest without interacting. They might be due to a background of positive protons or to antiprotons which give rise to no visible tracks. The third track gives rise to a small star after 9 cm path length. Mass measurements show that the particle is probably a deuteron.

Of the 10 identified antiprotons, 7 annihilate in flight and 3 at rest. We have carried out a special investigation to determine whether the last three antiprotons really reached the end of their path before annihilating or if they interacted in flight at low velocity. To do this we measured the length of all gaps between grains in the last 400 μm of the antiproton tracks. Positive protons were measured in the same way for calibration purposes. The measurements give as values for the rest ranges the negative lengths: -30 μm, -40 μm, and -40 μm respectively. The standard deviation is about ± 50 μm. Within the limits of experimental accuracy we conclude that all three antiprotons annihilated at rest. The total observed path length of antiprotons is 106.7 cm. For a computation of the mean free path in the energy interval between 230 MeV and 20 MeV we need the corresponding observed path which is 106.2 cm. The mean free path found by us is thus $\lambda = (15.2 \pm 5.8)$ cm, which corresponds to a cross-section $\sigma/\sigma_0 = 2.5 \pm 0.9$, where σ_0 is calculated for emulsion on the basis of a nuclear radius $R = 1.2 A^{\frac{1}{3}}$ fermis.

3. – Elastic p^--p^+ collision.

One event, number 6-6, was found which is interpreted as an elastic collision between the antiproton and a free proton of the emulsion. Such events are of extreme importance as the observation of many such events will enable us to calculate the elastic cross-section. Our measurements on this event constitute a proof that the interpretation is correct. We have also looked into the problem of determining the mass of the antiproton by a careful analysis of this event.

The antiproton, number 6-6, entered the emulsion stack with correct entrance criteria. After a path length of 6.39 cm it was scattered 21.3° and was finally captured in flight after an additional path length of 5.17 cm giving rise to an annihilation star. At the scattering point another track started which was found due to a proton.

The proton stopped in the emulsion with a range of 2.96 mm. The plane of the scattering event makes an angle of 47° with the plane of the emulsion. The coplanarity of the three tracks has been carefully measured. As a measure of lack of coplanarity we have taken the angle which any one of the three tracks forms with the base of the scattering tethraedron. This tethraedron has its top corner at the collision point and its base plane such that equal lengths are cut of all three tracks. Our measurements yielded the result that this angle is $\Delta = 0.02° \pm 0.07°$, thus consistent with coplanarity.

We measured all angles between the tracks and also the range of the proton. The latter was found to be $R = 2.956$ mm. Our emulsion density at exposure was (3.92 ± 0.02) g/cm^3. Converting the range to standard emulsion density and using the range-energy relation [1] we get the energy for this proton: $T = (26.40 \pm 0.25)$ MeV. The error is the standard deviation and takes into account the errors of the density measurements and the straggling. This error in T contributes by only 0.2% in the mass error of the antiproton. Of greater importance in a mass measurement from a collision event is the accuracy of the scattering angles. Besides the errors of measurement there are many factors which will have changed these angles since the exposure. Table I summarizes the various types of errors which we have considered and also their respective contribution to the error in the computed antiproton mass in our case.

We have made corrections for distortion (both first and second order), shrinkage of the emulsion, and for thermal drift of the microscope during measurements. The errors in the Table are the remaining estimated errors. The space angles were measured four times in each of two different ways and

(1) W. H. Barkas: UCRL-3769, April 9, 1957.

the final result after corrections is:

Scattering angle of p^-: $\omega = 21.28^\circ \pm 0.18^\circ$,

Space angle between outgoing p^- and p^+: $\omega = 89.25^\circ \pm 0.30^\circ$.

The scattering angle in the center of mass system is: $\omega^* = 45.8^\circ$.
The kinetic energy of the antiproton in the lab. system was 185 MeV.

TABLE I.

Type of error	Contribution to error in p^- mass
Range error of proton	0.2%
Error in shrinkage factor	0.7%
Error due to multiple scattering	3.0%
Error due to distortion	2.0%
Error in angle measurement	2.0%
Total error	4 %

The mass of the antiproton number 6-6 is then $m_{p^-} = (0.90 + 0.04)$ proton masses. It should be mentioned that the distortion correction was of considerable magnitude. Before this correction was applied the mass value was 1.03 proton masses. The best mass value for the antiproton has an error of about 3% ([2]). In order to achieve a superior mass measurement in a collision event several of the errors in the Table have to be reduced. Such would be the case if the plane of the event closely coincided with that of the emulsion, because then the distortion correction and its uncertainty would be greatly reduced. A similar statement holds for the shrinkage of the emulsion. It seems to us that a favorable collision event would permit the mass of the antiproton to be determined with an error less than 1%.

4. – The annihilation stars.

The identity of each track emitted has been established by various combinations of range, ionization, and multiple scattering measurements. Below twice minimum we generally measure ionization by blob count, above this value by the method of gap coefficient. Particles at or near minimum ioniz-

([2]) W. H. BARKAS *et al.*: *Phys. Rev.*, **105**, 1037 (1957).

ation have been assumed to be pions. Table II lists the stars with their total energy E_{vis} in charged particles and also the number of charged pions and heavy prongs, mainly protons. The energy release in visible prongs is generally only a fraction of the total available energy W. The missing energy is attributed to neutral radiation. Fig. 1 is a graph showing the fraction E_{vis}/W for every star.

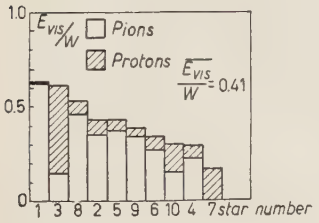

Fig. 1. – The fraction of the total energy emitted as charged particles.

The total number of charged pions is 22 in 10 stars, i.e. (2.2 ± 0.5) charged pions per star on the average. This figure does not include the number of reabsorbed pions. The energy distribution of the pions is plotted in Fig. 2. We have four tracks where we have given only a lower limit to the energy. These (cross hatched in Fig. 2) have been distributed above this limit in the same proportion as those measured. The average pion kinetic energy comes out as $\overline{T}_{pion}=128$ MeV.

TABLE II. – *Data on the antiproton annihilation stars.*

Columns 2 and 3 list the number of charged pions N_π and heavy prongs N_H: Columns 4, 5, and 6 list the total energy per star emitted in charged pions E_π, in heavy prongs E_H, and the total visible energy $E_{vis}=E_\pi+E_H$. Column 7 gives the kinetic energy of the antiproton T_{p^-} at the interaction. Column 8 gives the total visible energy expressed as a fraction of the total available energy W.

Star-number	N_π	N_H	E_π MeV	E_H MeV	E_{vis} MeV	T_{p^-} MeV	E_{vis}/W
6– 1	4	1	1144	31	1175	0	0.63
6– 9	3	1	645	85	730	53	0.38
6– 8	3	4	935	144	1079	150	0,53
6– 5	3	3+2 rec	688	110	798	0	0.43
6– 2	3	7	709	165	874	153	0.43
6– 4	2	5	421	113	534	0	0.29
6– 6	2	7	515	145	660	47	0.34
6–10	1	10	315	292	607	184	0.30
6– 3	1	15	290	900	1190	96	0.61
6– 7	0	10	0	346	346	210	0.17

The number of pions and their energy as observed are not the same as in the elementary annihilation process. In order to correct the number of pions and their average energy we need to know the nuclear excitation. The energy transferred to the nucleus is divided into two parts, the knock-on part $U_{k.o.}$ and the evaporation part $U_{ev.}$. The knock-on part is computed from all protons

above 40 MeV kinetic energy to which are added the neutrons with the same energy distribution. The number of neutrons is taken as 1.2 times the number of protons. We find $U_{\text{k.o.}} = 145$ MeV per star. The evaporation part $U_{\text{ev.}}$ has been estimated in two ways. In Fig. 3 we have tried to fit a curve calculated from evaporation theory to the proton spectrum. We find $U_{\text{ev.}}$ about 350 MeV. The other way was to add up all proton energies below 40 MeV, add the α-particle energies and also a number of neutrons. With reference to the Collaboration Paper (2) we have taken the neutrons to be 4 times as many as the protons and with 3 MeV kinetic energy. Finally we add the binding energies of these particles and find $U_{\text{ev.}} = 305$ MeV. An alternative way is to add the energy of all heavy particles as if protons, add neutrons in the same manner and finally the binding energies. The result has then to be reduced by an empirical 15%. We then find $U_{\text{ev.}} = 297$ MeV. The second approach thus gives $U_{\text{ev.}} = 300$ MeV. With regard to the fit in Fig. 3 we have taken $U_{\text{ev.}} = 325$ MeV. This figure is high compared to the one given in the Collaboration Paper (2), viz. 170 MeV. However, there is also another difference, namely in that our stars emit 4 evaporation protons per star on the average whereas the figure 170 MeV corresponds to 2 evaporation protons per star. These differences may be seen in the light of the kind of stars; our stars have occurred mainly in flight and it seems quite reasonable that the antiprotons have penetrated somewhat deeper into nuclear matter. We thus expect that more pions will have interacted with the nucleus. As we will see in the following we arrive at a number of 2.0 pions interacting per star, to be compared to 1.3 in the earlier data (2).

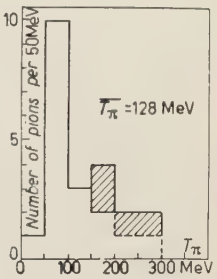

Fig. 2. – The pion energy distribution.

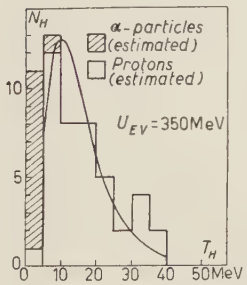

Fig. 3. – Energy spectrum of heavy particles with energies below 60 MeV. The curve has been calculated from evaporation theory and has been fitted to the proton energy spectrum by assuming $U_{\text{ev.}} = 350$ MeV.

We assume with reference to the Collaboration Paper (2) that in the elementary act of annihilation on the average a certain number, n, of charged and neutral pions are emitted. The average kinetic energy of the pions in the elementary act is T'. The problem is to determine both n and T' from the observed data. The fate of the emitted pions is that a number ν interact with the nucleus where the annihilation took place. A certain fraction, a, of the interacting pions is absorbed and its energy goes to an excitation of the

nucleus. The remaining fraction $(1 - a)$ is scattered and comes out with a lowered energy, T_0. The energy lost is $(T' - T_0)$ which adds to the nuclear excitation. Let the excitation be U. We then have

$$U = a\nu(T' + 140) + (1 - a)\nu(T' - T_0) , \tag{1}$$

140 MeV being the rest mass of the pion.

On the other hand we have observed n_0 charged pions with an average observed energy T. The value T is equal to T' minus the reduction in energy due to scattered pions. The number of charged scattered pions is $\frac{2}{3}(1 - a)\nu$. The factor $\frac{2}{3}$ corresponds to the assumed fraction of charged pions (based on charge independence).

We then have

$$T = T' - \frac{\frac{2}{3}(1-a)\nu}{n_0}(T' - T^0) \tag{2}$$

Our observed values are

$$U = 470 \text{ MeV}$$

$$T = 128 \text{ MeV}$$

$$n_0 = 2.2 .$$

We further assume that $T_0 = 50$ MeV (not a critical value), and $a = 0.75$.

The relations (1) and (2) give

$$\nu = 2.0$$

$$T' = 143 \text{ MeV} .$$

The number, n, of pions emitted in the elementary act is the sum of the observed number of pions (corrected for scanning efficiency $1/\varepsilon$) and a corresponding number of neutral pions and finally the number of absorbed pions, $a\nu$.

Thus

$$n = \varepsilon n_0 \cdot \tfrac{3}{2} + a\nu .$$

We have observed

$$n_0 = 2.2 \pm 0.5$$

and assume

$$\varepsilon = 1.1 \pm 0.1 .$$

The result is that the average number of pions in the elementary act is $n = 5.1 \pm 1.0$.

The sign of the charge on a pion is observable only for stopping pions. We have observed the following cases: $2\pi^-$ and $2\pi^+$. In order to obtain more

information on the sign of charge one should have access to rather large and expensive stacks in which a greater proportion of the pions would come to rest.

We have looked especially for charged K-mesons. No K-meson was found in all 10 stars.

5. – The annihilation process.

It was suggested by observations made in the Collaboration Paper (2) that the annihilation process takes place in a region outside the nuclear surface where the nucleon wave function is small. This conclusion was based on the fact that the fraction of pions absorbed or inelastically scattered is rather small. It was also concluded that stars with much energy released in heavy prongs correspond to annihilations in flight where the antiproton has penetrated deeper into nuclear matter. Among our 10 stars is one, number 6-3, which seems to further support this picture. The event was formed by an antiproton in flight at an energy of $T_{p^-} = 96$ MeV. The star consists of 15 heavy prongs and 1 pion. Among the 15 heavy particles are 5 high energy protons with the energies 68, 72, 102, 140 and 275 MeV, respectively. Another support to this picture is that our stars which mainly are due to annihilations in flight show a rather high nuclear excitation and the number of interacting pions is high, viz. $\nu = 2.0$.

* * *

We should like to express our gratitude to the Bevatron group and its head Dr. E. J. Lofgren for carrying out the exposure, and to Prof. E. Segrè, and Prof. G. Goldhaber for all help in planning the experiment. Thanks are due to Dr. Stephe White, A. Oliver, and G. Leipelt, Livermore, California, for carrying out the processing of the plates.

The interest in this work shown by Prof. K. Siegbahn has been of great value.

The support given by the Swedish Atomkommitté is gratefully acknowledged.

RIASSUNTO (*)

In un pacco di emulsioni nucleari esposto al bevatrone di Berkeley abbiamo trovato 10 eventi identificati come dovuti ad antiprotoni. Si sono analizzate e si riportano le caratteristiche dell'interazione. Di speciale interesse è l'osservazione di una collisione elastica tra un antiprotone e un protone libero.

(*) *Traduzione a cura della Redazione.*

Nucleon-antinucleon Forces in the Intermediate Coupling Theory (*).

M. Lévy

Ecole Normale Supérieure - Université de Paris

(ricevuto il 29 Dicembre 1957)

Summary. — A semi-phenomenological approach to meson theory is used in order to calculate the nucleon-antinucleon complex interaction responsible for the scattering and annihilation of antinucleons in hydrogen. It is assumed that the main part of the imaginary potential is due to processes involving virtual annihilation into an arbitrary number of mesons, all of them but one being emitted or absorbed in a p-state. An effective Hamiltonian is derived for such processes, from which a static interaction can be calculated, the nucleon and antinucleon being treated as fixed sources. The intermediate coupling theory of Tomonaga is extended to the two-body problem and applied first to the calculation of ordinary nuclear forces and of the real part of the nucleon-antinucleon interaction. The annihilation Hamiltonian is then treated approximately by the intermediate coupling method. The imaginary part of the potential is found to have a range of the order of 2 to $3 \cdot 10^{-13}$ cm, beyond which it becomes a weakly oscillating function of the nucleon-antinucleon distance. The physical meaning of this result is discussed, as well as the effects which would tend to sharpen the definition of the emitted pions multiplicity. In particular, a method is proposed to investigate, in the framework of the intermediate coupling theory, the influence of the excited states of the nucleon-antinucleon system.

1. – Introduction.

The experiments on the interaction of antinucleons with nucleons which have been performed at Berkeley ([1,2]) have revealed several features which seem, at first sight, surprising:

(*) Supported in part by the United States Air Force through the European Office, Air Research and Development Command.

([1]) B. Cork, G. Lambertson, O. Piccioni and W. Wenzel: *Phys. Rev.*, **107**, 248 (1957); see also the lecture notes by O. Chamberlain: *Summer School of Les Houches* (1957).

([2]) W. Barkas *et al.* (antiproton collaboration experiment): *Phys. Rev.*, **105**, 1037 (1957).

1) Total cross-sections are large (of the order of 100 millibarns) and approximately constant between 200 and 700 MeV. In this connection, it should be noted that the « geometrical » cross-section of a nucleon with a radius of $0.8 \cdot 10^{-13}$ cm ([3]) is equal to 20 mb; on the other hand, the quantity $4\pi\lambda^2$ in the center of mass system varies roughly from 40 mb at 300 MeV to 20 mb at 600 MeV.

2) The ratio ϱ between scattering and total cross-sections is relatively small, although its exact magnitude is still in doubt. Total cross-sections have been measured so far by attenuation of the beam in an hydrogen target, whereas the scattering cross-section is estimated indirectly from the production of anti-neutrons through charge exchange scattering of anti-protons. An upper limit of 0.2 has sometimes been given for ϱ.

3) A fairly high average multiplicity $\bar{n} = 5.3 \pm 0.3$ of π-mesons produced in the annihilation of anti-protons has been observed in photographic emulsions ([2]). In order to interpret this multiplicity in the framework of Fermi's statistical theory, it is necessary to assume an interaction volume which is much too large to appear reasonable at first sight ([4]).

It should be noted that the difficulty to interpret these experimental findings does not so much come from the fact that total cross-sections are large as has already been pointed out by Ball and Chew ([5]). Actually, those who have some experience in analyzing high-energy nucleon-nucleon scattering know that the difficulty there is rather to account for the *small* observed cross-sections. The feature which is hard to understand in these Berkeley experiments is *the combination of a large total cross- section with a small value of* ϱ.

In order to illustrate this point, let us consider, simply on the basis of the well-known general limits ([6]) which exist on $\sigma_{\text{scatt.}}$ and $\sigma_{\text{tot.}}$, the minimum number of partial waves required in order to obtain a given value of ϱ, if $\sigma_{\text{tot.}}$ is fixed to 100 mb. For simplicity, we assume that each partial wave contributes equally to the total cross-section for $l \ll L$, and gives no contribution for $l > L$ ([7]). We then find the following inequality

$$\frac{L^2}{s(L)} \geqslant \frac{\sigma_{\text{tot.}}}{4\pi\varrho\lambda^2}\,, \tag{1.1}$$

([3]) W. Chambers and R. Hofstadter: *Phys. Rev.*, **103**, 1454 (1956).

([4]) R. Gatto: *Nuovo Cimento*, **3**, 468 (1956); G. Sudarshan: *Phys. Rev.*, **103**, 777 (1956); see also ref. ([2]).

([5]) W. Ball and G. F. Chew: U.C.R.L. Report 3922, to be published.

([6]) See, for example: J. Blatt and V. F. Weisskopf: *Theoretical Nuclear Physics*, p. 317.

([7]) This assumption very probably underestimates L, since it is much more likely that the partial cross sections decrease when l increases.

where $s(L)$ is given by

$$s(L) = 1 + \frac{1}{3} + \ldots + \frac{1}{2L+1} . \tag{1.2}$$

The minimum number $L_{\min.}+1$ of partial waves, including S-waves ($L_{\min.}$ corresponds to a strict equality in Eq. (1.1)) is given in Table I for several values of ϱ and $E_{\text{cin.}}$, the kinetic energy of the antinucleons in the laboratory system.

TABLE I. – *Values of* $(L_{\min}+1)$.

E_{cin} (MeV)	$\varrho = 0.1$	$\varrho = 0.2$	$\varrho = 0.3$
150	6	5	4
300	8	6	5
500	11	8	7

These relatively large values of $L_{\min.}+1$, combined with the observed high pion-multiplicity n mentioned above, clearly indicate that what is needed, in order to account for the experimental results, *is a relatively weak annihilation force with a very long range.* This was already inferred by KOBA and TAKEDA [8] in their « black sphere » treatment of the antiproton-proton annihilation; it is also confirmed by a phenomenological analysis [9] based on a complex potential $V+iW$, where V and W are taken as square wells of different depths and ranges. In order to obtain a value of ϱ equal to 0.2, for example, the range of W must be at least equal to $3 \cdot 10^{-13}$ cm.

In the following, we shall also use the concept of a complex potential $V+iW$, the imaginary part of which being what we call « annihilation force » (although it also contributes, of course, to the scattering). It appears, at first sight, very difficult to reconcile the long range of W with meson theory, at least in the frame-work of its various weak coupling versions which have been proposed in the last few years. If one adopts the idea that nucleons and antinucleons are made of a core surrounded by a meson cloud, the range of the « ordinary force » V is determined by the overlapping of the clouds, whereas the range of W should be connected with the overlapping of the cores. The indication that the core is much bigger that one usually believes is perhaps not without relation with the problem of nucleon structure, where a similar indication is also found [10].

[8] Z. KOBA and G. TAKEDA: *Antinucleon Scattering*, to be published.

[9] M. GOURDIN, B. JANCOVICI and L. VERLET: private communication.

[10] See, for example, a discussion of this point in: D. YENNIE, M. LÉVY and D. RAVENHALL: *Rev. Mod. Phys.*, **29**, 144 (1957), especially footnote [38].

In any case, if the Berkeley experiments are to be explained on the basis of meson theory it is clear that a new mechanism must be found in order to describe the annihilation, and that it will have to be different from weak coupling. However, if this mechanism is obtained, there is no reason to give up in the nucleon-antinucleon problem, the semi-phenomenological approach which has been very successful in the past, at least in the low and intermediate energy regions. In this approach—which was first clearly formulated, in the case of the two nucleons problem, by TAKETANI ([11])—the π-meson field theory is believed to yield correct results for the « outer region », but has to be replaced by appropriate phenomenological boundary conditions at the « inner region », for which there is no trustful relativistic theory at present, and where, in any case, new effects due to other particles must play a large role. There remains an « intermediate region », where it has been found necessary to complete the predictions of meson theory by more or less phenomenological additional forces ([12]). The same approach can be used in the present problem because most of the absorption must occur at large distances. Then, only the contribution of the partial waves corresponding to low values of l will be sensitive to the phenomenological boundary conditions. As has been seen above, these partial waves contribute mostly to the scattering and very little to the annihilation. In other words, what we propose to do is to start from the fixed source meson theory, suitably modified to take into account absorption and to compute from it the complex potential; we shall then consider that the procedure is justified *a posteriori* if we obtain a long range for W. As for the real part, it will turn out, as will be seen in Sect. **3**, that it is not substantially different from the potential which is given by the ordinary charge symmetrical Yukawa theory:

$$V = -V_2 + V_4 - V_6 + \text{etc.} \ldots , \tag{1.3}$$

where V_{2n} is the corresponding $2n$-th order potential between two nucleons ($V_2 + V_4$ is essentially the Gartenhaus potential ([13])).

Apart from the problem of the range, another difficulty connected with W is that, according to the meson theoretical ideas on which were based the successful developments of recent years ([14]), it has always been thought that *virtual* creation and annihilation of nucleon—antinucleon pairs is a relatively rare process (small s-state contribution in π-p scattering; no « pair term » in

([11]) M. TAKETANI, S. NAKAMURA and M. SASAKI: *Progr. Theor. Phys.*, **6**, 581 (1951).
([12]) P. S. SIGNELL and R. MARSHAK: *Phys. Rev.*, **106**, 832 (1957).
([13]) S. GARTENHAUS: *Phys. Rev.*, **100**, 900 (1955).
([14]) G. F. CHEW and F. E. LOW: *Phys. Rev.*, **101**, 1570 (1956).

nuclear forces, etc. ([15])). This seems also to agree with the data on the *production* of real pairs at Berkeley, although they are not so easy to interpret, being obtained from experiments on complex nuclei (where the observed antiprotons are probably produced mostly at the nuclear surface). The question, therefore, arises why the absorption process is so highly probable.

The answer to that question must, of course, be looked for in the fact that the production of a pair is a single pion event, whereas the annihilation involves many pions (as indicated by the observed $\bar{n}$). This leads us naturally to the model which we have used. In addition to the processes which contribute only to V, we suppose that there are annihilation diagrams of the type drawn in Fig. 1. In this diagram many mesons are emitted in p-state by the nucleon-antinucleon pair (through the p-state coupling constant f of the Chew-Low theory) before it annihilates *once* virtually into an s-state meson through a vertex to which we suppose that a « small » coupling constant Γ is attached (its smallness comes from what is usually called the « pair damping » process, on which we do not intend to elaborate). In other words, we would like to compute the annihilation force to all orders in f^2, but to the lowest order in Γ^2. It can then be shown easily that the pair creation and annihilation processes can be eliminated entirely to this order by adding a new interaction term H_{II} to the familiar Hamiltonian H_I of the Chew-Low theory ([14]). The derivation of this « effective » interaction, which is essentially responsible for the appearance of an imaginary potential W, is given in Sect. 2.

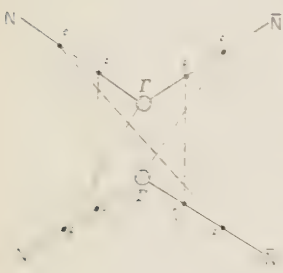

Fig. 1. – General diagram for the virtual annihilation of the nucleon-antinucleon system

The next problem is to compute the potential energy from the total Hamiltonian. It is clear that, for this purpose, weak coupling treatments are inadequate, since the calculation must essentially take into account those intermediate states where many pions are present. On the other hand, processes where few π-mesons are exchanged contribute so little to the annihilation that it is not necessary to calculate them accurately. Finally, when a large

([15]) In writing this etc., we have specifically in mind the evidence based on the π^0-lifetime (see, for example, the discussion in BETHE and DE HOFFMANN: *Mesons and Fields*, 2, pp. 7 and 404). The situation, however, has become much less clear, now that a new more precise upper limit has been obtained for this lifetime (G. HARRIS, J. OREAR and S. TAYLOR: *Phys. Rev.*, **106**, 327 (1957)). In any case, it should be kept in mind that, in this phenomenon, other effects than the virtual nucleon pairs damping can very well play a dominant role (see, for example, the discussion of the introduction of Pauli moments in the electromagnetic vertices, by H. KATSUMORI: *Progr. Theor. Phys.*, **12**, 241 (1954)).

number of mesons are exchanged, so many summations over all possible states have to be performed that, statistically, everything looks as if all the mesons had been emitted in the same state. For all these reasons, we decided that the intermediate coupling theory of Tomonaga [16] was best suited for our purpose. It has indeed been shown by STROFFOLINI [17] that the amplitudes for n mesons obtained through the intermediate coupling treatment of the one-body problem [18] represent a poor approximation to the exact amplitudes when n is small, but that the approximation becomes more adequate for higher values of n.

We have consequently been led to a generalization of the intermediate coupling method to the nuclear forces problem. A generalization of this type has already been attempted by NOGAMI and HASEGAWA [19] who, however, in order to remain in the spirit of the Chew-Low theory, limited their consideration to processes in which only one or two mesons are exchanged. Since this is obviously not sufficient in the present case, we have treated the two-body problem by a rather different method, where no formal difference is made between the «bound» mesons of each nucleon cloud and the «unbound» mesons exchanged between the two nucleons. This calculation of the nucleon-nucleon force and of the real part of the nucleon-antinucleon potential is given in Sect. 3. The problem of the complete interaction (in the nucleon-antinucleon case) is treated in Sect. 4. The main difficulty which arises when H_I and H_{II} are both present comes from the fact that, in the two-body problem, a meson emitted in a p-state with respect to one nucleon can be absorbed in an s-state around the other one, and inversely. There appear therefore, in the potential energy, interference terms between s- and p-state mesons, and an appropriate modification of the Tomonaga trial functions must be made. In Sect. 5, the asymptotic form of the imaginary part of the potential W is computed, using a special isotopic spin dependence of H_{II}. It has not been found, so far, necessary to compute W in a detailed fashion, owing to the present uncertainties over the experimental situation (especially concerning the charge distribution of the π-mesons produced). It is nevertheless clear that a long range force is obtained, and that its main characteristics do not depend strongly on the model used. The physical meaning of this result, as well as other predictions which can be tested experimentally, are discussed in the same Section. Finally, the influence of excited intermediate states of the nucleon-antinucleon system is examined. The interest of these excited

[16] S. TOMONAGA: *Progr. Theor. Phys.*, **2**, 6 (1947).

[17] R. STROFFOLINI: *Phys. Rev.*, **104**, 1146 (1956).

[18] M. H. FRIEDMAN, T. D. LEE and R. CHRISTIAN: *Phys. Rev.*, **100**, 1494 (1955).

[19] H. HASEGAWA: *Progr. Theor. Phys.*, **13**, 47 (1955); Y. NOGAMI and H. HASEGAWA: *Progr. Theor. Phys.*, **15**, 137 (1956).

states is that they tend to sharpen the definition of the multiplicity of the produced pions in accordance with the experimental results as they are known presently.

2. – Derivation of the annihilation hamiltonian.

This section, where we intend to derive the effective Hamiltonian responsible for the annihilation, is the only one of the present paper where relativistic operators (i.e. the nucleon-antinucleon field $\psi(x)$, the pseudoscalar matrix γ_5, etc.) are introduced. In doing this, we do not want to attach any special value to the relativistic pseudoscalar meson field theory; we simply use it as a means to obtain a plausible form for the annihilation Hamiltonian in the « outer region ». According to the semi-phenomenological approach described in the Introduction, the properties of this Hamiltonian in the relativistic region will be simulated by appropriate source functions ([20]).

When manipulating operators which deal with antinucleons, a certain care must be exercised since, as is well known, the invariance under charge conjugation produces new selection rules ([21,22]). In the following, we shall follow the elegant formulation of NAKAI ([23]), who introduces, in a field-theoretical manner, a new quantum number equivalent to the one of LEE and YANG ([22]).

We first write the complete Hamiltonian of the system in the following way

$$H = H_0 + H_D + H_{\text{int.}} . \tag{2.1}$$

where H_0 is the free meson field Hamiltonian:

$$H_0 = (2\pi)^{-3} \int \omega_k c_\alpha^*(\boldsymbol{k}) c_\alpha(\boldsymbol{k}) \, \mathrm{d}\boldsymbol{k} , \tag{2.2}$$

expressed in terms of meson creation and annihilation operators which obey the usual commutation relations and are introduced through the Fourier expansion of the meson field:

$$\varphi_\alpha(\boldsymbol{x}) \equiv (2\pi)^{-3} \int \varphi_\alpha(\boldsymbol{k}) \exp[i\boldsymbol{k}\boldsymbol{x}] \, \mathrm{d}\boldsymbol{k} = \tag{2.3}$$

$$= (2\pi)^{-3} \int (2\omega_k)^{-\frac{1}{2}} (c_\alpha(\boldsymbol{k}) \exp[i\boldsymbol{k}\boldsymbol{x}] + c_\alpha^*(\boldsymbol{k}) \exp[-i\boldsymbol{k}\boldsymbol{x}]) \, \mathrm{d}\boldsymbol{k} ;$$

([20]) The reader who is not interested in relativistic field theory can skip most of this Section; he simply will have to admit Eqs. (2.15) and (2.24) as a phenomenological basis for the calculations of the remaining Sections.

([21]) L. MICHEL: *Nuovo Cimento*, **10**, 319 (1953); D. AMATI and B. VITALE: *Nuovo Cimento*, **2**, 719 (1955); H. A. BETHE and J. HAMILTON: *Nuovo Cimento*, **4**, 1 (1956).

([22]) T. D. LEE and C. N. YANG: *Nuovo Cimento*, **3**, 749 (1956).

([23]) S. NAKAI: *Progr. Theor. Phys.*, **17**, 139 (1957).

α is the charge index ($\alpha = 1, 2, 3$) and $\omega_k = (k^2 + \mu^2)^{\frac{1}{2}}$. H_D is the sum of the free Dirac Hamiltonians of the nucleon and antinucleon. $H_{\text{int.}}$ is written as follows:

$$H_{\text{int.}} = \frac{i}{2}\int \mathrm{d}\boldsymbol{x}_1\,\mathrm{d}\boldsymbol{x}_2\,\mathrm{d}\boldsymbol{x}\,[\bar{\psi}_i(\boldsymbol{x}_1)\Gamma_5(\boldsymbol{x}_1 - \boldsymbol{x},\ \boldsymbol{x}_2 - \boldsymbol{x})\tau_\alpha^{ij}\psi_j(\boldsymbol{x}_2) + \\ + \bar{\psi}_i^c(\boldsymbol{x}_1)\Gamma_5(\boldsymbol{x}_1 - \boldsymbol{x},\ \boldsymbol{x}_2 - \boldsymbol{x})\tau_\alpha^{ji}\psi_j^c(\boldsymbol{x}_2)]\Phi_\alpha(\boldsymbol{x})\,, \tag{2.4}$$

where the isotopic indices i and j take the values 1 (proton or antiproton) and 2 (neutron or antineutron). The nucleon-antinucleon field ψ_i is given by:

$$\psi_i(\boldsymbol{x}) = (2\pi)^{-3}\int (a_{si}(\boldsymbol{p})u_s(\boldsymbol{p})\exp[i\boldsymbol{p}\boldsymbol{x}] + b_{si}^+(\boldsymbol{p})v_s(\boldsymbol{p})\exp[-i\boldsymbol{p}\boldsymbol{x}])\,\mathrm{d}\boldsymbol{p}\,, \tag{2.5}$$

where a_{si} and b_{si}^+ are the familiar anticommuting operators which respectively annihilate a nucleon or create an antinucleon of spin s and isotopic spin i; $u_s(\boldsymbol{p})$ is a free Dirac spinor of positive energy and momentum $\boldsymbol{p}$, $v_s(\boldsymbol{p})$ is a spinor of negative energy and momentum $-\boldsymbol{p}$. The charge conjugate field ψ_i^c is similar equal to:

$$\psi_i^c(\boldsymbol{x}) = (2\pi)^{-3}\int (b_{si}(\boldsymbol{p})u_s^c(\boldsymbol{p})\exp[i\boldsymbol{p}\boldsymbol{x}] + a_{si}^+(\boldsymbol{p})v_s^c(\boldsymbol{p})\exp[-i\boldsymbol{p}\boldsymbol{x}])\,\mathrm{d}\boldsymbol{p}\,, \tag{2.6}$$

where $u^c = C(\bar{v})^T = -(\bar{v}C)^T$, $v^c = C(\bar{u})^T = -(\bar{u}C)^T$, and similarly: $\bar{u}^c = -(v)^T C = = (Cv)^T$, $\bar{v}^c = -(u)^T C = (Cu)^T$, C being the usual conjugation matrix ($C^T = -C$; T means « transposed »). Since $\tau_\alpha^{ij} = \tau_\alpha^{*ij}$, it can be seen that the Hamiltonian (2.4) is invariant under charge conjugation if, at the same tine, $\varphi_1 \to \varphi_1$, $\varphi_2 \to -\varphi_2$, $\varphi_3 \to \varphi_3$. $\Gamma_5(\boldsymbol{x}, \boldsymbol{x}')$ is the pseudoscalar vertex operator which, in perturbation theory, would reduce to $G_0\gamma_5\,\delta(\boldsymbol{x})\,\delta(\boldsymbol{x}')$, where G_0 would then be the unrenormalized pseudoscalar coupling constant ($G_0 = f_0(2M/\mu)$, $f_0 =$ unrenormalized Chew-Low coupling constant).

Since we wish only to include diagrams like Fig. 1, where no more that one pair is present at a certain time, we write the state vector of the system:

$$\Psi = \Psi^{(0)} + \Psi^{(2)}\,, \tag{2.7}$$

where $\Psi^{(0)}$ corresponds to states where no nucleon or antinucleon are present:

$$\Psi^{(0)} = \sum_{n=0}^{\infty}(2\pi)^{-3n}\int B_n(0;\,0;\,\boldsymbol{k}_1\alpha_1, \ldots, \boldsymbol{k}_n\alpha_n)\Phi_0(\boldsymbol{k}_1\alpha_1, \ldots, \boldsymbol{k}_n\alpha_n)\,\mathrm{d}\boldsymbol{k}_1 \ldots \mathrm{d}\boldsymbol{k}_n\,. \tag{2.8}$$

In this last equation, Φ_0 is a free state of n non-interacting mesons of momenta and charge indices $\boldsymbol{k}_1, \alpha_1 \ldots \boldsymbol{k}_n, \alpha_n$:

$$\Phi_0(\boldsymbol{k}_1\alpha_1, \ldots \boldsymbol{k}_n\alpha_n) = \frac{1}{\sqrt{n!}}\,c_{\alpha_1}^*(\boldsymbol{k}_1)\ldots c_{\alpha_n}^*(\boldsymbol{k}_n)\Psi_0\,, \tag{2.9}$$

where Ψ_0 is the true vacuum for both meson and nucleon-antinucleon. Similarly, $\Psi^{(2)}$ includes states where a pair is present, written in the center of mass system:

$$(2.10)\quad \Psi^{(2)} = \sum_{n=0}^{\infty} (2\pi)^{-3n-6} \int A_n(\boldsymbol{p}_1, s_1, i_1; \boldsymbol{p}_2, s_2, i_2; \boldsymbol{k}_1\alpha_1 \dots \boldsymbol{k}_n\alpha_n)\, \delta(\boldsymbol{p}_1 + \boldsymbol{p}_2 + \boldsymbol{K}) \cdot \cdot a^+_{s_1 i_1}(\boldsymbol{p}_1) b^+_{s_2 i_2}(\boldsymbol{p}_2) \Phi_0(\boldsymbol{k}_1\alpha_1 \dots \boldsymbol{k}_n\alpha_n)\, \mathrm{d}\boldsymbol{p}_1\, \mathrm{d}\boldsymbol{p}_2\, \mathrm{d}\boldsymbol{k}_1 \dots \mathrm{d}\boldsymbol{k}_n ,$$

where $\boldsymbol{K} = \boldsymbol{k}_1 + \boldsymbol{k}_2 + \dots + \boldsymbol{k}_n$. After elimination of the annihilation process, the only state vector which will be considered in the rest of the paper will be $\Psi^{(2)}$ which, with the neglect of nucleon or antinucleon recoil, will be written alternatively:

$$(2.11)\quad \Psi^{(2)} = (2\pi)^{-3} \int \Phi(\boldsymbol{x}_1, \boldsymbol{x}_2; s_1 i_1, s_2 i_2) \cdot \exp[-i\boldsymbol{p}_1\boldsymbol{x}_1 - i\boldsymbol{p}_2\boldsymbol{x}_2] a^+_{s_1 i_1}(\boldsymbol{p}_1) b^+_{s_2 i_2}(\boldsymbol{p}_2) \Psi_0^{(N)}\, \mathrm{d}\boldsymbol{x}_1\, \mathrm{d}\boldsymbol{x}_2\, \mathrm{d}\boldsymbol{p}_1\, \mathrm{d}\boldsymbol{p}_2 ,$$

where $\Psi_0^{(N)}$ is the vacuum state vector for nucleons and antinucleons alone and Φ a new state vector corresponding to a nucleon-antinucleon pair located respectively at $\boldsymbol{x}_1$ and $\boldsymbol{x}_2$ which can also be written as a matrix in the s and i indices and expanded as follows:

$$(2.12)\quad \Phi(\boldsymbol{x}_1, \boldsymbol{x}_2) = \sum_{n=0}^{\infty} \frac{(2\pi)^{-3n}}{\sqrt{n!}} \int A_n(\boldsymbol{x}_1, \boldsymbol{x}_2; \boldsymbol{k}_1\alpha_1 \dots \boldsymbol{k}_n\alpha_n) \cdot \cdot c^*_{\alpha_1}(\boldsymbol{k}_1) \dots c^*_{\alpha_n}(\boldsymbol{k}_n) \Phi_0(\boldsymbol{x}_1, \boldsymbol{x}_2)\, \mathrm{d}\boldsymbol{k}_1 \dots \mathrm{d}\boldsymbol{k}_n ,$$

where $\Phi_0(\boldsymbol{x}_1, \boldsymbol{x}_2)$ is now simply the nucleon-antinucleon wave-function *multiplied by the meson vacuum state vector.* $\Phi(\boldsymbol{x}_1, \boldsymbol{x}_2)$ is normalized in the same way as Φ_0:

$$(2.13)\quad \Phi^*(\boldsymbol{x}_1, \boldsymbol{x}_2)\ \Phi(\boldsymbol{x}_1, \boldsymbol{x}_2) = \Phi_0^*(\boldsymbol{x}_1, \boldsymbol{x}_2)\, \Phi_0(\boldsymbol{x}_1, \boldsymbol{x}_2) ,$$

which means that the coefficients A_n are normalized as follows:

$$(2.14)\quad \sum_{n=0}^{\infty} (2\pi)^{-3n} \int |A_n(\boldsymbol{x}_1, \boldsymbol{x}_2; \boldsymbol{k}_1\alpha_1 \dots \boldsymbol{k}_n\alpha_n)|^2\, \mathrm{d}\boldsymbol{k}_1 \dots \mathrm{d}\boldsymbol{k}_n = 1$$

for all values of $\boldsymbol{x}_1$ and $\boldsymbol{x}_2$.

In the non-relativistic limit $\Phi(\boldsymbol{x})$ obeys the following Schrödinger equation

$$(2.15)\quad \Big(\sum_{i=1}^{2} T_i + 2M + H_0 + H_{\mathrm{I}} + H_{\mathrm{II}}\Big) \Phi(\boldsymbol{x}_1, \boldsymbol{x}_2) = E\, \Phi(\boldsymbol{x}_1, \boldsymbol{x}_2) ,$$

where T_i are the kinetic energies of the nucleon and antinucleon and H_{I} is

the usual Hamiltonian of the non-relativistic meson theory:

$$H_{\mathrm{I}}(\boldsymbol{x}_1, \boldsymbol{x}_2) = \frac{f_0}{\mu} \sum_{i=1}^{2} \int G(\boldsymbol{x} - \boldsymbol{x}_i) \tau_\alpha^{(i)} \boldsymbol{\sigma}^{(i)} \cdot \nabla \varphi_\alpha(\boldsymbol{x}) \, \mathrm{d}\boldsymbol{x} \,. \tag{2.16}$$

It is to the obtention of a suitable form for H_{II} that the remainder of this Section is devoted.

We first write the equation which is obeyed by the amplitude A_n in the state vector $\Psi^{(2)}$ of Eq. (2.10):

$$\begin{aligned}(E - E_0 - E_D) A_n(\boldsymbol{p}, s_1, i_1; -\boldsymbol{p} - \boldsymbol{K}, s_2, i_2; \boldsymbol{k}_1\alpha_1 \ldots \boldsymbol{k}_n\alpha_n) = \\ = \Phi_0^*(\boldsymbol{k}_1\alpha_1 \ldots \boldsymbol{k}_n\alpha_n) b_{s_2 i_2}(-\boldsymbol{p} - \boldsymbol{K}) a_{s_1 i_1}(\boldsymbol{p}) H_{\mathrm{int.}}(\Psi^{(0)} + \Psi^{(2)}) = U^{(0)} + U^{(2)} \,,\end{aligned} \tag{2.17}$$

where E_0 and E_D are the corresponding eigenvalues of H_0 and H_D. On the right hand side of (2.17), we need only to consider the first term, since the second is precisely the one which gives rise, in the non-relativistic limit, to H_{I} in Eq. (2.15). Using Eq. (2.4) one finds easily for the first term

$$U^{(0)} = i\Gamma_0 \Phi_0^*(\boldsymbol{k}_1\alpha_1 \ldots \boldsymbol{k}_n\alpha_n) F_{s_1 s_2}(\boldsymbol{p}, \boldsymbol{p} + \boldsymbol{K}) \tau_\alpha^{i_1 i_2} \varphi_\alpha(\boldsymbol{K}) \Psi^{(0)} \,, \tag{2.18}$$

where $\Gamma_0 F_{s_1 s_2}(\boldsymbol{p}, \boldsymbol{q})$ is simply the matrix element of the operator Γ_5:

$$\Gamma_0 F_{s_1 s_2}(\boldsymbol{p}, \boldsymbol{q}) = \int \bar{u}_{s_1}(\boldsymbol{p}) \Gamma_5(\boldsymbol{x}, \boldsymbol{x}') \exp[i\boldsymbol{p}\boldsymbol{x} + i\boldsymbol{q}\boldsymbol{x}'] v_{s_2}(-\boldsymbol{q}) \, \mathrm{d}\boldsymbol{x} \, \mathrm{d}\boldsymbol{x}' \,, \tag{2.19}$$

between a positive and a negative energy spinor which, in the non-relativistic limit *and for perturbation theory* would be equal to G_0.

In order to eliminate $\Psi^{(0)}$, it is sufficient to write now the equation which is satisfied by the amplitude B_n introduced in Eq. (2.8):

$$\begin{aligned}(E - E_0) B_n(0, 0; \boldsymbol{k}_1\alpha_1 \ldots \boldsymbol{k}_n\alpha_n) = \Phi_0^*(\boldsymbol{k}_1\alpha_1 \ldots \boldsymbol{k}_n\alpha_n) H_{\mathrm{int.}} \Psi^{(2)} = \\ = -i\Gamma \Phi_0^*(\boldsymbol{k}_1\alpha_1 \ldots \boldsymbol{k}_n\alpha_n) \int F_{s_1' s_2'}(\boldsymbol{p}', \boldsymbol{p}' + \boldsymbol{K}') \tau_\beta^{i_2' i_1'} \varphi_\beta(\boldsymbol{K}') \cdot \\ \cdot \sum_{m=0}^{\infty} (2\pi)^{-3m-3} A_m(\boldsymbol{p}', s_1', i_1'; -\boldsymbol{p}' - \boldsymbol{K}', s_2', i_2'; \boldsymbol{k}_1'\alpha_1' \ldots \boldsymbol{k}_n'\alpha_n') \Phi_0(\boldsymbol{k}_1'\alpha_1' \ldots \boldsymbol{k}_n'\alpha_n') \,.\end{aligned} \tag{2.20}$$

It is to be noted that no approximation is made on the right hand side of Eq. (2.20) (first line), since $\Psi^{(0)}$ can only be coupled, through $H_{\mathrm{int.}}$, to $\Psi^{(2)}$ and to no other state vector. The effective Hamiltonian H_{II} can now be written by eliminating the amplitudes B_n between Eqs. (2.18) and (2.10). Before writing it explicitly, however, it is convenient to make at this stage, the following approximation: the meson field operators $\varphi_\alpha(\boldsymbol{K})$ and $\varphi_\beta(\boldsymbol{K}')$ which appear

in these equations create or annihilate mesons of definite momentum, if $\boldsymbol{k}_1 \dots \boldsymbol{k}_n$, $\boldsymbol{k}'_1 \dots \boldsymbol{k}'_n$ are fixed; we will neglect, in the following, this correlation and consider $\boldsymbol{K}$ and $\boldsymbol{K}'$ as independent from momenta $\boldsymbol{k}_1 \dots \boldsymbol{k}_n$ or $\boldsymbol{k}'_1 \dots \boldsymbol{k}'_n$. If we concentrate our attention on states where many mesons are present, this approximation is obviously not serious. It is then seen that H_{II} is an integral operator, the matrix elements of which can be written as follows in configuration space (in the system where the center of mass is at rest and located at the origin)

$$(2.21) \quad (\boldsymbol{x}; s_1 i_1, s_2 i_2 | H_{\text{II}} | \boldsymbol{x}', s'_1 i'_1, s'_2 i'_2) = \Gamma_0^2 \tau_\alpha^{i_1 i_2} \tau_\beta^{i'_2 i'_1} \int F_{s_1 s_2}(\boldsymbol{x} - \boldsymbol{y}, \boldsymbol{y}) \varphi_\alpha(\boldsymbol{y}) \, \mathrm{d}\boldsymbol{y} \cdot$$

$$\cdot \frac{1}{E - H_0 + i\varepsilon} \int F_{s'_2 s'_1}(\boldsymbol{x}' - \boldsymbol{y}', \boldsymbol{y}') \varphi_\beta(\boldsymbol{y}') \, \mathrm{d}\boldsymbol{y}' \, ,$$

where the matrix element $F_{s_1 s_2}(\boldsymbol{x}, \boldsymbol{y})$ is simply the Fourier transform of $F_{s_1 s_2}(\boldsymbol{p}, \boldsymbol{q})$ defined by (2.19). It is seen that H_{II} is essentially a non-local separable interaction, which can take complex values, since the denominator $E - H_0$ can vanish when applied to states containing at least one meson (24). It is also possible to verify that the interaction (2.21) acts only on the isotopic spin triplet states.

In the frame work of our semi-phenomenological approach to the present problem, the features of the annihilation Hamiltonian which are really useful for our purpose are the following:

a) the bilinearity in the meson field operator,

b) the isotopic spin dependence,

c) the presence of the factor $(E - H_0 + i\varepsilon)^{-1}$,

d) the positive sign in front of the constant Γ_0^2 (as will be seen, this positive sign is essential in order to guarantee that H_{II} corresponds to an *absorption* of the antinucleons).

As to the source « matrix » F, we consider it, to a large extent, as arbitrary, since we do not want to take its connection to the matrix elements of the relativistic operator Γ_5 very seriously. The only information we have is that $F(\boldsymbol{x}, \boldsymbol{y})$ has presumably, with respect to *both* variables x and y, a range of the

(24) Actually, the energy denominator should only vanish for states containing at least *two* mesons (this is equivalent to saying that a nucleon-antinucleon pair cannot annihilate *really* into less than two mesons, if the total momentum is to be conserved). The term corresponding to the one meson annihilation enters Eq. (2.21) only because we have neglected the correlation between K and the sum of the other momenta. In practice, the source function cuts off the contribution of the terms involving less than *three* mesons, as will be seen in Sect. 5.

order of the nucleon Compton wave-length and that the coupling constant Γ_0 is probably relatively small, because of the so-called pair damping process, about which little is known with certainty.

Since an intermediate coupling treatment of a non-local interaction like (2.21) gives rise to many difficulties ([25]) we replace it by a local Hamiltonian having the same features *a*) to *d*) mentioned above:

$$(2.22)\quad (i_1,\ i_2\,|\,H_{\mathrm{II}}(\boldsymbol{x}_1,\boldsymbol{x}_2)\,|\,i_1',\ i_2') = \sum_{j=1}^{2} \Gamma_0^2 \tau_\alpha^{i_j i_1} \tau_\beta^{i_2' i_1} \int G_{\mathrm{II}}(\boldsymbol{y}-\boldsymbol{x}_j)\varphi_\alpha(\boldsymbol{y})\,\mathrm{d}\boldsymbol{y}\cdot$$
$$\cdot \frac{1}{E - H_0 + i\varepsilon} \int G_{\mathrm{II}}(\boldsymbol{y}'-\boldsymbol{x}_j)\varphi_\beta(\boldsymbol{y}')\,\mathrm{d}\boldsymbol{y}',$$

were we suppose, for simplicity, that the source function G_{II} is a spherically symmetrical scalar function which can eventually be taken equal to the function G_{I} of Eq. (2.16).

The disadvantage of this local form for H_{II} is that it introduces an imaginary self-energy which can, however, easily by substracted at the same time as the real one. H_{II} can also be written as a matrix in isotopic spin space, by means of the isotopic spin vector $\boldsymbol{T}$ of the nucleon antinucleon system:

$$(2.23)\quad H_{\mathrm{II}}(\boldsymbol{x}_1,\boldsymbol{x}_2) = \sum_{j=1}^{2} \Gamma_0^2 (\delta_{\alpha\beta} - T_\beta T_\alpha) \int G_{\mathrm{II}}(\boldsymbol{y}-\boldsymbol{x}_j)\varphi_\alpha(\boldsymbol{y})\,\mathrm{d}\boldsymbol{y}\cdot$$
$$\cdot \frac{1}{E - H_0 + i\varepsilon} \int G_{\mathrm{II}}(\boldsymbol{y}'-\boldsymbol{x}_i)\varphi_\beta(\boldsymbol{y}')\,\mathrm{d}\boldsymbol{y}'\,.$$

Since we suppose essentially in the following that $\Gamma_0^2 \ll f_0^2$, we can neglect the real part of H_{II} (when the principal part of $(E - H_0)^{-1}$ gives rise to no special effect at large distances) compared to H_{I} and keep only the imaginary part:

$$(2.24)\quad H_{\mathrm{II}} \simeq -i\pi\Gamma_0^2(\delta_{\alpha\beta} - T_\beta T_\alpha) \sum_j \int G_{\mathrm{II}}(\boldsymbol{y}-\boldsymbol{x}_i)\,\varphi_\alpha(\boldsymbol{y})\mathrm{d}\boldsymbol{y}\,\delta(E - H_0)\cdot$$
$$\cdot \int G_{\mathrm{II}}(\boldsymbol{y}'-\boldsymbol{x}_i)\varphi_\beta(\boldsymbol{y}')\,\mathrm{d}\boldsymbol{y}'\,.$$

This Hamiltonian can further be decomposed into several invariants in isotopic spin space, which it is interesting to consider separately. Denoting by $U_{\alpha\beta}$ the integral on the right hand side of the summation sign, in Eq. (2.24), it is

([25]) These difficulties come principally from the interference terms between *s*- and *p-state* mesons, which were mentioned in the Introduction. If H_{II} were the only interaction Hamiltonian, a separable non-local interaction like (2.21) would be relatively convenient to solve for the state vector.

seen that H_{II} can be written:

$$(2.25) \qquad H_{II} = -i\Gamma_0^2 \{U_{\alpha\alpha} - \tfrac{1}{2} \sum_{\alpha<\beta} [(T_\alpha T_\beta + T_\beta T_\alpha)(U_{\alpha\beta} + U_{\beta\alpha}) + iT_\gamma (U_{\alpha\beta} - U_{\beta\alpha})]\} ,$$

where the indices α, β, γ are used in a cyclic manner. This expression is very similar to the decomposition which is made in the one nucleon case where the s-state pion-nucleon interaction can be decomposed into a φ^2 and a $\boldsymbol{\tau} \cdot (\boldsymbol{\varphi} \times \boldsymbol{\pi})$ terms.

In particular, the last term on the right hand side of (2.25) can be very closely related to a $\boldsymbol{T} \cdot (\boldsymbol{\varphi} \times \boldsymbol{\pi})$ « spin-orbit » coupling term. In the one nucleon problem it has been found necessary ([26]), in order to account for the experimental data on π-p scattering near zero energy, to treat the coupling constants multiplying the two possible invariants as two independent parameters. In the present case too, it might turn out, when more is known about the charge distribution of the pions produced in the nucleon-antinucleon annihilation, that the three invariants on the right hand side of (2.25) will have to be treated as three independent interaction terms; it might also happen that only one of them is effective in the annihilation process ([27]).

3. – Intermediate coupling treatment of the real part of the hamiltonian.

In this Section, we apply the method of Tomonaga to the case where the Hamiltonian of the system contains only H_I (and not H_{II}): this application will be done in the case of the nucleon-nucleon (N-N) problem. The modifications which have to be made for the N-$\overline{\text{N}}$ problem (real part of the interaction) will be indicated at the end of this Section. Fort this last problem, however, the imaginary part of the Hamiltonian plays an important role which will be examined in Sect. **4**.

3·1. *General formalism.* – The interaction H_I can be expressed in terms of the operators $c_\alpha(\boldsymbol{k})$ and $c_\alpha^*(\boldsymbol{k})$, with the help of Eq. (2.3), as follows:

$$(3.1) \qquad H_I = \frac{f_0}{\mu} \sum_{j=1}^{2} (2\pi)^{-3} \int R(k) \tau_\alpha^{(j)} i(\boldsymbol{\sigma}^{(j)} \cdot \boldsymbol{k}) c_\alpha(\boldsymbol{k} \exp[i\boldsymbol{k}\boldsymbol{x}_j] - \\ - i(\boldsymbol{\sigma}^{(j)} \cdot \boldsymbol{k}) c_\alpha^*(\boldsymbol{k}) \exp[-i\boldsymbol{k}\boldsymbol{x}_j]) \, \mathrm{d}\boldsymbol{k} ,$$

where $R(k) = G_I(k)(2\omega_k)^{-\frac{1}{2}}$. $G_I(k)$ being the Fourier transform of the source function $G_I(\boldsymbol{x})$, normalized by $G_I(0) = 1$. The p-wave part of H_I *around each*

([26]) S. DRELL and W. ZACHARIASEN: *Phys. Rev.*, **104**, 236 (1956).

([27]) For simplicity, we shall consider, in the discussion of Sects. **4** and **5**, only the first term of (2.25).

nucleon can then be separated by introducing operators independent of $\boldsymbol{k}$ but depending on the co-ordinates $\boldsymbol{x}_1$ and $\boldsymbol{x}_2$ (for simplicity, we shall write them in the system where the center of mass is at the origin: $\boldsymbol{x}_1 = -\boldsymbol{x}_2 = \boldsymbol{r}/2$). Actually it is necessary to introduce two commuting sets of such operatros, respectively symmetrical and antisymmetrical with respect to the exchange of $\boldsymbol{x}_1$ and $\boldsymbol{x}_2$:

$$(3.2)\qquad \begin{cases} b^{+}_{\alpha i}(\boldsymbol{r}) = i\sqrt{6}\,(2\pi)^{-3}\int \varphi_1^{+}(k,\boldsymbol{r})\,Q^{+}_{ij}(k,\boldsymbol{r})\,\dfrac{k_j}{k}\cos\dfrac{\boldsymbol{kr}}{2}\,c_\alpha(\boldsymbol{k})\,\mathrm{d}\boldsymbol{k}\,, \\ b^{-}_{j}(\boldsymbol{r}) = i\sqrt{6}\,(2\pi)^{-3}\int \varphi_1^{-}(k,\boldsymbol{r})\,Q^{-}_{ij}(k,\boldsymbol{r})\,\dfrac{k_j}{k}\sin\dfrac{\boldsymbol{kr}}{2}\,c_\alpha(\boldsymbol{k})\,\mathrm{d}\boldsymbol{k}\,, \end{cases}$$

and similar definitions for $b^{+*}_{\alpha i}$ and $b^{-*}_{\alpha i}$. The functions $\varphi_1^{\mp}(k,\boldsymbol{r})$ (the index 1 is introduced only for the purpose of distinguishing these p-state functions from the s-state ones, which will be considered in next Section) are explicitly supposed to depend only on $|\boldsymbol{k}| = k$ and $\boldsymbol{r}$; they will be determined from a variational principle. For the time being, we consider them as real functions but they will have to take complex values when H becomes non-hermitian. The operators $Q^{\mp}_{ij}$ (which depend only on $\boldsymbol{r}$ and $|\boldsymbol{k}| = k$) come from a special complication of the p-state Hamiltonian: they are introduced to insure that the operators $b^{\mp}_{\alpha i}$ and $b^{\mp}_{\beta j}$ commute if $i \neq j$. Their essential property is the following:

$$(3.3)\qquad \frac{3}{4\pi}\,Q^{\pm}_{ij}\,Q^{\pm}_{kl}\int\frac{k_j k_l}{k^2}\,(1 \pm \cos\boldsymbol{kr})\,\mathrm{d}\Omega_k = \frac{\delta_{ik}}{4\pi}\int(1 \pm \cos\boldsymbol{kr})\,\mathrm{d}\Omega_k\,,$$

where $\int \mathrm{d}\Omega_k$ denotes an integration over the angles of $\boldsymbol{k}$ only. $Q^{\pm}_{ij}$ is proportional to δ_{ij} in three special cases:

— when $r \to 0$ or $r \to \infty$;

— when $\boldsymbol{r}$ is taken along one of the axes of co-ordinates.

Since it would be quite unelegant to specialize the system of co-ordinates in configuration space (especially with the presence of a tensor force), we prefer to keep the general form of Eq. (3.2). We will practically never need an explicit formula for the $Q^{\pm}_{ij}$. A relatively simple special one can be written:

$$(3.4)\qquad Q^{\pm}_{ij} = \left[\frac{1 \pm f(kr)}{1 \pm g(kr)}\right]^{\frac{1}{2}}\left[\delta_{ij} + u_{\pm}(kr)\,\frac{x_i x_j}{r^2}\right],$$

where $f(z) = (\sin z)/z$, $g(z) = (3/z^3)(\sin z - z\cos z)$ and $u_{\pm}(z)$ are suitable roots of the equation:

$$u_{\pm}^2 + 2u_{\pm} = \pm\frac{3(g-f)}{1 \pm g}\,(u_{+}+1)^2\,.$$

With the help of Eq. (3.3) and of the usual commutation relations obeyed by $c^*_\alpha(\boldsymbol{k})$ and $c_\alpha(\boldsymbol{k})$, we obtain the following relations:

$$[b^{\pm}_{\alpha i}, b^{\pm *}_{\beta j}] = \delta_{\alpha\beta}\delta_{ij}, \quad [b^{\pm}_{\alpha i}, b^{\mp *}_{\beta j}] = 0. \tag{3.5}$$

with all the other commutators vanishing. The functions $\varphi_1^{\pm}$ are supposed to be normalized as follows:

$$(2\pi)^{-3}\int \varphi_1^{\pm 2}(1 \pm \cos \boldsymbol{kr})\,\mathrm{d}\boldsymbol{k} = 1 \tag{3.6}$$

for all values of $\boldsymbol{r}$.

The reader who is familiar with the intermediate coupling treatment of the one-body problem will probably realize how much more complicated it becomes in the case of two bodies. However, this complication is fortunately purely formal. A close inspection of the present formalism will easily convince the reader that it really is the most straight forward extension, to the case of finite $\boldsymbol{r}$, of the usual treatment of the one-nucleon problem ([28]). (When $r \to \infty$, the system reduces to two separate nucleons interacting with their respective meson clouds; then φ_1^+ and φ_1^- go over *to the same function* $\varphi_1(k, \infty)$, which is the usual one-body trial function). In a first step, we would advise the reader to solve for himself, as an exercise, the same problem in the neutral scalar theory, where everything is much simpler. The Tomonaga trial function coincides then with the exact one (an outline of the solution of this exercise is given in the Appendix).

The general trial function for the state vector $\Phi(\boldsymbol{x})$ can now be written with the help of the operators of Eq. (3.2). It will eventually be necessary to express it in terms of eigenfunctions of the total angular momentum and the total isotopic spin. For the time being, we need only to know its most general form:

$$\Phi(\boldsymbol{r}) = \sum_{n=0}^{\infty}\sum_{p=0}^{n} C_{n,p}(\boldsymbol{r};\, \alpha, i;\, \beta, j)\,\frac{1}{[p!\,(n-p)!]^{\frac{1}{2}}}\,(b^{+*}_{\alpha i})^p (b^{-*}_{\beta j})^{n-p}\Phi_0(\boldsymbol{r})\,, \tag{3.7}$$

where it must be remembered that $\Phi_0(\boldsymbol{r})$ is the product of the two-body wave function by the meson vacuum state vector. The coefficients $C_{n,q}$ are normalized according to Eq. (2.13):

$$\sum_{n=0}^{\infty}\sum_{p=0}^{n} |\,C_{n,p}(\boldsymbol{r};\, \alpha, i;\, \beta, j)\,|^2 = 1 \tag{3.8}$$

for all values of $\boldsymbol{r}$.

([28]) There are several presentations of the intermediate coupling theory of the one-body problem, all equivalent of course. We follow here the elegant presentation of R. Riddell and H. Fried: *Phys. Rev.*, **94**, 1736 (1954).

The coefficient $C_{n,p}$, as well as the trial functions $\varphi_1^{\pm}$ themselves, will be determined by a variational principle which should, at the same time, define the energy. For this purpose, we consider first the two nucleons as fixed in space at the points $\boldsymbol{x}_1$ and $\boldsymbol{x}_2$, and treat therefore $\boldsymbol{r}$ as a fixed parameter. We separate, in the Hamiltonian of the system, the part which corresponds only to the meson field:

$$\bar{H}(\boldsymbol{r}) = H_0 + H_1(\boldsymbol{r}) \tag{3.9}$$

and solve the Schrödinger equation:

$$\bar{H}(\boldsymbol{r})\,\Phi(\boldsymbol{r}) = \mathcal{E}(\boldsymbol{r})\,\Phi(\boldsymbol{r})\,, \tag{3.10}$$

where $\mathcal{E}(\boldsymbol{r})$ is the total energy of the two fixed nucleons. $\mathcal{E}(\infty)$ is, as we have said above and will verify later, twice the self-energy δM of each nucleon interacting separately with its own meson cloud. We therefore define the potential energy as:

$$V(\boldsymbol{r}) = \mathcal{E}(\boldsymbol{r}) - \mathcal{E}(\infty)\,. \tag{3.11}$$

This separation of the self-energy corresponds to the mass renormalization; the charge renormalization will have to be performed later on $V(\boldsymbol{r})$. Making use of Eqs. (3.10), (3.11) and of the normalization condition (2.13), it is easily seen that the Schrödinger equation for the complete Hamiltonian (2.15) reduces to:

$$\Big(\sum_{i=1}^{2} T_i + V(\boldsymbol{r})\Big)\,\Phi_0(\boldsymbol{r}) = (E - 2M)\,\Phi_0(\boldsymbol{r})\,, \tag{3.12}$$

which is simply the non-relativistic Schrödinger equation with a potential $V(\boldsymbol{r})$ obeyed by the two-body wave function.

In order to solve Eq. (3.10) with the general trial function (3.7), the functions $\varphi_1^{\pm}(k, \boldsymbol{r})$ being subject to the conditions (3.6), we write the following variational principle:

$$\delta\Big\{\Phi^*(\boldsymbol{r})[\bar{H} - \mathcal{E}(\boldsymbol{r})]\Phi(\boldsymbol{r}) - \frac{2\nu_+}{(2\pi)^3}\int\varphi_1^{+2}\cos^2\frac{\boldsymbol{kr}}{2}\,\mathrm{d}\boldsymbol{k} - \frac{2\nu_-}{(2\pi)^3}\int\varphi_1{}^2\sin^2\frac{\boldsymbol{kr}}{2}\,\mathrm{d}\boldsymbol{k}\Big\} = 0\,, \tag{3.13}$$

where ν_+ and ν_- are two Lagrange multipliers to be determined later. This variation will be done in several steps: in the first one, an equivalent Hamiltonian $\bar{H}^T$, *depending only on the* $b_{\nu i}^{\pm}$ and $b_{\nu i}^{\pm *}$ will be determined from the relation:

$$\Phi^*(\boldsymbol{r})\bar{H}\,\Phi(\boldsymbol{r}) = \Phi^*(\boldsymbol{r})\bar{H}^T\Phi(\boldsymbol{r})\,. \tag{3.14}$$

The variation of (3.13) with respect to the coefficients C_{np} will then simply lead to the simplified Schrödinger equation of the intermediate coupling theory:

$$\overline{H}^T(\boldsymbol{r})\,\Phi(\boldsymbol{r}) = \mathcal{E}(\boldsymbol{r})\,\Phi(\boldsymbol{r})\,. \tag{3.15}$$

We shall then determine the form of the functions $\varphi_1^{\pm}$ by varying (3.13) with respect to an infinitesimal change of these functions.

3·2. *Determination of* $\overline{H}^T$. – Using Eqs. (3.2), we can write the following commutation relations

$$\begin{cases} [c_\alpha(\boldsymbol{k}),\, b^{+*}_{\alpha i}] = -\,i\sqrt{6}\varphi_1^+(k,\boldsymbol{r})\,Q^+_{ij}\,\dfrac{k_j}{k}\cos\dfrac{\boldsymbol{kr}}{2}\,, \\[2ex] [c_\alpha(\boldsymbol{k}),\, b^{-*}_{\alpha i}] = -\,i\sqrt{6}\varphi_1^-(k,\boldsymbol{r})\,Q^-_{ij}\,\dfrac{k_j}{k}\sin\dfrac{\boldsymbol{kr}}{2}\,, \end{cases} \tag{3.16}$$

and similar ones for $c^*_\lambda(\boldsymbol{k})$. Using relations (3.5) and the general expression (3.7), we can then write

$$c_\lambda(\boldsymbol{k})\,\Phi(\boldsymbol{r}) = -\frac{i\sqrt{6}}{k}\Big\{\varphi_1^+(k,\boldsymbol{r})\,Q^+_{\lambda j}k_j\cos\frac{\boldsymbol{kr}}{2}\,b^+_{\alpha i} + \varphi_1^-(k,\boldsymbol{r})\,Q^-_{ij}k_j\sin\frac{\boldsymbol{kr}}{2}\,b^-_{\lambda i}\Big\}\,\Phi(\boldsymbol{r}), \tag{3.17}$$

and, similarly

$$\Phi^*(\boldsymbol{r})\,c^*_\alpha(\boldsymbol{k}) = \frac{i\sqrt{6}}{k}\,\Phi^*(\boldsymbol{r})\Big\{\varphi_1^+(k,\boldsymbol{r})\,Q^+_{ij}k_j\cos\frac{\boldsymbol{kr}}{2}\,b^{+*}_{\alpha i} + \varphi_1^-(k,\boldsymbol{r})\,Q^-_{ij}k_j\sin\frac{\boldsymbol{kr}}{2}\,b^{-*}_{\alpha i}\Big\}\,. \tag{3.18}$$

The equations allow us then to write H^T as follows

$$H^T = H^T_+ + H^T_-\,, \tag{3.19}$$

with

$$\begin{cases} H^T_+ = \omega_+(\boldsymbol{r})\,b^{+}_{\lambda i}{}^{*}\,b^+_{\lambda i} + \sqrt{2}\,f^+_{ij}(T_\lambda S_i + \tau_\lambda\sigma_i)(b^+_{\lambda j} + b^{+}_{\lambda j}{}^{*}) \\ H^T_- = \omega_-(\boldsymbol{r})\,b_{\lambda i}{}^{*}\,b^-_{\lambda i} + i\sqrt{2}\,f^-_{ij}(\tau_\lambda S_i + T_\lambda\sigma_i)(b^-_{\lambda j} - b^{-}_{\lambda j}{}^{*})\,, \end{cases} \tag{3.20}$$

where the following notations have been used

$$\omega_\pm(\boldsymbol{r}) = (2\pi)^{-3}\int\omega_k\varphi_1^\pm(k,\boldsymbol{r})(1 \pm \cos\boldsymbol{kr})\,\mathrm{d}\boldsymbol{k}\,; \tag{3.21}$$

$\boldsymbol{T}$ and $\boldsymbol{S}$ are the total spin and isotopic spins defined as follows

$$T_\alpha = \frac{\tau_\alpha^{(1)} + \tau_\alpha^{(2)}}{2}, \qquad S_i = \frac{\sigma_i^{(1)} + \sigma_i^{(2)}}{2}.$$

whereas the « relative » spins and isotopic spins are defined as

$$\tau_\alpha = \frac{\tau_\alpha^{(1)} - \tau_\alpha^{(2)}}{2}, \qquad \sigma_i = \frac{\sigma_i^{(1)} - \sigma_i^{(2)}}{2}.$$

Finally the $f_{ij}^{\pm}$ are equal to

$$f_{ij}^{\pm} = \frac{1}{\sqrt{3}} \frac{f_0}{\mu} (2\pi)^{-3} \int \varphi_1^{\pm}(k, \boldsymbol{r}) k (1 \pm \cos \boldsymbol{kr}) R(\boldsymbol{k}) \bar{Q}_{ij}^{\pm} \, \mathrm{d}\boldsymbol{k}, \tag{3.22}$$

the $\bar{Q}^{\pm}$ being the inverse matrices of the $Q^{\pm}$

$$\bar{Q}_{ij}^{\pm} Q_{jk}^{\pm} = \delta_{ik}. \tag{3.23}$$

Since the $b_{\alpha i}^{+}$ commute with the $b_{\alpha i}^{-}$, etc., it can be seen that the simplified equation (3.15) splits into two separate equations

$$\bar{H}_{\pm}^{T} \Phi_{\pm} = \mathcal{E}_{\pm} \Phi_{\pm}, \tag{3.24}$$

with $\mathcal{E} = \mathcal{E}_{+} + \mathcal{E}_{-}$, the state vector Φ being written as a product involving separately the $b_{\alpha i}^{+*}$ and $b_{\alpha i}^{-*}$. Consequently, Eqs. (3.24) are not really much more difficult to solve than those corresponding to the one body problem ([29]). They involve separately as in the latter case, the wave equation of nine coupled harmonic oscillators, which can be simplified ([18]) by making use of invariance requirements. The only difference is in the spin and isotopic spin dependence. The complication introduced by the $f_{ij}^{\pm}$ matrices is only apparent, since a special system of co-ordinates can always be chosen to make them diagonal.

Nevertheless, the solution of Eqs. (3.24) can only be obtained by means of a fairly involved electronic computing program, which did not seem to us really necessary at this early exploratory stage of our work. An approx-

([29]) The problem of nuclear forces, when reduced to the solution of Eqs. (3.24) becomes analogous to the treatment of the interaction of one nucleon with its own meson cloud. Similarly, the calculation of the production of mesons in nucleon-nucleon collisions would become, in the present formalism, analogous to the intermediate coupling treatment of meson-nucleon scattering.

imation to the energy $\mathcal{E}(\boldsymbol{r})$ will be obtained by an indirect method in § 4 of the present Section.

3·3. *Form of the $\varphi_1^{\pm}$ functions.* – We now calculate the variation of Eq. (8.13) when an infinitesimal change

$$\varphi_1^{\pm} \to \varphi_1^{\pm} + \delta\varphi_1^{\pm}$$

is made on the meson trial functions. For the φ_1^{+} function, for example, the following relation is easily verified with the help of Eq. (3.7)

$$\delta_{\varphi_1^+}\Phi(\boldsymbol{r}) = -\frac{i\sqrt{6}}{(2\pi)^3}\int \delta\varphi_1^+(k,\boldsymbol{r})Q_{ij}^+\frac{k_j}{k}\cos\frac{\boldsymbol{kr}}{2}c_\alpha^* b_{\alpha i}^+\Phi(\boldsymbol{r}). \tag{3.25}$$

and similarly

$$\delta_{\varphi_1^+}\Phi^*(\boldsymbol{r}) = +\frac{i\sqrt{6}}{(2\pi)^3}\Phi^*(\boldsymbol{r})\int \delta\varphi_1^+(k,\boldsymbol{r})Q_{ij}^+\frac{k_j}{k}\cos\frac{\boldsymbol{kr}}{2}b_{\alpha i}^{+*}c_\alpha\,\mathrm{d}\boldsymbol{k}\,. \tag{3.26}$$

Eq. (3.13) then leads to the relation

$$\frac{1}{4\pi}\int \mathrm{d}\Omega_k\cos\frac{\boldsymbol{kr}}{2}\Big\{i\sqrt{6}Q_{ij}^+\frac{k_j}{k}[\Phi^* b_{\alpha i}^{+*}c_\alpha(\boldsymbol{k})(\overline{H}-\mathcal{E})\Phi - \\ -\Phi^*(\overline{H}-\mathcal{E})c_\alpha^*(\boldsymbol{k})b_{\alpha i}^+\Phi] - 4\nu_+\varphi_1^+\cos\frac{\boldsymbol{kr}}{2}\Big\} = 0\,. \tag{3.27}$$

Making now use of the commutation relation

$$[c_\alpha(\boldsymbol{k}),\overline{H}] = \omega_k c_\alpha(\boldsymbol{k}) - \frac{2if_0}{\mu}R(k)\Big\{\cos\frac{\boldsymbol{kr}}{2}(T_\alpha S_i+\tau_\alpha\sigma_i)k_i - \\ - i\sin\frac{\boldsymbol{kr}}{2}\tau_\alpha S_i + T_\alpha\sigma_i)k_i\Big\} \tag{3.28}$$

and a similar one for $c_\alpha^*(\boldsymbol{k})$, we obtain, with the help of Eqs. (3.17), (3.18)

$$\varphi_1^+(k,\boldsymbol{r})\{\Phi^* b_{\alpha i}^{+*}(\overline{H}-E+\omega_k)b_{\alpha i}^+\Phi - \nu_+\} = \\ = -\frac{f_0}{\mu\sqrt{6}}kR(k)\,\overline{Q}_{ij}^+\Phi^*(T_\alpha S_j+\tau_\alpha\sigma_j)(b_{\alpha i}^+ + b_{\alpha i}^{+*})\Phi\,. \tag{3.29}$$

(Notice that several of the integrals over angles vanish when going from (3.27) to (3.29).) It can now be verified that the left hand side of Eq. (3.29) is not changed if $\overline{H}$ is replaced by $\overline{H}^T$.

Using then the commutation relation

$$[b_{\alpha i}^+,\overline{H}^T] = \omega_+ b_{\alpha i}^+ + \sqrt{2}f_{ij}^+(T_\alpha S_z+\tau_\alpha\sigma_j) \tag{3.30}$$

and a similar one for $b_{i\nu}^{+*}$, we can simplify the left hand side of Eq. (3.29) by taking into account the fact that $\Phi(\boldsymbol{r})$ is a solution of (2.15):

$$\varphi_1^+(k, \boldsymbol{r})\{N_+(\omega_k - \omega_+) - \sqrt{2} f_{ij}^+ M_{ij}^+ - \nu_+\} = -\frac{f_0}{\mu}\sqrt{\frac{2}{3}}\, kR(k) Q_{ij}^+ M_{ij}^+ , \tag{3.31}$$

where we have set

$$N_\pm = \Phi^* b_{\nu i}^{\pm *} b_{\nu i}^{\pm} \Phi , \tag{3.32}$$

and

$$M_{ij}^+ = \tfrac{1}{2}\Phi^*(T_\alpha S_i + \tau_\alpha \sigma_i)(b_{\alpha j}^+ + b_{\alpha j}^{+*})\Phi . \tag{3.33}$$

Multiplying both sides of (3.31) by $\varphi^+(1+\cos \boldsymbol{kr})$ and integrating over $\boldsymbol{k}$ gives $\nu_+ = 0$. We obtain therefore finally

$$\varphi_1^+(k, \boldsymbol{r}) = -\frac{f_0}{\mu}\sqrt{\frac{2}{3}} Q_{ij}^+ \frac{M_{ij}^+}{N_+} \frac{kR(k)}{\omega_k + \Lambda_+(\boldsymbol{r})} , \tag{3.34}$$

where we have set

$$\Lambda_\pm(\boldsymbol{r}) = -\omega_\pm(\boldsymbol{r}) - \sqrt{2} f_{ij}^\pm \frac{M_{ij}^\mp}{N_\mp} . \tag{3.35}$$

By the same method, we would have obtained for $\varphi_1(k, \boldsymbol{r})$ a similar expression as Eq. (3.34) (by exchanging the + and — indices) with the definition

$$M_{ij}^- = \frac{i}{2}\Phi^*(\tau_\alpha S_i + T_\nu \sigma_i)(b_{\alpha j}^- - b_{\alpha j}^{-*})\Phi . \tag{3.36}$$

The coefficient $\bar{Q}_{ij}^\pm M_{ij}^\mp / N_\pm$ of $\varphi_1^\mp$ is completely determined by the normalization condition (3.6), so that the functions $\Lambda_\pm(\boldsymbol{r})$ are the only ones for the determination of which a solution of Eq. (3.15) is necessary. It is these functions which we will now try to estimate by an indirect method.

3·4. *The « potential equation ».* – Since we do not know the value of $\mathcal{E}(\boldsymbol{r})$ which would be obtained through the variational principle (3.13), we look for an approximation by connecting, through the Schrödinger equation obeyed by $\Phi(\boldsymbol{r})$, the amplitudes for zero and one meson. The expansion (3.7) can be re-expressed by writing explicitly the first two terms:

$$\Phi(\boldsymbol{r}) = \{C_0 + C_1^+(\boldsymbol{r};\ i, j)(T_\alpha S_i + \tau_\alpha \sigma_i) b_{\alpha j}^{+*} + \\ + C_1^-(\boldsymbol{r};\ i, j)(\tau_\nu S_i + T_\nu \sigma_i) b_{\nu j}^{*} + \text{etc.}\}\Phi_0 , \tag{3.37}$$

so that, by multiplying Eq. (2.15) (without H_{II}) on the left by $\Phi_0^*(\boldsymbol{r})$, we get the « exact » relation

$$(3.38)\qquad \Phi_1^*(E - 2M + 2\delta M - \sum T_i)C_0\Phi_0 - \Phi_0^*[V(\boldsymbol{r}) + 2\delta M]\Phi_0 = \Phi_0^*\mathcal{E}(\boldsymbol{r})\Phi_0 = \\ = \Phi_0^* H_I^-[C_{1ij}^+(T_\alpha S_i + \tau_\alpha\sigma_i)b_{\alpha j}^{+*} + C_1^-(i,j)(\tau_\alpha S_i + T_\alpha\sigma_i)b_{\alpha ij}^{-*}]\Phi_0\,,$$

where H_I is only the « absorbing » part of H_I. If we were going to proceed with this equation (calculating the $C_1^{\pm}(ij)$ coefficients through Eq. (3.15)) we would be facing again a special complication due to the $Q_{ij}^{\pm}$ operators. Since we only want an estimate of the $\Lambda_{\pm}$ functions, it is sufficient for our purpose to calculate *an average of* $\mathcal{E}(\boldsymbol{r})$ *over angles*, i.e. the central part of the energy $\mathcal{E}_c$. Then both the $Q_{ij}^{\pm}$ and $C_1^{\pm}(ij)$ are proportional to δ_{ij}, and Eq. (3.38) gives simply

$$(3.39)\qquad \mathcal{E}(r) = -\frac{f^2}{\mu^2(2\pi)^3}\int R^2(k)k^2\,\mathrm{d}\boldsymbol{k}\left\{\frac{[3 + \frac{1}{3}(\tau_1\cdot\tau_2)(\sigma_1\cdot\sigma_2)]}{\omega_k + \Lambda_+(r)}(1 + \cos\boldsymbol{k}\cdot\boldsymbol{r}) + \right. \\ \left. + \frac{3 - \frac{1}{3}(\tau_1\cdot\tau_2)(\sigma_1\cdot\sigma_2)}{\omega_k + \Lambda_-(r)}(1 - \cos\boldsymbol{k}\cdot\boldsymbol{r})\right\}.$$

In this equation, the ratios $f_0C_1^{\pm}/C_0$ multiplied by the normalization coefficients of $\varphi_0^{\pm}$ have been related to the renormalized coupling constant f^2 by comparison with the known expression of $\mathcal{E}_c$ obtained from perturbation theory to the second order in f. In other words Eq. (3.39) is essentially an improved Tamm-Dancoff approximation, in the sense that the replacement of $R(k)/\omega_k$ by $\varphi_1^{\pm}(k) \simeq R(k)[\omega_k + \Lambda_{\pm}]^{-1}$, the general form of which has been determined by a variation principle, means that higher order effects are, to a certain extent included. Naturally, in the spirit of the intermediate coupling theory, Eq. (3.39) should not give as good an approximation as the value directly determined from the variation (3.13).

The Λ_+ and Λ_- functions are proportional to f^2 (plus, of course, terms of higher order). We know, in addition, that they tend, when $r \to \infty$, to the same constant λ, which also appears in the $\varphi_1(k, \infty)$ function entering in the one-body problem [18]. We shall then write

$$(3.40)\qquad \Lambda_{\pm} = \lambda + \Lambda_{\pm}^{(1)}(r)\,,$$

where $\Lambda_{\pm}^{(1)}$ tends to zero for $r \to \infty$ at least like $\exp[-\mu r]$. These functions will be determined by comparison with $\mathcal{E}_c$ obtained from perturbation theory to the fourth order in the renormalized coupling constant

$$(3.41)\qquad \mathcal{E} \simeq -\frac{6f^2}{\mu^2}(2\pi)^{-3}\int\frac{R^2(k)k^2\,\mathrm{d}\boldsymbol{k}}{\omega_k} + \\ + \frac{4f^4}{\mu^4}(2\pi)^{-6}\int\frac{R^2(k)\,R^2(k')}{\omega}\,k^2k'^2\left(\frac{5}{\omega_{k'}} - \frac{4}{\omega_k + \omega_{k'}}\right)\mathrm{d}\boldsymbol{k}\,\mathrm{d}\boldsymbol{k}' + V_{2c}^{(G)} + V_{4c}^{(G)}\,,$$

where $V_{2c}^{(G)}$ and $V_{4c}^{(G)}$ are respectively the second and fourth order central parts of the Gartenhaus potential. In the following, we shall adopt the value, $f^2/4\pi = 0.10$, so that λ is equal to the number already determined by FRIEDMAN, LEE and CHRISTIAN ([18])

$$\lambda = 3.39 \,. \tag{3.42}$$

It is interesting to note that this value is not very different from the one which can be determined by fitting the second term of the expansion of (3.39) (with $r \to \infty$) with the fourth order self-energy (with a square cut-off at $\omega_{\max} - 6.0\,\mu$, one gets in this way: $\lambda \simeq 4.07$). This gives us a certain confidence in the determination of the $A_{\pm}^{(1)}$ by expansion, since an expansion of the self-energy is equivalent to an expansion of the potential at the origin. Keeping the value (3.42) we compare with $V_{2c}^{(G)}$ and $V_{4c}^{(G)}$ the potential of respective ranges $1/\mu$ and $1/2\mu$ obtained by expanding ([30]) (3.39) in powers of $A_{\pm}^{(1)}$. We then have, for the terms of range $1/\mu$

$$\frac{1}{(2\pi)^3}\int \frac{R^2(k)k^2\,\mathrm{d}\boldsymbol{k}}{(\omega_k+\lambda)^2}\left\{\left[3+\frac{1}{3}(\tau_1\cdot\tau_2)(\sigma_1\cdot\sigma_2)\right]A_+^{(1)}+\left[3-\frac{1}{3}(\tau_1\cdot\tau_2)(\sigma_1\cdot\sigma_2)\right]A_-^{(1)}\right\}= \tag{3.43}$$

$$= -\frac{2(\tau_1\cdot\tau_2)(\sigma_1\cdot\sigma_2)}{3(2\pi)^3}\int R^2\,\mathrm{d}\boldsymbol{k}\,k^2\left(\frac{1}{\omega_k}-\frac{1}{\omega_k+\lambda}\right)\exp\left[i\boldsymbol{k}\boldsymbol{r}\right]\mathrm{d}\boldsymbol{k}\,.$$

and, for the terms of range $1/(2\mu)$

$$V_{4c}^{(G)} = \frac{f^2}{(2\pi)^3}\int \frac{R^2(k)k^2\exp\left[i\boldsymbol{k}\boldsymbol{r}\right]}{(\omega_k+\lambda)^2}\left\{\left[3+\frac{1}{3}(\tau_1\cdot\tau_2)(\sigma_1\cdot\sigma_2)\right]A_+^{(1)}- \right. \tag{3.44}$$

$$\left. -\left[3-\frac{1}{3}(\tau_1\cdot\tau_2)(\sigma_1\cdot\sigma_2)\right]A_-^{(1)}\right\} - \frac{f^2}{(2\pi)^3}\int \frac{R^2(\boldsymbol{k})\,\mathrm{d}\boldsymbol{k}\,k^2}{(\omega_k+\lambda)^3}\cdot$$

$$\cdot\left\{\left[3+\frac{1}{3}(\tau_1\cdot\tau_2)(\sigma_1\cdot\sigma_2)\right]A_+^{(1)2}+\left[3-\frac{1}{3}(\tau_1\cdot\tau_2)(\sigma_1\cdot\sigma_2)\right]A_-^{(1)2}\right\}.$$

These equations allow, in principle, the determination of $A_{\pm}^{(1)}(r)$. It turns out, actually, that the quadratic terms on the right hand side of (3.44) contribute very little, due to the smallness of the coefficient in front of them, so that they can be neglected in first approximation (except at very short distances).

An interesting question is whether A_{+} can take, in certain states, negative values, which would lead, in Eq. (3.39), to the appearance, for r smaller than

([30]) It should be noted that this expansion is not made in powers of f^2, because we do not know the way in which λ depends on the coupling constant. We simply make use of the fact that a *renormalized* potential of order f^{2n} necessarily decreases at large distances like $\exp[-n\mu r]$.

a critical value r_c, of an oscillating potential rather than a repulsive core. To determine this, we have evaluated $\Lambda_\pm$ at the extreme value $r = 0$ for the different states of the N-N system (Table II), using the same square cut-off at $\omega_{\text{max}} = 6.0\,\mu$.

TABLE II. – *Values of* $\Lambda_\pm(0)$ *for the* N-N *system* (*in units of* μ).

States	Even Triplet and Singlet	Odd Triplet	Odd Singlet (*)
$\Lambda_+(0)$	13.3	— 1.9	— 2.7
$\Lambda_-(0)$	1.5	8.5	—

(*) In the case of the odd singlet states, the two Eqs. (III. 43, 44) give two independent values of $\Lambda_+^{(1)}$ (since the coefficient of $\Lambda_-^{(1)}$ vanishes) which turn out to be relatively close (— 2.7 and — 3.6); we have taken the first one, which is more reliable.

It hardly needs to be emphasized that the values given in Table II must only be considered as rough orders of magnitude, since they are calculated at the origin, where everything depends very much on the form chosen for the source function. There is an indication that Λ_+ becomes negative at short distances, but this occurs clearly practically at the core radius $r_c \simeq 0.4 \cdot 10^{-13}$ cm so that the consequences on the properties of the two body at low or intermediate energies are not really significant. It is only if one were to take seriously the fixed source semi-phenomenological potential at high energies that the replacement of a repulsive core by a rapidly oscillating potential would affect the theoretical predictions in a way which it is not easy to determine off-hand. In this case, however, the functions $\Lambda_\pm$ would have to be evaluated much more carefully.

3·5. *Case of the* N-N *system.* – We indicate briefly here the main characteristic of the real part of the interaction in the case of the nucleon-antinucleon system. The treatment in the intermediate coupling theory goes, of course, very much in the same way as for the N-N system. However, the result for the interaction is different. If one uses the approximate method of the preceding paragraph to determine the central part $\bar{\mathcal{E}}_c$ of the energy, one gets the following result

$$(3.45)\qquad \bar{\mathcal{E}}_c = -\frac{f^2}{(2\pi)^3}\int R^2(k)k^2\,\mathrm{d}k\left\{\frac{[3-\tfrac{1}{3}(\tau_1\cdot\tau_2)(\sigma_1\cdot\sigma_2)](1+\cos \boldsymbol{kr})}{\omega_k+\bar{\Lambda}_+}+\right.$$
$$\left.+\frac{[3+\tfrac{1}{3}(\tau_1\cdot\tau_2)(\sigma_1\cdot\sigma_2)](1-\cos \boldsymbol{kr})}{\omega_k+\bar{\Lambda}_-}\right\}.$$

The functions $\bar{A}_{\pm}$ take the form

$$\bar{A}_{\pm} = \lambda + \bar{A}_{\pm} , \tag{3.46}$$

where the constant λ is, of course, the same as before, but where the $A_{\pm}^{(1)}$ (which tend to zero at infinity as $\exp[-\mu r]$) are related to those of the N-$\bar{\text{N}}$ system by the relations

$$\begin{cases} A_{+}^{(1)} = -A_{-}^{(1)} , \\ A^{(1)} = -A_{-}^{(1)} . \end{cases} \tag{3.47}$$

The change of sign of these functions (together with their exchange) corresponds essentially to the fact that the series (1, 3) becomes alternating in the case of the N-N system. However, the sign of the complete functions $A_{\pm}$ of Eq. (3.46) does not change until r becomes fairly close to the core radius r_c since the energies $A_{\pm}^{(1)}$ must first grow in absolute value until they reach $\lambda = 3.39\,\mu \simeq 470$ MeV before a pole appears in the denominators of Eq. (3.45) and the potential becomes rapidly oscillating. Table III gives, as in the last Section, rough estimates of $\bar{A}_{\pm}$ at $r = 0$.

TABLE III. – *Values of* $\bar{A}_{\pm}(0)$ *for the* N-$\bar{\text{N}}$ *system (in units of* μ).

States	Even Triplet and Singlet	Odd Triplet	Odd Singlet
$\bar{A}_{+}$	5.3	— 1.7	—
$\bar{A}_{-}$	— 6.5	8.7	9.5

4. – Treatment of the non-hermitian part of the hamiltonian.

We now turn to the intermediate coupling treatment of the second part H_{II} of the interaction Hamiltonian. Since it will clearly involve the annihilation and creation of s-waves mesons, it would be natural to introduce, in a way analogous to what was done in the last Section, s-state operators $a_{\nu}^{\mp} \simeq \int \varphi_0^{\mp}(k, r)(1 \pm \cos kr)^{\frac{1}{2}} c_{\nu}(k)\,\mathrm{d}k$. However, one sees immediately that a_{ν}^{+}, defined in this way, does not commute with $b_{\nu i}^{-*}$, and similarly a_{α}^{-} with $b_{\nu i}^{+*}$. Physically, this corresponds to the fact mentionned in the Introduction, that a meson emitted in a p-state by one nucleon can be absorbed in an s-state by the other and inversely. To avoid this difficulty we have to define slightly different « s-state » operators, which actually contain a p-state part

$$a_{\alpha}^{+}(r) = \frac{\sqrt{2}}{(2\pi)^3} \int \varphi_0^{+}(k, r) X^{+}(kr) c_{\lambda}(k) \left[\cos \frac{kr}{2} - Q_{ij}^{-} Q_{il}^{-} D_j \frac{k_l}{k} \sin \frac{kr}{2} \right] \mathrm{d}k , \tag{4.1}$$

where the quantities D_j are defined as follows

$$D_j = \frac{\sqrt{3}}{4\pi}\int \mathrm{d}\Omega_k\, k_j \sin \boldsymbol{kr} = \frac{kx_j}{\sqrt{3}}\, g(kr)\,, \tag{4.2}$$

(the g function is defined in § 1 of last Section). Similarly,

$$a_\alpha^-(\boldsymbol{r}) = \frac{\sqrt{2}}{(2\pi)^3}\int \varphi_0^-(k,\boldsymbol{r})\, X^-(kr)\, c_\alpha(\boldsymbol{k})\left[\sin\frac{\boldsymbol{kr}}{2} - Q_{ij}^+ Q_i^+ D_j \frac{k_l}{k}\cos\frac{\boldsymbol{kr}}{2}\right]\mathrm{d}\boldsymbol{k}\,. \tag{4.3}$$

The functions X^- are simply introduced in order to normalize the functions $\varphi_0^\pm$

$$\frac{1}{(2\pi)^3}\int \varphi_0^{\pm 2}(1 \pm \cos \boldsymbol{kr})\,\mathrm{d}\psi = 1 \tag{4.4}$$

for all values of r. Their precise value is, in terms of the function $f(z)=(\sin z)/z$,

$$X^\pm(kr) = \frac{1 \pm f(kr)}{1 \pm f - (Q_{ik}^- D_k)^2}\,. \tag{4.5}$$

One verifies easily the following commutation relations

$$[a_\alpha^\pm, a_\beta^{\pm *}] = \delta_{\alpha\beta}\,, \qquad [a_\alpha^\pm, b_{\beta i}^{\mp *}] = 0\,; \tag{4.6}$$

all the other commutators vanish.

We suppose now that the state vector Φ contains simultaneously the operators $a_\alpha^{\pm *}$ and $b_{\alpha i}^{\pm *}$, so that Eqs. (3,17), (3.18) become

$$c_\alpha(\boldsymbol{k})\Phi = \left\{\sqrt{2}\varphi_0^+ X^+\left[\cos\frac{\boldsymbol{kr}}{2} - Q_{ij}^- Q_i^- D_j \frac{k}{k}\sin\frac{\boldsymbol{kr}}{2}\right] a_\alpha^+ - \right. \tag{4.7}$$

$$\left. - \frac{i\sqrt{6}}{k}\,\varphi_1^+ Q_{ij}^+ k_j \cos\frac{\boldsymbol{kr}}{2}\, b_{\alpha i}^+ + \text{similar terms with } (\,)^-\right\}\Phi(\boldsymbol{r})\,.$$

and another similar equation for $\Phi^* c_\lambda^*(\boldsymbol{k})$. One verifies however that H_1^T (the Tomonaga equivalent Hamiltonian for H_1) still does not involve the $a_\lambda^\pm$ operators so that the real part of the interaction remains unchanged ([31]). H_0^T, in addition to the terms involving the $b_{\alpha i}^\pm$, will now contain also:

$$H_0^T(s\text{-state}) = \omega_0^+ a_\alpha^{+ *} a_\alpha^+ + \omega_0^- a_\alpha^{- *} a_\alpha^-\,, \tag{4.8}$$

with

$$\omega_0^\pm = \frac{1}{(2\pi)^3}\int \omega_k \varphi_0^{\pm 2}(1 \pm \cos \boldsymbol{kr})\,\mathrm{d}\boldsymbol{k}\,. \tag{4.9}$$

([31]) This is the reason why we chose to represent the $b_{\alpha i}^\pm$ as pure p-state operators and the a_α as mixtures of s- and p-states. A different choice would produce interference terms in the real part of the interaction, and this would be quite unpleasant.

On the other hand, H_{II}^{T} will consist of three terms: two terms involving separately the $b_{\lambda i}^{-}$ and the $a_{\lambda}^{\mp}$, *plus an interference term* consisting of products of $a_{\lambda}^{+} b_{\lambda i}^{-}$ on one hand, and $a_{\lambda}^{-} b_{\lambda i}^{+}$ on the other.

In this Section, we shall be mostly interested in getting an approximate expression of the state vector Φ, and, particularly, of the s-state φ_0 function. To be able to do so, we shall unavoidably be obliged to simplify, to a certain extent, the expression of H_{II}^{T}. The imaginary part of the potential, however, will be computed directly, in the next Section, by calculating the matrix elements of the true Hamiltonian H_{II}, using the approximate state vector obtained here.

The part of H_{II}^{T} which is quadratic in the $b_{\lambda i}^{\mp}$ will simply add a small imaginary correction to the p-state Hamiltonian considered in the last Section. Its influence will become important only for those values of r where the p-state meson momentum distributions $\varphi_1^{\pm}$ contain a pole, since it will then remove the singularity, giving, so to speak, a width to the p-state excited level represented by the pole. However, we have seen that a singularity appears in the $\varphi_1^{\pm}$ functions only for values of r which are close to the core radius, so that it will have no influence in the asymptotic region in which we are mostly interested. In this region, actually, we will replace with a good approximation both φ_1^{+} and φ_1^{-} by their common limit, the one-body function $\varphi_1(k, \infty)$.

The interference terms between s- and p-states mesons create a difficult problem. When we discuss them in Sect. **5**, it will be shown that they very probably introduce only short range forces. A situation might arise, however, in which these « short range » forces consist actually of fairly weakly decreasing exponentials, which might influence the outer part of W in a significant manner. It would consequently be necessary to take them into account in the calculation of both φ_0 and φ_1, which would then become hopelessly complicated. However, even if these interference terms affect the details of the annihilation force, we do not believe that they will change its qualitative aspects, so that we did not think it necessary to worry too much about them at the present stage of our work.

The part of H_{II}^{T} which corresponds to a pure s-state interaction is obtained by substituting the first term of (4.7) (and a similar term for $c_{\lambda}^{*}(\boldsymbol{k})$) into the expression for H_{II} expressed in momentum space. The following relations have also to be used

$$\left\{\begin{array}{l} c_{\lambda}(\boldsymbol{k}) \dfrac{1}{E - H_0} = \dfrac{1}{E - H_0 - \omega_k} c_{\lambda}(\boldsymbol{k}) , \\ \\ c_{\lambda}^{*}(\boldsymbol{k}) \dfrac{1}{E - H_0} = \dfrac{1}{E - H_0 + \omega_k} c_{\lambda}^{*}(\boldsymbol{k}) . \end{array}\right. \tag{4.10}$$

The part of the Hamiltonian involving the δ-function is replaced by an average value to be evaluated later, so that H_{II}^{T} takes the approximate form

$$H_{II}^{T} = H_{II}^{T^+} + H_{II}^{T^-} + H_{II}^{(0)}, \tag{4.11}$$

with

$$H_{II}^{T\mp} = -i[\pm Y_{\pm}^{*} Z_{\pm}^{*} a_{\alpha}^{\pm 2} \pm Y_{\pm} Z_{\pm} a_{\alpha}^{\pm *2} + (Y_{\pm} Z_{\pm}^{*} + Y_{\pm}^{*} Z_{\pm}) a_{\alpha}^{\pm *} a_{\alpha}^{\pm})] \tag{4.12}$$

and

$$H_{II}^{(0)} = -2i \frac{\pi \Gamma^2}{(2\pi)^3} \int R^2(k) \langle \delta(E_0 - H_0 - \omega_k) \rangle \, \mathrm{d}\boldsymbol{k} \,. \tag{4.13}$$

In the expression (4.12) for $H_{II}^{T^{\pm}}$, a special isotopic spin dependence has been chosen, namely the one which corresponds to the first term of Eq. (2.25). This is simply for the purpose of illustrating the form which is taken by $\varphi_0^{\pm}$, since, in this case, the Tomonaga equivalent equation can be solved exactly. As was explained at the end of Sect. 2, the choice of one of the three possible isotopic invariants is, to a large extent, arbitrary at the present stage of the experimental situation, where little is known about the charge distribution of the π-mesons produced (and the relative annihilation probabilities of p-$\bar{\mathrm{p}}$, n-$\bar{\mathrm{p}}$, etc.).

In Eq. (4.12) the coefficients $Y_{\pm}$ and $Z_{\pm}$ are defined as follows

$$\begin{cases} Y_{\pm} = \dfrac{\Gamma}{(2\pi)^3} \displaystyle\int \frac{R(k)}{X_+} (1 \pm \cos \boldsymbol{kr}) \varphi_0^{\pm}(k, \boldsymbol{r}) \, \mathrm{d}\psi \,, \\ Z_{\pm} = \dfrac{\Gamma}{2(2\pi)^3} \displaystyle\int \frac{R(k)}{X_+} (1 \pm \cos \boldsymbol{kr}) [\langle \delta(E - H_0 - \omega_k) \rangle + \\ \qquad + \langle \delta(E - H_0 - \omega_k) \rangle] \cdot \varphi_0^{\pm}(k, \boldsymbol{k}) \, \mathrm{d}\boldsymbol{k} \,. \end{cases} \tag{4.14}$$

The Tomonaga equation for the pure s-states can be separated into two parts involving respectively the Φ_+ and Φ_- state vectors. Each part can then be diagonalized by appropriate canonical transformations. We do it here in the case of Φ_+, the operations in the case of Φ_- being entirely similar.

Putting $Y_+ = |Y_+| \exp[i\eta_+]$ and $Z_+ = |Z_+| \exp[i\zeta_+]$ and $Y_+ Z_+^{*} + Y_+^{*} Z_+ = 2\gamma_+^2$ (where γ_+ is a real function of r), we first make the transformation

$$\Phi_+ = (\exp[i\eta_+ a_{\alpha}^{+ *} a_{\alpha}^{+}] + \exp[i\zeta_+ a_{\alpha}^{+ *} a_{\alpha}^{+}]) \Phi_+' \,, \tag{4.15}$$

which leaves H_0^T unchanged and transforms H_{II}^{T+} into

$$H_{II}^{T+} = -i\gamma_+^2 (a_{\alpha}^{+} + a_{\alpha}^{+ *})^2 + i\gamma_+^2 \,. \tag{4.16}$$

A second canonical transformation

$$\Phi' = \exp\left[(\beta/2)(p_\alpha^+ q_\alpha^+ + q_\lambda^+ p_\lambda^+)\right]\Phi'' , \tag{4.17}$$

where

$$\begin{cases} q_\lambda^+ = (2\omega_a^+)^{-\frac{1}{2}}(a_\lambda^+ + a_\lambda^{+*}) , \\ p_\alpha^+ = -i\,(\omega_0^+/2)^{\frac{1}{2}}(a_\alpha^+ - a_\alpha^{+*}) , \end{cases} \tag{4.18}$$

and

$$\operatorname{tg} 4\beta = \frac{4\,|\gamma^+|^2}{\omega_0^+} , \tag{4.19}$$

brings then the complete Hamiltonian into the diagonal form

$$H_+'' = \frac{1}{2}\exp\left[-2i\beta\right](p_\alpha^{+2} + \Omega_+^2\, q_\alpha^{+2}) - \frac{3\omega_0^+}{2} - i(\varepsilon_0 - \gamma_+^2) , \tag{4.20}$$

where $\Omega_2^+ = \omega_0^2(1+(16\gamma_+^4/\omega_0^2))^{\frac{1}{2}}$ and ε_0 is the average value of $H_{\mathrm{II}}^{(0)}$. This leads easily to the following expression for the ground state energy

$$\mathcal{E}_+ = \frac{3}{2}\exp\left[-2i\beta\right]\Omega_+ - \frac{3\omega_0^+}{2} - i(\varepsilon_0 - \gamma_-^2) . \tag{4.21}$$

The form of the φ_0^+ function itself is determined by a variation principle similar to the one of Sect. 3·3, except that a certain care has to be taken in handling the non-hermitian part of the Hamiltonian. We write the variational principle

$$\delta\left\{\Phi^+(H-\mathcal{E})\Phi + \Phi^{+*}(H^*-\mathcal{E}^*)\Phi^* - \frac{\nu}{(2\pi)^3}\int\varphi_0^*\varphi_0\,\mathrm{d}\boldsymbol{k}\right\} = 0 , \tag{4.22}$$

where the complex conjugation sign in the second term means that, in the state vector itself, the role of φ_0 and φ_0^* have to be exchanged, φ_0^* appearing now in the definition of a_α and φ_0 in the definition of a_λ^*. One then obtains easily for φ_0^+, for example, the following expression

$$\varphi_0^+ \simeq \frac{iR(k)}{\omega_k - ((\mathcal{E}_+ + i\varepsilon_0)/N_+)} = \frac{iR(k)}{\omega_k - \omega_0^+ - i\xi_-^2} , \tag{4.23}$$

where $N_+ = \Phi_+^+ a_\alpha^{+*} a_\alpha \Phi_+$ and $\xi_+^2 = 2\sqrt{2}\gamma_+^2(1+\sqrt{(16\gamma_4^+/\omega_0^{+2})})^{-\frac{1}{2}}$. The $\simeq$ sign in Eq. (4.23) means, of course, that φ_0^+ has to be normalized according to (4.4). A similar expression can be obtained for φ_0^-.

The form (4.23) of the φ_0 functions is the main result of this Section. It

is seen that $|\varphi_0|^2$ has a resonant shape around ω^+, the resonance being fairly narrow, since the « width » ξ^2 is, as can be seen from (4.19) and (4.14), proportional to Γ^2. This expression of the s-state mesons momentum distribution, which is extremely different from the p-state corresponding function, can be seen to be fairly independent of the special form of the annihilation interaction which we have used in this Section. It follows entirely from the fact that there is no s-state interaction apart from the imaginary one, and that the latter is quadratic in the meson creation and annihilation operators ([32]).

The last result of interest in this Section is the form of the Φ^+ state vector itself, or, rather, of the transformed vector Φ_+, defined by (4.15)

$$\Phi'_+ \simeq \sum_{n=0}^{\infty} \frac{1}{n!} \left(\frac{iU_+}{2}\right)^n (a_\alpha^{+*})^{2n} \Phi_0 \,, \tag{4.22}$$

where

$$U_+ = \frac{\operatorname{tg} 2\beta}{\cos 2\beta + \sqrt{\cos 4\beta}} [\sqrt{\cos 4\beta} + i \sin 2\beta] \,. \tag{4.23}$$

In the limit of very small Γ^2, U_+ is simply given by

$$U_+ \simeq \frac{|\gamma_+|^2}{\omega_0^+} \,. \tag{4.24}$$

5. – Estimation of the imaginary potential.

We are now in the position of discussing directly the average value of the actual annihilation Hamiltonian H_{II}, using the information we have obtained in the last two Sections on the s- and p-parts of the state vector for the nucleon-antinucleon system in the Tomonaga approximation. For the calculation of the average value $\langle H_{\text{II}} \rangle$ it is convenient to write H_{II} in a form where always the creation operators are on the right and the annihilation operators on the left

$$\begin{aligned} H_{\text{II}} = H_{\text{II}}^{(0)} - \frac{2i\pi\Gamma^2}{(2\pi)^6} \int R(k)\, R(k') \cdot \\ \cdot \Big\{ [\delta(E - H_0 - \omega_k) c_\alpha(\boldsymbol{k}) c_\alpha(\boldsymbol{k}') + c_\alpha^*(\boldsymbol{k}) c_\alpha^*(\boldsymbol{k}')\, \delta(E - H_0 + \omega_{k'})] \cos(\boldsymbol{k} + \boldsymbol{k}') \frac{\boldsymbol{x}}{2} - \\ - c_\alpha^*(\boldsymbol{k}) [\delta(E - H_0 + \omega_k - \omega_{k'}) + \delta(E - H_0)] c_\alpha(\boldsymbol{k}') \cos(\boldsymbol{k} - \boldsymbol{k}') \frac{\boldsymbol{x}}{2} \Big\} \mathrm{d}\boldsymbol{k} \mathrm{d}\boldsymbol{k}' \,, \end{aligned} \tag{5.1}$$

where $H_{\text{II}}^{(0)}$ is given by Eq. (4.13).

We start first with the calculation of the p-state part of $\langle H_{\text{II}} \rangle$.

([32]) The situation is completely different for a complex linear interaction. In the case of the neutral scalar theory, for example, with an imaginary coupling constant, one would still obtain a *real* function φ_0.

5·1. *Contribution of p-state mesons to* $\langle H_{II} \rangle$. – Of all the terms contained in Eq. (5.1), the first namely $H_{II}^{(0)}$, is the only one which gives rise to a truly long range force, in the sense that it contains no exponentially decreasing factor ([33]). However, since it becomes, as will be seen, oscillatory after a distance which may vary from 2 to $3 \cdot 10^{-13}$ cm, the other terms which involve factors like $\exp[-\mu r]$ or $\exp[-2\mu r]$ will not be negligible.

We give now the detail of the calculation of $H_{II}^{(0)}$ in order to show clearly the approximations involved. The estimation of the other terms of (5.1) goes exactly along the same line, and only the result will be given. The first approximation which we make is to neglect the contribution of all non central forces, simply because the formalism is quite complicated when non-central forces are taken into account, as was seen in Sect. 3, and we are only interested now in getting a general idea of the type of imaginary force which might come out of an approach like ours. To be more definite, since we have shown in Sect. 2 that H_{II} acts only in isotopic spin triplet states, we will restrict ourselves to the states of the nucleon-antinucleon system which are, at the same time, singlet states with respect to the usual spin.

We need now an approximation in the outer region for the p-state part of the state vector. The study of Sect. 3 as well as the comparison with the case of the neutral scalar theory (see Appendix), indicate that the following expression is probably sufficiently accurate

$$\Phi_{(p)} = N Q_+ Q_- \Phi_0 , \tag{5.2}$$

where Q_+ and Q_- correspond respectively to the $b_{\lambda i}^+$ operators and are given by

$$Q_+ = \sum_{n=0}^{\infty} \frac{(-z\sqrt{2/3})^n}{n!} [(\tau_\alpha S_i + T_\alpha \sigma_i) b_{\alpha i}^{+*}]^n \tag{5.3}$$

and

$$Q_- = \sum_{n=0}^{\infty} \frac{(-z\sqrt{2/3})^n}{n!} [(T_\alpha S_i + \tau_\alpha \sigma_i) b_{\alpha i}^{-*}]^n , \tag{5.4}$$

N being a normalization factor which can easily be found equal to

$$N = \exp[-3z^2] . \tag{5.5}$$

The parameter z can be estimated from the formula

$$z = f_\pm \frac{\sqrt{3}}{\omega_+} , \tag{5.6}$$

([33]) $H_{II}^{(0)}$ represents an interaction where the same s-meson is first created, then annihilated. Because of the commutation relations of the $c_\lambda(k)$ operators, it would retain the form (4.13) even when the full isotopic dependence of (2.25) is taken into account.

(where $f_\pm$ and $\omega_\pm$, given by Eqs. (3.21), (3.22) tend to the same values at large distances) which agrees with the expression of the potential energy calculated in Sect. 3. We need also the connection between the renormalized and unrenormalized constants

$$f = \frac{f_0}{\sqrt{2}} \left(\frac{U_1}{U_1 - \lambda U_2} \right)^{\frac{1}{2}}, \tag{5.7}$$

where we have put

$$U_n = \frac{1}{(2\pi)^3} \int \frac{k^2 R^2(k)\, \mathrm{d}\boldsymbol{k}}{(\omega_k + \lambda)^n} . \tag{5.8}$$

The expression of $\varphi_1^\pm$ which enters in $f_\pm$, $\omega_\pm$ and in the $b_{\alpha_i}^\pm$ is taken to be the common asymptotic form

$$\varphi_1(k, \infty) = U_2^{-\frac{1}{2}} \frac{k R(k)}{\omega_k + \lambda} . \tag{5.9}$$

One then finds for z^2 the following expression (we express all energies in units of μc^2)

$$z^2 = 2f^2 \frac{U_1 U_2}{U_1 - \lambda U_2} . \tag{5.10}$$

In the one-body problem, the true expansion parameter which should be compared with the $\bar{f}$ of FRIEDMAN, LEE and CHRISTIAN [18] would be $6z^2$ which, if we take $\lambda = 3.39$ and $f^2/4\pi = 0.10$ is found to be exactly equal to 3, which serves as another check for the approximation.

We now find for the average value of $\langle H_{\mathrm{II}}^{(0)} \rangle$ due to p-states mesons

$$\langle H_{\mathrm{II}}^{(0)} \rangle = \sum_{n,m} - 2i\pi \Gamma^2 \exp[-6z^2] \frac{z^{2n+2m}}{n!\, m!} \left[3 - \frac{1}{3} (\tau_1 \cdot \tau_2)(\sigma_1 \cdot \sigma_2) \right]^n \cdot \tag{5.11}$$

$$\cdot \left[3 + \frac{1}{3} (\tau_1 \cdot \tau_2)(\sigma_1 \cdot \sigma_2) \right]^m \frac{1}{(2\pi^2)^{n+m+1}} \int R^2(k) k^2\, \mathrm{d}k\, k_1^2\, \mathrm{d}k_1 \ldots k_n^2\, \mathrm{d}k_n\, k_1'^2\, \mathrm{d}k_1' \ldots k_m'^2\, \mathrm{d}k_m' \varphi_1^2(k_1) \ldots$$

$$\ldots \varphi_1^2(k_n) \varphi_1^2(k_1') \ldots \varphi_1^2(k_m') [1 + g(k_1 r)] \ldots [1 + g(k_n r)] \cdot$$

$$\cdot [1 - g(k_1' r)] \ldots [1 - g(k_m' r)]\, \delta(E - \omega_k - \sum \omega_{k_i} - \sum \omega k_j).$$

In order to evaluate this complicated integral, we will make the following approximation

$$\delta(E - \sum_{i=1}^{N} \omega_{k_i}) = \frac{1}{N} \sum_{i=1}^{N} \delta(E - N\omega_{k_i}) , \tag{5.12}$$

which is based on the fairly reasonable assumption that, due to the source functions $R(\boldsymbol{k})$ and the form of the φ_1 functions themselves, the main contribution to the integral comes from values of $k_1 \ldots k_N$ which are relatively close to each other.

With this approximation, Eq. (5.11) becomes

$$(5.13)\quad \langle H_{11}^{(0)} \rangle = \sum_{n,m} -2i\pi\Gamma^2 C^2 \exp[-6z^2] \frac{z^{2n+2m}}{n!\,m!} \left[3 - \frac{1}{3}(\tau_1\cdot\tau_2)(\sigma_1\cdot\sigma_2)\right]^n \cdot$$
$$\cdot \left[3 + \frac{1}{3}(\tau_1\cdot\tau_2)(\sigma_1\cdot\sigma_2)\right]^m \frac{n-m}{(n+m+1)} \frac{1}{2\pi^2} \int_0^\infty \varphi_1^2(k) k^2 \,\mathrm{d}k \; g(kr)\, \delta(E - (n+m+1)\omega_k) \,,$$

where we have already subtracted the constant « self-energy » part which was mentioned in Sect. **2**. The constant C^2 is equal to

$$C^2 = \frac{1}{(2\pi)^3} \int R^2(k) \mathrm{d}k \,.$$

If we write $n+m = N$, the summation over n keeping N fixed, can be done immediatly. If we use for the source function a square cut-off ([34]) at $\omega_{\max}$, the summation over N is extended between two values

$$(5.14)\quad \begin{cases} N_{\min.} = \dfrac{E}{\omega_{\max}} - 1 \\ \text{and} \\ N_{\max} = \dfrac{E}{\mu} - 1 \,. \end{cases}$$

For $\omega_{\max} = 6\,\mu$, and a kinetic energy of antinucleons equal to 150 MeV in the laboratory system, we have $N_{\min} = 2$, $N_{\max} = 13$, $C^2 = 0.417$ and $U_2 = 0.116$. We write, in the following

$$(5.15)\quad \omega_N = \frac{E}{N+1} \qquad \text{and} \qquad k_N^2 = \omega_N^2 - \mu^2 \,.$$

Expressing also $g(y)$ in terms of the usual spherical Bessel function of order one

$$(5.16)\quad g(y) = \frac{3}{y} j_1(y) = \frac{3}{y} \sqrt{\frac{\pi}{2y}} J_{\frac{3}{2}}(y) \,,$$

([34]) Note that the oscillatory potential is *not* produced by « surface » effects on the edge of the square source function.

we obtain finally (with $6z^2 = 3$), for the singlet spin and triplet isotopic spin states

$$(5.17) \qquad \langle H_{11}^{(3)} \rangle = -i \frac{\Gamma^2 C^2}{4\pi} \cdot \frac{2 \exp[-6z^2]}{U_2} \frac{1}{r} \sum_{N=2}^{13} \frac{1}{(N+1)^2} \frac{(6z^2)^N}{(N-1)!} \frac{k_N^2 j_1(k_N r)}{(\omega_N + \lambda)^2} ,$$

which can easily be evaluated numerically. In practice, the summation does not need to be extended beyond $N = 10$, the error made being inferior to 1%.

A similar method can now be applied to the calculation of the average values of the remaining terms in Eq. (6.1). First, it is convenient to express these terms a little differently, making use of the relations (3.17), (3.18) obeyed by the p-state part of the state vector. For example, the mean value of the second term of (5.1) can be written, after averaging over space angles

$$(5.18) \qquad \left\langle -\frac{2i\Gamma^2}{(2\pi)^6} \int R(k) R(k') \, \mathrm{d}\boldsymbol{k} \, \mathrm{d}\boldsymbol{k}' \cos(\boldsymbol{k} + \boldsymbol{k}') \frac{\boldsymbol{x}}{2} \delta(E - H_0 - \omega_k) c_\nu(\boldsymbol{k}) c_\nu(\boldsymbol{k}') \right. =$$

$$= \left\langle -\frac{i\Gamma^2 r^2}{(2\pi)^3} \int_0^\infty \int_0^\infty R(k) R(k') k^3 \, \mathrm{d}k \, k'^3 \, \mathrm{d}k' \varphi_1(k) \varphi_1(k') g(kr) g(k'r) \delta(E - H_0 - \omega_k) \cdot \right.$$

$$\left. \cdot [(b_{\nu i}^+)^2 - (b_{\nu i}^-)^2] \right\rangle .$$

Using the relations

$$(5.19) \qquad (b_{\nu_i}^\pm)^2 \Phi^\pm = z^2 [3 \pm \tfrac{1}{3}(\tau_1, \tau_2)(\sigma_1, \sigma_2)] \Phi^\pm$$

and defining

$$(5.20) \qquad F(r) = \frac{1}{2\pi^2} \int_0^\infty R(k) k^3 \varphi_1(k) g(kr) \, \mathrm{d}k ,$$

we obtain for this second term

$$\left\langle \frac{i\Gamma^2 r^2}{3} F(r) z^2 \frac{1}{3} (\tau_1 \cdot \tau_2)(\sigma_1 \cdot \sigma_2) \int_0^\infty R(k) k^3 g(kr) \varphi_1(k) \delta(E - H_0 - \omega_k) \, \mathrm{d}k \right\rangle ,$$

which can then be evaluated exactly by the same method as the one used above for $H_{11}^{(3)}$. It is seen that the average value will be proportional to $F(r)$ and therefore have an exponentially decreasing character. After calculating in a similar manner all the remaining terms of (5.1), one gets finally (for singlet

spin and triplet isotopic spin states)

$$(5.21)\quad \langle H_{II} - H_{II}^{(0)} \rangle = -\, i \left(\frac{\Gamma^2}{2\pi}\right) \frac{r^2 F(r)}{9} \exp\left[-6z^2\right] \sum_{N_{\min}}^{N_{\max}} \frac{(6z^2)^{N+1}}{(N+1)(N+1)!} \cdot$$

$$\cdot \left\{ \left[N(N+3) + 36z^2(N+2) + 36z^4 \right] \frac{F(r)}{(N+3)\sqrt{U_2}} \frac{k_N^3}{(\omega_N + \lambda)^2} \left[1 + \frac{1}{k_N r} j_1(k_N r) \right] + \right.$$

$$+ \left[(N+2)(N+3) + 36z^2(N+1)(N+2) + 36z^4 \right] \cdot$$

$$\left. \cdot \frac{3}{(N+2)(N+3)} \frac{k_N^2}{\sqrt{U_2}(\omega_N + \lambda)} \frac{1}{r} j_1(k_N r) \right\} .$$

The complete imaginary interaction due to the p-state mesons is then equal to the sum of the two expressions (5.17) and (5.21).

5·2. *Discussion of* $\langle H_{II} \rangle$. – The two series (5.17) and (5.21) can be easily evaluated numerically. The only undetermined parameter is the coupling constant $\Gamma^2/4\pi$, which can be fixed, however, by comparing with the values obtained by DRELL and ZACHARIASEN ([26]) in their analysis of low energy pion-nucleon s-scattering; this leads to

$$(5.22)\qquad \frac{\Gamma^2}{4\pi} \simeq 0.4 ,$$

(note that $4\pi \simeq 2M/\mu$). This value of $\Gamma^2/4\pi$ also agrees with the expression obtained by KONUMA, MIYAZAWA and OTSUKI ([35]) for the nucleon-nucleon potential due to the exchange of two s-state mesons, which they express in terms of the meson-nucleon s-state scattering lengths. Using therefore (5.22) and the usual parameter of the Chew-Low theory (which corresponds here to $6z^2 = 3$ and $\lambda = 3.39$), we obtain for the imaginary potential W in the outer region the solid curve (I) represented in Fig. 2. It is seen that W is fairly large around the meson Compton wave length and extends approximately until a distance of the order of $2 \cdot 10^{-13}$ cm; it then starts to oscillate but remains very small in absolute value. These oscillations can be understood mathematically from the presence of the δ-function in the interaction in momentum space. They may have been introduced by the approximation (5.12) which fixes all the Fourier transforms to given values of the momenta.

In the following, we shall often define the « range » of the imaginary potential from the first zero of W. This « range » can be extended beyond

([35]) M. KONUMA, H. MIYAZAWA and S. OTSUKI: *Two-Pion Exchange Nuclear Potential*, to be published.

$2 \cdot 10^{-13}$ cm if, for example, a slightly lower value for the cut-off is chosen. The dotted curve (Ia) in Fig. 2 represents the variation of W which would result from a choice of $N_{\min} = 3$ instead of 2.

An aspect of these results which is not very satisfactory is the absence of a sharply defined multiplicity $\bar{n}$ of the emitted mesons. This comes from the shape of the φ_1 function which, in order to agree with the experimental results on $\bar{n}$, should be sharply peaked around a given value of ω_k. It can also be seen that, if such an effect were to occur, the range of W would also be appreciably increased. If φ_1 is peaked around, let us say, $\omega_k = \omega_0$, we can evaluate the expressions (5.17) and (5.21) for a fixed value of N, namely $N_0 = (E/\omega_0) - 1$. The range of W is then defined by

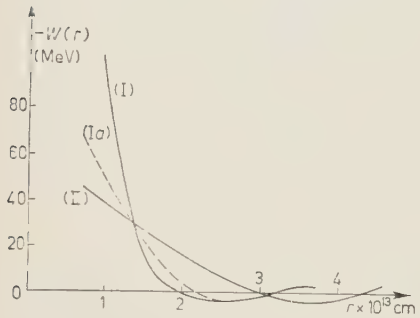

Fig. 2. – Variation of the imaginary potential as a function of r, for various forms of the p-state mesons weight function.

$$k_{N_0} r = x_0 \,, \tag{5.23}$$

where $x_0 \simeq 4.5$ is the first zero of the j_1 function. For $N_0 = 5$, for example, this would give a range of $3 \cdot 10^{-13}$ cm. On the other hand, the fact that only one term in the series (5.17) and (5.21) contributes to the interaction would not result in a drastic decrease of W, because, for this special value of N, φ_1^2 would be quite large if the width of the function were chosen small enough. In order to illustrate this argument we have plotted on Fig. 2 (curve II) the imaginary potential which would be obtained if the φ_1-function were such that

$$\varphi_1^2 \simeq \frac{k^2 R(k)}{(\omega_k - \omega_0)^2 + \delta^2} \,, \tag{5.24}$$

with $\omega_0 = 330$ MeV and $\delta \simeq 50$ MeV. It is seen that this is just the type of variation which is needed in order to account for all the experimental features of the antinucleon annihilation, including the sharply defined multiplicity of pions.

However, as we have seen in the discussion of Sect. **3** and **4**, the p-state functions $\varphi_1^{\pm}$ in the intermediate coupling theory behave like (5.24) only for distances which are fairly close to the core radius; in the outer region, they behave rather like (5.9). It has been noted by STROFFOLINI [17] that the intermediate coupling treatment of the one-body problem would yield results in better agreement with those of the one-meson approximation to the Chew-Low theory if the constant λ in the function $\varphi_1(k, \infty)$ were chosen equal to zero·

The function φ_1^- for singlet and triplet even states and φ_1^+ for odd triplet states would then have a resonant shape like (4.24) for all values of r. However, for distances of the order of the meson Compton wavelength, the corresponding value of ω_0 would already be too small, and the resulting value of $\bar{n}$ much too large to agree with experiment. Furthermore, the nucleon-nucleon potential would itself become very peculiar even at distances of the order of $\hbar/\mu c$. It is, in fact, an essential feature of the two nucleon potential in the Tomonaga approximation, as we have discussed in Sect. 3·4, that a value of $\lambda = 470$ MeV is necessary in order to guarantee that the interaction is well behaved for distances greater than the core radius for all spin and isotopic spin states.

We now turn to the discussion of two other effects which give contributions to the imaginary potential only with sharply defined multiplicity of exchanged pions:

a) contribution of the *s*-state mesons, since we have seen that the corresponding φ_1^- function has a resonant shape around the frequency ω_0;

b) influence of excited intermeditae states of the nucleon-antinucleon system.

5·3. *Contribution of the s-state mesons to* $\langle H_{II}\rangle$. – As was seen in Sect. **4** (Eq. (4.22)) the expansion parameter of the *s*-state vector, which defines the probability for having *s*-state mesons present before or after the annihilation, is $U_\pm/2 \simeq |\gamma_\pm|^2/2\omega_0^\pm$. Using the form of the $\varphi_0^\pm$ functions which was obtained through the variational principle, and assuming that $U_\pm/2 \ll 1$, we obtain the following approximate expression

$$\frac{U_\pm}{2} \simeq -i\sqrt{2}\,|\gamma_\pm|^2 \frac{\Gamma^2}{4\pi}\int_0^\infty \frac{R^2(k)k^2\,\mathrm{d}k[1+f(kr)]}{\omega_k-\omega_0-i2\sqrt{2}\,|\gamma_\pm|^2}\cdot \tag{5.25}$$
$$\cdot[\langle\delta(E-H_0-\omega_k)\rangle+\langle\delta(E-H_0+\omega_k)\rangle]\,.$$

In order to evaluate the average values of the δ-functions on the right hand side, it is natural—since we assume that $U_\pm/2$ will be small—to take only into account the *p*-state part of the state vector; we also assume that the $\varphi_0^\pm$ functions have a very narrow width. Writing then $\omega_0^2 = k_0^2+\mu^2$, and $E/\omega_0 = N_0+1$, we obtain

$$\frac{U_\pm}{2} \simeq \eta(N_0)\frac{\Gamma^2}{4\pi}\frac{k_0}{4E}[1\pm f(k_0 r)]\,; \tag{5.26}$$

(the function $f(x)$ is, like in Sect. **3**, equal to $((\sin x)/x)$; $\eta(N_0)$ is a small coefficient

$$\eta(N_0) = \exp[-6z^2]\frac{(6z^2)^{N_0}}{N_0!\,(N_0+1)}\left[1+\frac{(6z^2)^2}{(N_0+3)(N_0+2)}\right]. \tag{5.27}$$

Taking $6z^2 = 3$, we have $\eta(4) = 0.04$ and $\eta(5) = 0.07$. In any case, it is clear from Eq. (5.26) that $U_\pm$ is indeed a very small parameter, so that the contribution of the s-state mesons to $\langle H_{\text{II}} \rangle$ can safely be evaluated only to the lowest order in $U_\pm$. To this order, the average value of $\langle H_{\text{II}}^{(0)} \rangle$ evaluated with the same technique as in § 1, is found equal to

$$\langle H_{\text{II}}^{(0)} \rangle_s = -i \frac{\Gamma^2}{4\pi} C^2 \exp[-6z^2] \frac{\omega_0 k_0}{4E} \frac{(6z^2)^{N_0-2}}{(N_0+1)(N_0-2)!} \left(\frac{1}{U_0^-} + \frac{1}{U_0^-} \right), \tag{5.28}$$

where we have put

$$U_0^\pm = \frac{1}{2\pi^2} \int_0^\infty \frac{R^2 k(k) k^2 \, dk [1 \pm f(kr)]}{(\omega_k - \omega_0)^2 + 8\gamma_\pm^4}. \tag{5.29}$$

The dependence of $U_0^\pm$ on r being very weak, the expression (5.28) is approximately constant, and contributes mainly to the imaginary self-energy we have already mentioned which should therefore be subtracted. There are two interesting features however, which merit discussion: *a*) only one value of N contributes to the interaction, because $|\gamma_\pm|^2$ being a very small parameter, the term such that $E = (N_0+1)\omega_0$ is practically the only one which does not vanish; *b*) at first sight, it would appear that (5.28) is of the same order in Γ^2 as the p-state contribution; this is not so, however, because the $U_0^\pm$ are themselves of the order of $|\gamma_\pm|^2$, as can be seen be evaluating (5.29).

The remaining terms of $\langle H_{\text{II}} \rangle$ can now be evaluated easily to give

$$\langle H_{\text{II}} \rangle_s = -i \frac{\Gamma^2}{4\pi} r^2 F^2(r) \exp[-6z^2] \frac{(6z^2)^{N_0-1}}{(N_0-2)!\,(N_0+1)^2} \cdot \cdot \frac{\pi\sqrt{2}[|\gamma_+|^2 + |\gamma_-|^2]}{9} \left[1 + \frac{(6z^2)^2}{N_0(N_0-1)} + \frac{36z^2(N_0+2)}{(N_0-1)(N_0+3)} \right]. \tag{5.30}$$

This is, essentially, the first order interference term between p- and s-state mesons. As expected, it gives only a contribution for a fixed multiplicity of π-mesons exchanged. However, it is clear from Eq. (5.30) that it also yields a much smaller contribution to the imaginary potential than the p-state part. We conclude therefore that the s-state mesons will not be effective in sharpening the multiplicity of the emitted pions ([36]).

([36]) These s-state mesons do not include the one which is responsible for the annihilation and has, so to speak, already been eliminated in the calculation of H_{II}. They are s-mesons left over from previous virtual annihilations, which come into play only because, the state vector being a solution of the Schrödinger Eq. (2.15), it contains terms corresponding to the iteration of H_{II} an arbitrary number of times.

5.4. *Effect of excited states of the nucleon-antinucleon system.* – Since we are looking for the effects which would tend to give to the meson $\varphi(k)$ functions a more sharply peaked shape, it is natural to ask whether the influence of the excited states of the nucleon-antinucleon system would not have precisely this result. In the Appendix, the form of the $\varphi(k)$ function corresponding to the excited states is discussed in the case of the neutral scalar theory. It is seen that the constant λ changes sign and remains negative for all the states above the ground state. Now, in the case of the N-$\bar{\text{N}}$ system, the annihilation interaction H_{II} will add a small imaginary part to this constant λ, so that the p-state φ_1^+ functions will have indeed the sharply peaked shape. The question is how will this manifest itself in the complex potential W? As in the Appendix, we write

$$H' = H - H^T = H_0' + H_{\text{I}}' + H_{\text{II}}' \tag{5.31}$$

and treat this Hamiltonian as a perturbation. Writing, for an excited state m, the energy as

$$\mathcal{E}^{(m)} = \mathcal{E}_0^{(m)} - i\mathcal{E}_1^{(m)}, \tag{5.32}$$

we find, as a first order correction to the imaginary part of the energy in the ground state

$$\Delta\mathcal{E}_1^{(0)} = \left\{ \sum_{n \neq 0} \frac{[\Phi_0^*(H_0' + H_{\text{I}}')\Phi_n][\Phi_n^*(iH_{\text{II}}')\Phi_0]}{\mathcal{E}_0^{(0)} - \mathcal{E}_0^{(n)}} + \text{c. c.} \right\}. \tag{5.33}$$

Since the p-state part of the Φ_n state vector will involve the resonant like φ_1 functions, the main contribution to $\Delta\mathcal{E}_1^{(0)}$ should come from the emission of mesons at a well defined energy. To understand physically the meaning of this result one first has to note that, if the system consisting of one meson and one nucleon (or one antinucleon) has an isobaric state, the first « excited state » of the N-$\bar{\text{N}}$ system will be obtained roughly by leaving one particle in the ground state and lifting the other one to the isobaric state. Eq. (5.33) is therefore equivalent to a multiple scattering correction to diagrams like Fig. 1. Such multiple scattering corrections could, in principle, be evaluated directly using the technique of MIYAZAWA ([37]): in the framework of the fixed source theory, it is well

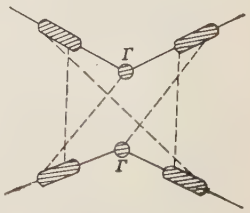

Fig. 3. – Diagram illustrating the multiple scattering corrections to the annihilation process.

([37]) H. MIYAZAWA: *Phys. Rev.*, **104**, 1741 (1956).

known that the two-meson vertices con be related directly to the meson-nucleon scattering amplitudes. In particular, since we know that the average meson-multiplicity is of the order of 5, it would be interesting to calculate multiple scattering corrections in a diagram like Fig. 3, where four p-state and one s-state mesons are exchanged the p-state mesons being emitted and absorbed in pairs, to take advantage of the $T = \frac{3}{2}$ resonance. However, the obvious weakness of such an approach is that the three- or four-mesons vertices may also give important contributions which it is impossible to relate to the meson-nucleon scattering amplitudes. We therefore believe that the introduction of the excited states in the framework of the Tomonaga intermediate coupling theory probably provides a more powerful method to look into this problem.

6. – Concluding remarks.

We hope to have shown, in the present paper, that a long range imaginary force between a nucleon and an antinucleon can emerge from a relatively plausible version of the usual meson theory. In spite of the heavy mathematical formalism we believe that the physical explanation for this long range force is rather clear and simple. The p-state mesons which are exchanged during the virtual annihilation tend to come out with a fixed momentum k_n which is close to the resonance momentum of meson-nucleon scattering in the $(\frac{3}{2}, \frac{3}{2})$ state. If we were dealing with virtual mesons, an exponentially decreasing potential would be obtained, and its range would be of the order of $\hbar/k_n$, too small therefore to account for the required extension of the interaction. However, in calculating the imaginary potential, we actually deal with mesons which are on the energy shell, so that the resulting interaction has an oscillatory character, the « range » of which can be defined in terms of the first zero ($x_0 = 4.5$) of the spherical Bessel function $j_1(x)$, so that it is rather equal to $x_0\hbar/k_n$; this accounts for the much larger range of the imaginary potential. Naturally, in our calculations, this clear picture has been somewhat obscured by the influence of the interaction terms corresponding to all the other possible numbers of exchanged mesons. This is partly due to the Tomonaga approximation and partly due, also, as was discussed at the end of Sect. 5, to the neglect of multiple scattering corrections to the imaginary potential. This is one of the points which should be carefully investigated in the future, another one being the charge dependence of the annihilation Hamiltonian, which it will be possible to state more precisely when more is known experimentally on the charge distribution of the pions produced in the annihilation process.

The extension of the intermediate coupling theory to the problem of nuclear forces (which is, so to speak, a by-product in our calculation of the antinucleon

annihilation) should also deserve further detailed investigation. In particular, it would be interesting to see if some of the features of the potential, as estimated approximately in Sect. 3·4, persist in a numerical solution of the more exact equations (3.24).

It is our general impression, after completing this work, that the Tomonaga intermediate coupling theory is a powerful method, the possibilities of which have not yet been fully utilized. In particular, it should be interesting to try to evaluate corrections to the one-state approximation, either by a perturbation method (as outlined, for example, in the Appendix and at the end of Sect. 5), or by complicating to a certain extent the general form of the trial function for the state vector.

Appendix

Nuclear forces in the neutral scalar theory.

We start from the Hamiltonian:

$$H - (2\pi)^{-3}\int c_k^* c_k \,\mathrm{d}\boldsymbol{k} - \frac{g}{(2\pi)^3}\sum_{i=1}^{2}\int R(k)\,\mathrm{d}\boldsymbol{k}\,(c_k \exp[i\boldsymbol{k}\boldsymbol{x}_i] + c_k^* \exp[-i\boldsymbol{k}\boldsymbol{x}_i]) , \tag{A.1}$$

which can be written, if we take the center of mass at the origin:

$$H = (2\pi)^{-3}\int c_k^* c_k \,\mathrm{d}\boldsymbol{k} - 2g\,(2\pi)^{-3}\int R(k)\,\mathrm{d}\boldsymbol{k}(c_k + c_k^*)\cos\frac{\boldsymbol{k}\boldsymbol{r}}{2} . \tag{A.2}$$

We define:

$$\begin{cases} c_+(\boldsymbol{r}) = \dfrac{\sqrt{2}}{(2\pi)^3}\displaystyle\int \varphi_+(k, \boldsymbol{r})\cos\frac{\boldsymbol{k}\boldsymbol{r}}{2}\, c_k \,\mathrm{d}\boldsymbol{k} , \\ c_-(\boldsymbol{r}) = \dfrac{\sqrt{2}}{(2\pi)^3}\displaystyle\int \varphi_-(k, \boldsymbol{r})\sin\frac{\boldsymbol{k}\boldsymbol{r}}{2}\, c_k \,\mathrm{d}\boldsymbol{k} , \end{cases} \tag{A.3}$$

the functions $\varphi_\pm$ being normalized as follows:

$$\frac{1}{(2\pi)^3}\int \varphi_\pm^2 (1 \pm \cos \boldsymbol{k}\boldsymbol{r})\,\mathrm{d}\boldsymbol{k} = 1 . \tag{A.4}$$

The Tomonaga equivalent Hamiltonian is easily found to be:

$$H^I = \omega_+ c_+^* c_+ + \omega_- c_-^* c_- - \sqrt{2}\, G_+(c_+ + c_+^*) \tag{A.5}$$

where we have put:

$$\omega_\pm = \frac{1}{(2\pi)^3}\int \varphi_\pm^2 \omega_k (1 \pm \cos \boldsymbol{kr})\, \mathrm{d}\boldsymbol{k}\,, \tag{A.6}$$

and

$$G_+ = \frac{g}{(2\pi)^3}\int R(k)\varphi_+(1 + \cos \boldsymbol{kr})\, \mathrm{d}\boldsymbol{k}\,. \tag{A.7}$$

It is then seen that the mesons in the q_- state remain always « free », so that the state vector will contain only the c_+^* operator:

$$\Phi = \sum_0^\infty \chi_n (c_+^*)^n \Phi_0\,. \tag{A.8}$$

Φ is a solution of the Schrödinger equation:

$$[\omega_- c_-^* c_+ - G_+\sqrt{2}\,(c_+ + c_+^*)]\Phi = \mathcal{E}\Phi\,. \tag{A.9}$$

If we write

$$\begin{cases} q_- = \dfrac{1}{\sqrt{2\omega_-}}(c_- - c_-^*)\,, \\[2ex] p_+ = i\sqrt{\dfrac{\omega_+}{2}}\,(c_+^* - c_+)\,, \end{cases} \tag{A.10}$$

and make the canonical transformation

$$\Phi = \exp\left[-i\,\frac{G_+\sqrt{2}}{\omega_+^{\frac{1}{2}}}\,p_-\right]\Phi\,; \tag{A.11}$$

the new state vector Φ' obeys simply the diagonal equation

$$\left(\omega_- c_-^* c_+ - \frac{2G_+^2}{\omega_-}\right)\Phi' = \mathcal{E}\Phi'\,. \tag{A.12}$$

In the ground state, $\Phi' = \Phi_0$ and

$$\mathcal{E}_0 = -2\,\frac{G_+^2}{\omega_-}\,. \tag{A.13}$$

The original state vector Φ is then found to be, for the ground state:

$$\Phi = \exp\left[-\frac{z^2}{2}\right] \sum_0^\infty \frac{z^n}{n!} (c_+^*)^n \Phi_0 , \tag{A.14}$$

with

$$z = \frac{G_+\sqrt{2}}{\omega_+} . \tag{A.15}$$

The variational principle shows also (as in Sect. 3·3) that the function φ_- has the form:

$$\varphi_+(k) = \frac{R(k)}{\omega_k + \lambda} \frac{1}{\sqrt{U_2}} , \tag{A.16}$$

with: $\lambda = -\omega_- - \sqrt{2} G_-(M_-/N_-)$, where we have defined $N_- = \Phi^* c_-^* c_- \Phi$ and $M_- = \frac{1}{2}\Phi^*(c_- - c_-^*)\Phi$. Using the solution (A.14) one verifies that, for the ground state, $\lambda = 0$. Putting (A.16) (with $\lambda = 0$) into (A.6) and (A.7) one verifies easily that:

$$\mathcal{E}_0 = -2g^2 \int \frac{R^2(k)}{\omega_k} (1 + \cos \boldsymbol{kx}) \, \mathrm{d}\boldsymbol{k} , \tag{A.17}$$

which is exactly the sum of the self-energy and the Yukawa potential ($R(k) = G(k)/\sqrt{2\omega_k}$, $G(k)$ being the Fourier transform of the source function). However, in the case of the excited states, for which the state vector Φ_n has the form:

$$\Phi_n = \frac{1}{\sqrt{n!}} \exp\left[-i \frac{G_+\sqrt{2}}{\omega_+^{\frac{3}{2}}} p_+\right] (c^*)^n \, \Phi_0 , \tag{A.18}$$

one sees easily that λ is no longer zero, but has the (always negative) value;

$$\lambda_n = -\frac{n\omega_+^2}{n\omega_+ + (2G_+^2/\omega_+)} . \tag{A.19}$$

Let us define;

$$H' = H - H^I \tag{A.20}$$

and treat H' as a perturbation. By definition, all diagonal matrix elements of H' are zero. The non-diagonal elements, however, do not vanish and a correction to the ground state energy can be written as

$$\Delta\mathcal{E}_0 = \sum_{n=0} \frac{|\Phi_0^* H' \Phi_n|^2}{\mathcal{E}_0 - \mathcal{E}_n} . \tag{A.21}$$

which takes then into account the possibility of excitation of the two nucleon system in intermediate states. In a theory where stable isobars can exist (this is not the case for the neutral scalar theory), Eq. (A.21) provides a simple way to calculate the effect of these isobars on the two nucleon forces in the ground state.

RIASSUNTO (*)

Si ricorre a una rappresentazione semifenomenologica della teoria dei mesoni per calcolare l'interazione complessa nucleone-antinucleone che dà luogo allo scattering e all'annichilamento degli antinucleoni nell'idrogeno. Si presume che la parte principale del potenziale immaginario sia dovuta a processi che coinvolgono l'annichilamento virtuale in un numero arbitrario di mesoni, tutti meno uno emessi o assorbiti in uno stato p. Si deriva per tali processi una Hamiltoniana effettiva, dalla quale si può calcolare un'interazione statica, trattando il nucleone e l'antinucleone come sorgenti fisse. La teoria di Tomonaga dell'accoppiamento intermedio si estende al problema dei due corpi e si applica dapprima al calcolo delle forze nucleari ordinarie e della parte reale dell'interazione nucleone-antinucleone. Si approssima poi l'hamiltoniana dell'interazione col metodo dell'accoppiamento intermedio. Si trova che la parte immaginaria del potenziale ha un'estensione dell'ordine di $(2 \div 3) \cdot 10^{-13}$ cm, oltre la quale diventa una funzione debolmente oscillante della distanza nucleone-antinucleone. Si discute il significato fisico di questo risultato, nonchè gli effetti che tenderebbero a rendere più stringente la definizione della molteplicità dei pioni emessi. Si propone, in particolare, un metodo per esaminare, nel quadro della teoria dell'accoppiamento intermedio, l'influenza degli stati eccitati del sistema nucleone-antinucleone.

(*) *Traduzione a cura della Redazione.*

Proton-Proton Collision in High Energy.

D. Ito, S. Minami (*) and H. Tanaka (+)

Institute of Physics, Tokyo University of Education - Tokyo, Japan
(*) *Department of Physics, Osaka City University - Osaka, Japan*
(+) *Istituto di Fisica, Università di Bologna - Bologna, Italy*

(ricevuto il 30 Dicembre 1957)

Summary. — The experimental results of the proton-proton collisions at 1.5 GeV and 2.75 GeV by Fowler *et al.* are analysed in a phenomenological way. It is found then that the partial waves of $l = 2 \div 5$ and $l = 2 \div 7$ are mainly responsible for the pion production at 1.5 GeV and 2.75 GeV respectively. Further, from our analysis in such an energy region it is shown that the effective size of the proton is nearly constant $((0.6 \div 0.7) \cdot 10^{-13}$ cm).

1. – Introduction.

The recent experiments on the nucleon-nucleon collisions, especially the proton-proton collision, in the energy region $1 \sim 3$ GeV have revealed us some natures of the pion-nucleon interactions or the nucleon structures. That is, *a*) the cross-section of the elastic proton-proton collision diminishes gradually with the energy, $((24 \pm 2)$ mb at 0.8 GeV and (15 ± 2) mb at 2.75 GeV), *b*) and its angular distribution (90° symmetry) has a sharp forward directed maximum, which may be interpreted as a shadow scattering, *c*) the cross-section of the inelastic collision in the energy region $(1 \div 2.75)$ GeV is nearly constant $((24 \pm 3)$ mb). Fowler *et al.* [1] tried to explain these features on

---

[1] W. B. Fowler, R. P. Shutt, A. M. Thorndike, W. L. Whittemore, V. T. Cocconi, E. Hart, M. M. Block, E. M. Harth, E. C. Fowler, J. D. Garrison and T. W. Morris: *Phys. Rev.*, **103**, 1489 (1956).

the basis of the optical model. On the other hand, LINDENBAUM-STERNHEIMER (2) and BARSHAY (3) treated the pion production on proton-proton collision with the nucleon isobar model supposing that the decaying proton and pions from one isobar do not interact with the decaying proton and pions from another isobar. This approach may be reasonable if the collision occurs in a peripheral region of each proton, but as they said the life time of the nucleon isobar being very short ($(10^{-23} \div 10^{-24})$ s) this approximation will lose a meaning if the collision takes place in the central part of the protons.

Then it will be of some importance to examine in which region of the proton the pions are produced by the collision, and the energy dependence of this region is an interesting question. In order to treat these problems we shall take the phenomenological approach which was applied by us for the analysis of the π^--p collision at 1.4 GeV (4), that is, considering the elastic scattering as an almost shadow scattering one estimates, from its angular distribution, the cross-section of the inelastic scattering.

At present, the experimental data at 0.8 GeV, 1.5 GeV and 2.75 GeV are available, but we shall confine ourselves to the data at 1.5 GeV and 2.75 GeV, because the angular distribution at 0.8 GeV containing a part rather isotropic will not be explained by the shadow scattering. Especially, the Pauli exclusion principle and the statistical factors which have not been considered in the optical model are taken into account in our analysis. In the Sect. **2** the method is described briefly and in the Sect. **3** the results are compared with the experiments. In spite of our somewhat crude estimation the obtained cross-section of the inelastic collision shows a fairly good agreement with the observed one. Further, it is shown there that for the pion production process the partial waves $l = 2 \div 5$ and $l = 2 \div 7$ are mainly responsible at the energies 1.5 GeV and 2.75 GeV respectively. Next, in the Sect. **4** our method is compared with the optical model. Translating our results in terms of the optical model it is proved that the parameter R is nearly independent of the incident proton energy, $R = (1.1 \div 1.3) \cdot 10^{-13}$ cm, while the other parameter γ changes with the incident energy, $\gamma = 1.09$ at 1.5 GeV and 0.63 at 2.75 GeV. Finally, in the Sect. **5** the extended size of the proton is estimated from the proton-proton collision, obtaining the nearly constant value $(0.6 \div 0.7) \cdot 10^{-13}$ cm which is consistent with the value $r_p = 0.7 \cdot 10^{-13}$ cm derived from the electron-proton scattering by HOFSTADTER *et al.* (5).

---

(2) S. J. LINDENBAUM and R. M. STERNHEIMER: *Phys. Rev.*, **105**, 1874 (1957).
(3) S. BARSHAY: *Phys. Rev.*, **106**, 572 (1957).
(4) D. ITO and S. MINAMI: *Prog. Theor. Phys.*, **14**, 108 (1954).
(5) R. HOFSTADTER: *Rev. Mod. Phys.*, **28**, 214 (1956).

2. – Method of analysis.

First, the reaction matrix R of the scattering for the angular momentum l is approximated very roughly as

$$R_l \equiv \eta_l \exp[2i\delta_l] - 1 \cong \eta_l - 1 , \qquad |\eta_l| \leqslant 1, \tag{1}$$

where η indicates the effects of the absorption. Here it must be noted that the following characters are remarkable in the proton-proton elastic collision.

i) The angular distribution is symmetric with respect to 90°.

ii) There exist the spin triplet and singlet states. The odd angular momentum contributes only to the former while the even angular momentum only to the latter. (Pauli exclusion principle). The statistical weights of both states are $\frac{3}{4}$ and $\frac{1}{4}$ respectively, and there is no interference between the two states.

In the previous paper (4) of the π^--p scattering we approximated the elastic angular distribution empirically by $b^2/(a - \cos\theta)^2$, so in the present case we could put it in a form (*) $c^2/(a^2 - \cos^2\theta)^2$ satisfying the symmetry condition i). With this form however, only the even states of the angular momentum are relevant, while with the form $b^2\cos^2\theta/(a^2 - \cos^2\theta)^2$ only the odd states appear. Then a combination of both, $(b^2\cos^2\theta + c^2)/(a^2 - \cos^2\theta)^2$ might be favourable, but the condition $|\eta_l| \leqslant 1$, cannot be satisfied in that case. Noting however that the elastic scattering at the energy in question should be an almost shadow scattering and that the experimental differential cross-section at 90° is nearly zero, we may eventually adopt the following form of the angular distribution

$$\frac{\mathrm{d}\sigma^{\mathrm{scatt}}}{\mathrm{d}\Omega} = (b^2\cos^2\theta + c^2)\left[\frac{1}{a^2 - \cos^2\theta} - d\right], \tag{2}$$

$$d \cong \frac{1}{a^2}, \tag{3}$$

where it is easily seen that all the necessary conditions are satisfied.

(*) We have no fundamental reason to put the denominator as $(a^2 - \cos^2\theta)^2$. However, if one calculates, by the perturbation, the matrix element of the p-p scattering corresponding to some diagram one obtains easily the form $A/(a - \cos\theta)$. Then, by the procedure of the symmetrization with $\theta \to (\pi - \theta)$ the denominator of the matrix element becomes $(a^2 - \cos^2\theta)$. Accordingly, in the expression of the cross-section the form of the denominator may be $(a^2 - \cos^2\theta)^2$.

Now, let us consider the proton-proton elastic scattering cross-section $\mathrm{d}\sigma^{\mathrm{scatt}}/\mathrm{d}\Omega$ and its scattering amplitudes $F(\theta)$ in the singlet states. In our approximation with the eq. (1) they are written as

$$\left(\frac{\mathrm{d}\sigma^{\mathrm{scatt}}}{\mathrm{d}\Omega}\right)_{l=\mathrm{even}} = \frac{1}{4}\frac{1}{4k_0^2}\left|\sum_{l=\mathrm{even}}(2l+1)T_l P_l(\cos\theta)\right|^2 \tag{4}$$

$$= \frac{1}{4}\frac{1}{4}\left|\sum_{l=\mathrm{even}}(2l+1)Q_l' P_l(\cos\theta)\right|^2 \tag{5}$$

$$= \frac{1}{4}\left|\sum_{l=\mathrm{even}}(2l+1)Q_l'' P_l(\cos\theta)\right|^2, \tag{6}$$

$$T_l \equiv 1-\eta_l\,, \qquad Q_l' \equiv T_l/k_0\,, \qquad Q_l'' \equiv Q_l'/2\,, \tag{7}$$

$$F(\theta)_{l=\mathrm{even}} = \frac{1}{2}\frac{1}{2ik_0}\sum_{l=\mathrm{even}}(2l+1)(\eta_l-1)P_l(\cos\theta) = \frac{i}{2}\sum_{l=\mathrm{even}}(2l+1)Q_l'' P_l(\cos\theta)\,, \tag{8}$$

where the first factors $\frac{1}{4}$ in the eqs. (4) and (5) are the statistical weight and k_0 is the incident momentum. In the case of the triplet scattering we assume here, as in the previous paper (1), that the R matrix be the same for the three states of the total angular momentum J, that is, $J=l+1$, l and $l-1$ corresponding to the orbital angular momentum l. Under such assumption the cross-section $(\mathrm{d}\sigma^{\mathrm{scatt}}/\mathrm{d}\Omega)_{l=\mathrm{odd}}$ and the scattering amplitude $F(\theta)_{l=\mathrm{odd}}$ are expressed in the same form as in the singlet case, only with the difference due to the change of the statistical factor. Defining the Q_l'' for $l=\mathrm{odd}$ as

$$Q_l'' = \frac{\sqrt{3}}{2}Q_l'\,, \qquad \text{for } l=\mathrm{odd}, \tag{9}$$

$F(\theta)_{l=\mathrm{odd}}$ takes the same form as $F(\theta)_{l=\mathrm{even}}$.

$$F(\theta)_{l=\mathrm{odd}} = \frac{i}{2}\sum_{l=\mathrm{odd}}(2l+1)Q_l'' P_l(\cos\theta)\,. \tag{8'}$$

Then, the contributions to the elastic scattering cross-section from the l-state are expressed, independently of the parity of the l value,

$$\sigma_l^{\mathrm{scatt}} = \pi(2l+1)Q_l''^2 \tag{10}$$

and the contributions to the pion production are

$$\sigma^{\mathrm{prod}}_{l=\mathrm{even}} = \frac{1}{4}\frac{\pi}{k_0^2}(2l+1)\,(1-\eta_l^2)\,, \tag{11}$$

$$\sigma^{\mathrm{prod}}_{l=\mathrm{odd}} = \frac{3}{4}\frac{\pi}{k_l^2}(2l+1)(1-\eta_l^2)\,. \tag{12}$$

On the other hand, noting that there is no interference between the odd and even states, the scattering amplitudes should be, from the eq. (2),

$$\underset{l=\text{even}}{F(\theta)} = e^{i\xi} c \left[\frac{1}{a^2 - \cos^2\theta} - d \right], \tag{13}$$

$$\underset{l=\text{odd}}{F(\theta)} = e^{i\xi'} b \cos\theta \left[\frac{1}{a^2 - \cos^2\theta} - d \right], \tag{13'}$$

where $e^{i\xi}$ and $e^{i\xi'}$ are undetermined phase factors. Then, the comparison of the two forms (8), (8') and (13), (13') gives us the relations

$$e^{i\xi} c \left[\frac{1}{a^2 - \cos^2\theta} - d \right] = \frac{i}{2} \sum_{l=\text{even}} (2l+1) Q_l'' P_l(\cos\theta), \tag{14}$$

$$e^{i\xi'} b \cos\theta \left[\frac{1}{a^2 - \cos^2\theta} - d \right] = \frac{i}{2} \sum_{l=\text{odd}} (2l+1) Q_l'' P_l(\cos\theta). \tag{15}$$

According to our picture, the Q_l'' being real, the right hand side of the eqs. (14) and (15) are pure imaginary, and so must be their left hand sides. This requires the phase factors $e^{i\xi} = e^{i\xi'} = i$, and we obtain finally the following equations

$$Q_l'' = c \left[\frac{1}{2a} \int_{-1}^{1} \left(\frac{1}{a-x} + \frac{1}{a+x} \right) P_l(x)\, \mathrm{d}x - 2d\delta_{l,0} \right] = 2c\left[(Q_l(a)/a) - d\delta_{l,0} \right], \tag{16}$$

for $l =$ even,

$$Q_l'' = b \left[\frac{1}{2} \int_{-1}^{1} \left(\frac{1}{a-x} - \frac{1}{a+x} \right) P_l(x)\, \mathrm{d}x - d \int_{-1}^{1} x P_l(x)\, \mathrm{d}x \right] = 2b \left[Q_l(a) - \frac{d}{3} \delta_{l,1} \right], \tag{17}$$

for $l =$ odd,

where $x = \cos\theta$ and

$$Q_l(a) = \frac{1}{2} \int_{-1}^{1} \frac{P_l(x)}{a-x}\, \mathrm{d}x. \tag{18}$$

As is seen in the formulae of Neuman-Hankel these $Q_l(a)$ are the Legendre functions of the second kind and easily calculated for the given value of a.

Consequently, with the known Q_l'' we find the η values by the eq. (7) and making use of the eqs. (10), (11) and (12), σ_l^{scatt} and σ_l^{prod} are estimated finally.

3. – Comparison with the experiments.

The angular distribution of the proton-proton elastic scattering given by FOWLER *et al.* [1] are reproduced in the Fig. 1 and 2, where the curves represent our empirical formula (2) calculated with the chosen parameters a^2,

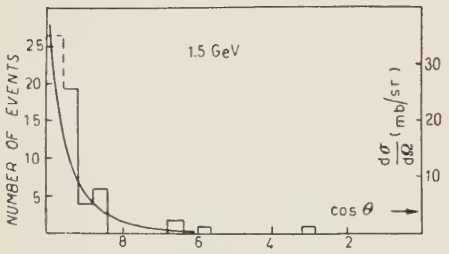

Fig. 1.

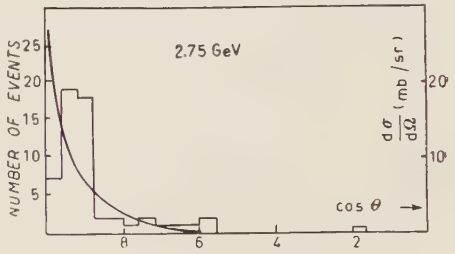

Fig. 2.

b^2, c^2 and d in the Table I. The elastic scattering cross-sections for such choice of the parameters are estimated by the method described in the Sect. 2, and we obtain $\sigma^{\text{scatt}} = \sum_l \sigma_l^{\text{scatt}} = 19$ mb at 1.5 GeV and 13 mb at 2.75 GeV con-

TABLE I.

Parameters	Energy	
	1.5 GeV	2.75 GeV
a^2	1.39	1.15
b^2 (mb)	5.00	0.56
c^2 (mb)	0.90	0.10
d	0.70	0.86

sistent with the experimental values (20 ± 2) mb and (15 ± 2) mb respectively. This fact will guarantee us that the choice of the parameter values a, b, c and d should be sufficiently adequate.

Now, after adjusting, as above, the parameters to the elastic collisions data, we shall look for the pion production cross-sections by the method given in the Sect. 2. The results are shown in the Tables II and III for each partial wave contribution. There, taking into account the statistical weights, the total production cross-sections are obtained by a summation of each contribution, resulting $\sigma^{\text{prod}} = 22$ mb and 21 mb at 1.5 GeV and 2.75 GeV respectively. In Fig. 3 the values are compared with the experiment.

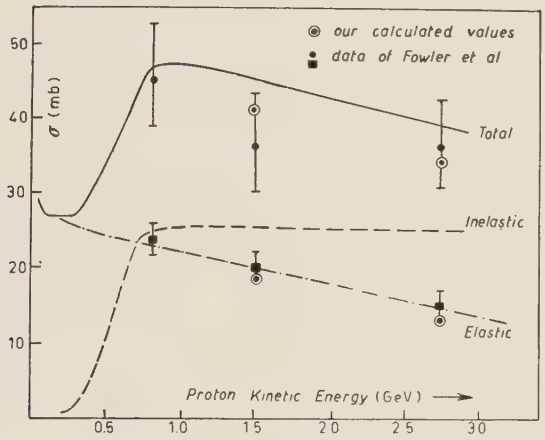

Fig. 3.

It is very interesting that in spite of our rather rough estimations they show a fairly good agreement with the experiment. Further, it should be noted that the calculated production cross-sections are, as observed in the experiments, nearly independent of the incident energy.

Now in the Tables II and III we can see the effective partial waves in the production process. The waves $l = 2 \div 5$ and $l = 2 \div 7$ are mainly responsible at the energies 1.5 GeV and 2.75 GeV respectively. Transforming to the impact parameters corresponding to these partial waves, one may say that with the largest contributions from $R = (0.7 \div 0.8) \cdot 10^{-13}$ cm the proton region up to $R = (1.2 \div 1.4) \cdot 10^{-13}$ cm plays an important role in the pion production. This fact is intimately related to the extended size of the proton which will be discussed in the Sect. 5. But before going to this problem we shall compare our results with those of the optical model.

TABLE II (at energy 1.5 GeV).

l	$\frac{\pi}{k_0^2}(2l+1)(1-\eta_l^2)$	l	$\frac{\pi}{k_0^2}(2l+1)(1-\eta_l^2)$
0	0.55 mb	1	2.94 mb
2	8.58	3	11.02
4	6.00	5	6.07
6	2.44	7	2.34
8	0.87	9	0.78
10	0.24	11	0.09

$$\sigma^{\text{prod}} = \frac{1}{4}\sum_{l=\text{even}} \frac{\pi}{k_0^2}(2l+1)(1-\eta_l^2) + \frac{3}{4}\sum_{l=\text{odd}} \frac{\pi}{k_0^2}(2l+1)(1-\eta_l^2) \cong 22 \text{ mb}$$

TABLE III (at energy 2.75 GeV).

l	$\frac{\pi}{k_0^2}(2l+1)(1-\eta_l^2)$	l	$\frac{\pi}{k_0^2}(2l+1)(1-\eta_l^2)$
0	0.53 mb	1	1.60 mb
2	4.71	3	6.47
4	5.04	5	5.79
6	3.32	7	3.64
8	1.90	9	2.04
10	1.03	11	1.09
12	0.54	13	0.57
14	0.27	15	0.29

$$\sigma^{\text{prod}} = \frac{1}{4}\sum_{l=\text{even}} \frac{\pi}{k_0^2}(2l+1)(1-\eta_l^2) + \frac{3}{4}\sum_{l=\text{odd}} \frac{\pi}{k_0^2}(2l+1)(1-\eta_l^2) \cong 21 \text{ mb}$$

4. – Relations with the optical model.

The diffraction scattering amplitudes $f(\theta)$ by a sphere of radius R is given, for a small scattering angle θ, by

$$f(\theta) \propto J_1(k_0 R \sin\theta)/(k_0 R \sin\theta) \cong 1 - (k_0 R)^2 \frac{\theta^2}{8} + \ldots = 1/[1 + (k_0 R)^2 \theta^2/8] .$$

Considering the quantities up to the order of θ^2, we may set

$$\cos\theta = 1 - \frac{\theta^2}{2} + \ldots$$

then, the cross-section at small angle θ is written

$$\frac{\mathrm{d}\sigma^{\mathrm{el}}}{\mathrm{d}\Omega} = \{\lambda\!\!\!^{-}\gamma/[(2\lambda\!\!\!^{-}R)^2 + 1 - \cos\theta]\}^2 , \qquad \lambda\!\!\!^{-} = \frac{1}{k_0} . \tag{19}$$

On the other hand, our empirical amplitude eq. (2) also can be approximated for small θ in the same form,

$$(b^2 \cos^2\theta + c^2)\left[\frac{1}{a^2 - \cos^2\theta} - d\right]^2 \cong \left[\frac{\{1 - d(a^2 - 1)\}\sqrt{b^2 + c^2}}{(a+1)(a - \cos\theta)}\right]^2 . \tag{20}$$

There, it is seen easily that our parameters are closely related to those of the optical model, that is,

$$a = (2\lambda\!\!\!^{-}/R)^2 + 1 , \qquad \lambda\!\!\!^{-}\gamma = \{1 - d(a^2 - 1)\}\sqrt{b^2 + c^2}/(a+1) . \tag{21}$$

Introducing the parameter values of Table I in these relations we obtain the corresponding optical model parameters R and γ, as given in Table IV. Then,

TABLE IV.

Parameters	Energy	
	1.5 GeV	2.75 GeV
R	$1.10 \cdot 10^{-13}$ cm	$1.30 \cdot 10^{-13}$ cm
γ	1.09	0.63

in terms of the optical model, our choiced values are somewhat different from those used by FOWLER *et al.* [1] in their proper optical approach. As was remarked in the Sect. 3, owing to such weak dependence of R on the incident energy, the higher l waves mainly aswer for the higher energy events.

5. – Proton size and proton-proton scattering.

We may rewrite the elastic scattering cross-section (19) in the following form

$$\left(\frac{\mathrm{d}\sigma^{\mathrm{el}}}{\mathrm{d}\Omega}\right)^{-\frac{1}{2}} = \frac{1}{\lambda\!\!\!^{-}\gamma}[(1-\cos\theta) + (2\lambda\!\!\!^{-}/R)^2]\,. \tag{22}$$

Then, if the high energy proton-proton scattering can be really interpreted as a shadow scattering, the experimental value $(\mathrm{d}\sigma^{\mathrm{el}}/\mathrm{d}\Omega)^{-\frac{1}{2}}$ plotted as a function of $(1-\cos\theta)$ must be linear in the region of small angles θ. In fact, it proves well to be so, as illustrated in the Fig. 4. Further, as a confirming example, in the Fig. 5, the same procedure is operated for the π-p scattering which is known to be the shadow scattering from the analysis of the dispersion relations. It shows also linear dependence as expected.

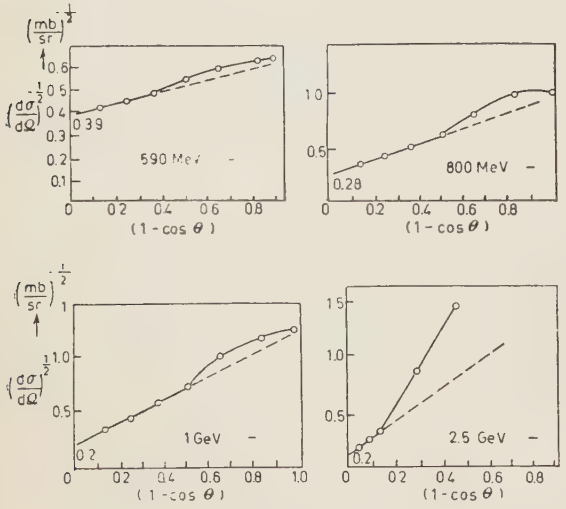

Fig. 4.

Now basing on such picture we shall estimate the order of the proton size in the following two ways.

a) The simplest way is to observe that the tangents of these lines are given by $1/\gamma\lambda\!\!\!^{-}$ and that the crossing points with the vertical axes are $4\lambda\!\!\!^{-}/\gamma R^2$. From these two values we can determine easily the values of R and γ. The obtained R value is almost independent on the incident energy, and at 1 GeV, for example,

$$R \cong 1.35\cdot 10^{-13}\ \mathrm{cm}\,. \tag{23}$$

As R corresponds to the radius of the optical model, it should be twice the proton radius r_{p}. Thus,

$$r_{\mathrm{p}} \approx 0.68\cdot 10^{-13}\ \mathrm{cm}\,, \tag{24}$$

which is consistent with Hofstadter's value $r_p = 0.70 \cdot 10^{-13}$ cm obtained from the electron-proton scattering.

The above method is very simple and it might introduce a large error because it relies only on the experimental differential cross-sections. So, assuming only a shadow scattering as to the elastic collision, we shall estimate the proton size from the total cross-section. Using the relation (21) between our model and the optical one, the cross-sections are given by (6)

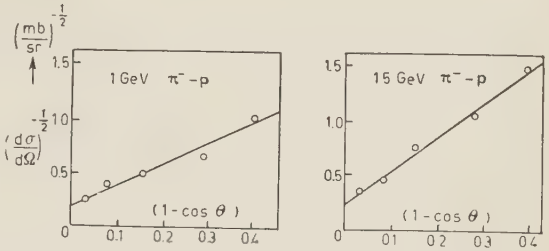

Fig. 5.

$$
(25) \qquad \begin{cases} \sigma^{\text{tot}} = \gamma \pi R^2 , \\ \sigma^{\text{el}} = \gamma^2 \pi R^2 / \{2 + (2/kR)^2\} , \\ \sigma^{\text{inel}} = \gamma \pi R^2 / (1 - \gamma / \{2 + (2/kR)^2\}) , \end{cases}
$$

from which γ and R are expressed by the cross-sections σ^{el} and σ^{tot},

$$
(26) \qquad \frac{2}{\gamma} = \frac{\sigma^{\text{tot}}}{\sigma^{\text{el}}} - \frac{1}{\sigma^{\text{tot}}} \frac{8\pi}{M^2} \frac{M}{T^{\text{lab}}} ,
$$

$$
(27) \qquad R^2 = \frac{\sigma^{\text{tot}}}{2\pi} \frac{2}{\gamma} ,
$$

where σ^{tot} is the total cross-section of the proton-proton collision $\sigma^{\text{tot}} \equiv \sigma^{\text{el}} + \sigma^{\text{inel}}$, σ^{el} the elastic scattering cross-section, M the proton mass ($\hbar = c = 1$) and T^{lab} the incident energy in the laboratory system. As the values of σ^{tot} and σ^{el} we used the experimental data given by CHEN-LEAVITT-SHAPIRO (7). The results are shown in the Table V.

As is seen in this Table R shows a weak dependence on the incident energy, confirming also the rough estimation in the Table IV. Such estimation would suggest, in a certain sense, the proton radius

$$
(28) \qquad r_p \cong (0.6 \div 0.7) \cdot 10^{-13} \text{ cm}
$$

in place of the Compton wave length $r_M = \hbar / Mc = 0.21 \cdot 10^{-13}$ cm.

(6) D. ITO, T. KOBAYASHI, M. YAMAZAKI and S. MINAMI: *Prog. Theor. Phys.*, **18**, 264 (1957).

(7) F. F. CHEN, C. P. LEAVITT and A. M. SHAPIRO: *Phys. Rev.*, **103**, 211 (1956).

TABLE V.

$T^{\text{lab.}}$ (GeV)	Experimental values			Our estimated values	
	σ^{tot} (mb)	σ^{el} (mb)	$\sigma^{\text{tot}}/\sigma^{\text{el}}$	$2/\gamma$	R (cm)
2.5	42	15	2.80	2.70	$1.33 \cdot 10^{-13}$
2.0	43	18	2.39	2.27	$1.25 \cdot 10^{-13}$
1.5	7	20	2.35	2.20	$1.28 \cdot 10^{-13}$
1.0	48	21	2.28	2.07	$1.26 \cdot 10^{-13}$
0.8	47	22	2.14	1.86	$1.18 \cdot 10^{-13}$

Though our radius is almost the same as that of HOFSTADTER ($r_p = 0.70 \cdot 10$ cm) [5], one may ask « What is the proton radius? ». There is no evidence that our radius should have the same meaning as that of HOFSTADTER. In any way however, it must be very suggestive that the same « proton size » is obtained from very different experiments.

RIASSUNTO (*)

Si esaminano sotto l'aspetto fenomenologico i risultati ottenuti da FOWLER *et al.* sulle collisioni protone-protone a 1.5 GeV e 2.75 GeV. Si trova così che le onde parziali con $l = 2 \div 5$ e $l = 2 \div 7$ sono le cause prevalenti della produzione di pioni a 1.5 GeV, rispettivamente a 2.75 GeV. Dalla nostra analisi risulta, inoltre, che in questo intervallo di energia le dimensioni effettive del protone sono pressochè costanti ($(0.6 \div 0.7) \cdot 10^{-13}$ cm).

(*) *Traduzione a cura della Redazione.*

On the Decay Modes of Interacting and Non-Interacting K^+-Mesons.

B. Bhowmik (*), D. Evans and D. J. Prowse (×)

H. H. Wills Physical Laboratory - University of Bristol

F. Anderson (+) D. Keefe and A. Kernan

University College - Dublin

(ricevuto il 9 Gennaio 1958)

Summary. — The decay modes of K^+-mesons which have been inelastically scattered from nuclei in emulsion have been determined and it is shown that their relative frequencies are consistent with those obtained for K^+-mesons which have not undergone nuclear interaction. Measurements were also made on a total of 286 decay events with a singly charged secondary with the object of discovering without detection bias, particles decaying in the rare τ' and the $K_{\mu 3}$ modes.

1. – Introduction.

The problem of whether the τ and the θ-particles ought to be considered as being identical or as two distinct particles is now well known. The analyses of τ-meson decay by Dalitz [1] and Fabri [2] suggested that the τ-meson was most likely to be a pseudoscalar particle, and as such forbidden to decay in the χ-mode to two π-mesons. The failure of parity conservation in weak interactions suggested by Lee and Yang [3] offers one way out of the dilemma

(*) Now at the University of Delhi.

(×) Now on leave at Phisics Department, U.C.L.A., Los Angeles.

(+) Now at the John Hopkins University, Baltimore, Maryland, U.S.A.

(1) R. H. Dalitz: *Phys. Rev.*, **94**, 1046 (1954).

(2) E. Fabri: *Nuovo Cimento*, **11**, 479 (1954).

(3) T. D. Lee and C. N. Yang: *Phys. Rev.*, **104**, 254 (1956).

if the breakdown holds also for decay processes not involving the neutrino. Other suggestions which have been made in order to explain the apparent equality in mass and lifetime of the τ and θ-particles include that of LEE and OREAR [4] involving a genetic relationship with a very small energy release between two distinct heavy mesons of different life-times, and that of LEE and YANG [5] in which the τ and θ-particles are envisaged as constituting a parity doublet. If the difficulty of reconciling the modes of decay does indeed imply the existence of two particles then their relative abundance in a sample of K-mesons which have interacted with nuclear matter might be different from that in the pure beam at production. In the first place this could arise from a difference in the interaction cross-sections of the two particles. Alternatively it is possible that upon interacting, a τ-particle might be transformed into a θ-particle and vice versa with certain probabilities; in particular, the case of nuclear scattering with change of parity has been considered by BERESTETSKY and BYCHKOV [6]. If the assignment of the τ, τ' and $K_{\mu 2}$ modes to the τ-particle and χ, $K_{\mu 3}$ and K_{β} modes to the θ-particles is correct [7], then the unscattered K^+ beam entering an emulsion stack consists of τ and θ-particles in the proportion of very nearly two-to-one. Unless the ratio of the probabilities for « τ to θ » and « θ to τ » transitions assumes the special value of one to two there will be a change in the beam composition after interacting. Even if the separation into distinct particles is more complex than this and interparticle transitions still occur, there will in general be a change in the relative frequencies after interaction.

In order to investigate this possibility, BISWAS *et al.* [8] selected 146 events in which a K-meson collided either elastically or inelastically with a nucleus and later decayed; they observed 10 to decay in the τ-mode and they made extensive measurements on 31 K_L-decays in which the secondary particle was in good geometry, and found two further low energy $K_{\mu 3}$ decay events on the basis of less accurate measurements on a sample of 55 further K_L-decays in poorer geometry. In their experiment about 30% of the K-mesons chosen suffered only elastic scattering with deflection $\geqslant 40°$, and the remainder made inelastic collisions. WIDGOFF *et al.* [9] have investigated the relative frequencies of decay modes in a stack exposed to a K^+-meson beam emerging from a uranium target at 120° to the Cosmotron beam. They grain-counted the

---

[4] T .D. LEE and J. OREAR: *Phys. Rev.*, **100**, 932 (1955).

[5] T. D. LEE and C. N. YANG: *Phys. Rev.*, **102**, 290 (1956).

[6] V. B. BERESTETSKY and YU. A. BYCHKOV: *Nuclear Physics*, **3**, 153 (1957).

[7] M. GELL-MANN: *Pisa Conference* (June 1955), unpublished.

[8] N. N. BISWAS, L. CECCARELLI-FABRICHESI, M. CECCARELLI, N. C. VARSHNEYA and P. WALOSCHEK: *Nuovo Cimento*, **4**, 631 (1956).

[9] M. WIDGOFF, A. M. SHAPIRO, R. SCHLUTER, D. M. RITSON, A. PEVSNER and V. P. HENRI: *Phys. Rev.*, **104**, 811 (1956).

tracks of 72 heavy meson secondary particles and in addition observed 28 τ-decays and 18 low energy τ' and $K_{\mu 3}$ decay events in area scanning. Under certain assumptions and approximations they have estimated the 120° beam to be 75% composed of scattered K-mesons and have compared their results with those obtained in a study of the K^+-beam produced at 60° from a copper target in the Cosmotron and reckoned to contain only 20% of scattered particles ([10]).

The present investigation was commenced after a considerable number of decays and interactions of K-mesons had been found in a systematic way described in full by Bhowmik *et al.* ([11]), in order to add significantly to the published data; in addition measurements have been made on those events where the primary particle had not interacted inelastically, with the object of discovering, without any detection bias dependent on the energy of the secondary products, particles decaying in the τ' and $K_{\mu 3}$ modes.

2. – Experimental procedure.

A stack of G5 emulsion sheets (the so-called K_2^+ stack) was exposed to the momentum analysed positive beam produced at 90° to the 6 GeV proton beam incident on a copper target in the Bevatron. The tracks of K^+-mesons of an energy between 100 and 150 MeV were found and followed to their end points in the stack, interactions occuring between the mesons and emulsion nuclei being recorded. Full details of the exposure, scanning procedure and the classification and analysis of the interactions are given in Bhowmik *et al.* ([11]). In scanning 148 metres of K^+-meson track length, 94 interactions were observed in which the K-meson was seen to emerge, having lost an amount of energy which was greater than 10 MeV; these mesons were classified as the « scattered K-meson beam ». About 2000 tracks due to K-mesons which did not suffer an inelastic collision were traced to their ends. From these a random sample was selected and 286 secondary tracks in good geometry were grain counted in order to yield information on the secondaries of the « unscattered K-meson beam ».

The frequency of occurrence of the different components of the K-meson beam, decaying into singly charged particles, was found from ionization measurements on the tracks of the decay products. Only tracks having a dip less than a prescribed cut-off angle in the unprocessed emulsion were used for these measurements. About half the sample was analysed with a cut-off angle of 34° on the scattered beam and 31° on the unscattered beam; later these

([10]) T. Hoang, M. F. Kaplon and G. Yekutieli: *Phys. Rev.*, **102**, 1185 (1956).

([11]) B. Bhowmik, D. Evans, S. Nilsson, D. J. Prowse, F. Anderson, D. Keefe, A. Kernan and J. Losty: *Nuovo Cimento*, **6**, 440 (1957).

cut-off angles were changed to 30° and 22° respectively for the remainder of the sample. The secondary tracks were followed through a number of emulsion sheets to enable the accumulation of sufficient statistics for an accurate estimate of the ionization. The statistical precision of the measurements on the secondaries of the K-mesons of the scattered beam was never worse than 3% while for events of the unscattered beam an average uncertainty of 4.5% was allowed. In every plate the grain density, g_π, of the tracks due to the beam π-mesons was measured with a precision of better than $\pm 2.5\%$ and the other grain counts on the secondary tracks normalized by dividing them by g_π. From the calibration curve of ALEXANDER and JOHNSTON [12] in this stack, g_π is known to be 1.01 times the minimum grain density so that the specific ionization g^+, normalized to g_π will be 1.04 for secondaries arising in the $K_{\mu 2}$ mode, 1.12 for the K_β mode, and 1.21 for the χ mode. In general the grain density of the tracks was obtained in the centre region of the emulsion only, but where necessary, correction was made for the development gradient (23% surface to glass) which was shown to be present from the normalization measurements.

A re-examination was made of all the secondary tracks from K-mesons of the scattered beam, which had values of g^+ lying between 1.06 and 1.30. Special efforts were made to distinguish the K_β decay mode and in every case where a value of g^+ consistent with 1.12 was obtained the track of the secondary particle was traced for 4 cm and examined carefully for evidence of energy degradation or change of ionization. Only one case was found to have exactly the right grain density and its identification as an electron secondary was confirmed by the discovery of an electron-electron collision along its path. In addition, for the K-mesons of both the scattered and the unscattered beams, all secondary tracks giving a value of $g^+ > 1.4$ from the initial measurements were followed a sufficient distance to ensure identification of the τ' and the $K_{\mu 3}$ decay modes.

A $K_{\mu 3}$-decay event would be detected with certainty as such only if the μ-meson had an energy less than about 55 MeV ($g^+ \geqslant 1.4$). Accordingly a division of $K_{\mu 3}$-decay events has been made into the two classes $\varkappa_{\text{high}}$ and $\varkappa_{\text{low}}$ according as the μ-meson energy is greater than or less than 55 MeV. Recent work on the energy spectrum of μ-mesons arising in this mode [13-15] suggests that the number of $\varkappa_{\text{low}}$ events is about one half of the number of $\varkappa_{\text{high}}$ events.

---

[12] G. ALEXANDER and R. H. W. JOHNSTON: *Nuovo Cimento*, **5**, 363 (1957).

[13] R. W. BIRGE, D. H. PERKINS, J. R. PETERSON, D. H. STORK and M. N. WHITEHEAD: *Nuovo Cimento*, **4**, 834 (1956).

[14] D. M. RITSON, A. PEVSNER, F. C. FUNG, M. WIDGOFF, G. T. ZORN, S. GOLDHABER and G. GOLDHABER: *Phys. Rev.*, **101**, 1085 (1956).

[15] G. ALEXANDER, R. H. W. JOHNSTON and C. O'CEALLAIGH: *Nuovo Cimento*, **6**, 478 (1957).

3. – Experimental results and discussion.

3·1. *The scattered beam.* – In all, 94 events were found corresponding to the inelastic interaction of a K-particle with an emulsion nucleus where the heavy meson emerged from the collision in the same charge state. In 6 cases the emergent K-particle left the stack before decaying, 5 decayed in the τ mode and 2 decayed in flight to a single charged secondary. Ionization measurements of the type described in Sect. 2 were made on the tracks of the 33 events where the single charged secondary had a dip less than the prescribed cut-off value, and where the event lay within the central 80% of the emulsion. The final distribution of normalized grain density, g^+, for these events is shown in Fig. 1. The event identified as being a decay in the K_β mode is marked « β » while in another case, marked by «2e», an electron pair was found to be associated with the end-point of a K-particle decaying in the χ mode.

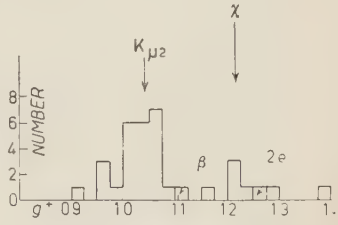

Fig. 1. – Histogram of the values of g^+ (normalized grain density) for all secondaries in geometry of the « scattered beam ». The event marked « β » is a K_β event and the event marked 2e is a χ-decay event with a Dalitz pair associated.

Neglecting the possible small contamination of $\varkappa_{high}$ events, Fig. 1 indicates that the sample analysed comprised 24 $K_{\mu 2}$ events and 8 χ events and 1 K_β event. In order to compute relative frequencies, 6 of the 12 K_0 events (*) lying within the central 80% of the emulsion, and 2 τ events have been included among the events of geometry acceptable for measurement. Of the K_0 events, 5 have bene assigned to the $K_{\mu 2}$ mode and one to the χ mode, i.e. in about the ratio found for the unscattered

TABLE I (*a*). – *Relative frequencies of the decay modes in the scattered beam.*

Decay mode	τ	τ' (*)	χ (+)	$K_{\mu 2}$ (+)	$\varkappa_{low}$	K_β
Relative frequency	5/88	0/41	9/41	29/41	0/41	1/41
Percentages	5.7±2.5	—	22±8	71±12	—	2
Combined with Göttingen percentages	6.3±1.6	0/91	23±6	64± 9	2/91 ~2%	2/57 ~4%

(*) 1 example of the τ' mode was found but it was out of geometry.
(+) These figures may contain a small contamination of $\varkappa_{high}$ events.

(*) K_0-events are K^+-meson decay events in which no secondary could be found. For a full treatment of this problem see reference [11].

TABLE I (*b*). – *Relative frequencies of the decay modes in the unscattered beam.*

Decay mode	τ	τ'	χ	$K_{\mu 2}$	$\varkappa_{low}$	$\varkappa_{high}$	K_β
Percentages This work	61/1 330= =4.6±.6	11/353= =3.1±.8	24±6 (*)	62±5 (*)	8/353= =2.3±.8	2 4 assumed	
ALEXANDER *et al.*	6.77±.43	2.15±.42	23.2±2.2	56.9±2.6	5.90±1.3		5.06±1.3
BIRGE *et al.*	5.56±.41	2.15±.47	27.7±2.7	58.5±3	2.8 ±1.0		3.2 ±1.3

(*) These errors are not only statistical but also take into account the uncertainty in the analysis of the g^+ distribution in Fig. 2.

beam (cf. 3·2). Since the K_0 correction is a small one, any error in this assignment is negligible compared with the statistical errors in the relative frequencies. These results are summarized in Table I (*a*).

In the third row of the table the figures of the Göttingen group, which are in agreement with the present results and obtained in a rather similar experiment, are added, and the summed data may be compared with the figures for the unscattered beam given in the second half of the table. Clearly, no statistically significant change in the relative frequency has been produced by allowing the beam to interact first with nuclei.

The two decay-in-flight events observed, in a time of flight for the scattered K-mesons of $1.6 \cdot 10^{-8}$ s, are in reasonable agreement with the lifetime value of $1.24 \cdot 10^{-8}$ s for the particles in the unscattered beam.

3·2. *The unscattered beam and the* $K_{\mu 3}$ *and* τ' *decay modes.* – Ionization measurements were made on a random sample of 286 decay events obeying the criteria of Sect. **2**, and the results are shown in Fig. 2. The bulk of the histogram lies in the region $g^+ = 0.9 \div 1.3$ as expected from the predominance of the $K_{\mu 2}$ and χ-decays and is well fitted by the combination of the Gaussian curves as shown. These curves give a ratio $\chi/K_{\mu 2} = 0.38$ in good agreement with that obtained by other workers ([13-15]); the detection efficiencies estimated were 0.84 for $K_{\mu 2}$ and 0.92 for χ events (cf. appendix to Ref. 13). The spread of the curves is that associated with the statistical errors in the grain counts.

As described in Sect. **2**, all secondaries giving an initial value of $g^+ \geqslant 14.$ were followed to allow the unbiassed discrimination of decays due to the τ' and the $K_{\mu 3}$ particles. The highest energy that a π-meson arising in the τ' decay mode may have is 54 MeV, corresponding to a track of $g^+ = 1.61$, and since the lower limit of g^+ for the following of tracks is about 3 standard

deviations below this, it is expected that all examples of this type of particle were found. The energy of a μ-meson having a track of $g^+ = 1.4$ is 55 MeV and so the efficiency of detection of the $K_{\mu 3}$ events is thought to be independent

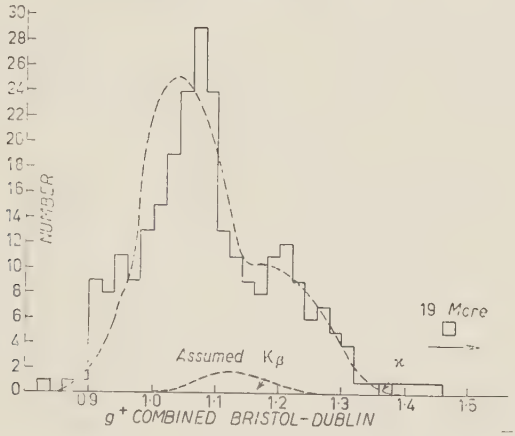

Fig. 2. – Histogram of the values of g^+ for all secondaries in geometry of the « unscattered beam ». There are 19 events with $g^+ \geqslant 1.46$ of which 11 are from the τ'-mode and 8 from the $\varkappa$-mode. In addition there was an event with $g^+ = 1.51$ (not shown) which appears to be a χ-decay event giving an anomalous ionization measurement. The number of K_β events has been estimated from published data (4%) and the gaussian marked K_β is the distribution in g^+ expected from such events. The relative number of $K_{\mu 2}$ and χ-events present in the sample has been estimated in the following way: two gaussian curves were centred at $g^+ = 1.04$ and 1.21, each with a width expected from the statistical accuracy of the ionization measurements. Their relative amplitudes were then adjusted to fit the observed distribution, the best fit being chosen by a simple χ^2 test.

of energy for secondaries of less than 50 MeV. The tracks of the decay products of all τ' and $K_{\mu 3}$ particles detected were followed to their ends in the stack and Table II shows the energies observed.

TABLE II. – *Energies of the secondary particles arising in the τ' and $K_{\mu 3}$ modes of decay.*

τ'	E (MeV)	4.5,	11,	11,	16,	18,	22,	24,	26,	32,	33,	34 .
$\varkappa_{\text{low}}$	E (MeV)	7.2,	7.7,	21,	22,	29,	35,	37,	39,	(59) (*) .		

(*) This event has $g^+ < 1.4$ and so is excluded from the analysis.

The relative frequency of occurrence of τ' is $(3.1 \pm .8)\%$; of τ is $(4.6 \pm .6)\%$ and $\varkappa_{\text{low}}$ is $(2.3 \pm .8)\%$; and the branching ratio $\tau'/\tau = .67 \pm .15$. Fig. 3 summarizes the present results on the τ' secondary spectrum together with those given at the Rochester Conference (1957) which are also unbiassed. The

figure is in general agreement with the hypothesis that the π-mesons are created in an even spin and odd parity state in the decay process. It is interesting to note that in the examination of the heavy meson decay events, electron pairs were observed to be associated in 3 cases. Assuming that the branching ratio for the alternative decay mode of the π^0 into an electron pair and a γ-ray is 1/80 and that a π^0-meson is involved in the decay modes $K_{\pi 2}$, $K_{\mu 3}$ and K_β, and two π^0 in the mode τ' then the number of electron pairs expected is 5.

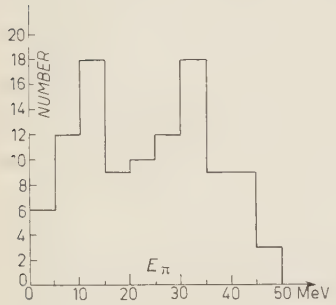

Fig. 3. – Energy spectrum of the π^+-mesons emitted in τ'-decay. These are the combined results of this work, the Dublin, Advanced Institute, work (ref. [15]) and the Columbia work (reported at the Rochester Conference, 1957),

* * *

We are very grateful to Professors E. J. Lofgren and R. W. Birge who made the exposure to the K^- beam at the Bevatron possible. We acknowledge with gratitude the work of Mr. C. Waller (Ilford Ltd.) in preparing the stack. Our thanks are due to Professors C. F. Powell F.R.S. and T. E. Nevin for their constant encouragement. The hard work in scanning by Misses J. Byrne and M. Pearce, Mrs. A. Boult and Mrs. A. Evans at Bristol, and Misses D. O'Brien and M. Smith at Dublin is greatly appreciated. Special thanks are due to Miss B. Maher and Mrs. A. Evans for their assistance with the measurements and to J. Losty and S. Nilsson for their contributions in the early stages of the experiment. We thank Dr. J. Orear for permission to include the published Columbia data in Fig. 3. One of us (B. B.) wishes to thank the University of Delhi for leave of absence; another (D. E.) the University of Bristol for a graduate scholarship.

RIASSUNTO (*)

Si sono determinati i modi di decadimento dei mesoni K^+ che hanno subito scattering anelastici in emulsione e si dimostra che le loro frequenze relative sono compatibili con quelle ottenute pei mesoni K^+ che non hanno subito interazioni nucleari. Si sono anche eseguite misure su un totale di 286 decadimenti con un secondario semplicemente carico allo scopo di scoprire, senza incorrere in errori d'osservazione, le particelle che decadono nei modi rari τ' e $K_{\mu 3}$.

(*) *Traduzione a cura della Redazione.*

Radiative β-Decay of the π-Meson.

E. Ferrari

Istituto di Fisica dell'Università - Roma
Istituto Nazionale di Fisica Nucleare - Sezione di Roma

(ricevuto l'11 Gennaio 1958)

Summary. — The probability of the process $\pi \to e + \nu + \gamma$ is calculated by means of a cut-off procedure. It is shown that for ST coupling the branching ratio $(\pi \to e + \nu + \gamma)/(\pi \to \mu + \nu)$ is practically independent of the cut-off parameter.

The problem of pion decay through a virtual nucleon pair is of much interest in the framework of the Universal Fermi Interaction. The theoretical result suggested by this scheme seems to be in contradiction with the experimental evidence.

It is well known that the pion decays into a μ-meson and a neutrino: radiative decays $\pi \to \mu + \nu + \gamma$ have been observed, but so far no events which could be interpreted without ambiguity as direct pion decays into an electron and a neutrino (accompanied or not by photons) have been detected. The scheme of the Universal Fermi Interaction, however, because of its symmetry between muon and electron (except for the masses) would make one to expect either decay.

We are assuming that the coupling in the Universal Fermi Interaction is mainly scalar and tensorial (ST), assuming the customary order of Fermi amplitudes [1]. We must also assume a small amount of axial coupling (A), in order not to forbid the $\pi \to \mu + \nu$ decay, which can occur only through the axial and pseudoscalar couplings. In this case the branching ratio of the probabilities of the two decays is

$$\text{Rate}\frac{\pi \to e + \nu}{\pi \to \mu + \nu} = 1.3 \cdot 10^{-4}.$$

[1] Recent evidence from recoil experiments has cast some doubt on the suitability of the ST theory.

If however we consider the radiative β-decay $\pi \to e+\nu+\gamma$ we arrive at a serious discrepancy with the experiment. We shall discuss this difficulty later.

1. – The radiative β-decay of the pion.

The radiative β-decay of the pion may occur through the 3-rd order graphs shown in Fig. 1.

For an ST interaction all the contributions of the various couplings between the fermions are ineffective or negligible in comparison with the contribution of graph (*c*) with tensorial coupling. In fact in the other graphs of type (*c*) the coupling constants are small in comparison with the tensorial, except the scalar: but in this case the process is forbidden. In the graphs of type (*a*) and (*b*) the corresponding 2-nd order processes, obtained by suppressing the photon, are forbidden for the tensorial and scalar couplings, and negligible for the other couplings, because of the smallness of the coupling constants.

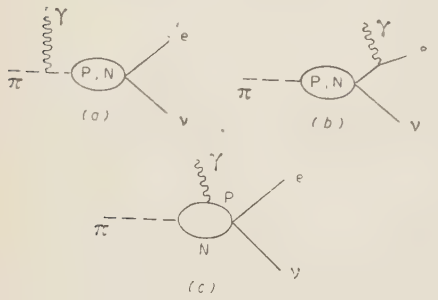

Fig. 1.

The process $\pi \to e+\nu+\gamma$ has already been calculated by several authors [2]; but all of them have made « approximate » calculations. The reason is that the matrix element of the process turns out to be logarithmically divergent for large momenta of the virtual nucleons. In order to make it finite, a cut-off procedure must be introduced. The value of the cut-off parameter is to be chosen so that it fits the other experimental data; but it remains to a large extent arbitrary. The approximate calculations consist in writing down for the contribution of the intermediate nucleon loop an adequate expression suggested by gauge invariance or symmetry requirements. Thus the calculations are much simplified; but it is not possible to see the influence of the cut-off procedure on the result, and one could doubt that, with a large var-

[2] M. Ruderman: *Phys. Rev.*, **85**, 157 (1952); S. B. Treiman and H. W. Wyld: *Phys. Rev.*, **101**, 1552 (1956); T. Eguchi: *Phys. Rev.*, **102**, 879 (1956). Experimental work on the problem has been performed by H. L. Friedman and J. Rainwater: *Phys. Rev.*, **84**, 684 (1951); S. Lokanathan and J. Steinberger: *Suppl. Nuovo Cimento*, **2**, 151 (1955); H. L. Anderson: unpublished; S. Lokanathan: *Ph. D. Thesis*; J. M. Cassels, M. Rigby, A. M. Wetherell and J. R. Wormald: *Proc. Phys. Soc.*, A **70**, 729 (1957).

iation of the cut-off parameter, the result might vary even by many orders of magnitude, since the original integral was divergent. In order to remove this objection, we have carried out the calculation as exactly as possible. The only approximation we have been compelled to make is an expansion of the matrix element in powers of the parameter m_{π}/M; in the final result the error to be ascribed to this cause is less than 2%.

The final result, which has been obtained with the Feynman-Dyson's covariant treatment of the perturbation method, gives for the transition probability $\tau_{e\gamma}^{-1}$ of the process $\pi \to e+\nu+\gamma$ the expression

$$\tau_{e\gamma}^{-1} = \frac{1}{2\pi^5}\left(\frac{e^2}{4\pi\hbar c}\right)\left(\frac{G^2}{4\pi\hbar c}\right)\frac{g_T^2 h_0^5}{\hbar^2 c}\,\frac{\eta^2}{192}\,\varphi(\varrho'), \tag{1}$$

where G is the pseudoscalar constant of the Yukawa interaction: g_T is the tensorial constant of the Fermi interaction: h_0^{-1} is the Compton wave length of the pion: η is a constant, cut-off dependent, which diverges as $\log \tau$ when the cut-off parameter τ goes to infinity; ϱ' is a parameter which ranges from 1 to 0 when τ varies from 0 to ∞; $\varphi(\varrho')$ is the following function of ϱ'

$$\varphi(\varrho') = 1 + \frac{11}{3}\,\varrho' + \frac{47}{12}\,\varrho'^2.$$

A graph of $\varphi(\varrho')$ in function of ϱ' and of the cut-off parameter τ is plotted in Fig. 2.

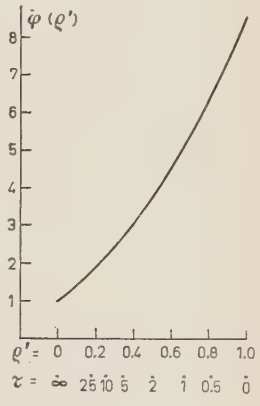

Fig. 2.

The meaning of τ and the explicit expressions of η and ϱ' in function of τ will be given in the last paragraph.

In the calculation the mass of the electron is neglected.

A remarkable feature of our calculation is the following. If we compute the transition probability τ_{μ}^{-1} for the non-radiative decay $\pi \to \mu+\nu$ we find ($\gamma = m_{\mu}/m_{\pi}$)

$$\tau_{\mu}^{-1} = \frac{1}{8\pi^4}\left(\frac{G^2}{4\pi\hbar c}\right)\frac{g_A^2}{\hbar^2 c}\,h_0^3\left(\frac{Mc}{\hbar}\right)^2 \gamma^2(1-\gamma^2)^2\eta^2\,, \tag{2}$$

where g_A is the axial constant of the Fermi interaction, M is the nucleon mass, and η is the same constant as in (1). Therefore the branching ratio $\varrho_{e\gamma} = \tau_{e\gamma}^{-1}/\tau_{\mu}^{-1}$ never diverges, and depends on the cut-off only through $\varphi(\varrho')$: that is very slightly. It is almost the same situation which occurs in the calculation of the ratio $(\pi \to e+\nu)/(\pi \to \mu+\nu)$, in which the divergences cancel out.

If we evaluate ϱ_γ numerically, we find

$$\varrho_\gamma = \frac{1}{48\pi}\left(\frac{e^2}{4\pi\hbar c}\right)\left(\frac{m_\pi}{M}\right)^2 [\gamma^2(1-\gamma^2)^2]^{-1}\left(\frac{g_T}{g_A}\right)^2 \varphi(\varrho') = 10^{-5}\left(\frac{g_T}{g_A}\right)^2 \varphi(\varrho') .$$

This result is in full agreement with the approximate result of TREIMAN-WYLD's calculation, which is [3]

$$\varrho_\gamma \geqslant 10^{-5}\left(\frac{g_T}{g_A}\right)^2 , \tag{3}$$

which, compared with ours, is equivalent to setting $\varphi(\varrho') \geqslant 1$, which is actually the case. Our calculation gives a quantitative expression for the $\geqslant$ which appears in (3), and fixes the variation of ϱ_γ with the cut-off parameter. Besides this it demonstrates that it is not possible to obtain large variations of ϱ_γ by choosing different cut-off parameters, provided the same cut-off is used in both calculations: the calculation of the radiative and that of the non-radiative decay.

2. – Conclusions.

As TREIMAN-WYLD have pointed out, the evidence from β-decay spectra gives us $|g_T/g_A| \simeq 50$. With this we find

$$\varrho_\gamma \geqslant 0.025 , \tag{4}$$

while the experiment shows that the branching ratio is of the order of 10^{-5}.

This calculation supports the conclusion that the pion decay is not consistent with the scheme of a « Universal » weak interaction, at least if we retain the ST coupling. In fact we have answered one of the objections which might be raised against the result (4): its possible strong cut-off dependence.

It is therefore difficult to see how one could avoid giving up the idea of Universal Fermi Interaction: in particular, it does not seem possible to explain the strong preference of the pion for decaying into μ instead of e with the only aid either of a particular selection rule, or of the mass difference between muon and electron [4]. An attempt could be made to investigate whether an unconventional order of the ψ's in the expression of the $\mathrm{pn}\mu\nu$ interaction might save the possibility of a quadrilinear universal interaction [5]; the

[3] S. B. TREIMAN and H. W. WYLD: *Phys. Rev.*, **101**, 1552 (1956).
[4] B. TOUSCHEK: private communication.
[5] G. MORPURGO: *Nuovo Cimento*, **5**, 1159 (1957).

consequences of such a rearrangement, however, are not so immediate, and the present stage of uncertainty about the values of the β-constants does not allow us to draw any definite conclusions on the subject.

In order to conclude, we would like to point out that in our calculation the cut-off procedure has been achieved (according to FEYNMAN: *Phys. Rev.*, **76**, 769 (1949)) by multiplying the integrals on the 4-momentum p of the virtual nucleon by a convergence factor $K^2/(p^2+K^2)$. We have set $K=\tau M$, in in order to deal with a pure number.

The values of η and ϱ' in function of τ are (6)

$$\eta=\frac{1}{2}\frac{\tau^2}{(\tau^2-1)^2}[1+\tau^2(\log\tau^2-1)]\,, \qquad \varrho'=\frac{1+\tau^2-[2\tau^2/(\tau^2-1)]\log\tau^2}{1+\tau^2(\log\tau^2-1)}\,.$$

* * *

We thank Prof. G. MORPURGO and Prof. B. TOUSCHEK for constant advice and helpful discussion.

(6) If we treat the problem with the usual procedure of the perturbative method, the cut-off procedure is different. The upper limit of an integral on the 3-momentum of the virtual nucleon is to be put equal to τM. The final conclusions are quite the same: the τ-dependence of η, ϱ', is, however, different, and becomes the same only asymptotically ($\tau\to\infty$). We have:

$$\eta=\log\left[\tau+\sqrt{1+\tau^2}\right]-\frac{\tau}{\sqrt{1+\tau^2}}\,, \quad \varrho'=\frac{\frac{1}{3}(\tau/\sqrt{1+\tau^2})^3}{\eta}\,.$$

We would like to point out that the energy and angular distributions for the electron, which are given in EGUCHI's and CASSELS' works, refer to the «extreme asymptotic» case ($\log\tau\gg 1$, $\varrho'\simeq 0$) apart from a multiplicative factor. The general energy distribution for an arbitrary cut-off is much more complicated, but the curve has always the same shape.

RIASSUNTO (*)

Si calcola la probabilità del processo $\pi\to e+\nu+\gamma$ con un procedimento di taglio. Si dimostra che per accoppiamento ST il rapporto $(\pi\to e+\nu+\gamma)/(\pi\to\mu+\nu)$ è praticamente indipendente dal parametro di taglio.

(*) *Traduzione a cura della Redazione.*

The External Magnetic Field of the Earth.

A. Beiser

Department of Physics, New York University, University Heights, New York, N.Y.

(ricevuto il 7 Gennaio 1958)

Recently it has been discovered [1] that the equivalent geomagnetic dipole required to account for the latitude variation in cosmic-ray neutron intensity is different from the equivalent dipole derived from surface observations. The cosmic-ray data indicate that the dipole component in the equatorial plane, as seen by a charged particle incident upon the earth from a distant source, is approximately 45° west of the equatorial component obtained from the harmonic analysis of the surface magnetic field. While not too much is known about the properties of interplanetary matter, there is little doubt that it is a fairly good conductor of electricity, and therefore it seems reasonable to suppose that the origin for the above discrepancy is to be found in magnetic fields set up in this matter by currents there that are induced by the rotation of the geomagnetic equatorial dipole.

In the system of co-ordinates we shall use in treating this problem a magnetic dipole of moment $\boldsymbol{M}$ is at the origin, and rotates about the z-axis with the angular velocity $\boldsymbol{\omega}$ corresponding to the rotation of the earth. $\boldsymbol{M}$ has the components

$$(1) \qquad \begin{cases} M_x = M \cos \varphi \\ M_y = M \sin \varphi \\ M_z = 0 \, , \end{cases}$$

where φ is the angle between $\boldsymbol{M}$ and the x-axis, and $\boldsymbol{\omega} = \omega_z$. The vector potential $\boldsymbol{A}$ at the point (x, y, z) due to $\boldsymbol{M}$ is

$$(2) \qquad \boldsymbol{A} = \frac{\boldsymbol{M} \times \boldsymbol{r}}{r^3} \, .$$

and since $\varphi = \omega t$, it is a function of time. This varying potential gives rise to an electric field

$$\boldsymbol{E} = - \frac{\partial \boldsymbol{A}}{\partial t}$$

in the interplanetary matter, and consequently to a current density $\boldsymbol{J}$ given by

$$(3) \qquad \boldsymbol{J} = \sigma \boldsymbol{E} = - \sigma \frac{\partial \boldsymbol{A}}{\partial t} \, .$$

[1] J. A. Simpson, K. B. Fenton, J. Katzman and D. C. Rose: *Phys. Rev.*, **102**, 1648 (1956).

where σ is the conductivity. $\boldsymbol{J}$ has the components

$$(4) \qquad \begin{cases} J_x = \dfrac{\sigma\omega M z \cos\varphi}{r^3}, \\ J_y = -\dfrac{\sigma\omega M z \sin\varphi}{r^3}, \\ J_z = \dfrac{\sigma\omega M(y\sin\varphi + x\cos\varphi)}{r^3}, \end{cases}$$

and evidently corresponds to current loops lying in planes parallel to the moving plane containing both $\boldsymbol{M}$ and the z-axis.

Owing to the physical state of the interplanetary matter spontaneous currents and associated magnetic fields may be expected to exist in it which, beyond some mean distance R from the earth, dominate the field of $\boldsymbol{M}$. We must therefore consider $\boldsymbol{J}$ to be contained within a spherical shell whose inner radius R_e is that of the earth and whose outer radius R we shall leave unspecified for the moment.

The dipole moment $\boldsymbol{M}^i$ of the currents $\boldsymbol{J}$ is

$$(5) \qquad \boldsymbol{M}^i = \frac{1}{2}\int \boldsymbol{r}\times\boldsymbol{J}\,\mathrm{d}V\,,$$

where the volume integral is to be taken over the spherical shell of the preceding paragraph. The induced dipole $\boldsymbol{M}^i$ turns out to have the components

$$(6) \qquad \begin{cases} M_x^i = \dfrac{2}{3}\pi\sigma\omega \cdot \\ \qquad \cdot M(R^2 - R_e^2)\cos\left(\varphi - \dfrac{\pi}{2}\right) \\ M_y^i = \dfrac{2}{3}\pi\sigma\omega \cdot \\ \qquad \cdot M(R^2 - R_e^2)\sin\left(\varphi - \dfrac{\pi}{2}\right) \\ M_z^i = 0\,. \end{cases}$$

Comparing this result with Eq. (1) we see that the magnetic field induced in interplanetary matter by the rotating equatorial dipole $\boldsymbol{M}$ is equivalent to that of a dipole of moment

$$(7) \qquad M^i = \frac{2}{3}\pi\sigma\omega M(R^2 - R_e^2)$$

rotating in the same plane and about the same axis as $\boldsymbol{M}$ but displaced by 90° behind it. Hence this analysis provides an explanation for the difference between the cosmic-ray and surface-field equatorial dipoles, since the net equatorial field influencing the motion of cosmic-ray primaries in the vicinity of the earth is that of $\boldsymbol{M}+\boldsymbol{M}^i$ beyond R. The field of $\boldsymbol{M}+\boldsymbol{M}^i$ is an angle

$$(8) \qquad \theta = \mathrm{tg}^{-1}\frac{M^i}{M} = \mathrm{tg}^{-1}\,\pi\sigma\omega(R^2 - R_e^2)$$

behind (i.e. to westward) of $\boldsymbol{M}$. The experimental observation [1] that $\theta \sim 45°$ means that $M^i \sim M$.

The resultant equivalent dipole representing the external magnetic field of the earth, consisting of $\boldsymbol{M}+\boldsymbol{M}^i+\boldsymbol{M}_{\text{axial}}$, should be tilted by several degrees farther from the rotational axis than $\boldsymbol{M}+\boldsymbol{M}_{\text{axial}}$ as well as being displaced westward. It seems likely that the small but definite discrepancies between the locations of the auroral maximum zones and those predicted on the basis of the surface-field dipole and between the actual positions of auroral corona radiation points and the surface-field magnetic zenith are due to $\boldsymbol{M}^i$. Certain anomalies in the propagation of radio whistlers may also result from the presence of $\boldsymbol{M}^i$. (A detailed consideration of these effects is in preparation.)

From the point of view of hydromagnetic theory, we can regard the interplanetary matter as exerting a kind of

viscous drag on the lines of force of $\boldsymbol{M}$ which causes them to lag behind their normal position with respect to $\boldsymbol{M}$. The work that must be done in overcoming this drag is at the expense of the rotational kinetic energy of the earth, and appears as Joule heat. In order to evaluate the power needed to maintain the rotation of $\boldsymbol{M}$, we begin by computing the energy W in the magnetic field $\boldsymbol{H}^i$ outside of the earth due to $\boldsymbol{M}^i$. This is

$$(9) \qquad \left\{ \begin{array}{l} W = \dfrac{1}{8\pi} \displaystyle\int H^{i2}\, \mathrm{d}V \,, \\ \qquad = \dfrac{M^{i2}}{3R_e^3} \,. \end{array} \right.$$

As we have found, $M^i \sim M$, while M, the equatorial component of the equivalenf geomagnetic dipole, is $1.59 \cdot 10^{25}$ G cm^3; hence $W = 3.26 \cdot 10^{23}$ ergs. The time τ required for the free decay of a magnetic field in a region whose linear dimensions are of order L and whose conductivity is σ is

$$(10) \qquad \tau \approx 4\pi\sigma L^2 \,.$$

Upon setting $\theta = 45°$ in Eq. (8) we have

$$(11) \qquad \frac{1}{\omega} = \frac{2}{3}\, \pi\sigma (R^2 - R_e^2) \,,$$

so that the magnetic field of $\boldsymbol{M}^i$ decays with a time scale approximately that involved in the rotation of the earth.

If now we suppose that the magnetic energy W must be replenished per radian of the earth's rotation, the power required amounts to $2.38 \cdot 10^{19}$ erg/s. This is slightly over twice the mean rate of energy dissipation resulting from tidal friction in the ocean basins. (Of course, the above figure is subject to a good deal of uncertainty, perhaps as much as an order of magnitude either way.) It is therefore possible that the maintenance of $\boldsymbol{M}^i$ may account for at least part of the discrepancy between the observed rate of lengthening of the day and the contribution of tidal friction to it.

Thus far it has not been necessary to evaluate either σ or R explicitly. The relation between them is given by Eq. (11). If $R \sim 10R_e$, which means that a field strength of 10^{-4} G due to $\boldsymbol{M}$ is the least that is effective in inducing $\boldsymbol{J}$ in interplanetary space, $\sigma \sim$ $\sim 10^{-16}$ emu. If $R > 10R_e$, σ is even lower. But the smallest plausible conductivity for cosmic matter that we can arrive at by orthodox means is $\sim 10^{-13}$ emu. However, it should be pointed out that Eq. (3) is valid in a plasma such as interplanetary matter only when the plasma is in a steady-state condition with its constituent ions having a vanishing mean velocity and in the absence of a gravitational potential. These conditions obviously do not obtain here, with the consequence that Eq. (3) may be employed as it is only by absorbing into the quantity σ a variety of effects not included in the usual expression for conductivity. An *effective* conductivity of 10^{-16} emu or less therefore does not seem unreasonable, and in fact estimates of its magnitude obtained in indirect ways such as this may contribute to an understanding of the properties of interplanetary matter.

* * *

I am indebted to Professor S. A. Korff for helpful discussions. This work was supported by the joint program of the U.S. Atomic Energy Commission and the U.S. Office of Naval Research.

Circular Polarization of Bremsstrahlung from High Energy Electrons with Arbitrary Polarization.

C. Fronsdal and H. Überall
CERN - Geneva, Switzerland

(ricevuto il 13 Gennaio 1958)

In view of the recently discovered possibilities of producing polarized electrons in parity violating weak interactions—β-decay ([1,2]) and μ-meson decay ([3])—circular polarization of bremsstrahlung becomes of interest as a means for detecting the polarization of such electrons ([2,3]). This electron polarization may not be entirely longitudinal ([4,5]). In the following, the bremsstrahlung circular polarization is indeed found to be sensitive to transverse electron polarization; thus at high energies $E_1 \gg mc^2$, where Coulomb scattering is no longer feasible, it offers another possibility for detecting transverse electron spins.

Born approximation calculations of circularly polarized bremsstrahlung were performed by McVoy and Dyson ([6]) for longitudinally polarized electrons and forward emission of radiation, and by Claesson ([7]) who obtained the differential cross-section. We derived the Born approximation differential cross-section and performed a summation over final electron spins and integration over final electron momenta, with a result feasible for experimental application. The following general results were found:

1) Bremsstrahlung is both linearly and circularly polarized.

2) The linear polarization is independent of any polarization of the initial electron.

3) Circular polarization occurs only for polarized initial electrons.

([1]) H. Frauenfelder, R. Bobone, E. von Goeler, N. Levine, H. R. Lewis, R. N. Peacock, A. Rossi and G. Pasquali: *Phys. Rev.*, **106**, 386 (1957).
([2]) M. Goldhaber, L. Grodzins and A. W. Sunyar: *Phys. Rev.*, **106**, 826 (1957).
([3]) G. Culligan, S. G. F. Frank, J. R. Holt, J. C. Kluyver and T. Massam: *Nature*, **180**, 751 (1957).
([4]) G. Györgyi and H. Überall: *Nuclear Physics*, **5**, 405 (1958).
([5]) H. Überall: *Nuovo Cimento*, **6**, 376 (1957); T. Kinoshita and A. Sirlin: *Phys. Rev.*, **108**, 844 (1957).
([6]) K. W. Mc Voy: *Phys. Rev.*, **106**, 828 (1957); K. W. Mc Voy and F. J. Dyson: *Phys. Rev.*, **106**, 1360 (1957).
([7]) A. Claesson: *Ark. f. Fys.*, **12**, 569 (1957).

4) If this circular polarization is not observed, the radiation has the same angular distribution and spectrum as that from unpolarized electrons.

The cross-section after summation of final electron variables and neglect of terms of order m/E_1, m/E_2, is found to be

$$\sigma = \tfrac{1}{2}\sigma_s + \tfrac{1}{2}\delta\sigma_c \,, \tag{1}$$

where σ_s is the cross-section given by SCHIFF [8]:

$$\sigma_s(x, U)\,\mathrm{d}x\,\mathrm{d}U\,\frac{\mathrm{d}\psi_1}{2\pi} = \frac{Z^2e^4}{137}\,\frac{\mathrm{d}x}{x}\,4U\,\mathrm{d}U\,\frac{\mathrm{d}\psi_1}{2\pi}\left\{\frac{1+(1-x)^2}{(1+U^2)^2}\left[\ln\frac{(1+U^2)^2}{\alpha}-1\right]-\right.$$
$$\left.-\,2\,\frac{1-x}{(1+U^2)^4}\left[2U^2\left[\ln\frac{(1+U^2)^2}{\alpha}-1\right]+1-4U^2+U^4\right]\right\}, \tag{2}$$

and σ_c is the circular polarized part:

$$\sigma_c(x, U, \psi_1)\,\mathrm{d}x\,\mathrm{d}U\,\frac{\mathrm{d}\psi_1}{2\pi} = \frac{Z^2e^4}{137}\,\mathrm{d}x\,4U\,\mathrm{d}U\,\frac{\mathrm{d}\psi_2}{2\pi}\left\{\cos\theta\left[\frac{2\quad x}{(1+U^2)^2}\left[\ln\frac{(1+U^2)^2}{\alpha}-1\right]-\right.\right.$$
$$\left.-\,2\,\frac{1-x}{(1+U^2)^4}\left[2U^2\left(\ln\frac{(1+U^2)^2}{\alpha}-1\right)+1-4U^2+U^4\right]\right]+$$
$$\left.+\sin\theta\cos\psi_1\,2\,\frac{1-x}{(1+U^2)^4}\,U(1-U^2)\left[\ln\frac{(1+U^2)^2}{\alpha}-4\right]\right\}; \tag{3}$$

$\delta = +1$ (-1) for right (left) circular polarization, x is the energy of the quantum divided by the initial electron energy, ε_1 the initial electron energy in units mc^2, $U = \theta_1\varepsilon_1$, θ_1 the angle between the momenta of initial electron and quantum, θ the angle between electron spin (in its rest system [9]) and electron momentum, ψ_1 the azimuth between the planes formed by electron spin-electron momentum and quantum momentum-electron momentum, and

$$\alpha = \left(\frac{Z^{\frac{1}{3}}}{111}\right)^2 + \left(\frac{1}{2\varepsilon_1}\,\frac{x}{1-x}\right)^2(1+U^2)^2 .$$

The circular polarization is given by

$$P_c = \sigma_c/\sigma_s \,. \tag{4}$$

It has the following properties:

1) for longitudinally polarized electrons ($\theta = 0$), P_c depends essentially on $x(2-x)$ and goes from zero at $x=0$ to one at $x=1$;

[8] L. I. SCHIFF: *Phys. Rev.*, 83, 252 (1951).
[9] H. A. TOLHOEK and S. R. DE GROOT: *Physica*, 17, 1 (1951).

2) for transversely polarized electrons ($\theta=\pi/2$), P_c is proportional to

   a) $\cos\psi_1$; thus P_c vanishes if the emission direction is perpendicular to the electron spin;

   b) $x(1-x)$; P_c goes from zero at $x=0$ through a maximum to zero at $x=1$;

   c) $U(1-U^2)(1+U^2)^{-2}$; thus it is zero for forward emission ($U=0$) and changes sign at $U=1$.

These results may be important for a determination of the transverse electron polarization from μ-meson decay. For β-decay electrons, which possess energies comparable to mc^2, the formulas cannot be used. An integration over the exact differential spectrum is being performed and will be published elsewhere.

About High Energy Interactions in Nuclear Emulsions.

P. Ciok, T. Coghen, J. Gierula, R. Hołyński, A. Jurak, M. Mięsowicz, T. Saniewska, O. Stanisz

Cosmic Ray Department, Institute of Nuclear Research Warszawa and Kraków, Poland

and

J. Pernegr

Institute for Physics of Czechoslovac Academy of Science Praha, Czechoslovakia

(ricevuto l'8 Febbraio 1958)

36 plates of the I-stack, which was exposed in the Po-Valley expedition in 1955, were scanned for photon-electron cascades to find interactions of the highest energy. The plates were also area scanned for jets of lower energy (in both scannings $N_h \leqslant 5$, $n_s \geqslant 6$). Measurements were made of the angular distribution (θ_L) of relativistic tracks. The energy γ_c of the colliding nucleons in the center of mass system was determined for every jet ($\log \gamma_c = \log \operatorname{ctg} \theta_L$) [1].

The jets were divided into three groups:

I)	$90 > \gamma_c > 23$	$(1.5 \cdot 10^{13} > E > 10^{12}$ eV)
II)	$23 > \gamma_c > 7.5$	$(10^{12} > E > 10^{11}$ eV)
III)	$7.5 > \gamma_c > 2.2$	$(10^{11} > E > 10^{10}$ eV)

$(E = 2\gamma_c^2 - 1)$

For each group the integral angular distribution is shown in Fig. 1 and 2 in co-ordinates of $\log F(\theta)/(1 - F(\theta))$ versus $\log \gamma_c \operatorname{tg} \theta_L$ [2,3], where $F(\theta)$ is the fraction of tracks with an angle less than θ with the jet axis. In these co-ordinates the isotropic distribution in center of mass system is represented as a line of slope 2 and the extreme anisotropic distribution of Heisenberg [4], as a line of slope 1.

[1] C. Castagnoli, G. Cortini, D. Moreno, C. Franzinetti and A. Manfredini: *Nuovo Cimento*, **10**, 1539 (1953).

[2] N. M. Duller and W. D. Walker: *Phys. Rev.*, **9**, 215 (1954).

[3] G. Bertolino and D. Pescetti: *Nuovo Cimento*, **12**, 630 (1954).

[4] K. Symanzik: in *Kosmische Strahlung* 2-nd ed. (W. Heisenberg ed., 1953), p. 561.

It is seen that the anisotropy in the center of mass system increases with the collision energy. Since the differential angular distribution predicted by the theories

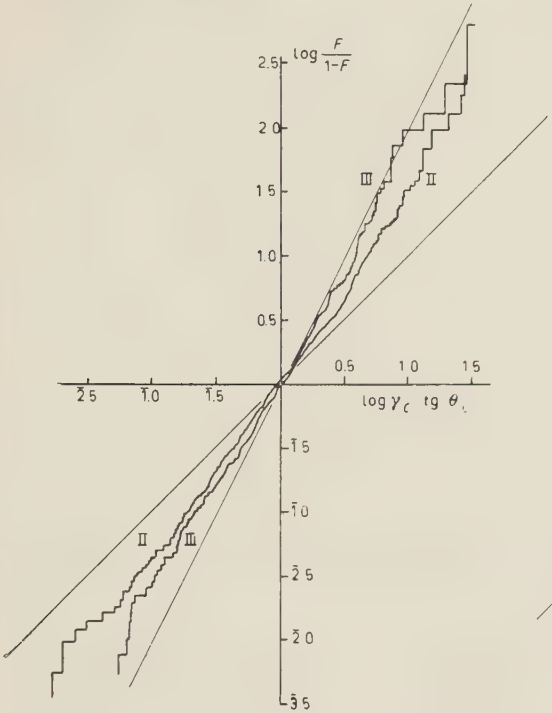

Fig. 1. – Integral angular distributions for jets of groups III and II. Group II consists of 32 jets with a total number of 470 tracks, group III consists of 35 jets with a total number of 345 tracks.

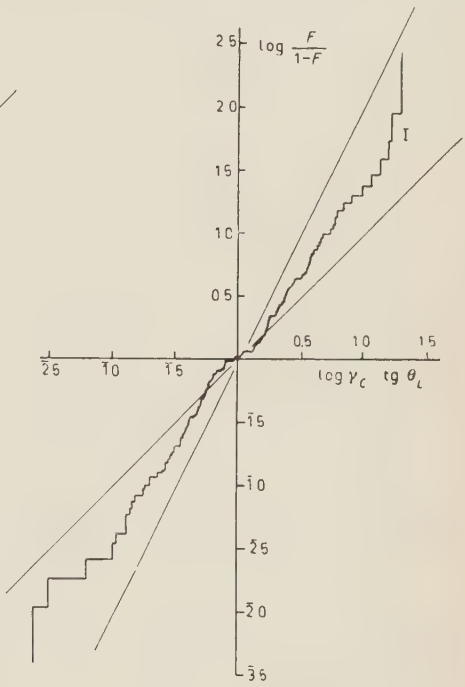

Fig. 2. – Integral angular distribution for jets of group I. It includes 11 jets with a total number of 138 tracks.

of Heisenberg and Landau may be approximated well by Gaussian curves [5], we therefore made such a comparison for our experimental material. The dispersion σ of this distribution is a measure of the degree of anisotropy ($\sigma=0.36$ corresponds to isotropy and $\sigma=0.7$ to the extreme anisotropy of Heisenberg). For group III we find $\sigma_{III}=0.46$, for group II $\sigma_{II}=0.56$ (Fig. 3 and 4). For group I $\sigma_{I}=0.55$, but the histogram obtained shows a significant deviation from the Gaussian curve (Fig. 5), (a χ^2 test gives a significant deviation on the 95% level).

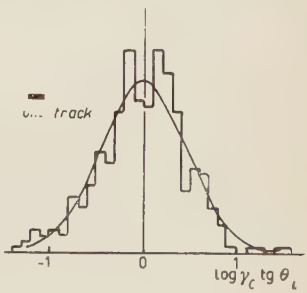

Fig. 3. – Differential angular distribution for jets of group III. The continuous curve represents the best fit of a Gaussian curve to the experimental data with $\sigma=0.46$.

[5] L. v. Lindern: *Nuovo Cimento*, **5**, 491 (1957).

If we could regard the distribution for group III and II as being in agreement with the curves predicted by the theories of Heisenberg and Landau ([6]), then we would observe a significant deviation for energies higher than 10^{12} eV (group I). The characteristic feature of this distribution is the scarcity of the tracks near the $\pi/2$ center of mass angle.

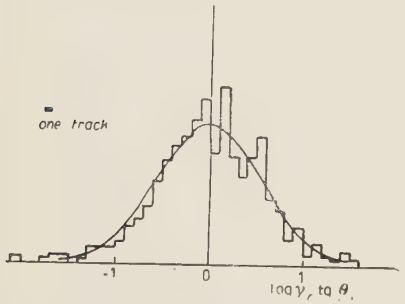

Fig. 4. – Differential angular distribution for jets of group II. The continuous curve represents the best fit of a Gaussian curve to the experimental data with $\sigma = 0.56$.

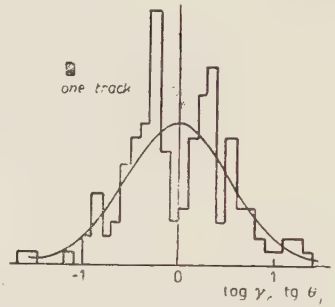

Fig. 5. – Differential angular distribution for jets of group I. The continuous curve represents a best fit of a Gaussian curve to the experimental data with $\sigma = 0.55$.

On the other hand an analysis of the results obtained may be attempted on the basis of the « excited nucleons » model ([7-9]) in which the nucleons emit mesons independently. The results of measurements of the angular distributions for two cones taken separately, presented in Fig. 6 as the integral distributions for three jets with well separated cones are not in contradiction with isotropic emission from two independent centres. As a consequence of the principle of the conservation of energy and the well-established experimental fact of the approximate constancy of the transverse momentum ([10,11]) ($p_T \approx 0.5$ GeV/c), we obtain for $\bar{\gamma}$, i.e. the γ-value of the radiating centres in the center of mass

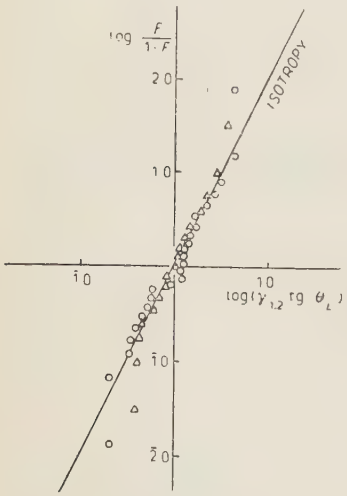

Fig. 6. – Integral angular distribution for diffuse and narrow cones treated separately as independent jets. Used here, are the jets: « S »-star ([12]), our recently described jet No 115 ([13]) and jet No 155 from group I of our statistical material. ○ narrow cones, Δ diffuse cones.

([6]) G. Bozóki, E. Fenyves and E. Gombosi: preprint.
([7]) H. W. Lewis, J. R. Oppenheimer and S. A. Wouthuysen: *Phys. Rev.*, **73**, 127 (1948).
([8]) S. Takagi: *Progr. Theor. Phys.*, **7**, 123 (1952).
([9]) W. L. Kraushaar and L. J. Marks: *Phys. Rev.*, **93**, 326 (1954).
([10]) S. Hayakawa: *Proc. of the VII Rochester Conference* (1957), Session XI, p. 3.
([11]) B. Edwards, J. Losty, D. H. Perkins, K. Pinkau and J. Reynolds: preprint. We are very much indebted to Dr. Perkins for sending us the preprint before publication.
([12]) M. Schein, R. G. Glasser and D. M.Haskin: *Nuovo Cimento*, **2**, 647 (1955).
([13]) P. Ciok, M. Danysz, J. Gierula, A. Jurak, M. Mięsowicz, J. Pernegr, J. Vrána and W. Wolter: *Nuovo Cimento*, **6**, 1409 (1957).

system the relation:

$$1.5 n_s E_\pi \bar{\gamma} = 2KM\gamma_c \,, \tag{1}$$

where E_π denotes the meson energy in the system of the emitting centre ($E \approx 0.5$ GeV), K is the inelasticity coefficient and M the nucleon rest mass. (In general $\bar{\gamma}$ is much smaller than γ_c). This formula is analogous to the formula for the cosec θ_{CM} given by the Bristol Group ([11]).

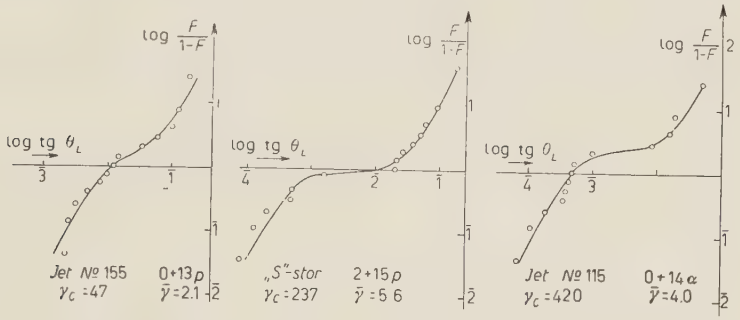

Fig. 7. – Integral angular distributions for jets from Fig. 6. The continuous curves represent the distributions predicted by the model under discussion, $\bar{\gamma}$ and γ_c being taken from the angular dstribution. ⊙ experimental points.

Fig. 7 shows the integral angular distributions for three jets of the highest energy obtained on the basis of the two-centre model. The $\bar{\gamma}$ (given in the figures) were determined from the angular distributions and are in agreement within the limits of error of K and γ_c with the values obtained by means of formula (1). The angular distributions in groups III and II can be roughly described in the same way by assuming $\bar{\gamma}_{III} \approx 1.3$ and $\bar{\gamma}_{II} \approx 1.5$. As may be seen, the model under consideration gives a consistent description of the observed experimental facts.

* * *

The authors wish to thank Professor M. Danysz for valuable discussions and Dr. P. Zieliński for his comments on the statistical analysis of the experimental material.

On the Convergence of Perturbative Expansions.

A. Buccafurri and E. R. Caianiello

Istituto di Fisica Teorica dell'Università - Napoli
Scuola di Perfezionamento in Fisica Teorica e Nucleare del C.N.R.N.

(ricevuto il 21 Febbraio 1958)

It was shown [1] that, when the space-time volume Ω of integration is taken finite and the free fermion and boson propagators $S^F(x, y)$ and $D^F(x, y)$ (in our notation, (xy) and $[xy]$) are bounded, in modulus, by finite quantities through some cut-off procedures, the perturbative expansions of the propagation kernels $K_{N_0 P_0}$ [2] of electrodynamics and similar theories are convergent, with a finite radius of convergence. Yennie [3] has further proved that, in the particular case in which the limitation of $S^F(x, y)$ is obtained by allowing only a finite number of modes to the free fermion field (already considered in ref. [1]), such perturbative expansions have an *infinite* radius of convergence, i.e. are holomorphic functions of the coupling constant λ in the whole plane (upon division by the vacuum-vacuum transition amplitude K_0, which is also holomorphic, the situation is thus similar to that occurring in the classical Fredholm theory; the radius of convergence of this ratio is expected to be *finite*). This result seems to us very relevant, both because it gives a final answer in all those cases in which the conditions which « regularize » the theory are inherent in the theory itself (field-theoretic models, problems of solid state physics, etc.), and because the extant field theories can, conceivably, be studied by analysing the behavior of the holomorphic kernels in the limit when these conditions are removed.

We think it appropriate, therefore, to offer a proof of Yennie's result which shows as clearly the mathematical reason of the holomorphy, and seems better suited to deeper investigations of this subject.

Assume that the free fermion field has only F modes for particles (and as many for antiparticles); let $|(xy)| < M$. Consider the determinant $\begin{pmatrix} \xi_1 \dots \xi_N \\ \xi_1 \dots \xi_N \end{pmatrix}$ formed with

[1] *Nuovo Cimento*, **3**, 223 (1956).
[2] For references and notation, see *Nuovo Cimento*, **11**, 492 (1954).
[3] D. R. Yennie and S. Gartenhaus: *Nuovo Cimento*, this issue.

the free propagators $(\xi_h\xi_k)((\xi_h\xi_h)=0)$. The following expansion theorem holds [4]:

$$(1)\qquad \begin{pmatrix}\xi_1 \dots \xi_N\\ \xi_1 \dots \xi_N\end{pmatrix} = \sum_{s=0}^{A}\sum_{C_s}(-1)^p \begin{pmatrix}\xi_{h_1'} \dots \xi_{h_r'}\\ \xi_{k_1'} \dots \xi_{k_r'}\end{pmatrix}\begin{pmatrix}\overset{0}{\xi}_{h_1''} \dots \overset{0}{\xi}_{h_s''} & \xi_{A+1} \dots \xi_N\\ \overset{0}{\xi}_{k_1''} \dots \overset{0}{\xi}_{k_s''} & \xi_{A+1} \dots \xi_N\end{pmatrix},$$

where: $r+s=A$, A any fixed number $>F$;

$h_1'<h_2'<\dots<h_r'$; $h_1''<h_2''<\dots<h_s''$ are any permutation Π_h of $1, 2 \dots N$ (row indices), and $k_1'<k_2'<\dots<k_r'$; $k_1''<k_2''<\dots<k_s''$ any permutation Π_k of $1, 2 \dots N$ (column indices);

p is the parity of Π_h with respect to Π_k, and $\sum_{C_s}$ is, for fixed s, the sum over all such $\binom{A}{s}^2$ Π_h and Π_k;

the last determinants are expanded with the rule:

$$(\overset{0}{\xi}_\alpha\overset{0}{\xi}_\beta) = 0\,; \qquad (\overset{0}{\xi}_\alpha\xi_\beta) = -(\xi_\alpha\overset{0}{\xi}_\beta) = (\xi_\alpha\xi_\beta)\,.$$

If $\xi_1\xi_2 \dots \xi_N$ are temporally ordered so that $(\xi_1)_0 \geqslant (\xi_2)_0 \geqslant \dots \geqslant (\xi_N)_0$, then it is trivially seen from the expansion of $(\xi_h\xi_k)$ in free-particle wave functions [5] that all terms at r.h.s. of (1) vanish for $s \geqslant F+1$ (physically, this is the exclusion principle). We can, therefore, replace in the first sum of (1) A with F.

For the sake of simplicity, we restrict our proof to the case of purely fermionic kernels $K_{N_0,0}$, taken with all external time-variables fitted to describe processes in which no antiparticles are involved [6]. This is, of course, no limitation of generality, and serves only to make simpler the application of theorem (1) to the expansion

$$(2)\qquad K_{N_0,0} = \sum_{n=0}^{\infty}\lambda^{2n}\int_{(V,T_{\text{in.}})}^{T_{\text{Fin.}}}\mathrm{d}\xi_1\int_{(V,T_{\text{in.}})}^{t_1}\mathrm{d}\xi_2 \dots \int_{(V,T_{\text{in.}})}^{t_{2n-1}}\mathrm{d}\xi_{2n}\sum\gamma^1\gamma^2 \dots \gamma^{2n}[\xi_1 \dots \xi_{2n}]\begin{pmatrix}\xi_1 \dots \xi_N & x_1 \dots x_{N_0}\\ \xi_1 \dots \xi_{2+1} & y_1 \dots y_{N_0}\end{pmatrix}.$$

Since $|[\xi_h\xi_k]|<L$ [1], a majorant of $K_{N_0,0}$ is given by:

$$(3)\qquad |K_{N_0,0}| < \sum_{n=0}^{\infty}\lambda^{2n}V^{2n}4^{6n}(2n-1)!!\,L^n \left|\begin{pmatrix}\xi_1 \dots \xi_{2n} & x_1 \dots x_{N_0}\\ \xi_1 \dots \xi_{2n} & y_1 \dots y_{N_0}\end{pmatrix}_{t_1>t_2>\dots>t_{2n}}\right|_{\text{Max.}} \cdot$$

$$\cdot\int_{T_{\text{in.}}}^{T_{\text{Fin.}}}\mathrm{d}t_1\int_{T_{\text{in.}}}^{t_1}\mathrm{d}t_2 \dots \int_{T_{\text{in.}}}^{t_{2n-1}}\mathrm{d}t_{2n} = \sum_{n=0}^{\infty}\left(\frac{\lambda^2}{2}\right)^n\cdot\frac{1}{n!}\cdot V^{2n}T^{2n}4^{6n}L^n\left|\begin{pmatrix}\xi_1 \dots x_{N_0}\\ \xi_1 \dots y_{N_0}\end{pmatrix}_{t_1>\dots>t_{2n}}\right|_{\text{Max.}},$$

where T is the time interval of integration.

---

[4] This is the classical theorem of Arnaldi, in our notation. We shall return on it in a subsequent paper.

[5] Ref. [2], rel. (13).

[6] Ref. [2], Sect. 2·3.

From (1) and from Hadamard's inequality it follows

$$\left(2n + N_0 = N;\ M^{A-s_1}\binom{A}{s_1}^2 (A-s_1)^{\frac{1}{2}(A-s_1)} = C(A, s_1)\right)$$

$$\left|\begin{pmatrix}\xi_1 \dots x_{N_0}\\ \xi_1 \dots y_{N_0}\end{pmatrix}_{t_1 > \dots > t_{2n}}\right|_{\text{Max.}} =$$

$$= D_N < \sum_{s_1=0}^{F} M^{A-s_1}\binom{A}{s_1}^2 (A-s_1)^{\frac{1}{2}(A-s_1)} \left|\begin{pmatrix} 0 & & 0 & & & & \\ \xi_{h_1''} \dots & \xi_{h_{s_1}''} & \xi_{A+1} \dots & \xi_{2n} & x_1 \dots & x_{N_0} \\ 0 & & 0 & & & & \\ \xi_{k_1''} \dots & \xi_{k_{s_1}''} & \xi_{A+1} \dots & \xi_{2n} & y_1 \dots & y_{N_0} \end{pmatrix}_{(t_1 > \dots > t_{2n})}\right|_{\text{Max.}} =$$

$$= \sum_{s_1=0}^{F} C(A, s_1) D_{s_1, N-A}\ .$$

Apply the same procedure to the first A rows and columns of $D_{s_1, N-A}$ (which we can do, because we find elements either $< M$ or $= 0$, so that in any case Hadamard's inequality holds):

$$D_{s_1, N-A} < \sum_{s_2=0}^{F} C(A, s_1) \left|\begin{pmatrix} 0 & & 0 & & & \\ \xi_{l_1''} & \dots & \xi_{l_{s_2}''} & \xi_{2A-s_1+1} \dots & x_{N_0} \\ 0 & & 0 & & & \\ \xi_{m_1''} & \dots & \xi_{m_{s_2}''} & \xi_{2A-s_1+1} \dots & y_{N_0} \end{pmatrix}_{(t_1 > \dots > t_{2n})}\right|_{\text{Max.}} =$$

$$= \sum_{s_2=0}^{F} C(A, s_2) D_{s_2, N-2A+s_1}\ ;$$

and, by iteration:

$$D_N < \sum_{s_1, \dots, s_p}^{0 \dots F} C(A, s_1) \dots C(A, s_p) D_{s_p, N-pA+s_1+s_2+\dots+s_{p-1}}\ .$$

The iteration will stop for values of p such that:

$$0 \leqslant \sum_{i=1}^{p} s_i + N - pA \leqslant A\ . \tag{5}$$

Since $\sum_{i=1}^{p} s_i \leqslant pF$, the p's cannot be greater than $N/(A-F)$. The last surviving determinants can be treated again with Hadamard's inequality, so that

$$D_N < \sum_{s_1, \dots, s_p}^{0 \dots F} C(A, s_1) \dots C(A, s_p) M^{\sum_{i=1}^{p} s_i + N - pA} \left(\sum_{i=1}^{p} s_i + N - pA\right)^{\frac{1}{2}\left(\sum_{i=1}^{p} s_i + N - pA\right)}$$

and « a fortiori »:

$$D_N < M^N A^{A/2} \left[\sum_{s=0}^{F}\binom{A}{s}^2 (A-s)^{\frac{1}{2}(A-s)}\right]^p < M^N A^{A/2} \left[A^{A/2}\sum_{s=0}^{F}\binom{A}{s}^2\right]^p <$$

$$< M^N A^{((p+1)/2)A} \left[\sum_{s=0}^{F}\binom{A}{s}\right]^{2p} < M^N A^{((p+1)/2)A} \left[\sum_{s=0}^{F}\binom{A}{s}\right]^{2p} = M^N A^{((p+1)/2)A}\, 2^{2pA}\ .$$

or:

$$D_N < A^{A/2}[M(2^4A)^{(A/2(A-F))}]^N . \tag{6}$$

It follows then, by substitution into (3), that $K_{N_0,0}$ is majorated by a series which, from a given term on, behaves like an exponential series, and has therefore an infinite radius of convergence.

It may be relevant to point out that, with this procedure, and of course under the same regularizing assumptions, also all perturbative expansions relative to Fermi-type couplings are shown to have an infinite radius of convergence.

* * *

We thank with pleasure Dr. D. R. YENNIE for kindly communicating his result to us previous to publication, and for interesting discussions on this subject.

On a Method of Covariant Quantization.

V. Nardi

Istituto di Fisica dell'Università - Padova
Istituto Nazionale di Fisica Nucleare - Sezione di Padova

(ricevuto il 21 Febbraio 1958)

1. – For the case of interacting fields (nucleons with neutral scalar mesons), with a non-local type interaction, the generalized Poisson brackets, defined by R. E. Peierls [1] have been evaluated for the in- and out-fields some time ago [2].

For $\{\varphi^{\text{in}}(y), \varphi^{\text{in}}(x)\} = \{\varphi^{\text{out}}(y), \varphi^{\text{out}}(x)\}$ and the similar for $\overline{\psi}^{\text{in}}_{\text{out}}(x)$, $\psi^{\text{in}}_{\text{out}}(x)$ the values $\Delta(y-x)$, etc., have been found. These results were possible only with the very extraordinary assumption that all the operators $\overline{\psi}(x)$, $\psi(x)$, $\varphi(x)$ of the Fermi and of the Bose fields are commuting quantities. Therefore the Peierls covariant rules of quantization $[\varphi^{\text{in}}(y), \varphi^{\text{in}}(x)]_- = i\hbar\{\varphi^{\text{in}}(y), \varphi^{\text{in}}(x)\}$, etc. seem, in this way, to be an inconsistent method in the Yang and Feldman formalism. In this note we [3] will show, without such unusual assumptions about the field operators, that it is possible to obtain for the generalized Poisson brackets of the in- and out-fields, the values $\Delta(x-y)$ etc., so that the covariant quantization rules appear to be consistent and give, obviously, the results of the canonical method. In order to obtain in a simple fashion the matrix element for scattering in a closed form S. S. Schweber [4] has calculated the commutation relation

$$[\varphi^{\text{in}}(y), \varphi^{\text{out}}(x)] \quad .$$

With the covariant rules of quantization one obtains, easily, identical results.

2. – The equations of motion for the Heisenberg operator of our system, are [5]:

$$(1) \qquad \begin{cases} (-i\not{\nabla} + m)\psi(x) = -G\psi(x)\varphi(x)\,, \\ i\partial_\nu\overline{\psi}(x)\gamma_\nu + m\overline{\psi}(x) = -G\overline{\psi}(x)\varphi(x)\,, \\ (\Box + \mu^2)\varphi(x) = -J(x)\,. \end{cases}$$

(1) R. E. Peierls: *Proc. Roy. Soc.*, **214**, 143 (1952).

(2) P. Gulmanelli: *Nuovo Cimento*, **10**, 1582 (1953).

(3) We consider here only a local type interaction. A non-local type interaction, in any case not advisable (see the work of G. E. C. Stueckelberg and Wanders: *Helv. Phys. Acta*, **27**, 667 (1954)) complicates only the formal expression. We have seen, with a general form factor, that the result is the same as that obtained with a local type interaction.

(4) S. S. Schweber: *Nuovo Cimento*, **2**, 397 (1955).

(5) Using a symmetrized interaction term $\frac{1}{2}[J(x), \varphi(x)]_-$ one obtains the same results.

The incoming and outgoing fields are defined by:

$$(2)\qquad \begin{cases} \varphi(x) = \overset{\text{in}}{\varphi}^{\text{out}}(x) - \int \underset{A}{\Delta_R}(x-x_1) J(x_1)\mathrm{d}x_1 , \\ \psi(x) = \overset{\text{in}}{\psi}^{\text{out}}(x) + G\int \underset{A}{S_R}(x-x_1)\psi(x_1)\varphi(x_1)\mathrm{d}x_1 , \\ \bar{\psi}(x) = \overset{\text{in}}{\bar{\psi}}^{\text{out}}(x) + G\int \bar{\psi}(x_1)\varphi(x_1)\underset{R}{S_A}(x_1-x)\mathrm{d}x_1 . \end{cases}$$

Adding to the action integral the operator $\lambda A = \lambda\varphi(y)$, where λ is an infinitesimal parameter, the equations of motion are changed. If B is a solution of (1) or a function of these solutions, and B' the changed operator, written as $B' = B + \lambda D_A B$ (or $B' = B + \lambda \mathcal{A}_A B$) to the first order in λ, we obtain the « retarded » variations:

$$(3)\qquad \begin{cases} D_{\varphi(y)}\varphi(x) = \Delta_R(x-y) - \int \Delta_R(x-x_1) D_{\varphi(y)} J(x_1)\mathrm{d}x_1 , \\ D_{\varphi(y)}\psi(x) = G\int S_R(x-x_1) D_{\varphi(y)}[\psi(x_1)\varphi(x_1)]\mathrm{d}x_1 , \\ D_{\varphi(y)}\bar{\psi}(x) = G\int \bar{\psi}(x_1)\varphi(x_1) S_A(x_1-x)\mathrm{d}x_1 , \end{cases}$$

uniquely determined from the conditions $D_A B \to 0$ as $t \to -\infty$, and the « advanced » variations:

$$(4)\qquad \mathcal{A}_{\varphi(y)}\varphi(x) = \Delta_A(x-y) - \int \Delta_A(x-x_1)\mathcal{A}_{\varphi(y)} J(x_1)\mathrm{d}x_1 , \quad \text{etc.}$$

uniquely determined from the condition $\mathcal{A}_A B \to 0$ as $t \to +\infty$. We have to evaluate the generalized Poisson brackets defined by

$$(5)\qquad \{A, B\} = D_A B - \mathcal{A}_A B ,$$

with $A = \varphi^{\text{in}}(y)$ and $B = \varphi^{\text{in}}(x)$.

From the modified equation (1) using $(2)_1$, $(3)_1$, $(4)_1$ and the general property

$$(a)\qquad \{A, B+C\} = \{A, B\} + \{A, C\} ,$$

it follows that:

$$D_{\varphi(y)}\varphi^{\text{in}}(x) = \Delta_R(x-y) , \qquad \mathcal{A}_{\varphi(y)}\varphi^{\text{in}}(x) = \Delta_A(x-y) - \int \Delta(x-x_1)\mathcal{A}_{\varphi(y)} J(x_1)\mathrm{d}x_1 ,$$

where $\Delta(x) = \Delta_A(x) - \Delta_R(x)$.

Still using $(2)_1$ and the property

$$(b) \qquad \{A + B, C\} = \{A, C\} + \{B, C\}\,,$$

one has

$$(6) \qquad \{\varphi^{\mathrm{in}}(y), \varphi^{\mathrm{in}}(x)\} - \Delta(y - x) = \int \Delta(x - x_1) \mathcal{A}_{\varphi(y)} J(x_1) \mathrm{d}x_1 + \\ + \int \Delta_B(y - y') \, [D_{J(y')} \varphi^{\mathrm{in}}(x) - \mathcal{A}_{J(y')} \varphi^{\mathrm{in}}(x)] \mathrm{d}y'.$$

It is easy to see that the right-hand side of (6) is identically zero. We obtain from the changed equations of motions, with $A = J(y)$, the following « advanced » variations:

$$(7) \qquad \begin{cases} \mathcal{A}_{J(y)} \varphi(x) = -\int \Delta_A(x - x_1) \mathcal{A}_{J(y)} J(x_1) \, \mathrm{d}x_1\,, \\ \mathcal{A}_{J,y)} \psi(x) = -GS_A(x - y)\psi(y) + G \int S_A(x - x_1) \mathcal{A}_{J(y)} [\psi(x_1)\varphi(x_1)] \mathrm{d}x_1\,, \\ \mathcal{A}_{J\,y)\,\bar{\psi}}(x) = -G\bar{\psi}(y) S_B(y - x) + G \int \mathcal{A}_{J(y)} [\bar{\psi}(x_1)\varphi(x_1)] S_B(x_1 - x) \mathrm{d}x_1\,, \end{cases}$$

and the analogous « retarded » variations.

From $(2)_1$ and $(7)_1$, it results that:

$$(8) \qquad \begin{cases} \mathcal{A}_{J(y)} \varphi^{\mathrm{in}}(x) = -\int \Delta(x - x_1) \mathcal{A}_{J(y)} J(x_1) \mathrm{d}x_1\,, \\ \text{and analogously:} \\ D_{J(y)} \varphi^{\mathrm{in}}(x) = 0\,. \end{cases}$$

If we make the iterative expansion in powers of the coupling constants G, of the two addends on the r.h.s. of (6), we obtain for the first addend, using (4) and the property of general validity [6]

$$(c) \qquad \{A, BC\} = \{A, B\} C + B \{A, C\}\,,$$

$$(9) \qquad G^2 \int \Delta(x - x_1) [\bar{\psi}(x_2) \Delta_A(x_2 - y) S_B(x_2 - x_1) \psi(x_1) + \\ + \bar{\psi}(x_1) S_A(x_1 - x_2) \psi(x_2) \Delta_A(x_2 - y)] \, \mathrm{d}x_1 \, \mathrm{d}x_2 + G^3 \ldots .$$

---

[6] We recall that on the contrary, the properties

$$(d) \qquad \{AB, C\} = \{A, C\} B + A \{B, C\}\,,$$

$$(e) \qquad \{A, B\} = -\{B, A\}$$

have not a general validity. For quantum operators, A and B, and C, one must determine their validity case by case.

For the second addend using (8) and then (7), we obtain:

$$(10) \qquad -G^2\int \Delta_R(y-y')\Delta(x-x_1)[\bar{\psi}(y')S_R(y'-x_1)\psi(x_1)+$$

$$+\bar{\psi}(x_1)S_A(x_1-y')\psi(y')]\mathrm{d}y'\mathrm{d}x_1+G^3\ldots.$$

With the change of notation $y'\to x_2$ and using the property

$$(11) \qquad \Delta_R(x)=\Delta_A(-x)\,,$$

the first term of one expansion is equal to the negative of the first term of the other.

Further, we can easily see that if (except for the sign) the n-order term of (9) is equal to the n-order term (10), then also the higher order terms of (9) and (10) are equal. In fact, in (9) one obtains terms of order $n+1$ from the n-order term by the substitutions

$$\ldots\psi(x_n)\Delta_A(x_n-y)S_R(x_n-x_{n-1})\ldots\to$$

$$\to\ldots\psi(x_{n+1})\Delta_A(x_{n+1}-y)S_R(x_{n+1}-x_n)\varphi(x_n)S_R(x_n-x_{n-1})\ldots$$

$$\ldots\bar{\psi}(x_n)\Delta_A(x_n-y)S_R(x_n-x_{n-1})\varphi(x_{n-1})\ldots\to\ldots-\bar{\psi}(x_{n-1})\Delta_A(x_{n-1}-x_n)\cdot$$

$$\cdot[\bar{\psi}(x_{n+1})\Delta_A(x_{n+1}-y)S_R(x_{n+1}-x_n)\psi(x_n)+\bar{\psi}(x_n)S_A(x_n-x_{n+1})\Delta_A(x_{n+1}-y)\psi(x_{n+1})]\ldots$$

etc., and in (10) by the substitutions

$$\Delta_R(y-y')\ldots\bar{\psi}(y')S_R(y'-x_{n-1})\ldots\to\Delta_R(y-y')\ldots\bar{\psi}(y')S_R(y'-x_n)\varphi(x_n)S_R(x_n-x_{n-1})\ldots$$

$$\Delta_R(y-y')\ldots\bar{\psi}(y')S_R(y'-x_{n-1})\,\varphi(x_{n-1})\ldots\to-\Delta_R(y-y')\ldots\bar{\psi}(x_{n-1})\Delta(x_{n-1}-x_n)\cdot$$

$$\cdot[\bar{\psi}(y')S_R(y'-x_n)\psi(x_n)+\bar{\psi}(x_n)S_A(x_n-y')\psi(y')]\ldots$$

etc. These latter substitutions, with the change $y'\to x_n$ and $y'\to x_{n+1}$ and for the property (11) coincide with the previous substitutions. The r.h.s. of (6) is therefore zero; by means of (8) and (2), it assumes the form:

$$\int\Delta(x-x_1)\mathcal{A}_{\varphi^{\mathrm{in}}_{(y)}}J(x_1)\,\mathrm{d}x_1,$$

and we have

$$(12) \qquad \mathcal{A}_{\varphi^{\mathrm{in}}_{(y)}}J(x)=0 \quad (7)\,.$$

Proceeding in a completely analogous way, we find that:

$$\{\bar{\psi}^{\mathrm{in}}(y),\psi^{\mathrm{in}}(x)\}=\{\psi^{\mathrm{in}}(y),\psi^{\mathrm{in}}(x)\}=0\,,\qquad \{\bar{\psi}^{\mathrm{in}}(y),\psi^{\mathrm{in}}(x)\}=-S(y-x)\,,$$

and the same for the outgoing fields.

(7) For a classical quantity the validity of (12) follows, by definition, from the $(8)_2$.

It is possible to affirm that the covariant quantization rules give the correct results for the incoming and outgoing fields. One also obtains correct results for the case of pseudoscalar-meson with direct or derivative couplings.

3. – In a similar way to the previous case, we evaluate:

$$\{\varphi^{\text{in}}(y), \varphi^{\text{out}}(x)\} .$$

Using the relations, corresponding to the expressions (8),

$$\mathcal{A}_{J(y)}\varphi^{\text{out}}(x) = 0 ,$$

$$D_{J(y)}\varphi^{\text{out}}(x) = \int \Delta(x - x_1) D_{J,y} J(x_1) \mathrm{d}x_1 ,$$

and

$$D\varphi^{\text{out}}(x) J(y) = 0 ,$$

obtained with the same iterative development used in order to obtain (12), we have:

$$\{\varphi^{\text{in}}(y), \varphi^{\text{out}}(x)\} = \Delta(y - x) - \int \mathrm{d}x_1 \cdot$$

$$\cdot \int \mathrm{d}y' \Delta(x - x_1)\Delta(y - y')\theta(y' - x_1) \left[D_{J(y')}J(x_1) - \mathcal{A}_{J(y')}J(x_1)\right] ,$$

where

$$\theta(x) = \begin{cases} 1 , & x^0 < 0 , \\ \frac{1}{2} , & x^0 = 0 , \\ 0 , & x^0 > 0 . \end{cases}$$

On the other hand for $A = J(y)$ and $B = \bar{\psi}(x)$, $\psi(x)$, $\varphi(x)$ it is easy to see with an iterative development of the type used above, that the property (e) is satisfied. The quantization covariant rules are therefore consistent and they give:

$$[\varphi^{\text{in}}(y), \varphi^{\text{out}}(x)]_- = i\hbar c \Delta(y - x) - \int \mathrm{d}x_1 \int \mathrm{d}y' \Delta(x - x_1)\Delta(y - y')\theta(y' - x_1)[J(y'), J(x_1)] .$$

Moreover, because the property (e) is demonstrable also for $A = \varphi^n(x)$ and $B = \bar{\psi}(x)$, $\psi(x)$, $\varphi(x)$, if one adds to $(1)_3$ the renormalization terms $a\,\varphi^2$, $b\varphi^3$ for scalar meson in order to remove the divergences due to the triangle and square diagrams (or $c\varphi^3$ for pseudo-scalar meson), the covariant quantization rules are still consistent and give, for pseudo-scalar meson, the same results obtained by SCHWEBER.

Renormalization of Axial Vector Coupling.

J. C. Polkinghorne
Tait Institute, University of Edinburgh, Scotland

(ricevuto il 4 Marzo 1958)

Feynman and Gell-Mann [1] have recently proposed a universal Fermi-interaction using V and A couplings. They point out that the effective coupling constant calculated from μ-decay agrees with that calculated from the decay of ^{14}O to a high degree and that this is rather surprising as the strong interactions present in the latter case would be expected to renormalize the effective coupling to a different value. They suggest that there may be a mechanism at work that prevents this, analogous to the mechanism in electrodynamics that ensures that all particles have the same renormalized charge. In fact this requires that the coupling should be through a current that is conserved by the strong interactions and they point out that such a current is available for the vector coupling, namely the isotopic-spin current, provided we also permit the π-meson field to participate in the four-field interaction. There remains the question of the axial vector coupling.

In this note we wish to point out that a recent suggestion of Schwinger [2] enables one to construct an axial vector current that is conserved to the extent that one neglects the medium strong [3] K-meson interactions.

Schwinger suggests that an isotopic scalar particle, σ, exists which is a scalar in Lorentz-space. If the real mass of σ is greater than twice the π-mass it is highly unstable and it will not have been seen. The existence of the σ enables one to construct an axial vector boson current from cross-terms with the π and so to construct an axial vector current that is conserved.

We shall consider first the nucleon-π-σ system, and suppose the nucleons have bare mass m_0, and that π and σ have *bare mass zero* and the same very strong coupling to the nucleons. The interaction Lagrangian is therefore

$$g[\bar{N}\gamma_5 \boldsymbol{\tau} N \cdot \boldsymbol{\pi} + \bar{N} N \sigma] \,. \tag{1}$$

[1] R. P. Feynman and M. Gell-Mann; *Phys. Rev.*, **109** 193 (1958).
[2] J. Schwinger: *Ann. of Physics*, **2**, 407 (1957).
[3] M. Gell-Mann: *Phys. Rev.*, **106**, 1296 (1957); J. Schwinger: *loc. cit.*; J. C. Polkinghorne: *Nuovo Cimento*, **6**, 864 (1957).

It is then easily verified that the equations of motion lead to the equation

$$\partial_\mu \left[i\bar{N}\gamma_5\gamma_\mu\tau_i N + 2\pi_i \cdot \partial_\mu \sigma - 2\partial_\mu \pi_i \cdot \sigma - \frac{2m^0}{g}\partial_\mu \pi_i \right] = 0 . \qquad i = 1, 2, 3 . \tag{2}$$

Thus we have constructed an axial vector isotopic current that is conserved. The extension to the case where all baryons interact with π and σ is trivial.

It is not possible to extend the current (2) to one conserved by the medium strong K-meson interactions unless the K-mesons are parity doublets. However, the greatest renormalization effects are presumably due to the π and σ interactions and the current experimental value of 1.3 for the ratio of Gamow-Teller to Fermi couplings may represent the effects of K-meson renormalization on the axial vector current.

Note added in proof.

Dr. J. C. Taylor has pointed out that if the pion bare mass is zero and its coupling to baryons is *pseudovector* then it follows that

$$\partial_\mu \left[i\bar{N}\gamma_5\gamma_\mu\tau_i N - \frac{1}{f}\partial_\mu \pi_i \right] = 0 . \tag{3}$$

This is an expression of the invariance of the equations for pseudovector coupling under the transformation $\boldsymbol{\pi} \to \boldsymbol{\pi} + \boldsymbol{\lambda}$, where $\boldsymbol{\lambda}$ is a constant isotopic vector. This would seem to imply that the pion real mass would also be zero for this case, in the approximation of neglecting meson-meson interactions.

The Symmetry Properties of Fermi Dirac Fields.

B. Touschek

Istituto di Fisica e Scuola di Perfezionamento in Fisica Nucleare dell'Università - Roma
Istituto Nazionale di Fisica Nucleare - Sezione di Roma

(ricevuto il 18 Marzo 1958)

A recent paper by Gürsey [1] and the proposal of a new universal theory by Heisenberg and Pauli [2] have shed a new light on the symmetry properties of Fermi Dirac fields. In the present note we study the maximum symmetry attainable in a space formed by an n-fold Majorana [3] field. This manifold is defined by

$$(1) \qquad \mu_\varrho^{i+}(\boldsymbol{x}) = \mu_\varrho^i(\boldsymbol{x});$$

$$2\{\mu_\varrho^i(x)\mu_\sigma^k(x')\} = \delta_{\varrho\sigma}\delta_{ik}\delta(\boldsymbol{x}-\boldsymbol{x}')\,,$$

where μ_ϱ^i is the (q-number) Majorana spinor, $^+$ denotes the Hermitian Conjugate, the indices i and k run from 1 to n, ϱ and σ are spinor indices and $\boldsymbol{x}$ and $\boldsymbol{x}'$ are space coordinates. The reality condition in (1) implies the use of the Majorana gauge

$$(2) \quad \gamma^{\mu+} = \gamma^\mu \quad \gamma^{i*} = \gamma^i \quad \gamma^{4*} = -\gamma^4,$$

with * denoting complex conjugation and $i = 1, 2, 3$.

It can be shown that the most general linear canonical and proper transformation of the μ's must be of the form

$$(3) \qquad \mu' = \exp[A + iS\gamma_5]\mu\,.$$

Here we have supressed the indices $i = 1, \ldots n$ as well as the spinor indices. A and S are real $n \times n$ matrices, A is antisymmetric, S is symmetric. It immediately follows from (3) that the full group of linear canonical and proper transformations has n^2 parameters. For $n = 1$ there is just one such parameter corresponding to the transformation

$$(4) \qquad \mu' = \exp[i\beta\gamma_5]\mu\,,$$

introduced by Touschek [4]. For $n = 2$ one has a reducible group of 4 parameters, which corresponds to the symmetries introduced by Pauli [5], one of which is a gauge group of the type (4) the other is isomorphic to the unitary group in two dimensions.

The full symmetry (3) in the case $n = 1$ and $n = 2$ does not allow the introduction of a mass operator. If it

(1) F. Gürsey: *Nuovo Cimento*, **7**, 411 (1958).
(2) W. Heisenberg and W. Pauli: preprint.
(3) E. Majorana: *Nuovo Cimento*, **14**, 171 (1937).
(4) B. Touschek: *Nuovo Cimento*, **5**, 754, 1281 (1957).
(5) W. Pauli: *Nuovo Cimento*, **6**, 204 (1957).

is required that such a mass operator should exist the group (3) has to be limited by the following requirement. It is postulated that there exist a symmetrical non singular (if all the masses are $\neq 0$) $n \times n$ matrix X such that

$$M = \mu\gamma_4(1 + \varepsilon\gamma_5)X\mu \,, \tag{5}$$

(with ε an arbitrary number) is invariant under a subgroup of (3). This subgroup is then represented by all the matrices A and S which satisfy the commutation relations

$$[AX] = 0 \,, \qquad \{S, X\} = 0 \,. \tag{6}$$

It is easily seen that in the case $n = 1$ this requirement eliminates the gauge transformation (4). In the case $n = 2$ one remains with a single parameter group which is equivalent to the ordinary gauge group for a complex spinor, viz.:

$$\psi' = \exp[i\alpha]\psi \,. \tag{7}$$

In the case $n = 4$ the requirement (5) reduces the number of available parameters to 6 and it can be shown that the resulting group is isomorphic to the group of rotations in a 4-dimensional euclidean space. If $X^2 = 1$, i.e. in the case of mass degeneracy its simplest representation is found with $X = 1$ which automatically gives $S = 0$ and A arbitrary. The transformations

$$\mu' = e^A\mu \,, \tag{8}$$

are isomorphic to two commuting unitary groups in two dimensions, a result which holds quite generally for $X^2 = 1$. If one of the two is identified with the isospin, the other bears the same relation to the conservation of the baryon number as the isospin group bears in relation to the conservation of charge. Invariance of a theory under (8) then has as a consequence the conservation of the quantum numbers

$$J^2, J_3; \quad K^2, K_3 \,, \tag{9}$$

where J^2 measures the multiplicity of the isotopic spin and K^2 that of the baryon number. It can be shown that a π-meson of isotopic spin 1 must necessarily destroy the conservation of K^2 — unless it is coupled to the baryon field by vector and tensor terms. Electromagnetic couplings on the other hand destroy both the symmetries J^2 and K^2.

* * *

I wish to thank Prof. CINI for helpful discussions and suggestions.

LIBRI RICEVUTI E RECENSIONI

B. T. Price, C. C. Horton and K. T. Spinney – *Radiation Shielding* (International Series of Monographs on Nuclear Energy). Ed. Pergamon Press, London, pag. IX+350, 60 s.

La protezione dalle radiazioni, anche di elevata energia e di grande intensità, non costituisce un problema nuovo: essa è stata realizzata praticamente con la costruzione dei reattori nucleari, delle macchine acceleratrici, e dei laboratori per alte attività; soltanto ora però le conoscenze teoriche e pratiche accumulate in questi anni appaiono nella letteratura in forma ordinata e completa.

Questo volume, scritto da scienziati del Laboratorio Atomico di Harwell, raccoglie infatti sia gli aspetti scientifici che quelli pratici della progettazione di schermi contro le radiazioni; pur dando maggior risalto ai primi, che formano una solida base per la trattazione dei problemi più complessi, gli autori non possono ignorare i secondi, che mettono in luce certi accorgimenti di dettaglio senza i quali anche uno schermo calcolato con ogni precisione risulterebbe inefficace.

La diversa natura delle radiazioni con le quali si può avere a che fare porta ad una spontanea suddivisione della materia: *a*) attenuazione dei raggi gamma e degli elettroni veloci, *b*) protezione contro i neutroni; ognuna di queste parti è basata su di uno studio preliminare delle interazioni con la materia ed è accompagnata da grafici e tabelle che rendono possibile il calcolo effettivo. Gli aspetti più strettamente pratici e costruttivi della schermatura dei reattori e dei materiali radioattivi e le questioni di dettaglio, come la costruzione di finestre protettive e di recipienti per il trasporto, sono poi esposti in un capitolo a parte in cui è anche preso in considerazione il costo relativo delle varie strutture.

Poichè la schermatura non può mai, in pratica, essere assoluta e poichè essa serve assai spesso per proteggere gli operatori, è naturale che le attuali conoscenze sugli effetti biologici delle radiazioni, almeno per quanto concerne i pericoli per gli esseri umani e le dosi che possono essere ammesse, costituiscano una necessaria premessa a questo studio. Questi argomenti sono esposti all'inizio del volume in un capitolo riassuntivo, completato, come tutti gli altri, da preziosa bibliografia.

Le formule matematiche più importanti sono discusse in un capitolo a parte che contiene i diagrammi delle funzioni che compaiono nel calcolo degli schermi.

Il volume è aggiornato al 1957; esso appare un'utile guida sia per lo studio che per il progetto e, dati i numerosi argomenti trattati, che vanno ben oltre i limiti del calcolo degli schermi, può presentare interesse per una larga cerchia di lettori.

Franco A. Levi

G. W. SERIES, *Spectrum of Atomic Hydrogen*, Oxford University Press 1957, pag. VII, 88, prezzo 8s. 6d.

Questo è il secondo volume della serie « Oxford Library of the Physical Science » (il primo volume della serie fu quello di Blin-Stoyle sui momenti nucleari).

Lo scopo principale del libro è quello di offrire una esposizione dei recenti lavori sui Lamb shift insieme ad una illustrazione delle relative idee teoriche. Tuttavia una prima parte del volume dà un quadro piuttosto completo anche del lavoro precedente sullo spettro dell'atomo di idrogeno.

Il primo capitolo, introduttivo, dà una sommaria descrizione del contenuto. Il secondo capitolo contiene una prima descrizione degli esperimenti principali di spettroscopia dell'atomo di idrogeno. Il terzo, quarto e quinto capitolo sono dedicati alla vecchia meccanica quantistica ed alle sue verifiche sperimentali. Il capitolo sesto introduce la nuova meccanica quantistica e si spinge sino alla equazione di Dirac ed al calcolo delle probabilità di transizione. Il capitolo settimo accenna al lavoro sperimentale svolto per confermare la teoria di Dirac. L'impossibilità di ottenere una conferma decisiva della teoria (a causa principalmente delle discrepanze tra i risultati di R. C. WILLIAMS e quelli di DRINKWATER, RICHARDSON e W. E. WILLIAMS) spinse LAMB e RETHERFORD a tentare nel 1945 con una tecnica originale l'ormai famoso esperimento sulla riga H_α che, confermando i risultati di R. C. WILLIAMS, mostrò l'inadeguatezza della teoria di Dirac. I punti salienti dell'esperimento sono descritti nel capitolo ottavo. Nel capitolo nono vengono riportate le spiegazioni proposte per il Lamb shift, che formarono la base fisica per gli sviluppi recenti dell'elettrodinamica e della teoria dei campi. Vengono riportati i calcoli di Bethe e di Welton. Il capitolo decimo descrive tutto il successivo lavoro sperimentale sui Lamb shift in idrogeno, deuterio, tritio e delio. Il capitolo undicesimo è dedicato alle teorie della struttura iperfina, dalla teoria originale di Fermi alle successive teorie elettrodinamiche. Infine il capitolo dodicesimo dà una breve ma accurata esposizione degli esperimenti sul positronio ed un cenno alle teorie relative.

Non ci si può naturalmente aspettare in un piccolo volume di meno di cento pagine una esposizione completa o molto dettagliata delle tante questioni trattate. Le principali idee sono però esposte con molta chiarezza e con particolare insistenza sul loro contenuto fisico. Per maggiori dettagli l'autore rimanda ai lavori originali ogni volta citati nella accurata bibliografia. In conclusione riteniamo che il libro, accuratamente scritto e di concezione piuttosto moderna, possa servire come guida, da estendere opportunamente, per la parte dei nostri corsi di spettroscopia relativa all'atomo di idrogeno.

R. GATTO

Direttore responsabile: G. POLVANI Tipografia Compositori - Bologna

Questo fascicolo è stato licenziato dai torchi il 18-4-1958